STUDIES ON HUMAN ARYLAMINE N-ACETYLTRANSFERASES

A THESIS SUBMITTED TO THE FACULTY OF GRADUATE SCHOOL OF THE UNIVERSITY OF MINNESOTA BY

LI LIU

IN PARTIAL FULFILLMENT OF THE REQUIREMENTS FOR THE DEGREE OF DOCTOR OF PHILOSOPHY

DR. PATRICK E. HANNA, ADVISOR

JANUARY, 2009

ACKNOWLEDGEMENT

Most of all my sincere thanks go to my adviser, Dr Patrick E. Hanna for his continuous encouragement and expert guidance. His scientific attitude, academic integrity, and energetic working style have influenced me greatly. He has trained me to design experiments independently, and to evaluate results critically. Many thanks go to Dr. Carston R. Wagner for his stimulating and helpful suggestions along the way. I thank the rest of my committee members, Dr Chengguo Xing and Dr Mark Distefano, for their valuable feedback, which helped me to improve this dissertation.

I thank the former members of Drs Hanna's and Wagner's laboratory, Dr Zhijun Guo, Dr Haiqing Wang, Dr Tsuifen Chou, and Dr Jonathan Carlson for their valuable help and for their great friendship. I thank current members of the laboratory, Xin Zhou, Yan Jia, Qing Li, Brian White, Dr Brahma Ghosh, Dr Adrian Fegan, and Dr Brandie Kovaleski for very helpful suggestions and for making my Ph. D a memorable experience. I thank Annette Von Vett for conducting the substrate specificities project, for her positive attitude and her friendship. I also thank other friends, Xiaodan Liu, Siyi Zhang, and Jignesh Doshi in the department of Medicinal Chemistry for their generous help and friendship.

I own my deepest gratitude to my parents, Jingchun Liu and Shuqing Zhao, for their love and support all these years. I owe my special thanks to my twin sister, Na Liu, who told me that whatever happened, I should smile and face it. Finally and most importantly, I am grateful to my beloved husband, Lei, for his unconditional love, support, patience, and encouragement.

ABSTRACT

Arylamine N-acetyltransferases (NATs, EC 2.3.1.5) are important phase II drug metabolism enzymes that are expressed in most human tissues. Humans express two NAT isozymes, NAT1 and NAT2, which share 81% sequence identity. NATs catalyze the AcCoA-dependent N-acetylation of arylamines to arylamides, which is a critical detoxification process and competes with cytochrome P450-catalyzed oxidation of arylamines to N-arylhydroxylamines. In this thesis, recombinant human NAT2 was successfully overexpressed and purified to homogeneity; the substrate specificities and molecular interactions of environmental arylamines with human NAT1 and NAT2 were characterized; the in vitro and intracellular inactivation of human NAT1 and NAT2 by the nitrosoarene and N-arylhydroxamic acid metabolites of toxic and carcinogenic arylamines was investigated.

To investigate the substrate specificities and inhibition of human NATs, we developed a method to produce homogeneous human “wild type” NAT2 in milligram quantities. Human NAT2 was overexpressed as a L54F dihydrofolate reductase (DHFR) fusion protein linked with a TEV protease-cleavage linker. Chromatography with a methotrexate affinity column, followed by a DEAE column, afforded partial purification of the fusion protein. The fusion protein was digested with TEV protease, and human NAT2 was purified to homogeneity with a second DEAE column. A total of 2.8 mg of human rNAT2 from 2 L of cell culture was purified to homogeneity with this methodology.

The kinetic specificity constants (k_{cat}/K_m) for N-acetylation of arylamine environmental contaminants were characterized for human NAT1 and NAT2. The dramatic effects of small alkyl substituents on the relative abilities of NAT1 and NAT2 to acetylate substituted anilines was reflected by the 1000-fold difference in the NAT1/NAT2 ratio of the specificity constants for monosubstituted and disubstituted alkylanilines containing methyl and ethyl ring substituents. A NMR-based model was used to interpret the interactions of binding site residues with the alkylanilines and to provide insight into how NATs achieve certain substrate specificities.

Arylamines and their N-hydroxylation products, N-arylhydroxylamines, can undergo oxidation to form nitrosoarenes in vivo. We investigated the inactivation of human NAT1 by the nitrosoarene metabolites of four environmental arylamines in vitro and in human cells. 4-Nitrosobiphenyl (4-NO-BP) and 2-nitrosofluorene (2-NO-F), which are nitroso metabolites of arylamines that are readily N-acetylated by NAT1, were found to be potent inactivators of human NAT1. 4-NO-BP is an affinity label for NAT1 (k_{inact}/K_I = 59,200 $M^{-1}s^{-1}$), whereas 2-NO-F inactivates NAT1 through an apparent bimolecular process (k_2 = 34,500 $M^{-1}s^{-1}$). Glutathione (GSH) afforded only partial protection of NAT1 from inactivation by the two nitrosoarenes in vitro. Nitrosobenzene (NO-B) and 2-nitrosotoluene (2-NO-T), which are nitroso metabolites of arylamines that are less readily acetylated by NAT1, were much weaker inhibitors of NAT1. Treatment of HeLa cells with 4-NO-BP (10 μM) for 15 minutes and 60 minutes caused 39% and 58% losses of NAT1 activity, respectively, without causing a decrease in either glyceraldehyde phosphate dehydrogenase (GAPDH) or glutathione

reductase (GR) activities. 2-NO-F was an even more effective inhibitor of HeLa cell NAT1 than 4-NO-BP. Tandem mass spectrometric analysis indicated that 4-NO-BP treatment of HeLa cells in which 3FLAG-NAT1 had been overexpressed resulted in a formation of (4-biphenyl)sulfinamide with the active site Cys68 of NAT1. This is consistent with the results obtained with recombinant NATs in vitro.

It was also demonstrated that the nitrosoarene metabolites of arylamines that are efficiently N-acetylated by NAT2 are potent inactivators of NAT2 in vitro and in human cells. The second order rate constants for inactivation of NAT2 by 4-NO-BP and 2-NO-F were 80,400 $M^{-1}s^{-1}$ and 50,500 $M^{-1}s^{-1}$, respectively; the values for NO-B and 2-NO-T were 14 $M^{-1}s^{-1}$ and 16 $M^{-1}s^{-1}$. Treatment of HeLa cells with 4-NO-BP (5 μM) for 1 h caused a 23% reduction in NAT2 activity, and exposure to 2-NO-F (2.5 μM) for 1 h caused a 22% loss of NAT2 activity, without inhibiting GAPDH and GR activities. Therefore, HeLa intracellular NAT2 is less susceptible to the effects of the lower concentrations of the two nitrosoarenes than is NAT1. It is concluded that NAT1 and NAT2 are intracellular targets of the nitrosoarene metabolites of 4-aminobiphenyl and 2-aminofluorene. Low concentrations of nitrosoarenes may cause a loss of NAT1 and NAT2 activities and impair a key detoxification pathway.

N-Arylhydroxamic acids, which are also potentially reactive metabolites of arylamines, have been shown to inactivate hamster NATs, in vitro and in vivo, and human recombinant NAT1. It was previously established that inactivation of NATs by N-hydroxy-4-acetylaminobiphenyl (N-OH-4-AABP) involves an initial

NAT-mediated deacetylation to form N-OH-4-aminobiphenyl, which undergoes oxidation to the electrophilic 4-nitrosobiphenyl (4-NO-BP), followed by reaction with the nucleophilic active site Cys68 to form a sulfinamide. We hypothesized that the relative stabilities of the acetyl-enzyme intermediates influence the susceptibilities of NATs to inactivation by N-arylhydroxamic acids. The second order rate constant for inactivation of human NAT2 by N-OH-AAF was 459 $M^{-1}s^{-1}$, which was 8-fold greater than that for NAT1. Mass spectrometric analysis of both NATs after treatment with N-OH-AAF revealed that the principal adducts were sulfinamide conjugates of Cys68. Kinetic analysis revealed that the hydrolysis rate of acetyl-NAT2 was 4.7-fold greater than that of acetyl-NAT1. Thus, the more rapid inactivation of NAT2 was facilitated by the rapid hydrolysis of the Cys68 thioacetyl ester to free the Cys68 thiol group for reaction with 2-NO-F. The hypothesis was further supported by the results from inactivation of human NATs by N-OH-4-AABP. Treatment of HeLa cells with N-OH-4-AABP (50 μM) for 6 hours had no effect on intracellular NAT2 activity, but caused a 24% decrease in NAT1 activity. Incubation with N-OH-4-AABP (100 μM) for 6 h reduced NAT2 and NAT1 activities by 19% and 56%, respectively. Treatment of HeLa cells with 50 μM N-OH-AAF for 6 hours reduced NAT2 and NAT1 activities by 11% and 33%, respectively. Therefore, approximately 10-fold greater concentrations and longer incubation times were required for the N-arylhydroxamic acids to produce effects on intracellular NATs than were required for 2-NO-F and 4-NO-BP. HeLa NAT1 is more susceptible to the effects of the N-arylhydroxamic acids than NAT2.

TABLE of CONTENTS

PAGE

LIST of FIGURES

PAGE

INTRODUCTION

PART I

PART II

PART III

PART IV

APPENDIX

LIST of TABLES

PAGES

PART I

PART II

PART III

PART IV

PART V

LIST OF ABBREVIATIONS

4-AABP	4-acetylaminobiphenyl
2-AAF	2-acetylaminofluorene
4-ABP	4-aminobiphenyl
AcCoA	acetyl coenzyme A
2-AF	2-aminofluorene
ANL	aniline
CYP	cytochrome P450
Da	Dalton
DEAE	diethylaminoethyl
DHFR	dihydrofolate reductase
DMAB	4-(dimethylamino)benzaldehyde
DMEM	Dulbecco modified Eagle medium
DMSO	dimethylsulfoxide
DNA	deoxyribonucleic acid
DNase	deoxyribonuclease
DTT	dithiothreitol
2,3-DMA	2,3-dimethylaniline
2,4-DMA	2,4-dimethylaniline
2,5-DMA	2,5-dimethylaniline
2,6-DMA	2,6-dimethylaniline
3,4-DMA	3,4-dimethylaniline
3,5-DMA	3,5-dimethylaniline
2-EA	2-ethylaniline
3-EA	3-ethylaniline

4-EA	4-ethylaniline
E. Coli	*Escherichia coli*
EDTA	ethylenediaminetetraacetic acid
ESI	electrospray ionization
FBS	fetal bovine serum
g	gram/gravitational force
GAPDH	glyceraldehyde 3-phosphate dehydrogenase
GR	glutathione reductase
GSH	glutathione
GSSG	oxidized glutathione
IPTG	isopropyl-D-thiogalactopyranoside
kDa	kilodalton
2-MA	2-methylaniline
4-MA	4-methylaniline
MALDI-TOF	matrix-assisted laser desorption/ionization time-of-flight
MOPS	3-(*N*-morpholino)propanesulfonic acid
MTX	methotrexate
m/z	mass over charge ratio
NAC	N-acetyl-L-cysteine
NAT	arylamine N-acetyltransferase
NO-B	nitrosobenzene
4-NO-BP	4-nitrosobiphenyl
2-NO-F	2-nitrosofluorene
N-OH-4-AABP,	N-hydroxy-4-acetylaminobiphenyl
N-OH-AAF	N-hydroxy-2-acetylaminofluorene

2-NO-T	2-nitrosotoluene
O.D.	Optical density
PABA	*p*-aminobenzoic acid
PAGE	polyacrylamide gel electrophoresis
PAS	*p*-aminosalicylic acid
PBS	phosphate-buffered saline
PE buffer	potassium phosphate buffer
PMSF	phenylmethanesulfonyl fluoride
PNP	*p*-nitrophenol
PNPA	*p*-nitrophenyl acetate
Q-TOF	quadrupole time-of-flight
SD	standard deviation
SMZ	sulfamethazine
SNPs	single nucleotide polymorphisms
TB	Terrific Broth
TBS	tris-buffered saline
TCA	trichloroacetic acid
TEV	tobacco etch virus
TFA	Trifluoroacetic acid
TMP	trimethoprim

INTRODUCTION

Arylamines and Heterocyclic Amines

Arylamines and heterocyclic arylamines are among the best documented human carcinogens and must be considered major candidates for contributing to human cancer because of the broad exposure to these compounds and the variability in activities of metabolic enzymes (*1-4*). In 1895, the occurrence of urinary bladder tumors among workers in aniline dye industry was first reported by Rehn, a German physician (*5*). Since that time, numerous experimental and epidemiological studies have demonstrated that occupational exposure to arylamines such as 4-aminobiphenyl (4-ABP), benzidine, and 1,2-naphthylamine can lead to bladder cancer in humans (Figure 1) (*5*). To date, it has been demonstrated that these carcinogens are a risk factor for a variety of human cancers, such as bladder cancer, lymphatic cancer, colorectal cancer, liver cancer, and breast cancer (*6-9*).

Although the amounts of arylamines produced in dye and rubber industries, and agricultural activities have been greatly reduced in recent years because of strict regulation, humans are still extensively exposed to arylamines and heterocyclic arylamines from cigarette smoking, therapeutic agents, permanent hair dyes, and dietary contaminants (*10-13*). Cigarette smoking causes 48% of the bladder cancer deaths in men and 28% of the bladder cancer deaths in women (*14*). Arylamines, such as 4-ABP and 2-naphthylamine, found in tobacco smoke are believed to contribute to bladder cancer development in smokers (*15, 16*). Recently, arylamines coming from non-smoking-related sources are drawing scientists' attention (*6, 8, 11, 15, 17*). 4-

ABP has been identified in commercial hair dyes, and the amount of 4-ABP can be as high as 1130 ng per application. In comparison, the amount of 4-ABP in mainstream smoke is less than 3.6 ng per cigarette (*11*). 2-Methylaniline (o-toluidine) is a primary metabolite of prilocaine, a widely used local anesthetic, and is responsible for hemoglobin adduct formation after prilocaine treatment (Figure 1) (*12*). Certain therapeutic agents, such as sulfamethazine (SMZ), procainamide, and dapsone are also arylamines (Figure 1) (*1*). Heterocyclic amines, such as 2-amino-3-methylimidazo[4,5-f]quinoline (IQ), 2-amino-1-methyl-6-phenylimidazo [4,5-b]pyridine (PhIP), and 2-amio-6-methyldipyrido[1,2-a:3',2'-d]imidazole (Glu-P-1), are generated during cooking, when amino acids (proteins) and reducing sugars (carbohydrates) are cooked together at high temperature (Figure 2) (*2, 18*). Arylamine compounds coming from unidentified environmental sources may be human carcinogens as well (*6*). For example, 2,6-dimethylaniline (2,6-DMA), 3,5-dimethylaniline (3,5-DMA), and 3-ethylaniline (3-EA) have been identified as risk factors for non-smoking-related bladder cancer (Figure 1) (*6, 19*).

Metabolism of arylamines involves several competing and interacting pathways that result in detoxification or bioactivation. One major reaction is the transformation of arylamines to arylamides by AcCoA: arylamine N-acetyltransferases (NATs. E. C. 2.3.1.5), which is usually considered to be a detoxification step (Figure 3, pathway A); the other major reaction is the N-hydroxylation of arylamines to arylhydroxylamines by cytochrome P450, leading to bioactivation (Figure 3, pathway C) (*1, 20*). The arylamides can be further

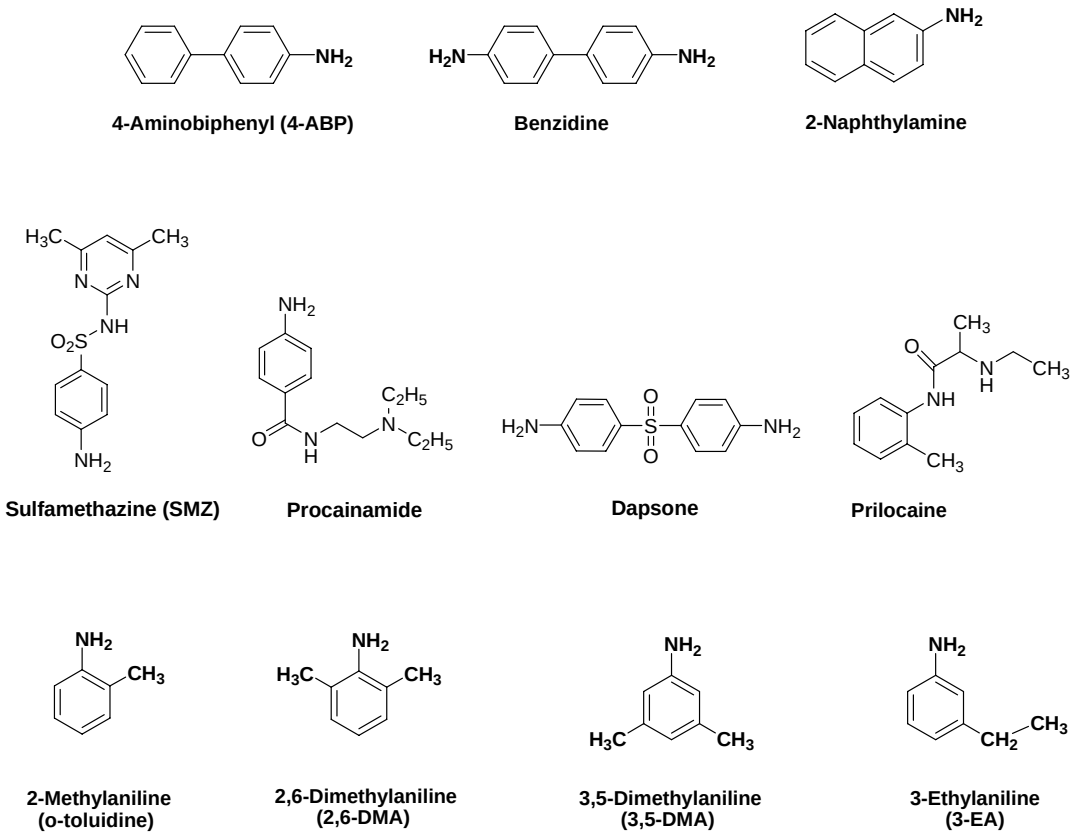

Figure 1. Examples of environmental and therapeutic arylamines.

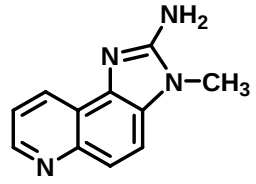

2-Amino-3-methylimidazo[4,5-f]quinoline (IQ)

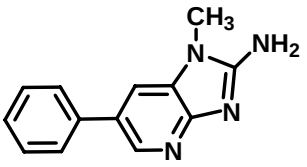

2-Amino-1-methyl-6-phenylimidazo[4,5-b]pyridine (PhIP)

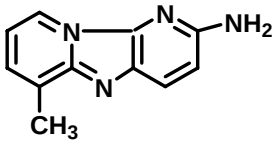

2-Amino-6-methyldipyrido[1,2-a:3',2'-d]imidazole (Glu-P-1)

Figure 2. Examples of carcinogenic heterocyclic amines.

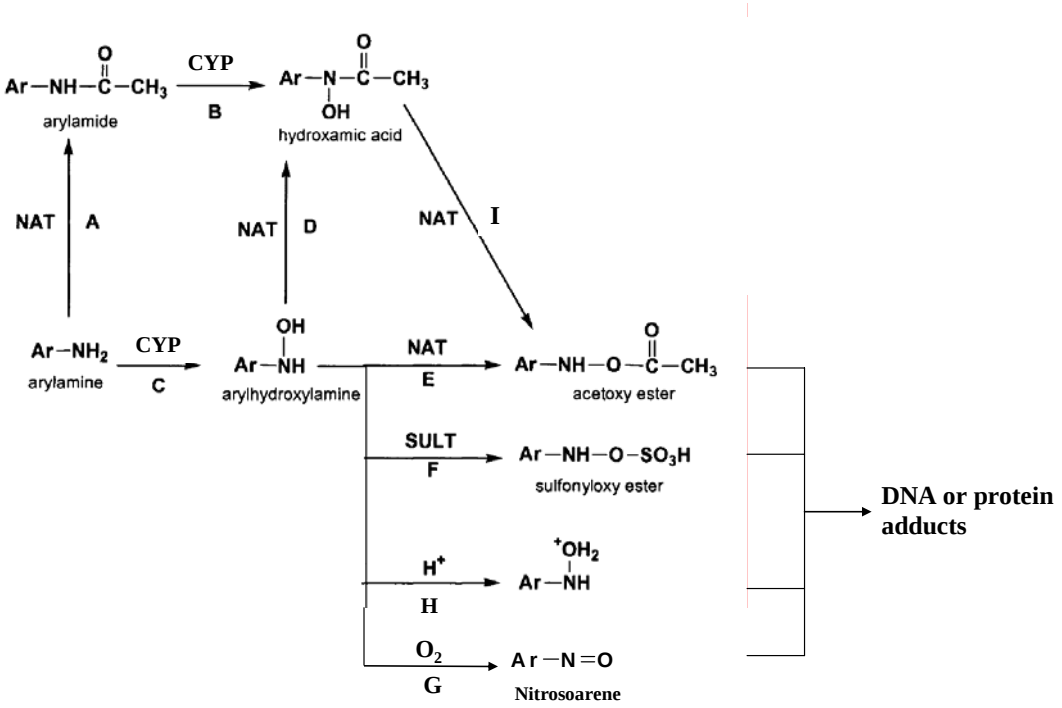

Figure 3. Arylamine detoxification and bioactivation pathways. Enzyme abbreviations are: CYP, cytochrome P450; NAT, Arylamine N-Acetyltransferase ; SULT, sulfotransferase.

metabolized to form carcinogenic N-arylhydroxamic acids via cytochrome P450 (Figure 3, pathway B) (*21, 22*). Protonation of N-arylhydroxylamines can make the compounds reactive (Figure 3, pathway H). But, in vivo, it is more likely that the N-arylhydroxylamines will undergo NAT-mediated O-esterification and sulfotransferase (SULT)-mediated O-sulfation to form N-acetoxy (Figure 3, pathway E) and N-sulfonyloxy esters (Figure 3, pathway F), which are electrophilic metabolites and are involved in mutagenesis and carcinogenesis by forming covalent adducts with DNA and proteins (*23*). A generally accepted mechanism for this reaction is an S_N1 reaction mechanism, in which a highly reactive nitrenium ion is formed through heterolytic cleavage of the N-O bond before reaction with nucleophilic functional groups in macromolecules (*20*). N-arylhydroxylamines might undergo NAT-mediated N-acetylation to produce N-arylhydroxamic acids (Figure 3, pathway D). Further oxidation of N-arylhydroxylamines can produce electrophilic nitrosoarenes, which may cause DNA and protein damage (Figure 3, pathway G) (*24*).

Nitrosoarenes and N-arylhydroxamic acids are two critical classes of arylamine reactive metabolites. The oxidation of arylamines is not the only source of nitrosoarenes. The metabolic reduction of environmental and therapeutic nitroarenes can also produce nitrosoarenes (*25, 26*). The eletrophilicity of the nitroso compounds makes it possible for them to react with nucleophilic thiol groups in proteins and glutathione (GSH) (*27-29*). N-Arylhydroxamic acids, such as N-OH-AAF, are strong carcinogens and are found to be irreversible metabolic inhibitors of hamster NATs

(*30-32*). The susceptibility of human NATs to inactivation by nitrosoarenes and N-arylhydroxylamines is investigated in this thesis (see Parts III and Part IV).

The bioactivation pathways of heterocyclic amines are similar to those for arylamines, involving an initial cytochrome P450 catalyzed N-hydroxylation followed by NAT-mediated O-acetylation to yield the eletrophilic N-acetoxy esters (*1*). NATs cannot catalyze N-acetylation of many heterocyclic amines, such as IQ and PhIP (Figure 2). Thus, NATs play a role in metabolic activation of heterocyclic amines instead of detoxification of the compounds (*1*).

The formation of arylamine-DNA adducts in vivo and in vitro has been well documented (*23, 33-35*). The principal adducts contain a covalent bond between the C8 atom of a guanine residue and the primary amino group of the arylamine or arylamide (*23, 33*). When 2-aminofluorene (2-AF) was used as a model compound, the major DNA covalent adducts formed with the bioactivated arylamine included N-(deoxyguanosin-8-yl)-2-acetylaminofluorene (dG-C8-AAF), and N-(deoxyguanosin-8-yl)-2-aminofluorene (dG-C8-AF) (Figure 4) (*34*). The C^8-dG-adduct is not expected because the C^8-position is not a strongly nucleophilic site in purines. The mechanism involving an initial adduct formation at the N^7 position followed by a rearrangement to produce a more stable C^8-dG-adduct was proposed and supported by experimental evidence (Figure 5) (*33, 35*).

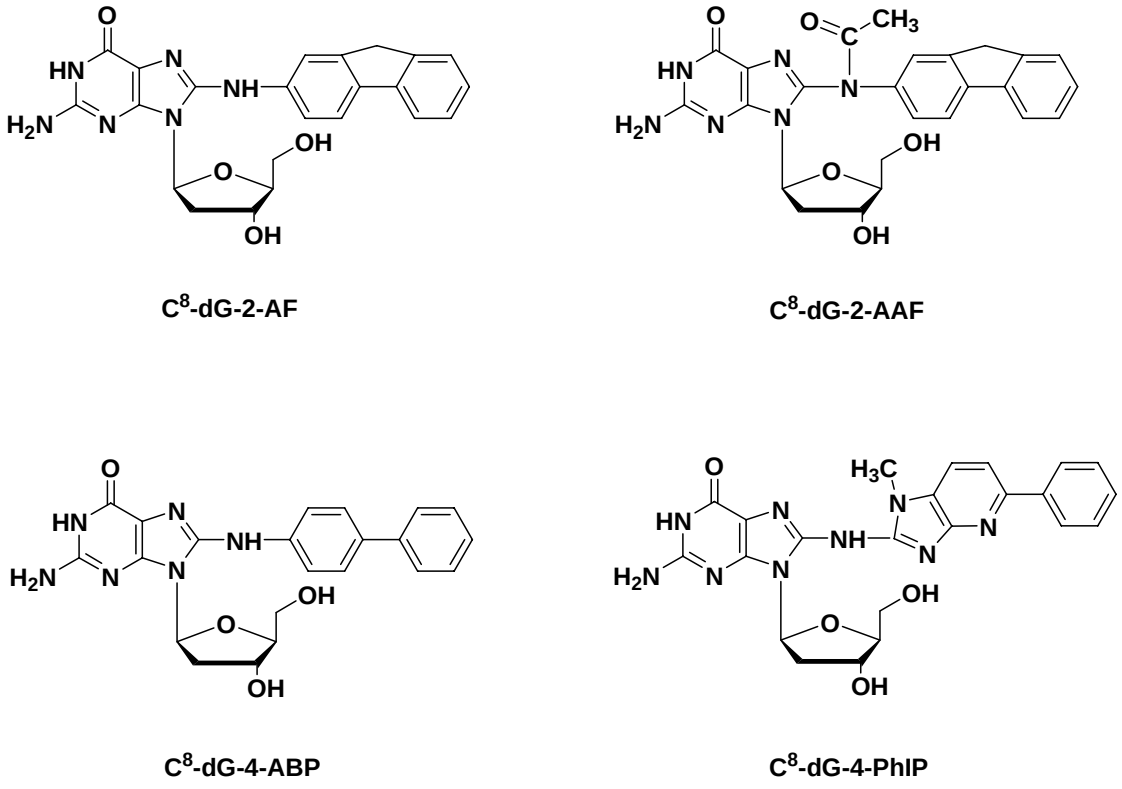

Figure 4. Examples of arylamine- and heterocyclic amine-deoxyguanosine adducts.

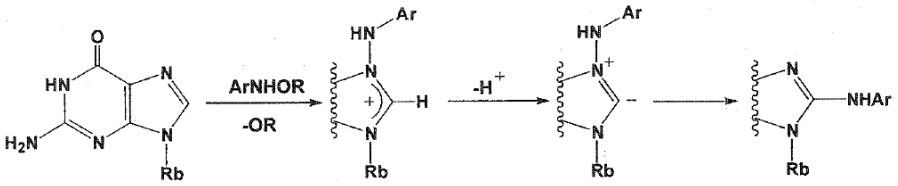

Figure 5. Proposed mechanism for the formation of C8-guanyl arylamine adducts. (Reproduced from reference 33)

Recently, more DNA adducts of arylamines were identified and their relationships to mutation and gene expression were investigated (*19, 36*). DNA adduct formation by three environmental arylamines, 2,6-DMA, 3,5-DMA, and 3-EA, in mouse bladder was identified and suggested to play a role in bladder cancer induction (*19*). The formation of (N-deoxyguanosin-8-yl)-4-aminobiphenyl (dG-C8-ABP) in human lymphoblastoid TK6 cells treated with N-OH-4-AABP was detected and quantified (Figure 4) (*36*). It was concluded that many genes related to mutagenicity and toxicity showed significant dose responses to dG-C8-ABP adduct formation (*36*).

In summary, arylamines and heterocyclic amines are considered to be procarcinogens and require metabolic activation to be carcinogenic (*1, 20*). Arylamines are subject to several competing metabolic pathways, and NATs and cytochrome P450 are major metabolism enzymes involved in detoxification and bioactivation of these xenobiotics.

Arylamine N-Acetyltransferases

Arylamine N-Acetyltransferases (NATs, EC 2.3.1.5) are important phase II drug metabolism enzymes which play a critical role in the detoxification and bioactivation of arylamines, hydrazines, and hydrazides (*1, 20*). NATs catalyze the transfer of an acetyl group from AcCoA to the nitrogen or oxygen atom of arylamine substrates and their N-hydroxylated metabolites (*20*). As shown in figure 6a, NATs can convert arylamines to arylamides, which is usually considered a detoxification process. This reaction competes with the N-hydroxylation of arylamines. However, the AcCoA-dependent O-acetylation of N-hydroxylamines and the AcCoA-independent intramolecular N, O-transacetylation of N-arylhydroxamic acids can produce electrophilic N-acetoxyarylamines, which can react with DNA and proteins (Figure 6b and 6c) (*20*). Thus, the later two processes are considered as toxification processes. Because of the apparent importance of NATs' dual functions, it is not surprising that the study of NATs has been a topic of interest for eighty years (*37*).

Humans express two polymorphic NAT isozymes, NAT1 and NAT2, both of which are 290 amino acids in length, with molecular masses of about 33.5 kDa. Although the two isozymes share 81% sequence identity, they exhibit differences in substrate specificity profiles (*38*). NAT1 specific substrates include *p*-aminobenzoic acid (PABA), an ingredient in sun screens, and *p*-aminobenzoylglutamic acid (pABglu), a folic acid metabolite and likely endogenous substrate (Figure 7) (*39, 40*). NAT2 substrates include SMZ, a medicine used to treat a variety of infections, and

isoniazid, an antituberculosis drug (*39, 41*). One critical task of biochemical studies of NATs is to further elucidate substrate specificities. In this thesis, the second order rate constants (k_{cat}/K_m) for N-acetylation of arylamine therapeutic agents and environmental contaminants, some of which are associated with bladder cancer risk, were determined with homogeneous recombinant NAT1 and NAT2 (see Part II).

Detailed enzyme kinetic and protein chemistry studies require large quantities of purified enzymes. Previously, due to the lack of homogenous enzyme, bioactivation and substrate specificity studies were conducted with partially purified tissue preparations, or with bacterial or mammalian cell cytosols in which NAT was overexpressed (*31, 39, 40, 42*). In the past fifteen years, this laboratory has made substantial progress in the purification of recombinant mammalian NAT proteins (*43, 44*). Hamster NAT1 and NAT2 were overexpressed and purified as a DHFR fusion protein from bacterial cell cultures by double DEAE anion-exchange column chromatography (*43-45*). Human NAT1 was successfully purified from a modified expression system, in which the human NAT1 gene replaced the hamster gene, and a similar purification protocol was applied (*45*). In this thesis, we developed a method to produce homogeneous human NAT2, for which the overexpression level in bacteria is only 10% of that of human NAT1, in milligram quantities (see Part I).

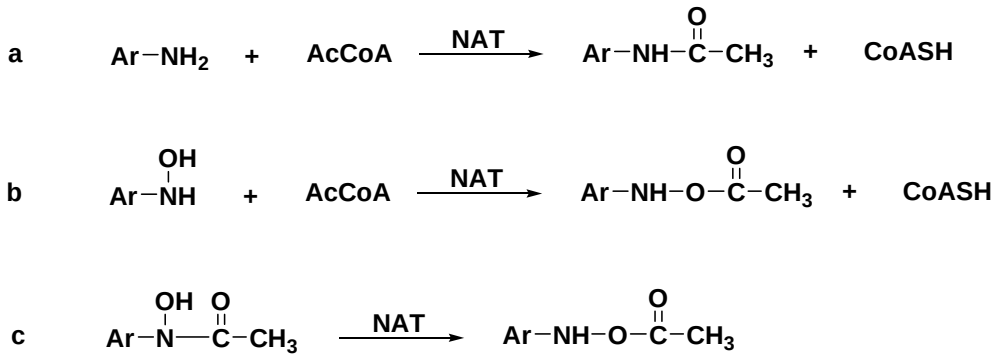

Figure 6. Reactions catalyzed by NATs.

Substrates for human NAT1

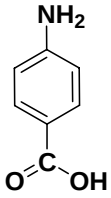

p-Aminobenzoic acid (PABA)

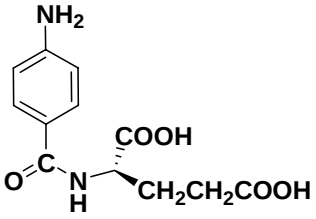

p-Aminobenzoylglutamic acid (pABglu)

Substrates for human NAT2

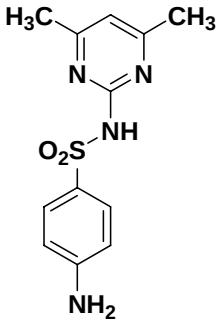

Sulfamethazine (SMZ)

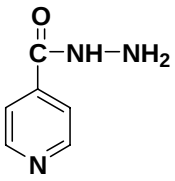

Isoniazid

Figure 7. Examples of NAT1 and NAT2 specific substrates.

Structural studies of NATs provided insight into catalytic mechanisms and structural determinants of substrate specificities. *Salmonella typhimurium* NAT (*St*NAT) was the first member in the NAT family whose X-ray crystal structure was resolved (*46*). The overall fold of *St*NAT consists of three domains which are about equal in length. The N-terminal domain comprises residues 1-85 and consists of five α-helices, the second domain (residues 86-175) contains eight β-strands, and the third domain contains four β-strands and two α-helices. The major breakthrough was that the 3D structure of *St*NAT revealed a cysteine protease-like catalytic triad containing Cys69, His107, and Asp122 (Figure 8a) (*46*). However, the active site of *St*NAT is sequestered in a deep and hydrophobic cleft by the C-terminal domain, which is different from the long and shallow active site of cysteine proteases. X-Ray crystal structures of other bacterial NATs and human NATs, and an NMR-based structural model of hamster NAT2, also revealed catalytic triads (*46-51*). The overall fold of human NAT1 and NAT2 are very similar to that of *St*NAT; the catalytic triads of human NATs are shown in figure 8b and 8c (*48*). This catalytic triad is conserved in all known NATs (*46*).

Kinetically, NAT-catalyzed reactions proceed through a ping-pong bi bi mechanism, in which the acetyl group is transferred from AcCoA to the active site Cys68 to form the acetylated enzyme intermediates, releasing CoA, followed by the transfer of the acetyl group to the arylamine substrates, forming arylamides (*52, 53*) (Figure 9).

a

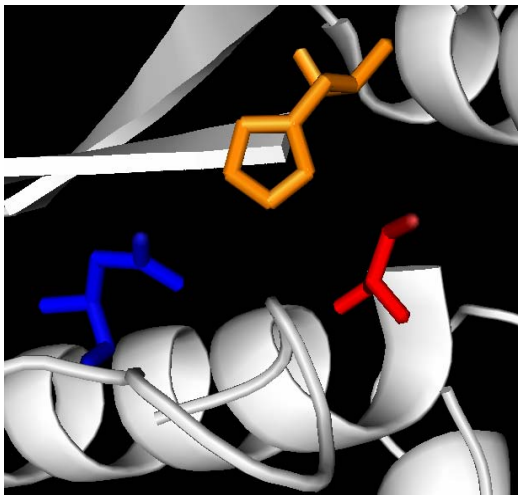

b

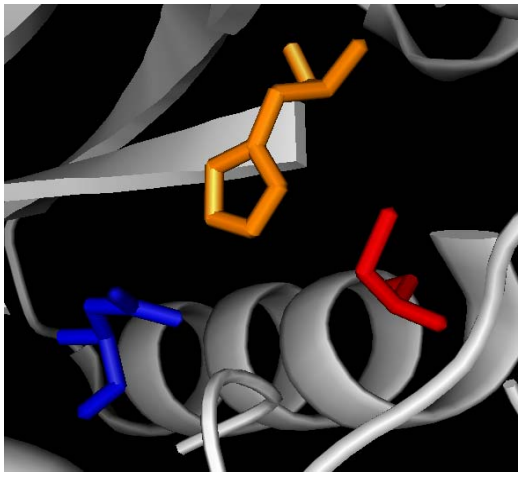

c

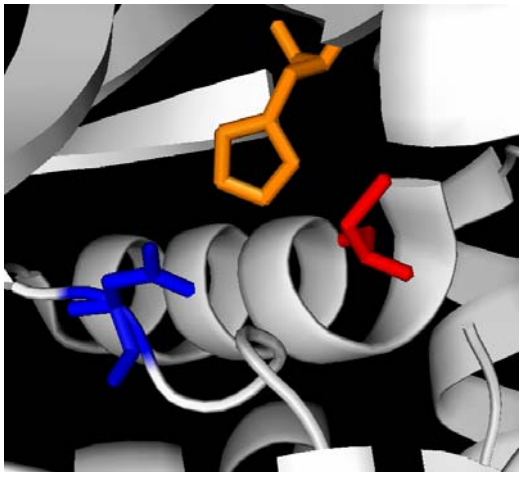

Figure 8. Catalytic triad of (a) *St*NAT (PDB ID: 1e2t), (b) human NAT1 (PDB ID: 2IJA), (c) human NAT2 (PDB ID: 2PFR) (Created with PyMOL). Cys68 (human) or Cys69 (bacterial), His107, and Asp122 are displayed in red, orange, and blue, respectively.

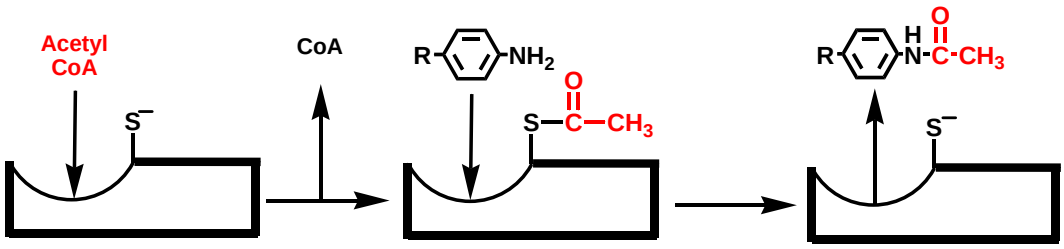

Figure 9. Ping-pong bi bi mechanism.

Recently, our laboratory investigated the catalytic mechanism of hamster NAT2 and demonstrated that the active site Cys68 is highly nucleophilic with a pKa of 5.2 (*54*). The exceptional reactivity of the active site Cys68 is the result of the formation of a thiolate-imidazolium ion pair, which is buried in a hydrophobic cleft. His107, the second member of the catalytic triad, showed a pKa greater than 9.5 (*55*). It is different from typical cysteine proteases, in which the histidine has a pKa of 8 to 9 (*56*). The third member of the thiolate-imidazolium ion pair, Asp122, was found to be both structurally and catalytically essential (*51, 54*). The high nucleophilicity of Cys68 causes NATs to react readily with electrophiles, such as 4-nitrosobiphenyl (4-NO-BP) to form sulfinamides, resulting in the inactivation of the enzyme (Figure 10) (*28*).

Genetically, human NATs are encoded adjacent to each other on chromosome 8p22 (*57*). There are over nine exons in the NAT1 gene and only two exons in the NAT2 gene. Both NATs contain only one coding exon (*58*). NAT1 and NAT2 mRNA has been identified in most human tissues (*59, 60*). It has been found that both NAT isoforms are expressed in hepatic and intestinal tissues, and NAT1 appears to be present in all human tissues (*61, 62*). The tissue distributions of NATs are important for their roles in the local detoxification or bioactivation of the arylamines and heterocyclic amines. In this research, the levels of NAT1 and NAT2 in several human cancer cell lines were determined by activity assays with NAT1 and NAT2 specific substrates and Western blotting with an NAT1-specific antibody. The results are presented in this thesis (see Parts III and IV). Recently, it was shown that the

expression of NAT1 may be a candidate prognostic marker in estrogen receptor (ER)-positive breast cancer (*63*). Thus, the methodology described in this thesis might have clinical implications.

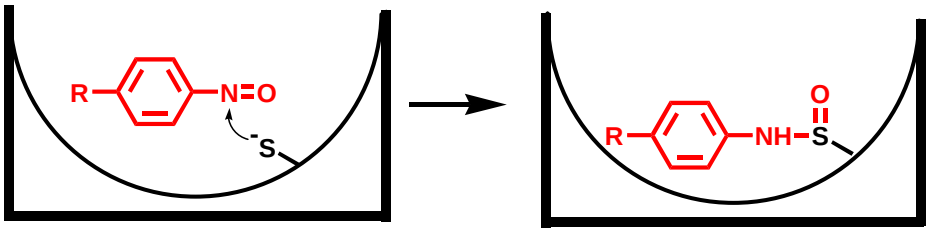

Figure 10. Inactivation of NATs by nitrosoarenes.

Genetic and Environmental Effects on the Activity of Arylamine N-Acetyltransferases

NATs are key cellular defense enzymes. The intracellular enzymatic activity of NAT depends on genetic polymorphisms and environmental factors. The attenuation of NAT activity by these factors might increase the amount of arylamine that is N-hydroxylated by increasing the amount that is available for oxidation, which is the primary step for toxification of the arylamines, resulting in enhanced cell toxicity and carcinogenesis (*1*, *2*, *4*).

It was over fifty years ago that NAT2 polymorphism was first discovered following the observations of differences in the vulnerability of tuberculosis (TB) patients to isoniazid toxicity. The importance of NAT2 polymorphism broadened when it was discovered that many environmental arylamines and hydrazine drugs are subject to N-acetylation (*64*). Slow acetylator status was predicted to cause an increase of urinary bladder cancer risk due to decreased detoxification of arylamines (*65*). To date, 26 NAT1 alleles and 36 NAT2 alleles possessing single nucleotide polymorphisms (SNPs) have been identified in the human population (http://louisville.edu/medschool/pharmacology/NAT. html). Studies have suggested that the genetic attenuation of NAT activities in humans is related to many diseases, such as non-Hodgkin lymphoma (*66*), breast cancer (*67*), bladder cancer (*68*), pancreatic cancer (*69*), and lung cancer (*70*).

Some of the NAT variants, such as NAT1 14 (R187Q), NAT1 15 (R187stop), NAT1 17 (R64W), and NAT1 22 (D25V), exhibit reduced cellular abundance and undergo constitutive ubiquitination (*71*). Recently, it was demonstrated that protein aggregation is one mechanism that causes NAT1 17 to be constitutively ubiquitylated and degraded in an ER-dependent manner as a quantity control process (*72*). Steady state kinetic analysis showed that the replacement of arginine (R64) with tryptophan in hamster NAT2 protein (the hamster counterpart of human NAT1) does not affect the catalytic activity of NAT or the stability of the acetylated enzyme. The results from NMR and circular dichroism spectroscopy revealed that the R64W mutation does not perturb the overall NAT protein structure, although the mutation caused protein aggregation in vitro and in human cells (Figure 11) (*72*). The recently resolved high resolution crystal structures of human NAT1 and NAT2 made it possible to rationalize the structure-function relationships of NAT variants (Figure 12) (*48*, *73*, *74*). R64 is partially surface exposed in domain I and forms critical hydrogen bonds with E38 and N41 (Figure 12b and 13) (*73*). The replacement of arginine with tryptophan will lead to the loss of those key hydrogen bonding interactions and result in a reduction in protein thermostability, which may trigger protein aggregation and degradation (*73*). This evidence supported the quality control mechanism.

In addition to genetic factors, recent evidence showed that non-genetic factors, such as exogenous and endogenous chemical agents, may affect NAT activities. These non-heritable factors could be useful to explain the inconsistency in some

a b

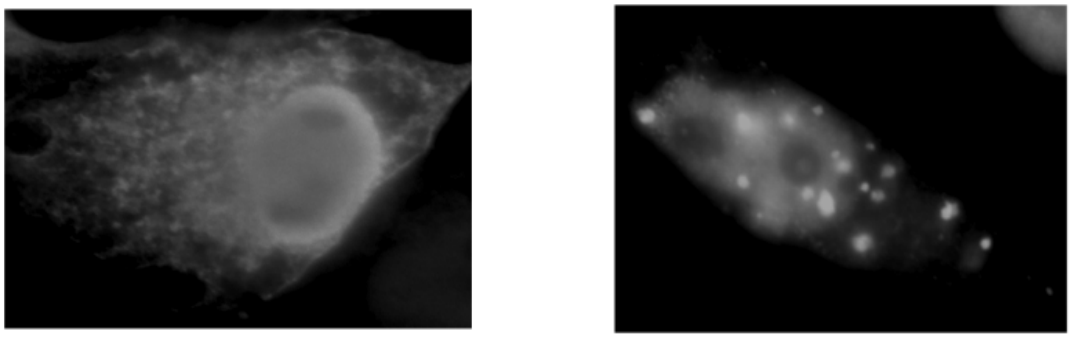

Figure 11. The NAT1 17 (R64W) causes it to form cytoplasmic microaggregates. Immunofluorescence microscopy was performed on HeLa cells transfected with either 3FLAG-tagged NAT1 (a) wild-type, or (b) R64W variant. NAT1 protein was visualized by using anti-FLAG antibody (From reference 71).

a

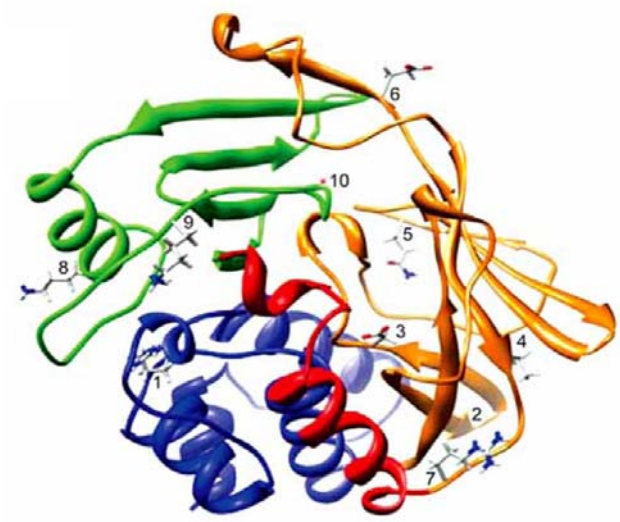

b

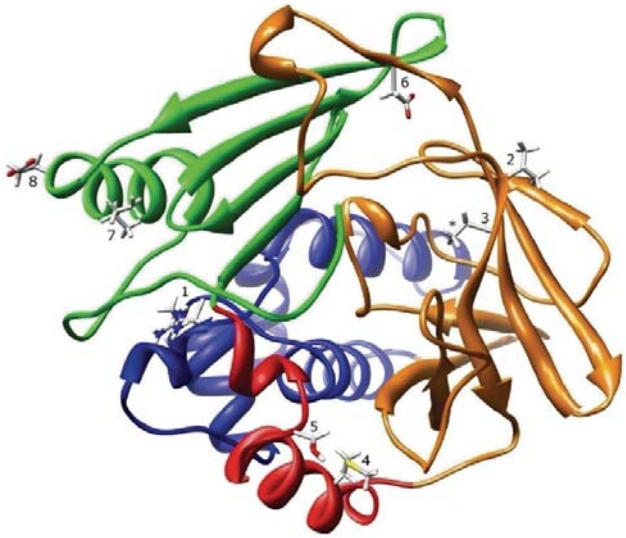

Figure 12. Human NAT1 and NAT2 crystal structure ribbon diagram. The ribbon is colored to indicate NAT protein domain I (blue), the interdomain region (red), domain II (orange), and domain III (green). (a) NAT1 structure. The location of residues R64 (1), I114 (2), D122 (3), L137 (4), Q145 (5), E167 (6), R197 (7), K268 (8), K282 (9), and G286 (10) are shown. (b) NAT2 structure. The location of residues R64 (1), V149 (2), R187 (3), M205 (4), S214 (5), D251 (6), E261 (7), I263 (8) are shown. (From reference 72 and 73).

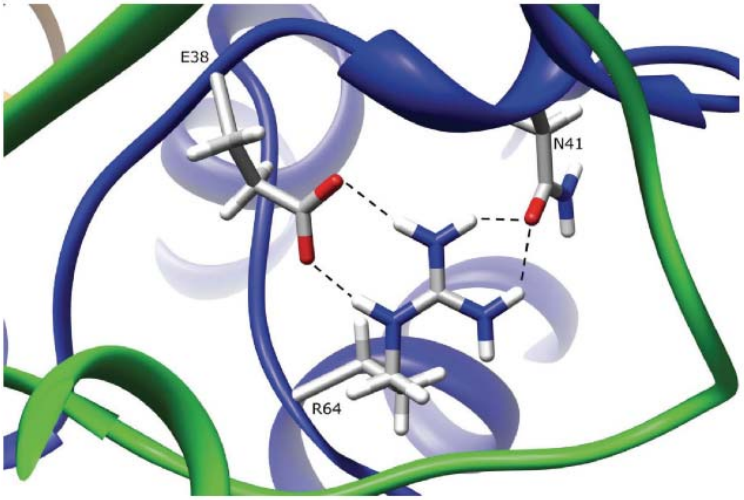

Figure 13. The NAT1 R64 side-chain makes multiple hydrogen bonds to E38 and N41 (From reference 72).

reported relationships between NAT genotypes and phenotypes in certain individuals. These environmental factors affect NAT activity through various mechanisms and have the potential to modulate cancer risk in individuals (*75-80*).

Substrate-dependent regulation of NAT1 was found when human peripheral blood mononuclear cells (PBMC) were treated with PABA (*75*). PABA decreased intracellular NAT1 activity by decreasing NAT1 protein content without changing mRNA level. Proteasome-dependent degradation was believed to be the mechanism (*75*). Androgen-dependent induction of NAT1 was found in androgen receptor-positive prostate cancer cells (*80*). Methyltrienolone (R1881, Figure 14) induced NAT1 activity by increasing NAT1 mRNA level, resulting in up-regulation of the enzyme expression (*80*). The induction of NAT1 by androgen could increase detoxification of arylamines and also might affect the bioactivation of arylamines and heterocyclic amines, leading to increased cancer risk in individuals (*80*).

Oxidation-dependent inactivation of NAT1 has been shown in several studies and NAT may be a target of biological oxidants (*77, 78, 81*). Physiological concentrations of peroxynitrite (Figure 14) irreversibly inactivated NAT1 in MCF7 breast cancer cells and human lens epithelial cells (HLE) by conversion of the active site Cys68 thiol group to a sulfinic or sulfonic form (*77, 78*). NAT1 was inactivated rapidly by peroxynitrite with a second order inactivation rate constant (k_{inact}) of 5 x 10^4 $M^{-1}s^{-1}$ (*77*). Hydrogen peroxide (H_2O_2) and UVB irradiation impaired NAT1 activities in HLE by oxidation the Cys68 thiol group to a sulfenic acid (*78, 81*). The

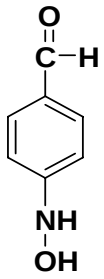

N-OH-PABA

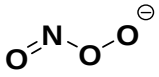

Peroxynitrite

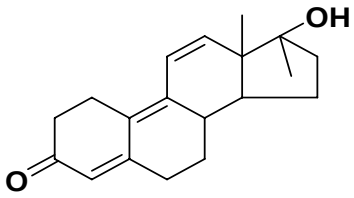

Methyltrienolone (R1881)

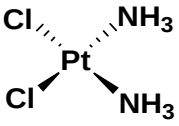

Cisplatin

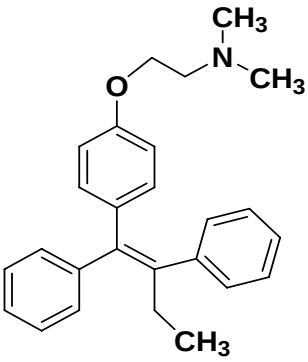

Tamoxifen

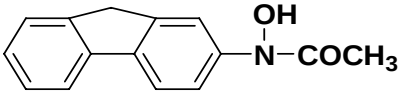

N-OH-AAF

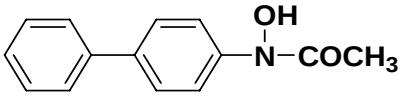

N-OH-4-AABP

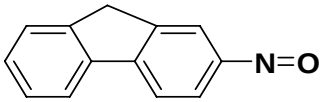

2-NO-F

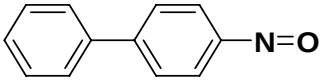

4-NO-BP

Figure 14. Examples of chemicals that inhibit NAT activity.

k_{inact} for inactivation of NAT1 by H_2O_2 was 420 $M^{-1}min^{-1}$ (*81*).

Covalent modification of the NAT active site cysteine by chemical agents is another mechanism that contributes to the inactivation of NAT (*76, 79*). N-OH-PABA (Figure 14) irreversibly inactivated endogenous NAT1 in PBMC in a time- and concentration-dependent manner, but did not change NAT1 protein content (*76*). Preincubation of cell cytosol with AcCoA protected NAT1 against inactivation by N-OH-PABA indicating that the inactivation involved a reaction with the active site Cys68 (*76*). Therapeutically relevant concentrations of cis-diaminedicholoroplatinum II (cisplatin) (Figure 14), an important anticancer drug used in chemotherapy, irreversibly reduced NAT1 activity in human breast cancer cells and mouse NAT2 (the mouse counterpart of human NAT1) activity in the tissues of mice treated with cisplatin (*79*). Cisplatin reacted with active site Cys68 directly with a k_{inact} of 700 $M^{-1}min^{-1}$ (*79*). It was suggested that the inhibition of NAT1 enzymatic functions by cisplain could contribute to the toxicological effects of the drug (*79*). Tamoxifen (Figure 14), the most widely prescribed selective estrogen receptor (ER) modulator for ER positive breast cancer treatment, has been shown to inhibit NAT1 activity in cytosols from breast cancer tissues and inhibit recombinant mouse NAT2 activity with an IC_{50} of 57 ± 3 μM (*82, 83*).

For more than 25 years this laboratory has investigated arylamine metabolites that may impair NAT activities (*31, 32, 84, 85*). In 1979, it was found that carcinogenic N-arylhydroxamic acids, such as N-hydroxy-2-acetylaminofluorene (N-

OH-AAF) and N-hydroxy-4-acetylaminobiphenyl (N-OH-4-AABP), irreversibly inactivated certain NAT activities when the compounds were incubated with partially purified hamster hepatic preparations (*31*). In in vivo experiments, N-OH-AAF was found to selectively inactivate hamster hepatic NAT1 (*84*). Recently, the successful purification of recombinant NAT enzymes and the use of modern mass spectrometry techniques made it possible to elucidate the molecular mechanism of inactivation of NATs by N-arylhydroxamic acids (*28, 32*). It was demonstrated that the major adduct formed between hamster NAT1 and N-OH-AAF was a sulfinamide, which was produced between the active site Cys68 and 2-nitrosofluorene (2-NO-F) generated during the bioactivation process (Figure 10) (*32*). Study of the inactivation of hamster NATs and human NAT1 by N-OH-4-AABP confirmed the overall mechanism of this reaction (*28*). It was also found that nitrosoarenes, such as 2-NO-F and 4-NO-BP irreversibly inactivate hamster NATs by reacting with the highly reactive active site Cys68 to form sulfinamides (*28, 32*). The effects of N-arylhydroxamic acids and nitrosoarenes on human NATs in vitro and in human cells were studied and the results are presented in this thesis (see Parts III and IV).

References

(1) Hanna, P. E. (1996) Metabolic activation and detoxification of arylamines. *Curr. Med. Chem. 3*, 195-210.

(2) Kim, D. and Guengerich, F. P. (2005) Cytochrome P450 activation of arylamines and heterocyclic amines. *Annu Rev Pharmacol Toxicol 45*, 27-49.

(3) Hein, D. W. (2002) Molecular genetics and function of NAT1 and NAT2: role in aromatic amine metabolism and carcinogenesis. *Mutat Res 506-507*, 65-77.

(4) Rodrigues-Lima, F., Dairou, J. and Dupret, J. M. (2008) Effect of environmental substances on the activity of arylamine N-acetyltransferases. *Curr Drug Metab 9*, 505-509.

(5) Parkes, H. G., Evans, A. E. J. (1984) Epidemiology of aromatic amine cancers. In: Searle C. E. (ed) Chemical carcinogens, vol 1, American Chemical Society, Washington DC, pp 277-301.

(6) Gan, J., Skipper, P. L., Gago-Dominguez, M., Arakawa, K., Ross, R. K., Yu, M. C. and Tannenbaum, S. R. (2004) Alkylaniline-hemoglobin adducts and risk of non-smoking-related bladder cancer. *J Natl Cancer Inst 96*, 1425-1431.

(7) Gorlewska-Roberts, K., Green, B., Fares, M., Ambrosone, C. B. and Kadlubar, F. F. (2002) Carcinogen-DNA adducts in human breast epithelial cells. *Environ Mol Mutagen 39*, 184-192.

(8) Gago-Dominguez, M., Bell, D. A., Watson, M. A., Yuan, J. M., Castelao, J. E., Hein, D. W., Chan, K. K., Coetzee, G. A., Ross, R. K. and Yu, M. C. (2003) Permanent hair dyes and bladder cancer: risk modification by cytochrome P4501A2 and N-acetyltransferases 1 and 2. *Carcinogenesis 24*, 483-489.

(9) Hazardous substances databand (HSDB) (2008) http:// toxnet.nlm.nih.gov.

(10) Yu, M. C., Skipper, P. L., Tannenbaum, S. R., Chan, K. K. and Ross, R. K. (2002) Arylamine exposures and bladder cancer risk. *Mutat Res 506-507*, 21-28.

(11) Turesky, R. J., Freeman, J. P., Holland, R. D., Nestorick, D. M., Miller, D. W., Ratnasinghe, D. L. and Kadlubar, F. F. (2003) Identification of aminobiphenyl derivatives in commercial hair dyes. *Chem Res Toxicol 16*, 1162-1173.

(12) Gaber, K., Harreus, U. A., Matthias, C., Kleinsasser, N. H. and Richter, E. (2007) Hemoglobin adducts of the human bladder carcinogen o-toluidine after treatment with the local anesthetic prilocaine. *Toxicology 229*, 157-164.

(13) Felton, J. S., Knize, M. G., Roper, M., Fultz, E., Shen, N. H. and Turteltaub, K. W. (1992) Chemical analysis, prevention, and low-level dosimetry of heterocyclic amines from cooked food. *Cancer Res 52*, 2103s-2107s.

(14) http://cancer.org.

(15) Jiang, X., Yuan, J. M., Skipper, P. L., Tannenbaum, S. R. and Yu, M. C. (2007) Environmental tobacco smoke and bladder cancer risk in never smokers of Los Angeles County. *Cancer Res 67*, 7540-7545.

(16) Vineis, P. and Pirastu, R. (1997) Aromatic amines and cancer. *Cancer Causes Control 8*, 346-355.

(17) Talaska, G. (2003) Aromatic amines and human urinary bladder cancer: exposure sources and epidemiology. *J Environ Sci Health C Environ Carcinog Ecotoxicol Rev 21*, 29-43.

(18) Messner, C. and Murkovic, M. (2004) Evaluation of a new model system for studying the formation of heterocyclic amines. *J Chromatogr B Analyt Technol Biomed Life Sci 802*, 19-26.

(19) Skipper, P. L., Trudel, L. J., Kensler, T. W., Groopman, J. D., Egner, P. A., Liberman, R. G., Wogan, G. N. and Tannenbaum, S. R. (2006) DNA adduct formation by 2,6-dimethyl-, 3,5-dimethyl-, and 3-ethylaniline in vivo in mice. *Chem Res Toxicol 19*, 1086-1090.

(20) Hanna, P. E. (1994) N-acetyltransferases, O-acetyltransferases, and N,O-acetyltransferases: enzymology and bioactivation. *Adv Pharmacol 27*, 401-430.

(21) Cramer, J. W., Miller, J. A. and Miller, E. C. (1960) N-Hydroxylation: A new metabolic reaction observed in the rat with the carcinogen 2-acetylaminofluorene. *J Biol Chem 235*, 885-888.

(22) Miller, J. A., Wyatt, C. S., Miller, E. C., and Hartmann, H. A. (1961) The N-hydroxylation of 4-acetylaminobiphenyl by the rat and dog and the strong carcinogenicity of N-hydroxy-4-acetylaminobiphenyl in the rat. *Cancer Res. 21*, 1465-1473.

(23) Beland, F. A., and Kadlubar, F. F. (1990) Metabolic activation and DNA adducts of aromatic amines and nitroaromatic hydrocarbons. *Handbook Exp. Pharmacol 94/I*, 267-325.

(24) Murata, M., Tamura, A., Tada, M. and Kawanishi, S. (2001) Mechanism of oxidative DNA damage induced by carcinogenic 4-aminobiphenyl. *Free Radic Biol Med 30*, 765-773.

(25) Zwirner-Baier, I. and Neumann, H. G. (1999) Polycyclic nitroarenes (nitro-PAHs) as biomarkers of exposure to diesel exhaust. *Mutat Res 441*, 135-144.

(26) Boelsterli, U. A., Ho, H. K., Zhou, S. and Leow, K. Y. (2006) Bioactivation and hepatotoxicity of nitroaromatic drugs. *Curr Drug Metab 7*, 715-727.

(27) Kazanis, S., and Mc Clelland, R. A. (1992) Electrophilic intermediate in the reaction of glutathione and nitrosoarenes. *J. Am. Chem. Soc. 114*, 3052-3059.

(28) Wang, H., Wagner, C. R. and Hanna, P. E. (2005) Irreversible inactivation of arylamine N-acetyltransferases in the presence of N-hydroxy-4-acetylaminobiphenyl: a comparison of human and hamster enzymes. *Chem Res Toxicol 18*, 183-197.

(29) Eyer, P. (1994) Reactions of oxidatively activated arylamines with thiols: reaction mechanisms and biologic implications. An overview. *Environ Health Perspect 102 Suppl 6*, 123-132.

(30) Miller, E. C., Miller, J. A. and Enomoto, M. (1964) The Comparative Carcinogenicities Of 2-Acetylaminofluorene And Its N-Hydroxy Metabolite In Mice, Hamsters, And Guinea Pigs. *Cancer Res 24*, 2018-2031.

(31) Banks, R. B. and Hanna, P. E. (1979) Arylhydroxamic acid N,O-acyltransferase. Apparent suicide inactivation by carcinogenic N-arylhydroxamic acids. *Biochem Biophys Res Commun 91*, 1423-1429.

(32) Guo, Z., Wagner, C. R. and Hanna, P. E. (2004) Mass spectrometric investigation of the mechanism of inactivation of hamster arylamine N-acetyltransferase 1 by N-hydroxy-2-acetylaminofluorene. *Chem Res Toxicol 17*, 275-286.

(33) Humphreys, W. G., Kadlubar, F. F. and Guengerich, F. P. (1992) Mechanism of C8 alkylation of guanine residues by activated arylamines: evidence for initial adduct formation at the N7 position. *Proc Natl Acad Sci U S A 89*, 8278-8282.

(34) Heflich, R. H. and Neft, R. E. (1994) Genetic toxicity of 2-acetylaminofluorene, 2-aminofluorene and some of their metabolites and model metabolites. *Mutat Res 318*, 73-114.

(35) Kennedy, S. A., Novak, M., Kolb, B.A. (1997) Reactions of ester derivatives of carcinogenic N-(4-biphenyl)hydroxylamine and the corresponding hydroxamic acid with purine nucleosides. *J. Am. Chem. Soc. 119*, 7654-7664.

(36) Ricicki, E. M., Luo, W., Fan, W., Zhao, L. P., Zarbl, H. and Vouros, P. (2006) Quantification of N-(deoxyguanosin-8-yl)-4-aminobiphenyl adducts in human lymphoblastoid TK6 cells dosed with N-hydroxy-4-acetylaminobiphenyl and their relationship to mutation, toxicity, and gene expression profiling. *Anal Chem 78*, 6422-6432.

(37) Agundez, J. A. (2008) N-acetyltransferases: lessons learned from eighty years of research. *Curr Drug Metab 9*, 463-464.

(38) Josephy, P. D., and Mannervik, B. (2006) *Molecular Toxicology 2nd edition*, pp 426-447, Oxford University Press, New York.

(39) Grant, D. M., Blum, M., Beer, M. and Meyer, U. A. (1991) Monomorphic and polymorphic human arylamine N-acetyltransferases: a comparison of liver isozymes and expressed products of two cloned genes. *Mol Pharmacol 39*, 184-191.

(40) Minchin, R. F. (1995) Acetylation of p-aminobenzoylglutamate, a folic acid catabolite, by recombinant human arylamine N-acetyltransferase and U937 cells. *Biochem J 307 (Pt 1)*, 1-3.

(41) Kawamura, A., Graham, J., Mushtaq, A., Tsiftsoglou, S. A., Vath, G. M., Hanna, P. E., Wagner, C. R. and Sim, E. (2005) Eukaryotic arylamine N-acetyltransferase. Investigation of substrate specificity by high-throughput screening. *Biochem Pharmacol 69*, 347-359.

(42) Hein, D. W., Doll, M. A., Rustan, T. D., Gray, K., Feng, Y., Ferguson, R. J. and Grant, D. M. (1993) Metabolic activation and deactivation of arylamine carcinogens by recombinant human NAT1 and polymorphic NAT2 acetyltransferases. *Carcinogenesis 14*, 1633-1638.

(43) Sticha, K. R., Sieg, C. A., Bergstrom, C. P., Hanna, P. E. and Wagner, C. R. (1997) Overexpression and large-scale purification of recombinant hamster polymorphic arylamine N-acetyltransferase as a dihydrofolate reductase fusion protein. *Protein Expr Purif 10*, 141-153.

(44) Sticha, K. R., Bergstrom, C. P., Wagner, C. R. and Hanna, P. E. (1998) Characterization of hamster recombinant monomorphic and polymorphic arylamine N-acetyltransferases: bioactivation and mechanism-based inactivation studies with N-hydroxy-2-acetylaminofluorene. *Biochem Pharmacol 56*, 47-59.

(45) Wang, H., Vath, G. M., Kawamura, A., Bates, C. A., Sim, E., Hanna, P. E. and Wagner, C. R. (2005) Over-expression, purification, and characterization of recombinant human arylamine N-acetyltransferase 1. *Protein J 24*, 65-77.

(46) Sinclair, J. C., Sandy, J., Delgoda, R., Sim, E. and Noble, M. E. (2000) Structure of arylamine N-acetyltransferase reveals a catalytic triad. *Nat Struct Biol 7*, 560-564.

(47) Holton, S. J., Dairou, J., Sandy, J., Rodrigues-Lima, F., Dupret, J. M., Noble, M. E. and Sim, E. (2005) Structure of Mesorhizobium loti arylamine N-acetyltransferase 1. *Acta Crystallogr Sect F Struct Biol Cryst Commun 61*, 14-16.

(48) Wu, H., Dombrovsky, L., Tempel, W., Martin, F., Loppnau, P., Goodfellow, G. H., Grant, D. M. and Plotnikov, A. N. (2007) Structural basis of substrate-binding specificity of human arylamine N-acetyltransferases. *J Biol Chem 282*, 30189-30197.

(49) Zhang, N., Liu, L., Liu, F., Wagner, C. R., Hanna, P. E. and Walters, K. J. (2006) NMR-based model reveals the structural determinants of mammalian arylamine N-acetyltransferase substrate specificity. *J Mol Biol 363*, 188-200.

(50) Rodrigues-Lima, F., Dairou, J., Diaz, C. L., Rubio, M. C., Sim, E., Spaink, H. P. and Dupret, J. M. (2006) Cloning, functional expression and characterization of Mesorhizobium loti arylamine N-acetyltransferases: rhizobial symbiosis supplies leguminous plants with the xenobiotic N-acetylation pathway. *Mol Microbiol 60*, 505-512.

(51) Sandy, J., Mushtaq, A., Holton, S. J., Schartau, P., Noble, M. E. and Sim, E. (2005) Investigation of the catalytic triad of arylamine N-acetyltransferases: essential residues required for acetyl transfer to arylamines. *Biochem J 390*, 115-123.

(52) Andres, H. H., Kolb, H. J., Schreiber, R. J. and Weiss, L. (1983) Characterization of the active site, substrate specificity and kinetic properties of acetyl-CoA:arylamine N-acetyltransferase from pigeon liver. *Biochim Biophys Acta 746*, 193-201.

(53) Westwood, I. M. and Sim, E. (2007) Kinetic characterisation of arylamine N-acetyltransferase from Pseudomonas aeruginosa. *BMC Biochem 8*, 3.

(54) Wang, H., Vath, G. M., Gleason, K. J., Hanna, P. E. and Wagner, C. R. (2004) Probing the mechanism of hamster arylamine N-acetyltransferase 2 acetylation by active site modification, site-directed mutagenesis, and pre-steady state and steady state kinetic studies. *Biochemistry 43*, 8234-8246.

(55) Wang, H., Liu, L., Hanna, P. E. and Wagner, C. R. (2005) Catalytic mechanism of hamster arylamine N-acetyltransferase 2. *Biochemistry 44*, 11295-11306.

(56) Storer, A. C. and Menard, R. (1994) Catalytic mechanism in papain family of cysteine peptidases. *Methods Enzymol 244*, 486-500.

(57) Hickman, D., Risch, A., Buckle, V., Spurr, N. K., Jeremiah, S. J., McCarthy, A. and Sim, E. (1994) Chromosomal localization of human genes for arylamine N-acetyltransferase. *Biochem J 297 (Pt 3)*, 441-445.

(58) Butcher, N. J., Tiang, J. and Minchin, R. F. (2008) Regulation of arylamine N-acetyltransferases. *Curr Drug Metab 9*, 498-504.

(59) Husain, A., Zhang, X., Doll, M. A., States, J. C., Barker, D. F. and Hein, D. W. (2007) Functional analysis of the human N-acetyltransferase 1 major promoter:

quantitation of tissue expression and identification of critical sequence elements. *Drug Metab Dispos 35*, 1649-1656.

(60) Husain, A., Zhang, X., Doll, M. A., States, J. C., Barker, D. F. and Hein, D. W. (2007) Identification of N-acetyltransferase 2 (NAT2) transcription start sites and quantitation of NAT2-specific mRNA in human tissues. *Drug Metab Dispos 35*, 721-727.

(61) Upton, A., Johnson, N., Sandy, J. and Sim, E. (2001) Arylamine N-acetyltransferases - of mice, men and microorganisms. *Trends Pharmacol Sci 22*, 140-146.

(62) Minchin, R. F., Hanna, P. E., Dupret, J. M., Wagner, C. R., Rodrigues-Lima, F. and Butcher, N. J. (2007) Arylamine N-acetyltransferase I. *Int J Biochem Cell Biol 39*, 1999-2005.

(63) Wakefield, L., Robinson, J., Long, H., Ibbitt, J. C., Cooke, S., Hurst, H. C. and Sim, E. (2008) Arylamine N-acetyltransferase 1 expression in breast cancer cell lines: a potential marker in estrogen receptor-positive tumors. *Genes Chromosomes Cancer 47*, 118-126.

(64) Hein, D. W. (1988) Acetylator genotype and arylamine-induced carcinogenesis. *Biochim Biophys Acta 948*, 37-66.

(65) Lower, G. M., Jr., Nilsson, T., Nelson, C. E., Wolf, H., Gamsky, T. E. and Bryan, G. T. (1979) N-acetyltransferase phenotype and risk in urinary bladder cancer: approaches in molecular epidemiology. Preliminary results in Sweden and Denmark. *Environ Health Perspect 29*, 71-79.

(66) Morton, L. M., Bernstein, L., Wang, S. S., Hein, D. W., Rothman, N., Colt, J. S., Davis, S., Cerhan, J. R., Severson, R. K., Welch, R., Hartge, P. and Zahm, S. H. (2007) Hair dye use, genetic variation in N-acetyltransferase 1 (NAT1) and 2 (NAT2), and risk of non-Hodgkin lymphoma. *Carcinogenesis 28*, 1759-1764.

(67) Ambrosone, C. B., Kropp, S., Yang, J., Yao, S., Shields, P. G. and Chang-Claude, J. (2008) Cigarette smoking, N-acetyltransferase 2 genotypes, and breast cancer risk: pooled analysis and meta-analysis. *Cancer Epidemiol Biomarkers Prev 17*, 15-26.

(68) Sanderson, S., Salanti, G. and Higgins, J. (2007) Joint effects of the N-acetyltransferase 1 and 2 (NAT1 and NAT2) genes and smoking on bladder carcinogenesis: a literature-based systematic HuGE review and evidence synthesis. *Am J Epidemiol 166*, 741-751.

(69) Li, D., Jiao, L., Li, Y., Doll, M. A., Hein, D. W., Bondy, M. L., Evans, D. B., Wolff, R. A., Lenzi, R., Pisters, P. W., Abbruzzese, J. L. and Hassan, M. M. (2006) Polymorphisms of cytochrome P4501A2 and N-acetyltransferase genes, smoking, and risk of pancreatic cancer. *Carcinogenesis 27*, 103-111.

(70) Zienolddiny, S., Campa, D., Lind, H., Ryberg, D., Skaug, V., Stangeland, L. B., Canzian, F. and Haugen, A. (2008) A comprehensive analysis of phase I and phase II metabolism gene polymorphisms and risk of non-small cell lung cancer in smokers. *Carcinogenesis 29*, 1164-1169.

(71) Butcher, N. J., Arulpragasam, A. and Minchin, R. F. (2004) Proteasomal degradation of N-acetyltransferase 1 is prevented by acetylation of the active

site cysteine: a mechanism for the slow acetylator phenotype and substrate-dependent down-regulation. *J Biol Chem 279*, 22131-22137.

(72) Liu, F., Zhang, N., Zhou, X., Hanna, P. E., Wagner, C. R., Koepp, D. M. and Walters, K. J. (2006) Arylamine N-acetyltransferase aggregation and constitutive ubiquitylation. *J Mol Biol 361,* 482-492.

(73) Walraven, J. M., Trent, J. O. and Hein, D. W. (2008) Structure-function analyses of single nucleotide polymorphisms in human N-acetyltransferase 1. *Drug Metab Rev 40,* 169-184.

(74) Walraven, J. M., Zang, Y., Trent, J. O. and Hein, D. W. (2008) Structure/Function evaluations of single nucleotide polymorphisms in human N-acetyltransferase 2. *Curr Drug Metab 9*, 471-486.

(75) Butcher, N. J., Ilett, K. F. and Minchin, R. F. (2000) Substrate-dependent regulation of human arylamine N-acetyltransferase-1 in cultured cells. *Mol Pharmacol 57*, 468-473.

(76) Butcher, N. J., Ilett, K. F. and Minchin, R. F. (2000) Inactivation of human arylamine N-acetyltransferase 1 by the hydroxylamine of p-aminobenzoic acid. *Biochem Pharmacol 60,* 1829-1836.

(77) Dairou, J., Atmane, N., Rodrigues-Lima, F. and Dupret, J. M. (2004) Peroxynitrite irreversibly inactivates the human xenobiotic-metabolizing enzyme arylamine N-acetyltransferase 1 (NAT1) in human breast cancer cells: a cellular and mechanistic study. *J Biol Chem 279,* 7708-7714.

(78) Dairou, J., Malecaze, F., Dupret, J. M. and Rodrigues-Lima, F. (2005) The xenobiotic-metabolizing enzymes arylamine N-acetyltransferases in human

lens epithelial cells: inactivation by cellular oxidants and UVB-induced oxidative stress. *Mol Pharmacol 67*, 1299-1306.

(79) Ragunathan, N., Dairou, J., Pluvinage, B., Martins, M., Petit, E., Janel, N., Dupret, J. M. and Rodrigues-Lima, F. (2008) Identification of the xenobiotic-metabolizing enzyme arylamine N-acetyltransferase 1 as a new target of cisplatin in breast cancer cells: molecular and cellular mechanisms of inhibition. *Mol Pharmacol 73*, 1761-1768.

(80) Butcher, N. J., Tetlow, N. L., Cheung, C., Broadhurst, G. M. and Minchin, R. F. (2007) Induction of human arylamine N-acetyltransferase type I by androgens in human prostate cancer cells. *Cancer Res 67*, 85-92.

(81) Atmane, N., Dairou, J., Paul, A., Dupret, J. M. and Rodrigues-Lima, F. (2003) Redox regulation of the human xenobiotic metabolizing enzyme arylamine N-acetyltransferase 1 (NAT1). Reversible inactivation by hydrogen peroxide. *J Biol Chem 278*, 35086-35092.

(82) Lee, J. H., Chung, J. G., Lai, J. M., Levy, G. N. and Weber, W. W. (1997) Kinetics of arylamine N-acetyltransferase in tissues from human breast cancer. *Cancer Lett 111*, 39-50.

(83) Kawamura, A., Westwood, I., Wakefield, L., Long, H., Zhang, N., Walters, K., Redfield, C. and Sim, E. (2008) Mouse N-acetyltransferase type 2, the homologue of human N-acetyltransferase type 1. *Biochem Pharmacol 75*, 1550-1560.

(84) Smith, T. J. and Hanna, P. E. (1988) Hepatic N-acetyltransferases: selective inactivation in vivo by a carcinogenic N-arylhydroxamic acid. *Biochem Pharmacol 37*, 427-434.

(85) Wick, M. J. and Hanna, P. E. (1990) Bioactivation of N-arylhydroxamic acids by rat hepatic N-acetyltransferase. Detection of multiple enzyme forms by mechanism-based inactivation. *Biochem Pharmacol 39*, 991-1003.

PART I: CLONING, EXPRESSION AND PURIFICATION OF RECOMBINANT HUMAN ARYLAMINE N-ACETYLTRANSFERASE 2

Introduction

Human arylamine N-acetyltransferase 2 (NAT2) (EC 2.3.1.5) is one of two functional NAT isoforms expressed in human tissues. NAT2 shares 81% sequence identity with its isoform, NAT1 (*1*). Although they have high sequence similarity, human NAT1 and NAT2 show different substrate specificities and behaviors in carcinogen bioactivation (*2, 3*). However, the exact biological functions of each isozyme are still unclear.

A detailed investigation of substrate specificity and drug bioactivation, as well as other studies, requires large quantities of purified NAT enzymes. Initially, the NAT enzymes were purified from various animal sources, such as pigeon (*4*), rabbit (*5*), and hamster (*6, 7*), which required the sacrifice of a large number of animals and multi-step procedures to obtain microgram quantities of purified enzyme. Obtaining human NAT enzymes was even more difficult. The development of molecular biology techniques made it possible to clone the NAT genes and express the proteins in bacterial and mammalian cells (*8-10*). It was in 1995 that a recombinant hamster NAT was first purified to homogeneity by this laboratory (*11*). Hamster NAT1 expression plasmid, pPH4-2 (Figure 1), was constructed and hamster NAT1 was purified as a fusion protein to an amino terminal FLAG marker peptide by anti-FLAG M2 immunoaffinity chromatography (*11*). To release NAT1 from the FLAG

octapeptide, a thrombin recognition site was inserted into pPH4-2 plasmid between the FLAG peptide and the amino terminus of hamster NAT1 to yield pPH7 (Figure 1a) (*12*).

Recombinant hamster NAT2 protein was purified from a modified expression system, pPH70, in which the hamster NAT2 gene replaced the hamster NAT1 gene present in pPH7 (Figure 1b) (*12*). To overcome the low capacity, high expense and instability of the anti-FLAG M2 immunoaffinity column, a unique expression system, pPH70D, was developed by inserting the *E. coli* L54F dihydrofolate reductase (DHFR) mutant gene between the FLAG and the thrombin cleavage linker (Figure 1c) (*13*). During the purification process, DHFR-hamster NAT2 fusion protein was partially purified by an initial DEAE anion-exchange column. Thrombin was applied to remove DHFR from the fusion protein. Hamster NAT2 was purified to homogeneity with a second DEAE column, and the yield was as high as 8 mg from 1 liter of cell culture (*13*). The map of pPH70D is shown in Figure 2. pPH70D has been used as a vector to develop several mammalian protein expression and purification systems, such as human histidine triad nucleotide-binding protein 1 (HINT1) and mouse translation initiation factor eIF4E (*14, 15*). To obtain a human NAT1 expression system, the human NAT1 gene was used to replace the hamster NAT2 gene in pPH70D, to yield pPH80D (Figure 3) (*16*). Similar to the purification of hamster NAT2, human NAT1 was successfully purified by double DEAE columns with a yield of 4 mg per liter of cell culture (*16*).

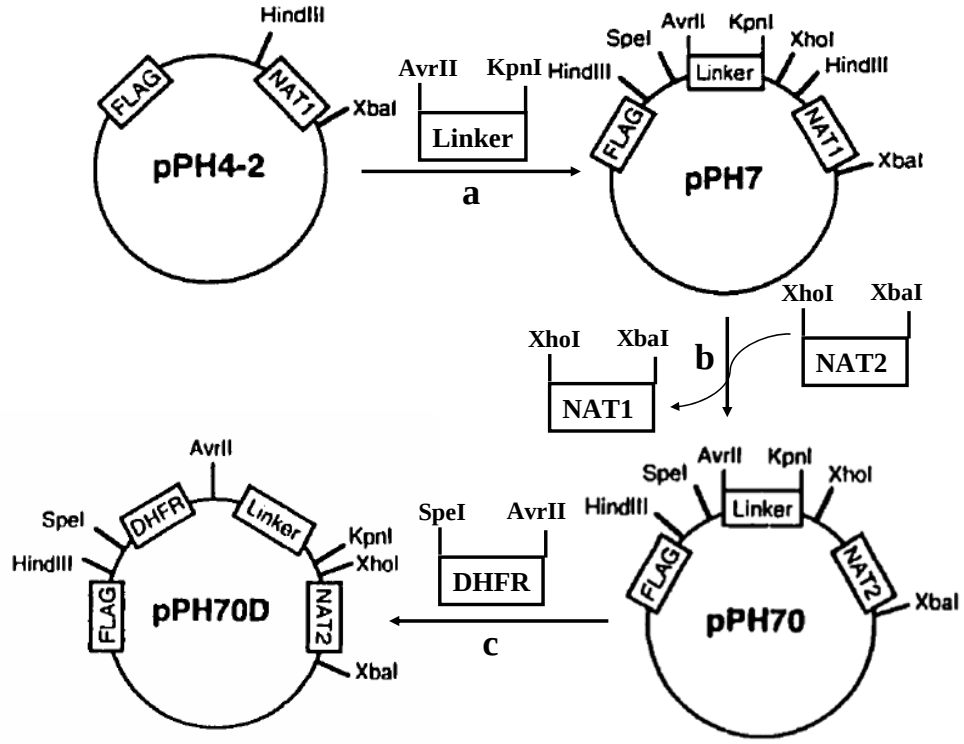

Figure 1. Construction of bacterial expression plasmids pPH7, pPH70, pPH70D. (From reference 12 and 13).

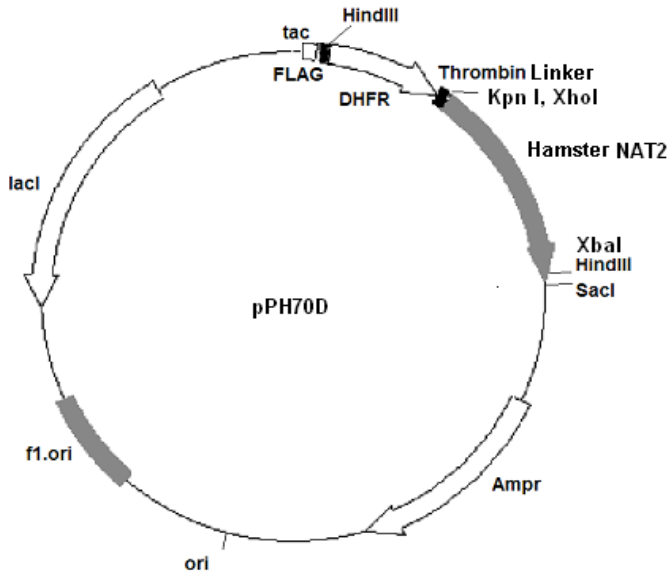

Figure 2. Hamster NAT2 expression plasmid pPH70D.

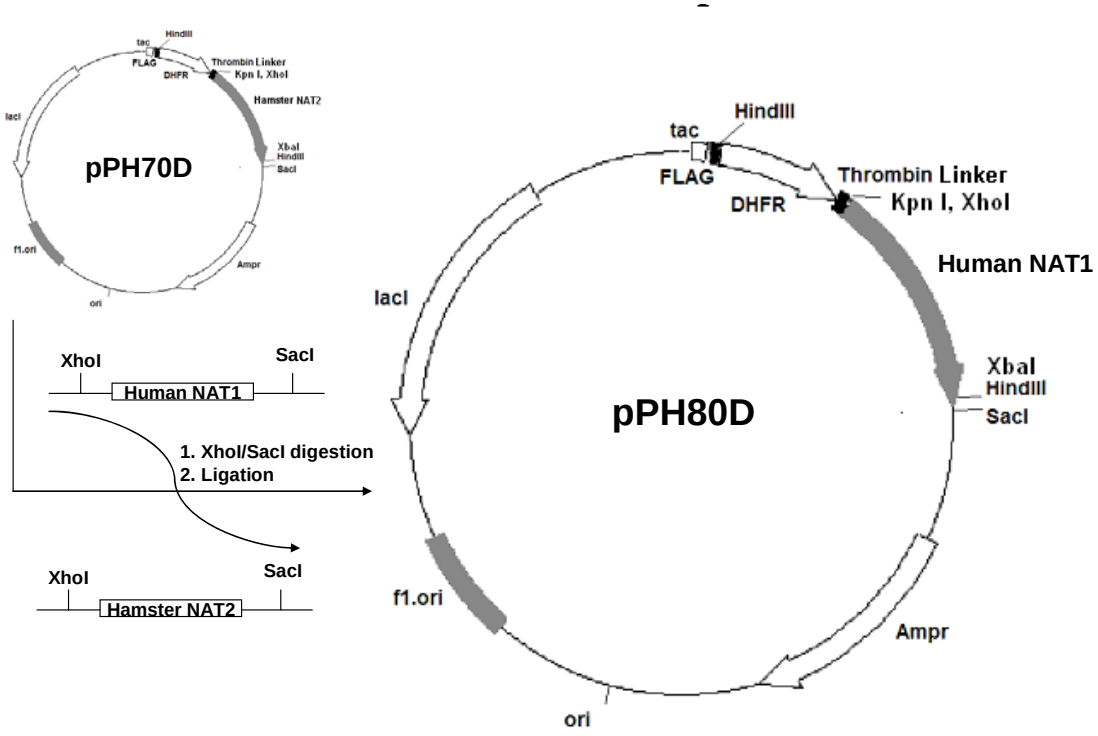

Figure 3. Construction of pPH80D.

In this part of the thesis, we describe a method to express and purify human NAT2 (NAT2 4) in milligram quantities. In the following parts, we describe the characterization of human NAT2 and NAT1.

Materials and Methods

Recombinant human NAT1 was overexpressed and purified as described previously (*16*). *p*-Anisidine, 3-(*N*-morpholino)propanesulfonic acid (MOPS), *p*-nitrophenyl acetate (PNPA), methotrexate (MTX) agarose, lysozyme, ampicilin, chloramphenicol, and isopropyl-β-D-thiogalactopyranoside (IPTG) were purchased from Sigma (St. Louis, MO). Trimethoprim (TMP) was purchased from MP Biomedicals (Irvine, CA). Competent BL-21 Codon Plus RIL *Escherichia. coli* cells were purchased from Stratagene (La Jolla, CA), and supercompetent *E. coli* DH5α cells were from Invitrogen (Carlsbad, CA). Restriction enzymes were purchased from New England Biolabs (Ipswich, MA). DEAE Sepharose Fast Flow anion-exchange resin was obtained from Amersham Pharmacia (Piscataway, NJ). Dialysis tubing (Spectra/Por® membrane, molecular weight cut off 12-14,000) was from Spectrum Laboratories (Rancho Dominguez, CA). Oligodeoxynucleotides were synthesized by the MicroChemical Facility of the University of Minnesota, and DNA sequences were determined by the BioMedical Genomics Center of the University of Minnesota. Protein concentrations were determined by the method of Bradford (*17*). Spectrophotometric data were acquired on a Varian Cary 50 UV-vis spectrophotometer. All buffers were degassed under vacuum, and all incubations were conducted under aerobic conditions. The concentrations of all solutions reported as percentages are v/v. Proteins were concentrated with Amicon ultrafiltration cells (model 202, 52, or 12). Kinetic data were analyzed with the JMP IN software suite (SAS Institute, Inc.).

Construction of Plasmid pPH90D. To allow use of the XhoI and XbaI restriction cloning sites in the pPH70D plasmid (*13*), a silent mutation was incorporated in the coding region of human nat2*4 to eliminate an XhoI restriction site by using QuickChange^{TM} site-directed mutagenesis kit (Stratagene, La Jolla, CA). The oligonucleotide primer was 5'- G TGG CAG CCG CTA GAA TTA ATT TCT GGG -3'. The coding region of human nat2*4 was amplified by PCR with the forward primer 5'-GCGACG*TCT*AGAATGGACATTGAAGCATATTTTG-3', which includes an XhoI restriction site, and the reverse primer 5'-CG *CTC*GAGCGCGCTAAATAGTAAGGGATCCATCACCAGG-3', which includes an XbaI restriction site. The PCR was conducted with 2 U Taq polymerase, 1 μg genomic DNA as template, 200 μ dNTP, and 30 pmol each of the primers. The reactions were heated at 94°C for 2 min, followed by 30 cycles of 30 s at 94°C, 45 s at 50°C, and 2 min at 72°C. To ensure complete extension, the reaction mixture was incubated at 72°C for 10 min after the 30 cycles. The PCR products were purified with a QIAquick PCR Purification Kit (Qiagen). The purified PCR product and the plasmid vector pPH70D were digested with XhoI and XbaI separately. The digestion products were isolated with a QIAquick Gel Extraction Kit (Qiagen). The vector DNA was ligated with the human nat2*4 insert with T4 ligase (Invitrogen). Supercompetent *E coli.* DH5α cells were transformed with the ligation mix according to the supplier's protocol, and ampicillin-resistant plasmid-containing clones were selected on LB agar plates. The plasmids from positive colonies were isolated with the Wizard Plus SV Miniprep DNA purification system. The cloned sequence was confirmed by automated DNA sequencing, and the plasmid was designated pPH90D.

Construction of Plasmid pPH100D. The oligonucleotide insert for the TEV protease cleavage linker encodes a space arm region and a TEV protease cleavage site, Asp-Tyr-Asp-Ile-Pro-Thr-Thr-Glu-Asn-Leu-Tyr-Phe-Gln-Gly. The single-stranded DNA (CTAGGTGATTACGATATCCCGACAACGGAAAACCTGTATTTTCAGG GCC and TCGAGGCCCTGAAAATACAGGTTTTCCGTTGTCGGGATATCGT AATCAC) was annealed by heating to 65°C and allowing the mixture to cool slowly to room temperature. Plamid pPH90D was digested with AvrII and XhoI and purified with a QIAquick Gel Extraction Kit (Qiagen). The vector was ligated with the annealed double stranded DNA insert with T4 ligase. Supercompetent *E. coli* DH5α cells were transformed and selected as described above. The constructed plasmid was designated pPH100D; the sequence was confirmed by automated DNA sequencing.

Expression and Purification of Human Recombinant NAT2. Competent BL-21 Codon Plus RIL *E. coli* cells were transformed with plasmid pPH100D according to the supplier's protocol. The cells were grown at 37 ºC in TB to an O.D. 600 of 1.2. IPTG (final concentration 100 μM) was added after the culture had been quickly cooled to 17 ºC. The growth was continued for 16 h at 17 ºC. The cells were harvested by centrifugation at 5000 x g for 15 min at 4 ºC. The cell pellets were frozen at -80 °C or on dry ice.

All purification steps were performed at 4°C in degassed buffers. The cell pellets from 2 L of BL-21 (RIL)/pPH100D culture were lysed as reported (*16*). The

soluble fraction of the bacterial cell lysate was acidified to pH 6.5 by dialysis against 6 L (three 2-L portions) of PE buffer (potassium phosphate 20 mM, pH 6.5; 1 mM EDTA; 1 mM DTT). The acidified soluble fraction was applied to a methotrexate (MTX)-affinity column (10 mm x 200 mm) that had been equilibrated with PE buffer (pH 6.5) and pre-saturated by treatment with the soluble fraction from transformed cells. The column was washed with 1 L of high salt PE buffer (1 M NaCl; pH 6.5), followed by elution with 150 mL of trimethoprim (TMP) buffer (300 μM TMP; 1 M NaCl; potassium phosphate 20 mM, pH 9.0; 1 mM EDTA; 1 mM DTT). Fractions (9 mL) were collected at a flow rate of 1 mL/min. The absorbance at 280 nm was determined for each fraction and an aliquot (1 μL) of each fraction was assayed for transacetylation activity. The fractions containing the highest levels of activity were combined and concentrated to 2 mg/mL of protein.

To separate the fusion protein from truncated fusion protein and other contaminating proteins, the protein solution from the MTX column was dialyzed against 6 L (three 2-L portions) of PE buffer (pH 7.4) and loaded onto a DEAE anion-exchange column (25 mm x 200 mm) which was packed with fast flow DEAE resin and had been equilibrated with PE buffer (pH 7.4). The column was washed with 200 mL of PE buffer (pH 7.4), followed by a 0-0.4 M NaCl gradient in PE buffer (pH 7.4, 720 mL). Fractions (9 mL) were collected at a flow rate of 1 mL/min. The fractions with the highest levels of transacetylation activity were combined and concentrated to 1.5 mg/mL of protein. The concentrated solution was dialyzed against 6 L (three 2-L portions) of TEV protease cleavage buffer (50 mM Tris-HCl, pH 8.0; 0.5 mM EDTA;

1 mM DTT). Human NAT2 was cleaved from the fusion protein by a 12 h incubation with recombinant TEV protease (350 units/mg of fusion protein) at 4°C. The solution was dialyzed against PE buffer (pH 7.4), and loaded onto a second DEAE column. The column was washed with 200 mL of PE buffer (pH 7.4), followed by a 0-0.2 M NaCl gradient in PE buffer (pH 7.4). Fractions (9 mL) were collected at a flow rate of 1 mL/min, and the fractions with the highest transacetylation activity were combined and concentrated to 1 mg/mL of protein. The second DEAE chromatography step resulted in the purification of human NAT2 to homogeneity according to SDS-PAGE and Nano-ESI-Q-TOF MS. The homogeneous recombinant protein was stored at -80°C as a 10% glycerol-PE (pH 7.4) solution.

NAT2 Activity Assay. The assay mixture contained NAT2 (96 ng/mL, 2.84 nM), PNPA (2 mM) as the acetyl donor, *p*-anisidine (1 mM) as the acetyl acceptor, and MOPS buffer (100 mM, pH 7.0; 150 mM NaCl; 0.1 mM DTT) in a final volume of 500 μL. The reaction was initiated by addition of PNPA dissolved in DMSO (5 μL). The final concentration of DMSO was 1%. Incubations were conducted at either 23 °C or 37 °C in acryl cuvetts in a Varian Cary 50 UV-Vis spectrophotometer equipped with a circulation water bath. The reaction rates were determined by monitoring the increase in absorbance at 400 nm, due to the formation of *p*-nitrophenol (PNP) (ε_{400nm} = 9400 M^{-1} cm^{-1}). The results were corrected for nonenzymatic PNPA hydrolysis by conducting the reaction in the absence of enzyme. The specific activities were expressed as μmol of product formed per mg of protein per min.

Results

Construction of Plasmid pPH90D. The two restriction sites, upstream of the hamster NAT2 gene in plasmid pPH70D, are KpnI and XhoI, which are both contained in the nat2*4 gene (*13*). Thus, T^{401} to G, a silent mutation, was incorporated into nat2*4 to allow double digestion with XhoI and XbaI to construct plasmid pPH90D, which was accomplished by replacement of the hamster NAT2 gene of pPH70D with nat2*4 (Figure 4).

The expression and purification of FLAG-mutant DHFR-thrombin site-NAT2 4 fusion protein from *E.coli* was successful, but treatment of the fusion protein with thrombin for 19 hours caused a loss of 25% of the NAT2 activity (Figure 5). Hamster and human NATs contain a R64-G65 pair which is a potential thrombin cleavage site. However, incubation of hamster NATs and human NAT1 fusion proteins with thrombin to free the NATs did not result in a loss of NAT activities. Human NAT2 contains a unique potential thrombin cleavage site (R156-G157), which is not present in the other NATs (Figure 6). We suspected that this site could be affected by thrombin and is responsible for the loss of specific activity upon incubation with thrombin.

Construction of Plasmid pPH100D. There is no TEV protease cleavage site in the human NAT2 sequence. Thus, the thrombin-sensitive linker of pPH90D was replaced with a TEV protease-sensitive linker to accomplish the construction of pPH100D (Figure 7). It was also found that replacement of the original linker with

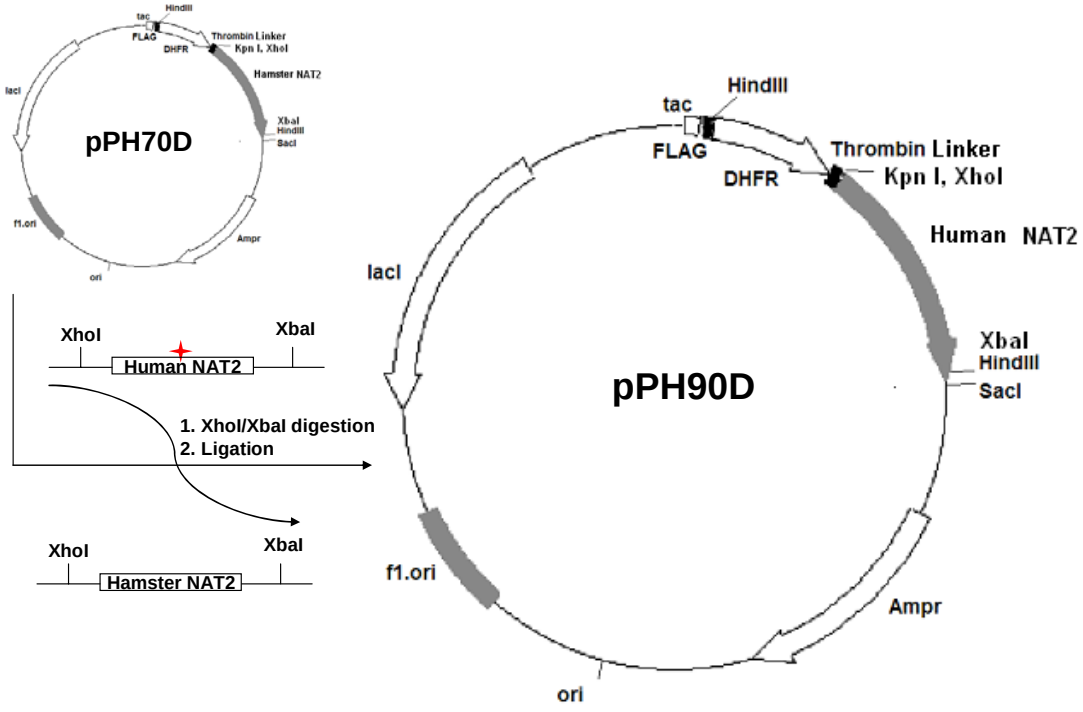

Figure 4. Construction of plasmid pPH90D.

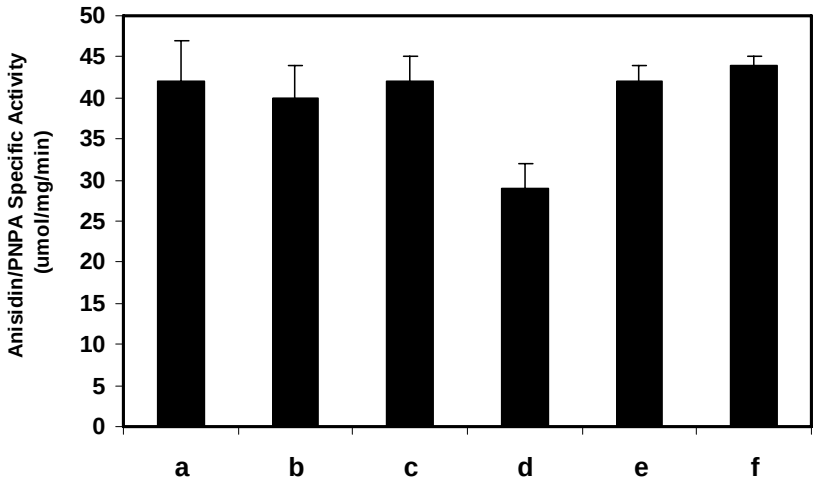

Figure 5. Change of NAT2 activity after incubation of the FLAG-DHFR-thrombin site-NAT2 fusion protein with thrombin or TEV protease. (a) fusion protein 0 hour at 4 °C; (b) fusion protein 19 hours at 4 °C; (c) fusion protein after incubation with thrombin for 0 hour at 4 °C; (d) fusion protein after incubation with thrombin for 19 hours at 4 °C; (e) fusion protein after incubation with TEV protease for 0 hour at 4 °C; (f) fusion protein after incubation with TEV protease for 19 hours at 4 °C.

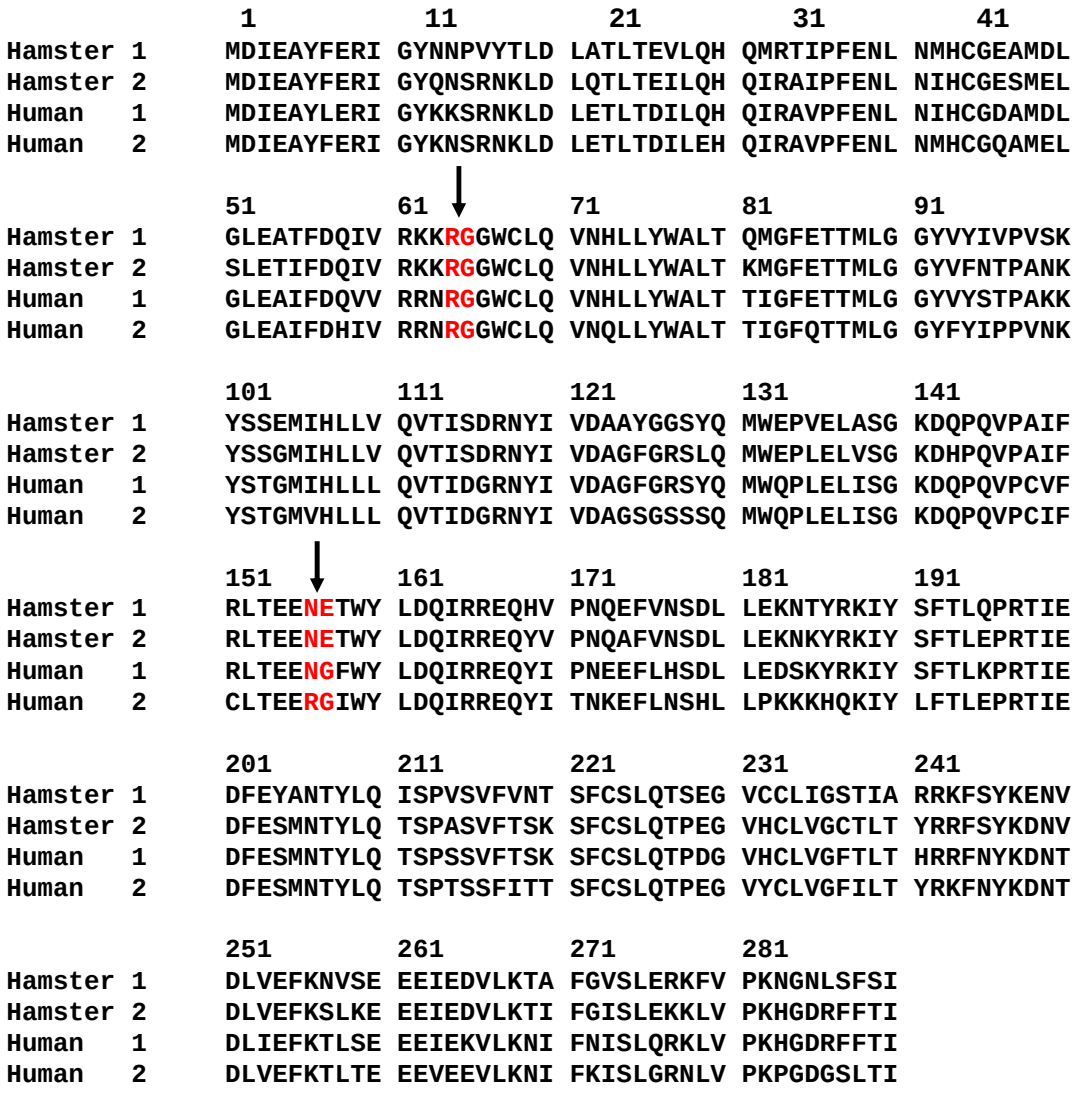

Figure 6. Alignment of hamster NATs and human NATs sequences. As indicated by the arrows, hamster NATs and human NAT1 contain one potential thrombin recognition site, R64-G65, while human NAT2 contains two potential thrombin recognition sites, R64-G65 and R156-G157.

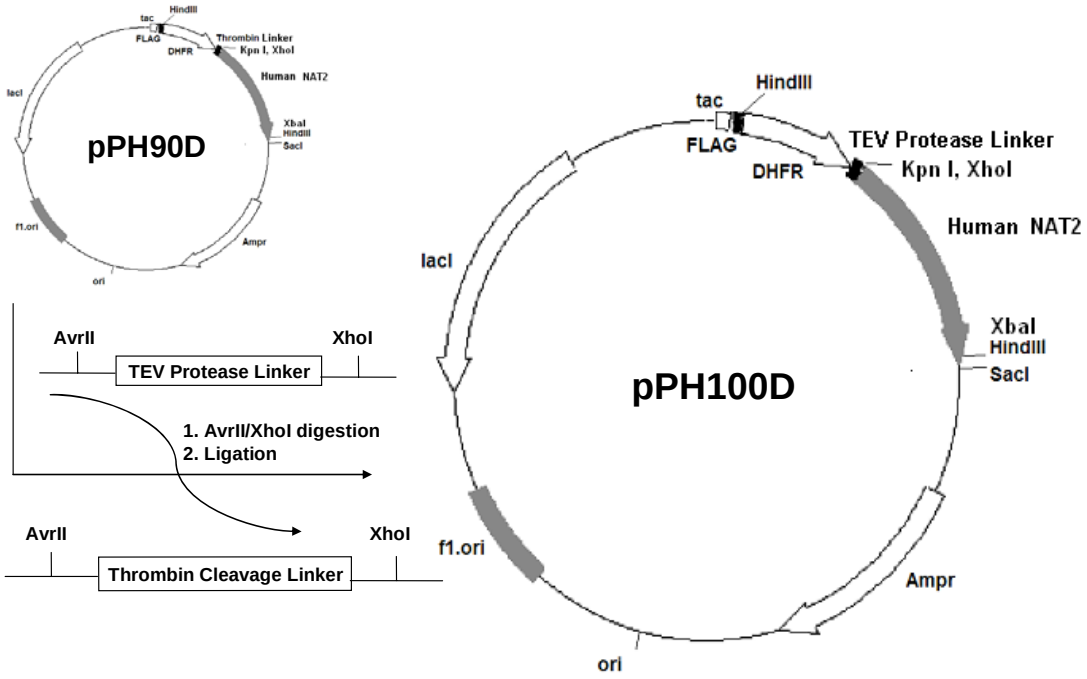

Figure 7. Construction of plasmid pPH100D.

the TEV protease site increased the level of expression of the soluble NAT2 fusion protein around 2-fold.

Overexpression of the Fusion Protein. In order to optimize the conditions for expression of the soluble fusion protein, different promoters, different bacterial cell lines, different media, and different induction conditions were tested. The DHFR-linker-NAT2 gene was inserted into plasmid pSGA02 (*18*), which contained a powerful bacteriophage T7 promoter. However, this expression system did not give a better result than pPH100D, which contained a tac promoter, a functional hybrid of two strong promoters (trp and lac) (*19*). To correct expression problems caused by codon bias, BL-21 Codon Plus RIL *E.coli* cells, BL-21 Codon Plus RP *E.coli* cells, and Rosseta *E.coli* cells, were tested for expression of the fusion protein. BL-21 Codon Plus RIL *E.coli* cells gave the highest expression of the soluble fusion protein. Effects of IPTG concentrations, induction temperatures, and induction durations were also examined. The optimized conditions are described in Experimental Procedures. After optimization, the overexpression level of soluble human NAT2 fusion protein was less than 10% of that of hamster NAT2 fusion protein (*13*) (Figure 8).

Purification of Human Recombinant NAT2. It had been reported that purification of DHFR-hamster NAT2 fusion protein by methotrexate (MTX) affinity chromatography resulted in a recovery of less than 10% of the hamster NAT2 activity (*13*). In the purification of the human NAT2 fusion protein, it again was found that over 70% of the human NAT2 activity was lost upon attempted elution from an MTX

a

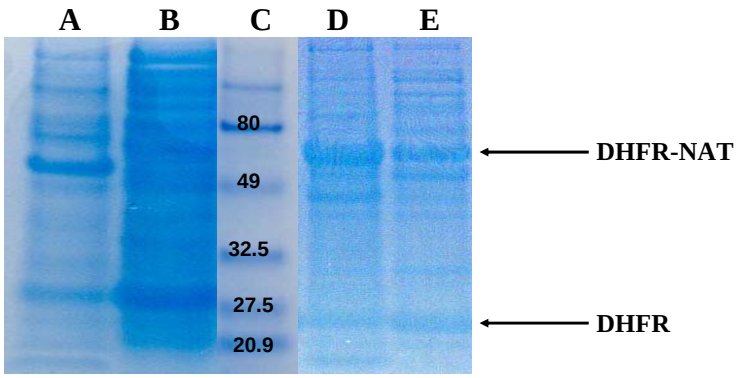

b

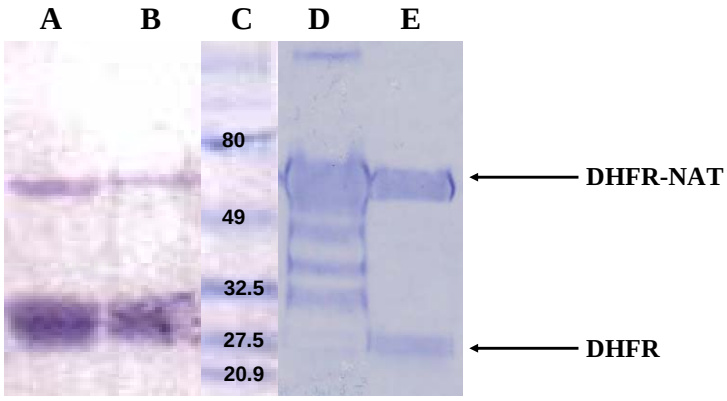

Figure 8. SDS-PAGE and Western Blot analysis of overexpression of human NAT2 fusion protein. (a) Coomassie blue-stained SDS-PAGE. Lane A: soluble part of pPH-100D *E. coli* lysates, Lane B: insoluble part of pPH-100D *E. coli* lysates, Lane C: molecular weight marker, Lane D: soluble part of pPH-70D *E. coli* lysates, Lane E: insoluble part of pPH-70D *E. coli* lysates. (b) Western Blot analysis of SDS-PAGE: lanes are as in (a). Anti-FLAG M2 monocolonal antibody was the primary antibody used in the Western Blot analysis.

column. The resin was boiled with SDS-PAGE loading buffer and the DHFR-human NAT2 fusion protein bound to the resin was identified by SDS-PAGE (Figure 9).

The method that we developed to prevent this apparent irreversible binding of human NAT2 to MTX involved purification of the fusion protein with an MTX column that had been previously treated with cell cytosol containing the recombinant fusion protein. As a result, the purification of the DHFR-fusion protein was accomplished by passage of cell cytosol, in which fusion protein had been expressed, through the cytosol-treated MTX column, followed by elution with trimethoprim (TMP). This method afforded an 86% recovery of NAT2 activity and a 17-fold purification of the 60 kD fusion protein from bacterial cell lysate (Figure 10, lane D; Table 1). The treated column could be stored at 4 °C and used repeatedly.

To improve the efficiency of TEV protease cleavage of the fusion protein, an initial DEAE anion exchange chromatography was applied to separate NAT2 fusion protein from apparent truncated fusion protein (Figure 10, lane E; Table 1). The fusion protein was eluted at approximately 0.2 *M* NaCl (Figure 11a). After incubation of TEV protease with the protein mixture from the first DEAE column, a new band with a molecular mass of approximately 34 kDa, corresponding to NAT2, appeared (Figure 10, lane F). Because of the difference between the theoretical isoelectric point of human NAT2 (p*I* 5.6) and that of FLAG-DHFR (p*I* 4.8), a second DEAE column

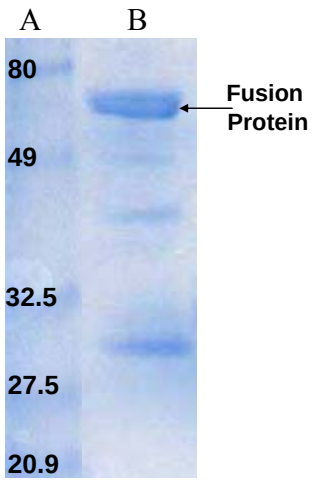

Figure 9. Irreversible binding of human NAT2-fusion protein to MTX. Cell cytosol, in which fusion protein had been expressed, was loaded on the MTX column followed by elution with TMP. The resin was boiled with SDS-PAGE loading buffer. Lane A: molecular weight marker, Lane B: MTX resin after boiling with SDS-PAGE loading buffer.

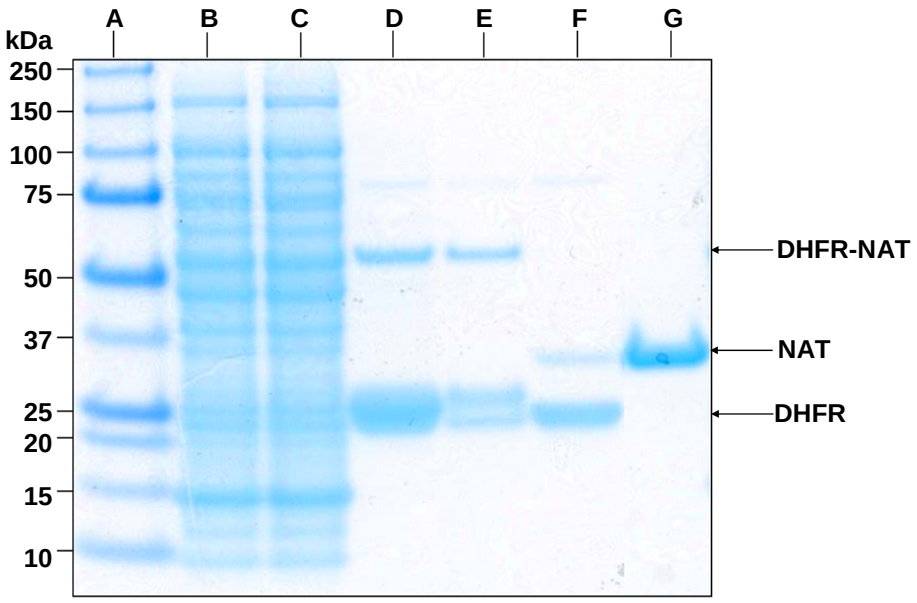

Figure 10. SDS-PAGE analysis of human NAT2 purification. Lane A: Molecular weight markers, Lane B: BL21 (RIL)/pPH100D cell lysate (without IPTG induction), Lane C: BL21 (RIL)/pPH100D cell lysate (with IPTG induction), Lane D: partially purified fusion protein after the MTX column, Lane E: partially purified fusion protein after the first DEAE column, Lane F: protein mixture after TEV protease cleavage, Lane G: purified human NAT2 after the second DEAE column.

purification step	total protein (mg)	anisidine/PNPA specific activity (μmol/mg/min)	total activity (μmol/min)	% recovery	fold purification
cell lysate	1560	1.8	2980	100	1.0
MTX column	62	31	2570	86	17
1st DEAE column	32	73	2340	78	40
2nd DEAE column	2.8	689	1920	64	373

Table 1. Purification of Human NAT2. These data were obtained from 2L of cell culture.

was applied to separate the human NAT2 from FLAG-DHFR and other contaminating proteins. NAT2 was eluted as a well separated peak at approximately 0.06 *M* NaCl (Figure 11b).

This methodology afforded a 373-fold purification of the human recombinant NAT2 and 64% of the anisidin/PNPA activity in the bacterial lysates was recovered as pure NAT2. The yield was 2.8 mg homogeneous NAT2 from 2 liters of cell culture. The homogeneity of purified NAT2 was confirmed by SDS-PAGE (Figure 10, lane G). The deconvoluted Nano-ESI-Q-TOF mass spectrum of purified NAT2 exhibited a molecular mass of 33844.0 Da, which agrees well with the theoretical mass of 33841.8, including the three additional amino acids (Gly-Leu-Glu) at the N-terminus of the recombinant protein (Figure 12).

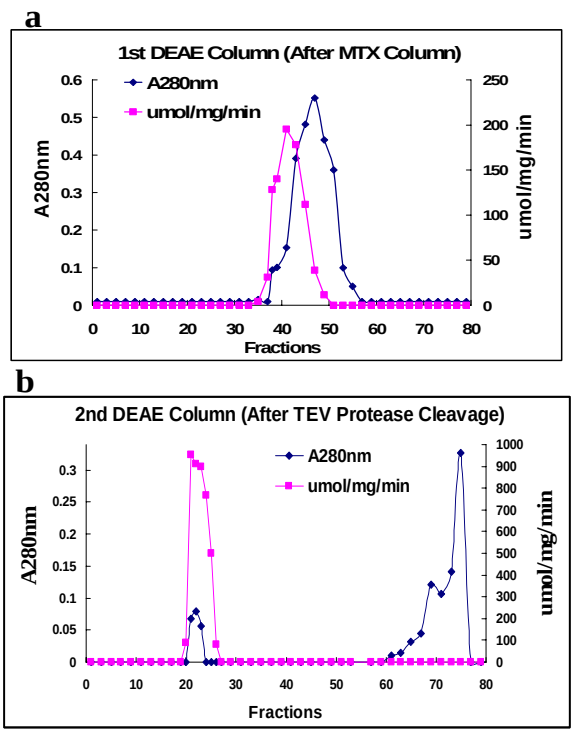

Figure 11. DEAE anion-exchange profile of (a) FLAG-DHFR-human NAT2 fusion protein, and (b) TEV protease cleaved human NAT2. The absorbance at 280 nm was determined, and selected fractions were assayed for anisidine/PNPA transacetylation activity (μmon/mg/min).

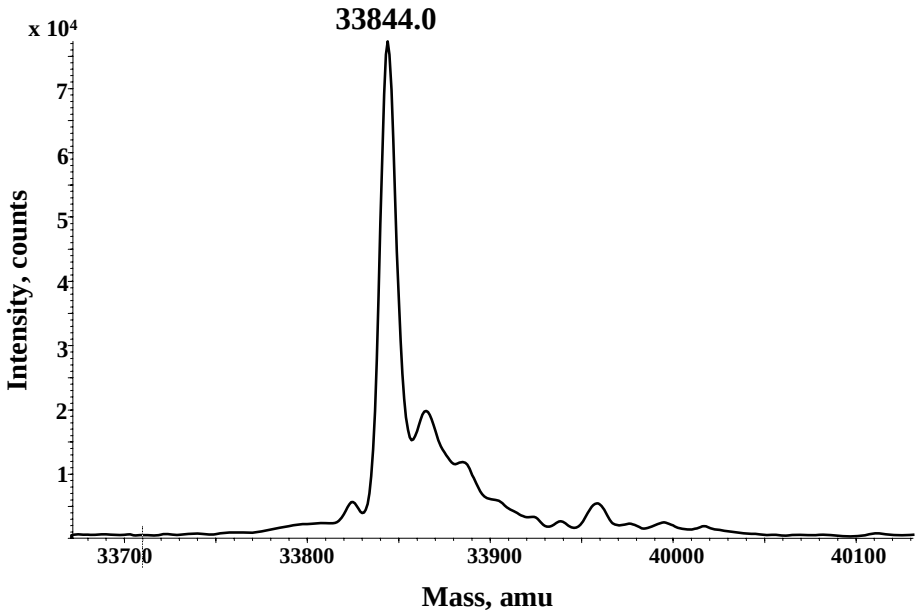

Figure 12. Nano-ESI-Q-TOF mass spectrum of purified recombinant human NAT2.

Discussion

Previously our laboratory designed and constructed hamster NAT2 and human NAT1 expression systems, pPH70D and pPH80D, which expressed a FLAG-DHFR L54F mutant-NAT fusion protein (*13, 16*). Recombinant hamster NAT2 and human NAT1 proteins were successfully purified by a double DEAE column strategy, which made it possible to study the substrate specificities and carcinogen bioactivations (*13, 16, 20, 21*). However, the overexpression level of soluble human NAT2 fusion protein was no more than 10% of that of hamster NAT2 or human NAT1 fusion protein. The double DEAE column method, which afforded approximately a 40-fold purification, did not give a high purity and yield of human NAT2. We needed to develop a new methodology that afforded a greater than 300-fold purification to produce recombinant human NAT2.

Dihydrofolate reductase (DHFR, 5,6,7,8-tetrahydrofolate:$NADP^+$ oxidoreductase, EC 1.5.1.3) has been used as a "affinity handle" for the expression and purification of a variety of peptides and proteins, such as human HINT1 and mouse eIF4E (*14, 15, 22*). MTX and TMP are both potent competitive inhibitors of DHFR and the K_i values are around 10^{-9} to 10^{-12} (*23*). Passage of the bacterial cell cytosol through a cytosol-treated MTX column followed by elution with TMP resulted in a mixture of DHFR-containing proteins. As shown in lane B of figure 13, the partially purified fusion protein eluted from the MTX column in the purification of NAT2 contained a 60 kD fusion protein and a mixture of approximately 30 kD DHFR-containing proteins. After 19 hours of treatment with TEV protease, the

protein mixture contained two bands, 34 kD recombinant NAT2 and 22 kD Flag-DHFR (Figure 13, Lane C). Thus, not only the fusion protein was cleaved by TEV protease, producing NAT2 and Flag-DHFR, but also the 30 kD DHFR-containing protein mixture was cleaved by TEV protease, yielding Flag-DHFR and small peptides, which could not be visualized by SDS-PAGE. It is concluded that the protein mixture that eluted from the MTX column contained a DHFR-TEV protease linker-NAT2 fusion protein and a mixture of truncated fusion proteins, which contained DHFR, TEV protease linker, and several amino acids from the N-terminus of NAT2. Because the truncated fusion proteins comprised the majority of the protein mixture (Figure 13, Lane B) and would consume TEV protease, DEAE anion exchange chromatography was used to remove the truncated fusion proteins prior to cleavage of the desired fusion protein with TEV protease.

Another challenge of purification of human NAT2 is that NAT2 contains a potential thrombin cleavage site (R156-G157) which is not present in human NAT1 or hamster NATs. To overcome this problem, plasmid pPH100D, which expresses a TEV protease sensitive linker, was constructed. Incubation of partially purified fusion protein with TEV protease for 19 hours gave complete cleavage of the fusion protein without loss of NAT2 activity.

In summary, to facilitate bioactivation and mechanistic studies with human NATs, a human NAT2 expression system, pPH100D, was constructed. Flag-DHFR-TEV protease linker-NAT2 fusion protein was overexpressed from *E.coli* under

optimized conditions. The high affinity of the MTX column afforded much greater purification of the fusion protein than a DEAE column, which made it possible to purify human NAT2 to homogeneity by DEAE anion exchange chromatography following TEV protease cleavage of the partially purified fusion protein. This is the only published method for the production of milligram quantities of homogenous human recombinant NAT2 with high specific activity (*24*). The characterization of human NAT2 will be described in the following chapters.

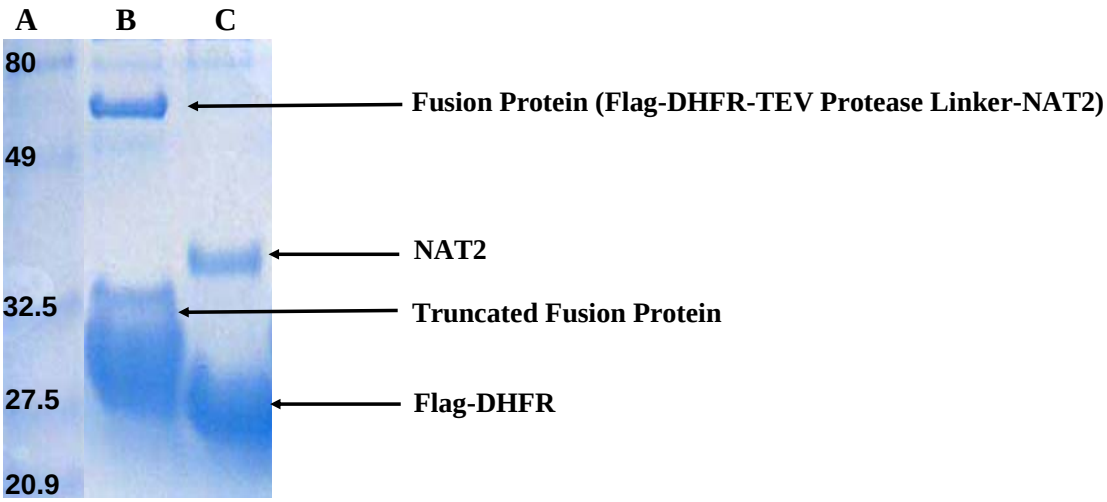

Figure 13. SDS-PAGE analysis of partially purified fusion protein aftre the MTX column. Lane A: molecular weight marker, Lane B: partially purified fusion protein after the MTX column, Lane C: protein mixture after incubation of the partially purified fusion protein with TEV protease for 19 hours.

References

(1) Josephy, P. D., and Mannervik, B. (2006) *Molecular Toxicology 2nd edition*, pp 426-447, Oxford University Press, New York.

(2) Grant, D. M., Blum, M., Beer, M. and Meyer, U. A. (1991) Monomorphic and polymorphic human arylamine N-acetyltransferases: a comparison of liver isozymes and expressed products of two cloned genes. *Mol Pharmacol 39*, 184-191.

(3) Glatt, H. and Meinl, W. (2004) Use of genetically manipulated Salmonella typhimurium strains to evaluate the role of sulfotransferases and acetyltransferases in nitrofen mutagenicity. *Carcinogenesis 25*, 779-786.

(4) Andres, H. H., Kolb, H. J., Schreiber, R. J. and Weiss, L. (1983) Characterization of the active site, substrate specificity and kinetic properties of acetyl-CoA:arylamine N-acetyltransferase from pigeon liver. *Biochim Biophys Acta 746*, 193-201.

(5) Andres, H. H., Vogel, R. S., Tarr, G. E., Johnson, L. and Weber, W. W. (1987) Purification, physicochemical, and kinetic properties of liver acetyl-CoA:arylamine N-acetyltransferase from rapid acetylator rabbits. *Mol Pharmacol 31*, 446-456.

(6) Ozawa, S., Abu-Zeid, M., Kawakubo, Y., Toyama, S., Yamazoe, Y. and Kato, R. (1990) Monomorphic and polymorphic isozymes of arylamine N-acetyltransferases in hamster liver: purification of the isozymes and genetic basis of N-acetylation polymorphism. *Carcinogenesis 11*, 2137-2144.

(7) Cheon, H. G., Boteju, L. W. and Hanna, P. E. (1992) Affinity alkylation of hamster hepatic arylamine N-acetyltransferases: isolation of a modified cysteine residue. *Mol Pharmacol 42*, 82-93.

(8) Doll, M. A. and Hein, D. W. (1995) Cloning, sequencing and expression of NAT1 and NAT2 encoding genes from rapid and slow acetylator inbred rats. *Pharmacogenetics 5*, 247-251.

(9) Dupret, J. M. and Grant, D. M. (1992) Site-directed mutagenesis of recombinant human arylamine N-acetyltransferase expressed in Escherichia coli. Evidence for direct involvement of Cys68 in the catalytic mechanism of polymorphic human NAT2. *J Biol Chem 267*, 7381-7385.

(10) Minchin, R. F., Reeves, P. T., Teitel, C. H., McManus, M. E., Mojarrabi, B., Ilett, K. F. and Kadlubar, F. F. (1992) N-and O-acetylation of aromatic and heterocyclic amine carcinogens by human monomorphic and polymorphic acetyltransferases expressed in COS-1 cells. *Biochem Biophys Res Commun 185*, 839-844.

(11) Bergstrom, C. P., Wagner, C. R., Ann, D. K. and Hanna, P. E. (1995) Hamster monomorphic arylamine N-acetyltransferase: expression in Escherichia coli and purification. *Protein Expr Purif 6*, 45-55.

(12) Wagner, C. R., Bergstrom, C. P., Koning, K. R. and Hanna, P. E. (1996) Arylamine N-acetyltransferases. Expression in Escherichia coli, purification, and substrate specificities of recombinant hamster monomorphic and polymorphic isozymes. *Drug Metab Dispos 24*, 245-253.

(13) Sticha, K. R., Sieg, C. A., Bergstrom, C. P., Hanna, P. E. and Wagner, C. R. (1997) Overexpression and large-scale purification of recombinant hamster polymorphic arylamine N-acetyltransferase as a dihydrofolate reductase fusion protein. *Protein Expr Purif 10*, 141-153.

(14) Chou, T. F., Bieganowski, P., Shilinski, K., Cheng, J., Brenner, C. and Wagner, C. R. (2005) 31P NMR and genetic analysis establish hinT as the only Escherchia coli purine nucleoside phosphoramidase and as essential for growth under high salt conditions. *J Biol Chem 280*, 15356-15361.

(15) Ghosh, P., Cheng, J., Chou, T. F., Jia, Y., Avdulov, S., Bitterman, P. B., Polunovsky, V. A. and Wagner, C. R. (2008) Expression, purification and characterization of recombinant mouse translation initiation factor eIF4E as a dihydrofolate reductase (DHFR) fusion protein. *Protein Expr Purif 60*, 132-139.

(16) Wang, H., Vath, G. M., Kawamura, A., Bates, C. A., Sim, E., Hanna, P. E. and Wagner, C. R. (2005) Over-expression, purification, and characterization of recombinant human arylamine N-acetyltransferase 1. *Protein J 24*, 65-77.

(17) Bradford, M. M. (1976) A rapid and sensitive method for the quantitation of microgram quantities of protein utilizing the principle of protein-dye binding. *Anal Biochem 72*, 248-254.

(18) Ghosh, S. and Lowenstein, J. M. (1996) A multifunctional vector system for heterologous expression of proteins in Escherichia coli. Expression of native and hexahistidyl fusion proteins, rapid purification of the fusion proteins, and removal of fusion peptide by Kex2 protease. *Gene 176*, 249-255.

(19) de Boer, H. A., Comstock, L. J. and Vasser, M. (1983) The tac promoter: a functional hybrid derived from the trp and lac promoters. *Proc Natl Acad Sci U S A 80*, 21-25.

(20) Sticha, K. R., Bergstrom, C. P., Wagner, C. R. and Hanna, P. E. (1998) Characterization of hamster recombinant monomorphic and polymorphic arylamine N-acetyltransferases: bioactivation and mechanism-based inactivation studies with N-hydroxy-2-acetylaminofluorene. *Biochem Pharmacol 56*, 47-59.

(21) Wang, H., Wagner, C. R. and Hanna, P. E. (2005) Irreversible inactivation of arylamine N-acetyltransferases in the presence of N-hydroxy-4-acetylaminobiphenyl: a comparison of human and hamster enzymes. *Chem Res Toxicol 18*, 183-197.

(22) Takasuga, A., Banba, K., Yoshino, K., Izutsu, H., Iwakura, M. and Ohashi, S. (1992) Efficient production of a small peptide by expression as a multimeric form fused with the dihydrofolate reductase affinity handle. *J Biochem 112*, 652-657.

(23) Blakley, R. L. Dihydrofolate reductase, in: R.L. Blakley, S.J. Benkovic (Eds.), Folates and Pterins, Wiley, New York, 1984, pp. 191-253.

(24) Liu, L., Von Vett, A., Zhang, N., Walters, K. J., Wagner, C. R. and Hanna, P. E. (2007) Arylamine N-acetyltransferases: characterization of the substrate specificities and molecular interactions of environmental arylamines with human NAT1 and NAT2. *Chem Res Toxicol 20*, 1300-1308.

PART II: CHARATERIZATION OF SUBSTRATE SPECIFICITIES AND MOLECULAR INTERACTIONS OF ENVIRONMENTAL ARYLAMINES WITH HUMAN NAT1 AND NAT2

Introduction

Arylamines constitute one of the most extensively studied classes of human carcinogens (*1, 2*). Exposure to arylamines can occur from many different sources and are associated with various cancer risks in humans (*3-8*). In a population-based study conducted by Gan and co-workers, nine alkylanilines, known to be present in cigarette smoke, were studied for their level of arylamine-hemoglobin adducts formed in peripheral blood collected from study subjects (*4*). It was found that levels of all arylamine-hemoglobin adducts, except for 2,6-DMA (Figure 1), were higher in smokers than in nonsmokers. The hemoglobin adducts of 2,6-DMA, 3,5-DMA, and 3-EA were independently correlated with bladder cancer risk in both smokers and non-smokers (*4*). Administration of small doses of these three compounds to mice resulted in DNA adduct formation in several tissues, including bladder, colon, liver, kidney, and lung, and 3,5-DMA was shown to have greater carcinogenic potential than the other two (*9*). However, the complex mechanisms involved in the detoxification and bioactivation of these environmental alkylanilines are still unclear.

Arylamine N-acetyltransferases (NATs) are important because they catalyze the N-acetylation of arylamines, which contributes to their detoxification. (*10, 11*). There are two NAT isoforms in human, NAT1 and NAT2, which showed overlapping

but distinct substrate-specificities (*12-14*). The successful purification of recombinant human NAT1 and NAT2 made it possible to investigate the substrate specificities of NATs for N-acetylation of a series of ring-substituted alkylanilines, including the nine alkylanilines studied by Gan and co-workers, as well as ANL, 2-MA, and 4-MA.

The objective of this research is two-fold: to determine k_{cat}/K_m values for N-acetylation of a group of toxicologically significant environmental arylamines, some of which are linked to bladder cancer, and to understand how NATs achieve substrate specificities. The results of this research might provide valuable information on why certain arylamines are detoxified in an NAT-delendent manner whereas others are not.

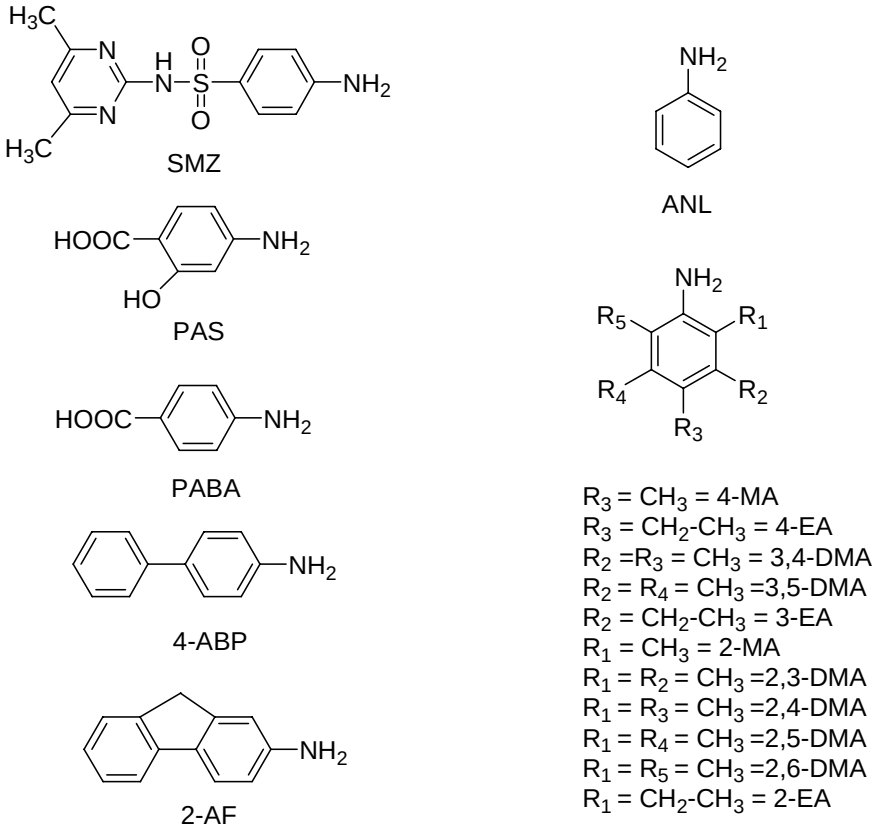

Figure 1. Structures of arylamines (aromatic amines) used in this study.

Materials and Methods

Recombinant human NAT1 was overexpressed and purified as described previously (*15*). Recombinant human NAT2 was overexpressed and purified as described in Part I. *p*-Anisidine, 4-aminobiphenyl (4-ABP), 3-(*N*-morpholino)propanesulfonic acid (MOPS), *p*-aminobenzoic acid (PABA) (sodium salt), *p*-aminosalicylic acid (PAS), and *p*-nitrophenyl acetate (PNPA) were purchased from Sigma (St. Louis, MO). Other arylamines were from Aldrich (Milwaukee, WI) or Acros Organics (Morris Plains, NJ). Protein concentrations were determined by the method of Bradford (*16*). Spectrophotometric data were acquired on a Varian Cary 50 UV-vis spectrophotometer. All buffers were degassed under vacuum, and all incubations were conducted under aerobic conditions. Kinetic data were analyzed with the JMP IN software suite (SAS Institute, Inc.). **Caution:** *4-ABP and alkylanilines should be handled in accordance with NIH Guidelines for the Laboratory Use of Chemical Carcinogens* (*17*)

NAT1 and NAT2 Activity Assay. The NAT2 activity assay was performed with PNPA as the acetyl donor and *p*-anisidine as the acetyl acceptor as described previously (Part I of this thesis). The NAT1 activity assay was conducted as described for NAT2, except the final concentration of NAT1 was 0.5 μg/mL (14.6 nM), and PABA (0.5 mM) was used as the acetyl acceptor (*15*).

Substrate Specificities of Human NAT1 and NAT2. In a final volume of 500 μL, purified NAT1 or NAT2 was incubated with PNPA (2 mM) and various

concentrations of arylamine substrates in MOPS buffer (100 mM, pH 7.0; 150 mM NaCl; 0.1 mM DTT). Protein concentrations were adjusted to obtain reaction rates that were linear with time during the incubation period. The reactions were initiated by addition of PNPA dissolved in DMSO. The final concentration of DMSO was 1%. The initial velocities of the reactions were determined at 37 °C as described for the NAT activity assays. The nonenzymatic hydrolysis of PNPA was measured by conducting incubations in the absence of enzyme. Substrate concentrations (μM) for NAT1 were: SMZ, 3000; PABA, 40-350; PAS, 25-400; 4-ABP, 20-1000; 2-AF, 20-600; ANL, 200-10000; 4-MA, 100-1000; 4-EA, 100-1000; 3,4-DMA, 50-1000; 3,5-DMA, 70-2000; 3-EA, 80-1500; 2-MA, 500-10000; 2,3-DMA, 300-7000; 2,4-DMA, 300-7000; 2,5-DMA, 3000-50000; 2,6-DMA, 50000; 2-EA, 20000. Substrate concentrations (μM) for NAT2 were: SMZ, 400-8000; PABA, 4000-60000; PAS, 2000-12000; 4-ABP, 50-1000; 2-AF, 50-600; ANL, 800-10000; 4-MA, 500-15000; 4-EA, 500-8000; 3,4-DMA, 100-1200; 3,5-DMA, 50-1000; 3-EA, 250-8000; 2-MA, 2000-15000; 2,3-DMA, 1000-8000; 2,4-DMA, 600-10000; 2,5-DMA, 200-10000; 2,6-DMA, 50000; 2-EA, 200-8000.

Nano-ESI-Q-TOF MS of Purified Recombinant Human NAT2. Human NAT2 samples were desalted with Millipore C18 ZipTips according to the supplier's instructions for peptides in solution with a high concentration of salt. ESI mass spectra were obtained with a QSTAR Pulsar I quadrupole time-of-flight (Q-TOF) mass spectrometer (ABI, Foster City, CA) equipped with a nano-ESI source (Protana Engineering). The ESI voltage was 1000 V; the TOF region acceleration voltage was

4 kV; and the injection pulse repetition rate was 6.0 kHz. Mass spectra were the average of 300 scans collected in the positive ion mode. Protein zero-charge mass was acquired by deconvolution of the series of multiply charged protein peaks from 700-3000 m/z with the Bayesian Reconstruct tool in the BioAnalyst software package (ABI).

Modeling of Arylamines into the Catalytic Cavities of Human NAT1 and NAT2. The lowest energy model structure of the human NAT1/PABA complex obtained as previously described was used to produce models for human NAT1 complexed with 4-MA, 3,5-DMA, and 3-EA (*18*). The substrates were generated by using the BUILDER module in Insight II, and their aryl ring carbon atoms were superimposed onto those of PABA. Ligplot was used to analyze the interactions between human NAT1 and the bound substrate (*19*). Similarly, the lowest energy model structure of the human NAT1/PABA complex obtained as described was used to generate the structural model of human NAT2 complexed with 3,5-DMA (*18*). In particular, the MODELER module of Insight II was used to produce a model structure of human NAT2 based on that of human NAT1 complexed with PABA. The backbone atoms of this NAT2 structure were superimposed onto those of human NAT1 in its structural complex with 3,5-DMA to produce the NAT2/3,5-DMA structure. Ligplot was used to analyze the interactions between human NAT2 and the bound substrate (*19*).

Results

Kinetic Data Analysis. The substrate specificities of human NAT1 and NAT2 were determined by steady-state kinetics experiments as previously described (*15*). Scheme 1 shows the equations and derivations used to determine specificity constants. Since catalysis by NATs involves a ping-pong bi-bi mechanism, initial velocity (V), k_{cat}, K_{ma}, and K_{mb} are determined by equations 1 to 4, respectively (Scheme 1) (*20*). All the derivations from equation 1 to equation 15 are shown, and $k_{cat,app}$ and $K_{mb,\ app}$ are determined with equations 16 and 10, respectively (Scheme 1).

The initial velocities of the N-acetylation reactions were measured with a fixed concentration (2 mM) of PNPA as the acetyl donor and various concentrations of arylamine acetyl acceptors. The $k_{cat,app}$ and $K_{mb,\ app}$ values were determined by using nonlinear regression analysis to fit the initial velocities to equation 15 (Scheme 1). The $k_{cat,app}/K_{mb,app}$ ratio is quantitatively equal to the specificity constant (k_{cat}/K_{mb}), which is determined by $k_3k_4/(k_{-3} + k_4)$ (Scheme 1, equation 17). Because NATs catalyze the reactions through a ping-pong bi-bi mechanism and the values of k_{-3}, k_3, and k_4 are independent of the properties of the acetyl donor, $k_{cat,app}/K_{mb,app}$, corresponding to k_{cat}/K_{mb}, is independent of the acetyl donor, and represents the specificity of the enzyme for the arylamine substrates. The arylamine substrates investigated in this study are shown in Figure 1 and the kinetic constants are reported in Table 1.

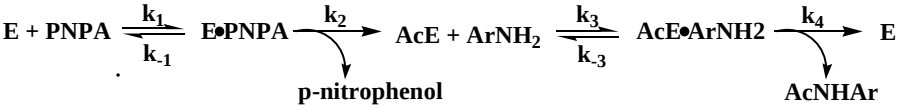

$$V = \frac{V_{max}[A][B]}{K_{ma}[B] + K_{mb}[A] + [A][B]} \qquad [A] = [PNPA]=2\ mM,\ [B] = [ArNH2] \quad (1)$$

$$k_{cat} = \frac{k_2k_4}{k_2 + k_4} \quad (2) \qquad K_{ma} = \frac{k_{-1} + k_2}{k_1} \times \frac{k_4}{k_2 + k_4} \quad (3) \qquad K_{mb} = \frac{k_{-3} + k_4}{k_3} \times \frac{k_2}{k_2 + k_4} \quad (4)$$

$$V = \frac{V_{max}[B]}{K_{ma}\frac{[B]}{[A]} + K_{mb} + [B]} \quad (5)$$

$$V = \frac{V_{max}[B]}{K_{mb} + K_{ma}\frac{[B]}{[A]} + [B]} \quad (6)$$

$$V = \frac{V_{max}[B]}{K_{mb} + [B](1 + \frac{K_{ma}}{[A]})} \quad (7)$$

$$V = \frac{\frac{V_{max}}{(1 + \frac{K_{ma}}{[A]})}[B]}{\frac{K_{mb}}{(1 + \frac{K_{ma}}{[A]})} + [B]} \quad (8) \qquad (V_{max})_{app} = \frac{V_{max}}{1 + \frac{K_{ma}}{[A]}} \quad (9) \qquad (K_{mb})_{app} = \frac{K_{mb}}{1 + \frac{K_{ma}}{[A]}} \quad (10)$$

$$V = \frac{(V_{max})_{app}[B]}{(K_{mb})_{app} + [B]} \quad (11) \qquad V = k_{obs}[E] \quad (12) \qquad (V_{max})_{app} = (k_{cat})_{app}[E] \quad (13) \qquad V_{max} = k_{cat}[E] \quad (14)$$

$$k_{obs} = \frac{(k_{cat})_{app}[B]}{(K_{mb})_{app} + [B]} \quad (15) \qquad (k_{cat})_{app} = \frac{k_{cat}}{(1 + \frac{K_{ma}}{[A]})} \quad (16)$$

$$\frac{(k_{cat})_{app}}{(K_{mb})_{app}} = \frac{\frac{k_{cat}}{(1 + \frac{K_{ma}}{[A]})}}{\frac{K_{mb}}{1 + \frac{K_{ma}}{[A]}}} = \frac{k_{cat}}{K_{mb}} = \frac{k_4}{\frac{k_{-3} + k_4}{k_3}} = \frac{k_3k_4}{k_{-3} + k_4} \quad (17)$$

Scheme 1

compound	NAT1[a]			NAT2[a]			k_{cat}/K_m (NAT1) / k_{cat}/K_m (NAT2)
	$K_{mb,app}$ (μM)	$k_{cat,app}$ (s^{-1})	k_{cat}/K_m (s^{-1} mM^{-1})	$K_{mb,app}$ (μM)	$k_{cat,app}$ (s^{-1})	k_{cat}/K_m (s^{-1} mM^{-1})	
SMZ	ND[b]	ND[b]		5390 ± 520	387 ± 20	72	
PABA	84 ± 7.9	298 ± 10	3550	152000 ± 39100	38 ± 7.5	0.25	14200
PAS	59 ± 9.2	591 ± 32	10000	5390 ± 530	27 ± 1.1	5.0	2000
4-ABP	191 ± 13	243 ± 5.4	1270	486 ± 23	256 ± 5.6	527	2.41
2-AF	109 ± 11	449 ± 17	4120	286 ± 38	759 ± 46	2650	1.55
ANL	2490 ± 140	281 ± 5.1	113	11200 ± 1790	711 ± 70	63	1.79
4-MA	483 ± 28	303 ± 8.2	627	11800 ± 1290	1600 ± 120	136	4.61
4-EA	205 ± 20	430 ± 14	2100	3270 ± 390	700 ± 34	214	9.80
3,4-DMA	352 ± 21	461 ± 12	1310	688 ± 30	800 ± 18	1160	1.13
3,5-DMA	742 ± 27	308 ± 5.2	415	280 ± 21	1220 ± 37	4360	0.10
3-EA	576 ± 27	310 ± 7.0	538	1320 ± 150	1960 ± 68	1490	0.36
2-MA	2320 ± 170	12 ± 0.33	5.2	7180 ± 130	111 ± 8.1	15	0.35
2,3-DMA	1110 ± 47	27 ± 0.37	24	5530 ± 590	256 ± 16	46	0.52
2,4-DMA	2060 ± 130	67 ± 1.7	32	5030 ± 610	661 ± 39	131	0.24
2,5-DMA	6730 ± 880	5.7 ± 0.23	0.85	3120 ± 305	313 ± 12	100	0.01
2,6-DMA	ND[c]	ND[c]		ND[c]	ND[c]		
2-EA	ND[d]	ND[d]		2110 ± 180	61 ± 5.0	29	

Table 1. Substrate Specificities of Human NAT1 and Human NAT2**.** (From reference 22)

[a] Results are expressed as the means (± SD) of three experiments.

[b] ND, not determined. At an SMZ concentration of 3 mM, the rate of N-acetylation was 7.1 μmol/mg/min. The limit of detection was 2-3 nmol. The lowest quantifiable rate was defined as an absorbance change of 0.1/min.

[c] Not determined. N-acetylation was not detectable at a concentration of 50 mM of 2,6-DMA.

[d] Not determined. The N-acetylation rate of 2-EA (20 mM) by NAT1 was 2.2 μmol/mg/min.

Substrate Specificities of SMZ, PAS, PABA, 4-ABP, and 2-AF. Initially, the second order rate constants for N-acetylation of SMZ, PAS, PABA, 4-ABP, and 2-AF by NAT1 and NAT2 were measured. The second order rate constant for N-acetylation of SMZ by recombinant NAT2 was 72 $s^{-1}mM^{-1}$, whereas the rate of acetylation by NAT1 was so low that the k_{cat}/K_{mb} value could not be determined. This is consistent with previous reports that SMZ is a NAT2 substrate (*12*). PABA and PAS, known NAT1 substrates (*12*), showed 14200- and 2000-fold greater specificity constants with NAT1 than with NAT2. 4-ABP and 2-AF are substrates for both NAT1 and NAT2, but each showed a greater k_{cat}/K_{mb} value with NAT1, which is consistent with the observations of Hein and co-workers (*21*). Thus, the recombinant NAT2 obtained from the purification described in Part I gave consistent results with previous studies (*21, 22*).

Substrate Specificities of 4-Alkyl Substituted Anilines and the NMR-Based Model. Aniline (ANL) was N-acetylated with similar specificity constants by both NAT1 and NAT2 (Table 1). This might be a consequence of the small size of the unsubstituted aromatic ring, which may bind in the substrate binding pocket of both NAT1 (162 $Å^3$) and NAT2 (257 $Å^3$) similarly (*23*). However, 4-MA (p-toluidine) and 4-EA are better substrates for NAT1, which is consistent with previous observations reported by Hein and co-workers (*21*). An NMR-based model, which was constructed by Drs Kylie Walter and Naixia Zhang, showed that the preferred binding of 4-MA by NAT1 is a consequence of one key residue at position 216, namely V216 in NAT1, whereas in NAT2, S216 occupies that position. The 4-methyl group of 4-MA makes

favorable nonbond contacts with a side chain methyl group of V216 in NAT1, but in NAT2, this interaction does not exist (Figure 2) (*22*).

Substrate Specificities of 3-Alkyl Substituted Anilines and the NMR-Based Model. The presence of a 3-alkyl substituent in ANL and 4-methylaniline (4-MA) caused increases in the k_{cat}/K_{mb} values obtained with both NAT1 and NAT2. As shown in Table 1, 3,4-DMA, 3,5-DMA, and 3-EA are all N-acetylated efficiently by both NATs. Compared with 4-MA, the 3-methyl group of 3,4-DMA caused a 2-fold increase in the NAT1 specificity constant and a 9-fold increase in the NAT2 specificity constant. The addition of two meta-methyl substituents to ANL, 3,5-DMA, increased the k_{cat}/K_{mb} value with NAT1 by 4-fold and with NAT2 by 70-fold. The incorporation of 3-ethyl group in ANL, 3-EA, increased the specificity constant with NAT1 by 5-fold and with NAT2 by 20-fold (Table 1). Thus, small 3-alkyl substituents contribute favorable binding interactions with both NATs, with the interaction being more favorable with NAT2 than with NAT1.

NMR model structures of NAT1 and NAT2 complexed with 3,5-DMA are shown in panels A and B of Figure 3. In NAT1, one of the methyl groups of 3,5-DMA engages in favorable bonding interactions with residues S215 and L209, and the other methyl group probably interacts with F217, F215, and V93. In NAT2, the bonding interactions of one methyl group with S215 and L209 are also present, and favorable interactions appear to exist between F217 and the other methyl substitutent. Moreover, several nonbond contacts can occur between the other methyl group and

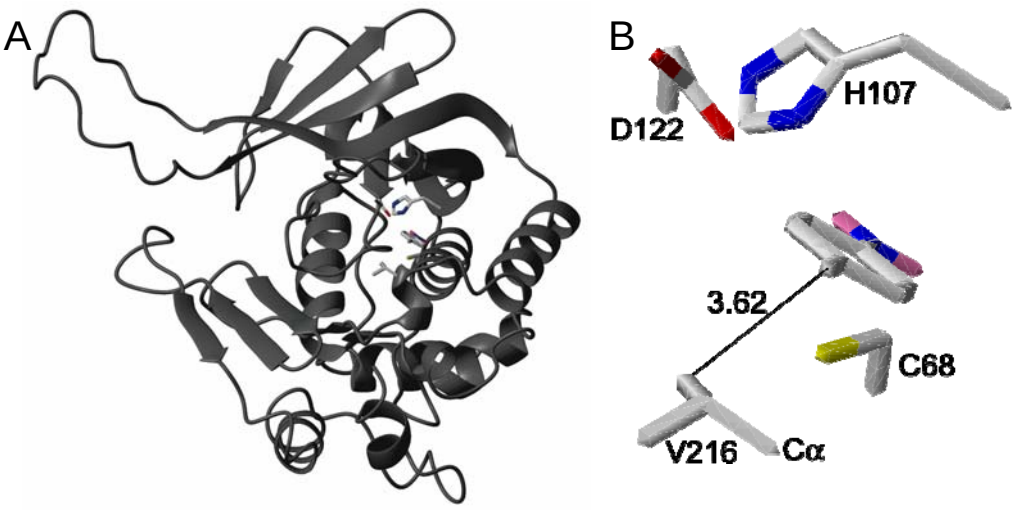

Figure 2. Model structure of human NAT1 bound to 4-MA. (A) Illustrates the position of 4-MA in the protein's interior with secondary structural elements and the bonds of the side chain heavy atoms of the catalytic triad, C68, H107 and D122, as well as V216 and 4-MA displayed. (B) An expanded view is provided to illustrate the contacts between human NAT1 and 4-MA. Carbon, nitrogen, oxygen, sulfur and hydrogen atoms are colored white, blue, red, yellow and pink, respectively, and a hydrophobic contact with V216 is highlighted. (By Dr Naixia Zhang) (From reference 22)

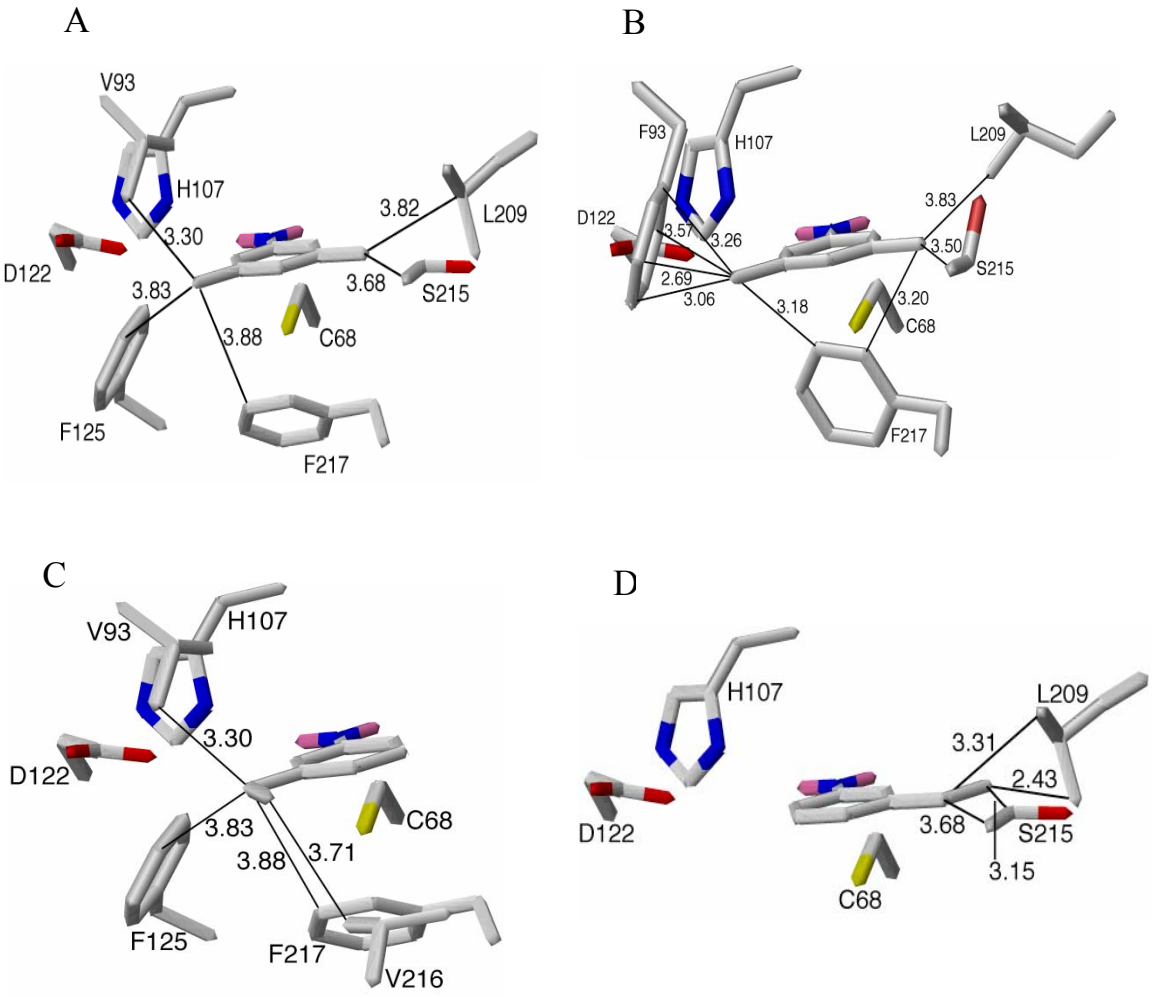

Figure 3. A. Expanded view of 3,5-dimethylaniline (3,5-DMA) bound to human NAT1. B. Expanded view of 3,5-DMA bound to human NAT2. C., D. Model structures of 3-ethylaniline (3-EA) bound to NAT1 in two different orientations. The labeling and color scheme are the same as in Figure 3. The lengths of hydrophobic contacts are represented by the dark lines. (By Dr Naixia Zhang) (From reference 22)

the aromatic ring of F93. These interactions are not available with NAT1, which contains V93, and compensate for the interaction provided by F125 in NAT1, which is substituted by a serine in NAT2. F93 is believed to be a key residue that contributes to the 10-fold higher specificity constant of NAT2, compared to that of NAT1.

The NMR-based model structures of human NAT1 complexed with 3-EA are shown in panels C and D of Figure 3. The 3-ethyl group forms favorable interactions with the same residues in NAT1 and NAT2 as the methyl groups of 3,5-DMA. Due to the larger size and hydrophobicity of the ethyl substituent, a greater number of nonbond contacts can occur between 3-EA and NATs. The more favorable interactions provided between F93 in NAT2 and 3-EA are believed to contribute to the 3-fold higher specificity of NAT2 over NAT1.

Substrate Specificities of 2-Alkyl Substituted Anilines and the NMR-Based Model. The influence of 2-alkyl substituents on the N-acetylation of the ring-substituted anilines was reflected by the results obtained with 2-MA, 2,3-DMA, 2,4-DMA, 2,5-DMA, 2,6-DMA, and 2-EA, which were inefficiently N-acetylated by both NAT1 and NAT2 (Table 1). We observed a 22-fold and 4-fold decrease in the second order rate constant for N-acetylation of 2-MA, relative to that of aniline, for NAT1 and NAT2, respectively. 2,6-DMA, which is a rodent nasal cavity carcinogen (*24*), was not N-acetylated by either NAT1 or NAT2. 2-EA was a substrate for NAT2, but not for NAT1. Thus, 2-alkyl groups decreased N-acetylation rates catalyzed by both NAT1 and NAT2, but were more detrimental to N-acetylation by NAT1 than NAT2.

The unfavorable interactions of the 2-methyl group of 2-MA with F125 in NAT1 was suggested by the NMR-based structural model (*18*). The steric clash involving the 2-methyl group and F125 may hinder binding of 2-MA in the NAT1 catalytic cavity. In NAT2, F125 is substituted with a smaller serine residue, which causes less hindrance to binding with 2-MA and contributes to the 3-fold greater specificity constant of NAT2, compared to that of NAT1. The 20-fold difference in the specificity constants for N-acetylation of 4-MA and 2,4-DMA by NAT1 can be rationalized by the steric hindrance between the 2-methyl substituent and F125 as well. The steric effect of residue 125 in the binding pockets of NAT1 and NAT2 was emphasized by the results obtained with 2-EA, which was N-acetylated by NAT2, but not by NAT1 (Table 1).

Discussion

N-acetylation of amino compounds was first identified as an important biotransformation pathway in humans in 1926 (*25*). In 1965, it was shown that humans express separate enzymes for metabolizing PABA and PAS, or isoniazid and SMZ (*26*). The substrate specificities of human NATs for N-acetylation and detoxification of arylamines have attracted numerous scientists' attention (*12, 14, 21*).

In this study, we determined the specificity constants (k_{cat}/K_{mb}) for N-acetylation of a group of arylamine drugs, environmental contaminants and carcinogens with human NAT1 and NAT2. There is an almost 1000-fold range in the differences in the NAT1/NAT2 ratios of specificity constants for the monosubstituted and disubstituted alkylanilines (Table 1). Subtle changes in substrate structure have pronounced influences on the relative abilities of NAT1 and NAT2 to acetylate the alkylanilines, which triggered the elucidation of the structural determinants of substrate specificity by an NMR-based model (*18, 22*).

One striking effect reflected by the data presented in Table 1 is the influence of 3-alkyl substituents on NAT2 selectivity. The addition of a 3-methyl group to 4-MA, which is a preferential substrate for NAT1, increases the k_{cat}/K_{mb} value for 3,4-DMA with NAT2 by approximately 9-fold over that observed for acetylation of 4-MA. The specificity constant for 3,5-DMA, which contains two meta-methyl groups, obtained with NAT2 is more than 10-fold greater than that with NAT1. The selectivity of NAT2 for N-acetylation of the meta-substituted alkylanilines can be

explained by favorable bonding interactions between the 3-alkyl group and F93 in the binding pocket of NAT2 (Figure 3B). The crystal structures of NAT2 also revealed that F93 introduced a "lip" in the Van der Waals surface of the binding pocket. It is the presence of F93 in NAT2 that makes the sulfonamide class of compounds bind selectively to NAT2 (*23*).

Several studies revealed that residue 125 is a key residue for substrate binding and can determine substrate specificity. Mutagenesis studies with NAT1 showed that conversion of the single amino acid F125 to a serine, which is the 125 residue in NAT2, produced a 220-fold change in apparent K_m for the sulfonamide, SMZ (*27*). An X-ray crystal structure revealed that the F125S mutation in NAT1 does not alter the volume of the substrate binding pocket, but changes the extent of the hydrophobic interactions with the pocket surface (*23*). Another consequence of this steric effect is the selective binding of 2-substituted alkylanilines to NAT2. The steric effect of a 2-alkyl substituent on the formation of the tetrahedral intermediate between the enzyme bound thioacetyl ester and the arylamine substrate would be expected to be similar for reactions catalyzed by both NAT1 and NAT2. Therefore, the steric clash of the F125 with the 2-methyl group of 2-MA, illustrated by the NMR-based model, is an important factor (*18*).

The dramatic decrease of specificity constants caused by the unfavorable interaction between 2-alkyl substituents and F125 was also reflected by the results obtained with PABA and 4-amino-3-methylbenzoic acid (Figure 4). The specificity

constant for N-acetylation of 4-amino-3-methylbenzoic acid by NAT1 showed an approximately 8-fold reduction compared to that of PABA (Table 2) (*18*).

The metabolism of arylamines in vivo is a complicated process, involving several metabolism enzymes and competing pathways, and we should study it in a global way. Genetically manipulated mice are useful models for studying the N-acetylation of the metabolism of arylamines (*28*). The results of the present study, obtained from kinetic and structural investigations, defined how NATs achieve certain substrate specificities and contribute to the in-depth knowledge needed for understanding arylamine metabolism.

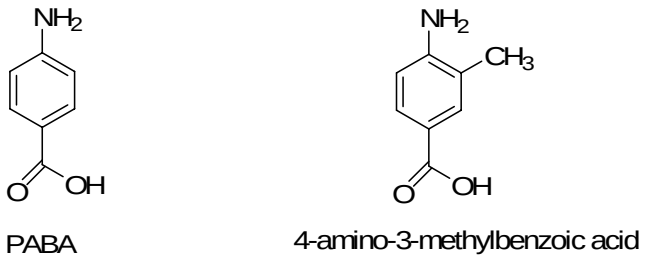

Figure 4. Structures of PABA and 4-amino-3-methylbenzoic acid.

Substrates	NAT1[a,,b]			NAT2[a,,b]		
	$K_{mb,app}$ (μM)	$k_{cat,app}$ (s^{-1})	k_{cat}/K_{mb} ($s^{-1}mM^{-1}$)	$K_{mb,app}$ (μM)	$k_{cat,app}$ (s^{-1})	k_{cat}/K_{mb} ($s^{-1}mM^{-1}$)
PNPA/PABA	49 ± 6	127 ± 5	2599	166000 ± 20000	21 ± 3	0.13
PNPA/4-amino-3-methylbenzoic acid	170 ± 20	16.6 ± 0.5	96.8	11000 ± 1000	1.3 ± 0.05	0.11

Table 2. Substrate Specificities Obtained with PABA and 4-Amino-3-Methylbenzoic Acid**.** (From reference 18)

[a] Results are expressed as the means (± standard deviation) of three experiments.

[b] Experiments were conducted at 23 ° C.

References:

(1) Vineis, P. and Pirastu, R. (1997) Aromatic amines and cancer. *Cancer Causes Control 8*, 346-355.

(2) Talaska, G. (2003) Aromatic amines and human urinary bladder cancer: exposure sources and epidemiology. *J Environ Sci Health C Environ Carcinog Ecotoxicol Rev 21*, 29-43.

(3) Turesky, R. J., Freeman, J. P., Holland, R. D., Nestorick, D. M., Miller, D. W., Ratnasinghe, D. L. and Kadlubar, F. F. (2003) Identification of aminobiphenyl derivatives in commercial hair dyes. *Chem Res Toxicol 16*, 1162-1173.

(4) Gan, J., Skipper, P. L., Gago-Dominguez, M., Arakawa, K., Ross, R. K., Yu, M. C. and Tannenbaum, S. R. (2004) Alkylaniline-hemoglobin adducts and risk of non-smoking-related bladder cancer. *J Natl Cancer Inst 96*, 1425-1431.

(5) Yu, M. C., Skipper, P. L., Tannenbaum, S. R., Chan, K. K. and Ross, R. K. (2002) Arylamine exposures and bladder cancer risk. *Mutat Res 506-507*, 21-28.

(6) Gaber, K., Harreus, U. A., Matthias, C., Kleinsasser, N. H. and Richter, E. (2007) Hemoglobin adducts of the human bladder carcinogen o-toluidine after treatment with the local anesthetic prilocaine. *Toxicology 229*, 157-164.

(7) Gorlewska-Roberts, K., Green, B., Fares, M., Ambrosone, C. B. and Kadlubar, F. F. (2002) Carcinogen-DNA adducts in human breast epithelial cells. *Environ Mol Mutagen 39*, 184-192.

(8) Gago-Dominguez, M., Bell, D. A., Watson, M. A., Yuan, J. M., Castelao, J. E., Hein, D. W., Chan, K. K., Coetzee, G. A., Ross, R. K. and Yu, M. C. (2003)

Permanent hair dyes and bladder cancer: risk modification by cytochrome P4501A2 and N-acetyltransferases 1 and 2. *Carcinogenesis 24*, 483-489.

(9) Skipper, P. L., Trudel, L. J., Kensler, T. W., Groopman, J. D., Egner, P. A., Liberman, R. G., Wogan, G. N. and Tannenbaum, S. R. (2006) DNA adduct formation by 2,6-dimethyl-, 3,5-dimethyl-, and 3-ethylaniline in vivo in mice. *Chem Res Toxicol 19*, 1086-1090.

(10) Hanna, P. E. (1996) Metabolic activation and detoxification of arylamines. *Curr. Med. Chem. 3*, 195-210.

(11) Hanna, P. E. (1994) N-acetyltransferases, O-acetyltransferases, and N,O-acetyltransferases: enzymology and bioactivation. *Adv Pharmacol 27*, 401-430.

(12) Grant, D. M., Blum, M., Beer, M. and Meyer, U. A. (1991) Monomorphic and polymorphic human arylamine N-acetyltransferases: a comparison of liver isozymes and expressed products of two cloned genes. *Mol Pharmacol 39*, 184-191.

(13) Hickman, D., Palamanda, J. R., Unadkat, J. D. and Sim, E. (1995) Enzyme kinetic properties of human recombinant arylamine N-acetyltransferase 2 allotypic variants expressed in Escherichia coli. *Biochem Pharmacol 50*, 697-703.

(14) Kawamura, A., Graham, J., Mushtaq, A., Tsiftsoglou, S. A., Vath, G. M., Hanna, P. E., Wagner, C. R. and Sim, E. (2005) Eukaryotic arylamine N-acetyltransferase. Investigation of substrate specificity by high-throughput screening. *Biochem Pharmacol 69*, 347-359.

(15) Wang, H., Vath, G. M., Kawamura, A., Bates, C. A., Sim, E., Hanna, P. E. and Wagner, C. R. (2005) Over-expression, purification, and characterization of recombinant human arylamine N-acetyltransferase 1. *Protein J 24*, 65-77.

(16) Bradford, M. M. (1976) A rapid and sensitive method for the quantitation of microgram quantities of protein utilizing the principle of protein-dye binding. *Anal Biochem 72*, 248-254.

(17) *NIH Guidelines for the Laboratory Use of Chemical Carcinogens* (1981) NIH Publication No. 81-2385, U.S. Government Printing Office, Washington, DC.

(18) Zhang, N., Liu, L., Liu, F., Wagner, C. R., Hanna, P. E. and Walters, K. J. (2006) NMR-based model reveals the structural determinants of mammalian arylamine N-acetyltransferase substrate specificity. *J Mol Biol 363*, 188-200.

(19) Wallace, A. C., Laskowski, R. A. and Thornton, J. M. (1995) LIGPLOT: a program to generate schematic diagrams of protein-ligand interactions. *Protein Eng 8*, 127-134.

(20) Segel, I. H. (1975) Enzyme kinetics: behavior and analysis of rapid equilibrium and steady-state enzyme systems. *pp. 606-612*.

(21) Hein, D. W., Doll, M. A., Rustan, T. D., Gray, K., Feng, Y., Ferguson, R. J. and Grant, D. M. (1993) Metabolic activation and deactivation of arylamine carcinogens by recombinant human NAT1 and polymorphic NAT2 acetyltransferases. *Carcinogenesis 14*, 1633-1638.

(22) Liu, L., Von Vett, A., Zhang, N., Walters, K. J., Wagner, C. R. and Hanna, P. E. (2007) Arylamine N-acetyltransferases: characterization of the substrate

specificities and molecular interactions of environmental arylamines with human NAT1 and NAT2. *Chem Res Toxicol 20*, 1300-1308.

(23) Wu, H., Dombrovsky, L., Tempel, W., Martin, F., Loppnau, P., Goodfellow, G. H., Grant, D. M. and Plotnikov, A. N. (2007) Structural basis of substrate-binding specificity of human arylamine N-acetyltransferases. *J Biol Chem 282*, 30189-30197.

(24) U. S. National Toxicology Program (1990) *Toxicology and Carcinogenesis Studies of 2,6-Xylidine (2,6-Dimethylaniline) (CAS No. 87-62-7) in Charles River CD Rats (Feed Studies).* Technical Report Series No. 278, NTP, Research Triangle Park, NC.

(25) Muenzen, J. B., Cerecedo, L. R., and Sherwin, C. P. (1926) Comparative Metabolism of Certain Aromatic Acids. VIII Acetylation of Amino Compounds. *Journal of Biological Chemistry 67*, 469-476.

(26) Jennne, J. W. (1965) Partial purification and properties of the isoniazid transacetylase in human liver. Its relationship to the acetylation of p-aminosalicylic acid. *J Clin Invest 44*, 1992-2002.

(27) Goodfellow, G. H., Dupret, J. M. and Grant, D. M. (2000) Identification of amino acids imparting acceptor substrate selectivity to human arylamine acetyltransferases NAT1 and NAT2. *Biochem J 348 Pt 1*, 159-166.

(28) Sugamori, K. S., Brenneman, D. and Grant, D. M. (2006) In vivo and in vitro metabolism of arylamine procarcinogens in acetyltransferase-deficient mice. *Drug Metab Dispos 34*, 1697-1702.

PART III: HUMAN ARYLAMINE N-ACETYLTRANSFERASE 1: IN VITRO AND INTRACELLULAR INACTIVATION BY NITROSOARENE METABOLITES OF TOXIC AND CARCINOGENIC ARYLAMINES

Introduction

N-Acetylation of arylamines to arylamides by arylamine N-acetyltransferases (NATs) is considered to be a detoxification pathway (Figure 1a), which competes with oxidation of arylamines to N-arylhydroxylamines by cytochrome P450s (Figure 1b) (*1*, *2*). Inactivation of intracellular NATs by exogenous or endogenous chemical agents would impair the key detoxification pathways and could result in enhanced cell toxicity and carcinogenesis.

Arylamines and their N-hydroxylation products, N-arylhydroxylamines, can undergo oxidation to form nitrosoarenes in vivo (Figure 1b and 1c). Nitrosoarenes also can be formed from metabolic reduction of therapeutic agents, containing aromatic nitro groups, and environmental nitroarenes, such as 2-nitrofluorene and 1-nitropyrene (Figure 1d) (*3*-*5*). It has been found that 2-nitrosofluorene (2-NO-F) uncouples oxidative phosphorylation in isolated mitochondrial preparations and reacts with double bonds in microsomal membrane lipids to produce nitroxyl free radicals (*6*). Nitrosoarenes attracted our interest because the electrophilicity of nitrosoarenes makes them react readily with intracellular nucleophilic thiols, such as those present in glutathione (GSH) and proteins (*7*-*11*).

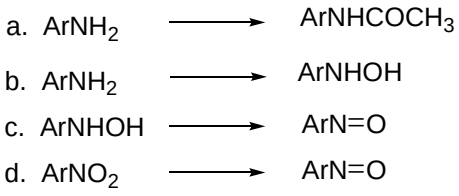

Figure 1. Metabolism of arylamines and formation of nitrosoarenes.

4-Nitrosobiphenyl (4-NO-BP), the nitroso metabolite of the tobacco smoke component, 4-aminobiphenyl (4-ABP), has been shown to cause irreversible inactivation of human NAT1 in vitro. Mass spectrometric analysis revealed that the reaction between 4-NO-BP and the catalytically essential and highly nucleophilic Cys68 of human NAT1 formed a sulfinamide adduct in vitro (*11*). It is critical to understand that exposure to nitrosoarene metabolites of environmental arylamines may result in inactivation of NAT1 and a decreased ability to detoxify environmental arylamines.

In this study, we investigated the inactivation of human NAT1 by the nitrosoarene metabolites of four environmental arylamines in vitro and in human cells. The objective of this research is to test the hypothesis: the nitroso derivatives of arylamines, that are good substrates for human NAT1, would be potent NAT1 inactivators. In contrast, the nitrosoarene metabolites of arylamines, that are poor substrates for NAT1, would be much less effective inactivators of the enzyme. The k_{cat}/K_m values for N-acetylation 4-aminobiphenyl (4-ABP) and 2-aminofluorene (2-AF) by recombinant NAT1 are 1270 $s^{-1}mM^{-1}$ and 4120 $s^{-1}mM^{-1}$. However, the corresponding rate constants for aniline (ANL) and 2-methylaniline (o-toluidine) (2-MA) are 113 $s^{-1}mM^{-1}$ and 5.2 $s^{-1}mM^{-1}$ (*12*). Thus, 4-nitrosobiphenyl (4-NO-BP) and 2-nitrosofluorene (2-NO-F) are proposed to be potent inactivators of NAT1 and nitrosobenzene (NO-B) and 2-nitrosotoluene (2-NO-T) are anticipated to be much weaker inhibitors (Figure 2).

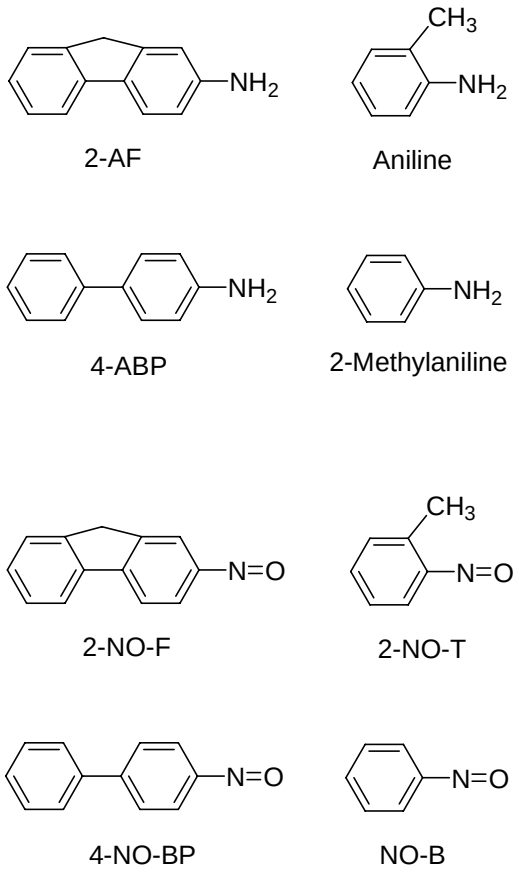

Figure 2. Structures of arylamines and their nitrosoarene metabolites used in this study.

Materials and Methods

Recombinant human NAT1 and NAT2 were prepared as described previously (*12, 13*). N-OH-4-AABP, N-OH-AAF, 4-NO-BP, and 2-NO-F were synthesized as reported (*10, 11, 14, 15*). Human NAT1 polyclonal antibody was provided by Prof. E. Sim (University of Oxford, Oxford, UK) (*16*). Acetyl coenzyme A (AcCoA), *p*-anisidine, anti-beta actin, glyceraldehyde 3-phosphate, GSH, GSSG, goat anti-rabbit IgG horseradish peroxidase, monoclonal anti-beta EZview^{TM} Red ANTI-FLAG M2 Affinity Gel, 3-(*N*-morpholino)propanesulfonic acid (MOPS), NO-B, NADPH, p-aminobenzoic acid (PABA), *p*-nitrophenylacetate (PNPA), pepsin A, sulfamethazine (SMZ) were purchased from Sigma (St. Louis, MO). Bio-Spin 6 Tris columns were obtained from Bio-Rad (Hercules, CA). 2-NO-T was purchased from Aldrich (Milwaukee, WI). HeLa, MDA-MB-231, MDA-MB-468, and MCF-7 cells, and Minimum Essential Medium (MEM) were obtained from American Type Culture Collection (Rockville, MD). Dulbecco modified Eagle medium (DMEM) was purchased from Mediatech (Herndon, VA). Fetal bovine serum (FBS) was purchased from Atlanta Biologicals (Lawrenceville, GA). Phosphate-buffered saline (PBS), trypsin-EDTA, penicillin-streptomycin-fungizome, Lipofectamine 2000 transfection kit, 4-12% SDS-polyacrylamide gels, and PVDF membranes were obtained from Invitrogen (Carlsbad, CA). Goat anti-rabbit IgG horseradish peroxidase was obtained from Amersham Biosciences (Piscataway, NJ). Restore Plus Western Blot Stripping Buffer was purchased from Pierce (Rockford, IL). Protein concentrations were determined by the method of Bradford (*17*). All experiments were conducted in degassed buffers and under aerobic conditions. Spectrophotometric data were acquired on a Varian Cary 50 UV-vis

spectrophotometer equipped with a circulation water bath. Kinetic data were analyzed with the JMP IN software suite (SAS Institute, Inc.). Statistical significance of differences between means was assessed with Student's *t* test. IC_{50} and LC_{50} values were calculated with Kaleidagraph 3.6 (Synergy Software). **Caution:** *N-OH-4-AABP, N-OH-AAF; 4-NO-BP, 2-NO-F, NO-B, and 2-NO-T should be handled in accordance with NIH Guidelines for the Laboratory Use of Chemical Carcinogens (18).*

NAT1 Activity Assay. The activity assay with human recombinant NAT1 was conducted as described previously (Part II of this thesis).

Time-Dependent Inactivation of NAT1 by Nitrosoarenes at 37 °C. The incubation mixtures contained NAT1 (35 μg/mL, 1 μM), 4-NO-BP (0.1-5 μM), 2-NO-F (0.1-2 μM), NO-B (100-1250 μM), or 2-NO-T (100-1200 μM) and potassium phosphate buffer (20 mM, pH 7.4; 1 mM EDTA) in a total volume of 75 μL. The reaction was initiated by addition of nitrosoarene dissolved in DMSO (1.5 μL). The final concentration of DMSO was 2%. Aliquots (2 μL) were withdrawn at 15 s (4-NO-BP, 2-NO-F), 30 s (2-NO-T), or 60 s (NO-B) intervals and transferred to an assay cuvett. The controls contained DMSO, but not nitrosoarene.

Inactivation of NAT1 by NO-B and 2-NO-T in the Presence of AcCoA. In a total volume of 98 μL, NAT1 (35 μg/mL, 1 μM) was incubated with AcCoA (20 μM) in potassium phosphate buffer (20 mM, pH 7.4; 1 mM EDTA) at 37 ºC. After 1 min, 2-NO-T or NO-B dissolved in DMSO (2 μL) was added. The final

concentrations of 2-NO-T and NO-B were 300 μM and 250 μM, respectively. After incubation for 2 min (2-NO-T) or 4 min (NO-B), aliquots (2 μL) were withdrawn and assayed for NAT1 activity.

Inactivation of NAT1 by 4-NO-BP and 2-NO-F in the Presence of GSH. To NAT1 in potassium phosphate buffer (20 mM, pH 7.4; 1 mM EDTA) was added GSH dissolved in 1 μL of potassium phosphate buffer. After 2 min at 37 °C, either 4-NO-BP or 2-NO-F dissolved in DMSO (3 μL) was added. The final concentrations were: NAT1, 25 μg/mL (0.72 μM); GSH, 0.5, 1, or 5 mM; 4-NO-BP or 2-NO-F, 1, or 5 μM; DMSO, 2%, in a total volume of 150 μL. After a 30 or 60 s incubation, aliquots (2 μL) were withdrawn and transferred to an assay cuvett. Controls contained only potassium phosphate buffer and DMSO. There was no significant difference between control activities determined in the presence and absence of GSH ($p > 0.2$).

Sample Preparation for Nano-ESI-Q-TOF MS of 2-NO-F-Treated NAT1. To NAT1 (120 μg, 43 μM) in potassium phosphate buffer (80 μL, 20 mM, pH 7.4; 1 mM EDTA; 10% glycerol; 0.1 mM DTT) was added 2-NO-F dissolved in 2 μL of DMSO. The final concentration of 2-NO-F was 250 μM. DMSO only was added to the control incubation mixtures. After a 5 min incubation at 37 °C, a portion (10 μL) of the reaction mixture was used to measure the residual activity. The reaction mixture was loaded onto a Bio Spin 6 Tris Column. After centrifugation, the sample was concentrated to 30 μL by freeze drying.

Nano-ESI-Q-TOF MS of 2-NO-F-Treated NAT1. The NAT1 samples were desalted with Millipore C4 ZipTips according to the supplier's protocol. ESI mass spectra were acquired as described (*11*).

Pepsin Digestion of 2-NO-F-Treated NAT1. NAT1 was inactivated with 2-NO-F under conditions identical with those described above for the sample preparation for Nano-ESI-Q-TOF MS. The digestion was conducted as previously reported (*11*).

MS Screening and Sequencing of Peptides. Peptides were desalted and analyzed by MALDI Q-TOF MS and sequenced by MALDI Q-TOF MS/MS as previously reported (*11*).

Cell Culture Conditions. HeLa, MDA-MB-231, and MDA-MB-468 cells were maintained as monolayers in DMEM supplemented with 10% FBS and 1% penicillin-streptomycin-fungizome in a humidified, 5% CO_2 atmosphere at 37 ºC. MCF-7 cells were grown as an adherent monolayer in MEM supplemented with 10% FBS, and 1% penicillin-streptomycin-fungizome in a humidified, 5% CO_2 atmosphere at 37 ºC.

Western Blot Analysis of Endogenous NAT1 in HeLa Cells. At approximately 90% confluence, cell monolayers (100 mm plate, 3.45 x 10^6 cells) were washed with 5 mL of PBS. Cell monolayers were exposed to 2 mL of trypsin-EDTA and incubated for 3 min at 37 ºC. Monolayers were washed with PBS buffer (10 mL) and centrifuged for 5 min at 1000g (4 ºC). Cells were

resuspended in 0.8 mL of lysis buffer (20 mM Tris-HCl, pH 7.5; 1 mM EDTA; 0.1% Triton X-100; 1 mM PMSF; 1 mM benzamidine; 1.4 μM pepstatin A; 2.0 μM leupeptin) and disrupted at 4 ºC by sonication (5 x 5-s bursts). The cell lysate was centrifuged for 15 min at 13,000 rpm (4 ºC) and the supernatant was withdrawn for analysis. The cell cytosol was subjected to electrophoresis on 4-12% SDS-polyacrylamide gels and transferred to PVDF membranes (30 V, 70 min, room temperature). Membranes were blocked with TBS/Tween 20 (0.05%) supplemented with 5% (w/v) nonfat milk powder. The membranes were incubated overnight at 4 °C with primary antibody (anti-NAT1, 1:4000) in TBS/Tween 20 supplemented with 5% (w/v) nonfat milk powder. The membranes were washed three times for 10 min with TBS/Tween 20. Secondary conjugated antibody (goat anti-rabbit IgG horseradish peroxidase, 1: 4000) in TBS/Tween 20 supplemented with 5% (w/v) nonfat milk powder was added and the membrane was incubated at room temperature for 1 h followed by four 10-min washes with TBS/Tween 20. The Enhanced Chemiluminescence Western Blotting analysis system (Amersham Biosciences, Piscataway, NJ) was used for detection. The membranes were scanned with a Chemifluorescence Workstation (Molecular Dynamics Storm 840, Sunnyvale, CA) and analyzed with Glyko BandScan Analysis Software (Glyko, Inc., Novato, CA) or the relative densities of the bands were analyzed with a Bio-Rad Model GS-700 Imaging Densitometer.

The membranes were incubated with 20 mL of Restore Plus Western Blot Stripping Buffer for 15 min at room temperature to remove primary and secondary antibodies and washed with TBS/Tween 20 according the supplier's protocol. Membranes were blocked with TBS/Tween 20 supplemented with 5% nonfat milk

powder. The membranes were incubated with primary antibody (anti-beta actin, 1:4000) in TBS/Tween 20 for 1 h and washed with TBS/Tween 20. Secondary conjugated antibody (goat anti-mouse IgG horseradish peroxidase, 1: 4000) in TBS/Tween 20 was added. After the membrane was incubated for 1 h and washed with TBS/Tween 20, the signal was detected and quantified as described above.

NAT1 Activity in HeLa Cell Cytosol. Cell cytosol (50 μL) and PABA, dissolved in 40 μL of assay buffer (20 mM Tris-HCl, 1 mM EDTA, pH 7.5) were incubated at 37 ºC for 5 min. AcCoA dissolved in 10 μL of assay buffer was added. The final concentrations were: PABA, 200 μM; AcCoA, 400 μM. The incubation was continued at 37 ºC for various lengths of time (2-10 min). Cold trichloroacetic acid (20% w/v) (100 μL) was added, followed by centrifugation for 5 min at 12000g. The supernatant was added to 4-dimethylaminobenzaldehyde (800 μL, 5% w/v in 9:1 acetonitrile/water). The unreacted PABA was quantitated by measuring the absorbance at 450 nm (ε_{450nm} = 6400 $M^{-1}cm^{-1}$) (*19*). All assays were performed in triplicate under initial rate conditions. The controls contained either assay buffer only, AcCoA without PABA, or PABA without AcCoA. When PAS (200 μM) was used as acetyl acceptor, the unreacted PAS was quantitated by measuring the absorbance at 405 nm (ε_{405nm} = 1300 $M^{-1}cm^{-1}$) (*19*).

GAPDH Activity in HeLa Cell Cytosol. Cell cytosol (20 μL), glyceraldehyde 3-phosphate (4 mM), and NAD^+ (1 mM) were dissolved in 100 mM potassium phosphate buffer (10 mM EDTA, 0.1 mM DTT, pH 7.4). The final volume was 1 mL. NADH formation was monitored at 340 nm for 1min at 37 °C (*20*).

GR Activity in HeLa Cell Cytosol. Cell cytosol (40 μL) was incubated with 40 μL of 6 mM EDTA, 40 μL of 22 mM GSSG, and 240 μL of 180 mM sodium phosphate buffer (pH 7.2) for 5 min. The reaction was started by the addition of 40 μL of 4.5 mM NADPH. The rate of disappearance of NADPH was measured at 340 nm for 3 min at 37 °C (*21*).

Effect of 4-NO-BP, 2-NO-F, NO-B, and 2-NO-T on NAT1 Activity in HeLa Cell Cytosol. In a total volume of 50 μL, cell cytosol (48 μL) was incubated with either 4-NO-BP (10-300 nM), 2-NO-F (10-300 nM), NO-B (50-750 μM), or 2-NO-T (25-1000 μM) at 37 ºC for 10 min. The reaction was initiated by the addition of the nitrosoarenes dissolved in DMSO (2 μL). PABA and AcCoA dissolved in assay buffer (50 μL) and warmed to 37 ºC for 5 min, were added to the mixtures. The final concentrations were: PABA, 200 μM; AcCoA, 400 μM. Residual NAT1 activity was measured as described above. The control incubations contained DMSO, but not nitrosoarene.

Effect of AcCoA on 4-NO-BP, 2-NO-F, NO-B, and 2-NO-T Inactivation of NAT1 in HeLa Cell Cytosol. To cell cytosol (46 μL) was added AcCoA dissolved in assay buffer (2 μL). The mixture was incubated for 5 min at 37 ºC followed by the addition of 4-NO-BP, 2-NO-F, NO-B, or 2-NO-T in DMSO (2 μL). The final concentrations were: AcCoA, 400 μM; 4-NO-BP, 100 nM; 2-NO-F, 50 nM; NO-B, 500 μM; 2-NO-T, 100 μM. After incubation for 10 min at 37 ºC, PABA and AcCoA dissolved in assay buffer (50 μL) were added. The final concentrations were: PABA, 200 μM; AcCoA, 400 μM. Residual NAT1 activity

was measured as described above. For experiments without AcCoA, cell cytosol (46 μL) was incubated with 2 μL of assay buffer for 5 min. Nitrosoarenes (2 μL) were added and incubations were continued for 10 min. PABA and AcCoA dissolved in 50 μL of assay buffer were added and NAT1 activity was measured.

Effect of Nitrosoarenes on GAPDH Activity in HeLa Cell Cytosol. In a total volume of 50 μL, cell cytosol (48 μL) was incubated with 4-NO-BP (100-3000 nM), 2-NO-F (100-3000 nM), NO-B (200-4000 μM), or 2-NO-T (500-2000 μM) at 37 ºC for 10 min. The reaction was initiated by the addition of the nitrosoarenes dissolved in DMSO (2 μL). A 20 μL portion of the incubation mixture was withdrawn to determine residual GAPDH activity. The controls contained DMSO, but not nitrosoarenes.

Effect of Nitrosoarenes on GR Activity in HeLa Cell Cytosol. In a total volume of 100 μL, cell cytosol (96 μL) was incubated with 4-NO-BP (100-1500 nM), 2-NO-F (100-2000 nM), NO-B (800-5000 μM), or 2-NO-T (500-3000 μM) at 37 °C for 10 min. The reaction was initiated by the addition of the nitrosoarenes dissolved in DMSO (4 μL). A 40 μL portion of the incubation mixture was withdrawn for the GR activity assay. The controls contained DMSO, but not nitrosoarenes.

Determination of the Comparative Cytotoxicities of 4-NO-BP, 2-NO-F, NO-B, and 2-NO-T. Cell viability was determined by the 96 AQ_{ueous} One Solution Cell Proliferation Assay (Promega Co., Madison, WI). HeLa cells were seeded into 96-well plates at a density of 6000 cells per well and allowed to

adhere overnight. Media was changed with 100 μL of serum-free DMEM, which contained 4-NO-BP (final concentration 1-250 μM), 2-NO-F (final concentration 1-500 μM), NO-B (final concentration 1-500 μM), or 2-NO-T (final concentration 10-400 μM) dissolved in DMSO. DMSO only was added to the controls. The final concentration of DMSO was less than 1%. After a 4 h incubation at 37 ºC, media was changed with 100 μL of serum-containing DMEM. After 40 h of growth, 20 μL of CellTiter 96 AQ_{ueous} One Solution Reagent was added to each well. The plate was incubated at 37 ºC for an additional 2 h. The absorbance at 490 nm was recorded with a FL600 Microplate Fluorescence Reader (Key Scientific, Mt. Prospect, IL).

Effect of Nitrosoarenes on Endogenous NAT1, GAPDH, and GR Activities in HeLa Cells. At approximately 90% confluence, cell monolayers (100 mm plate, 3.45 x 10^6 cells) were washed twice with PBS. The cells were exposed to 4-NO-BP (1-40 μM), 2-NO-F (0.5-20 μM), NO-B (100-250 μM), or 2-NO-T (50-200 μM) in 10 mL of serum-free DMEM media containing DMSO. The final concentration of DMSO was 0.1%. The incubation was continued at 37 ºC for various periods of time. Cells were washed with PBS buffer, trypsinized, and harvested by centrifugation at 1000g for 5 min at 4 ºC. The controls contained DMSO only. Cytosol was prepared as described above, and the NAT1, GAPDH, and GR activities were measured. After treatment with either 4-NO-BP or 2-NO-F, cell viability was confirmed with the trypan blue assay. Cells were washed with PBS buffer and trypsinized, and 0.2 mL of the cell suspension was mixed with trypan blue solution (0.5 mL, 0.4% w/v) (Sigma, St. Louis, MO), and 0.3 mL of Hanks' Balanced Salts (HBSS). The mixture (10 μL) was used to count the viable

cells with a standard hemocytometer according to the instructions from the supplier.

Effect of 4-NO-BP and 2-NO-F on Cytosolic NAT1 and Intracellular NAT1 Activity in Breast Cancer Cells. In a total volume of 50 μL, MDA-MB-231 cell cytosol (48 μL) was incubated with either 4-NO-BP (20-500 nM), or 2-NO-F (20-1000 nM) at 37 ºC for 10 min. The reaction was initiated by the addition of the nitrosoarenes dissolved in DMSO (2 μL). PABA and AcCoA dissolved in assay buffer (50 μL) and warmed to 37 ºC for 5 min, were added to the mixtures. The final concentrations were: PABA, 200 μM; AcCoA, 400 μM. Residual NAT1 activity was measured as described above. The control incubations contained DMSO, but not nitrosoarene.

At approximately 90% confluence, MDA-MB-231 or MDA-MB-468 cell monolayers (100 mm plate, 3.45 x 10^6 cells) were washed twice with PBS. The cells were exposed to 4-NO-BP (1-20 μM) in 10 mL of serum-free DMEM media containing DMSO. The final concentration of DMSO was 0.1%. The incubation was continued at 37 ºC for 4 h. Cells were washed with PBS buffer, trypsinized, and harvested by centrifugation at 1000g for 5 min at 4 ºC. The controls contained DMSO only. Cytosol was prepared as described above for HeLa cells, and the NAT1 activity was measured.

Effect of N-Acetyl-L-Cysteine (NAC) on Inactivation of HeLa Cell NAT1 by 4-NO-BP. At approximately 90% confluence, cell monolayers were washed twice with PBS (5 mL). The cells were exposed to NAC (20 mM) in 10

mL of serum-free DMEM media for 4 h (*22*). The cell monolayers were washed five times with PBS (5 mL). Serum-free DMEM media (10 mL) containing 4-NO-BP (10 μM) dissolved in DMSO (10 μL) was added. The incubation was continued at 37 ºC for 1 h. Cells were washed twice with PBS buffer (5 mL), trypsinized, and harvested by centrifugation at 1000g for 5 min (4 ºC). Cytosol was prepared as described above, and NAT1 activity was measured.

Sample Preparation for in-Gel Digestion of FLAG-NAT1 from 4-NO-BP Treated p3FLAG-NAT1*4 Transfected HeLa Cells. At 90-95% confluence, cell monolayers (100 mm plate, 15 plates) were transfected with p3FLAG-NAT1*4 plasmid with Lipofectamine 2000 (*23*). After 24 h, the media was replaced with serum-free media (10 mL) containing 4-NO-BP (200 μM) dissolved in DMSO (10 μL). After 1.5 h, the media was again replaced with serum-free media (10 mL) containing 4-NO-BP (200 μM) dissolved in DMSO (10 μL) and incubation was continued for 1.5 h. Cells were washed three times with PBS and were harvested. The controls contained DMSO, but not 4-NO-BP.

Cell cytosol (60 mg of protein from p3FLAG-NAT1*4 transfected HeLa cells; 59 mg of protein from 4-NO-BP treated p3FLAG-NAT1*4 transfected HeLa cells) was incubated with 300 μL (packed gel volume) of EZview^{TM} Red ANTI-FLAG M2 Affinity Gel with shaking at 4 ºC overnight. After centrifugation at 8200g for 30 s, the supernatant was removed. Gel pellets were washed three times with 5000 μL of TBS (50 mM Tris HCl, 150 mM NaCl, pH 7.4) containing 0.5 M NaCl for 10 min and twice with 5000 μL of TBS for 10 min. Non-reducing SDS-PAGE sample buffer (300 μL) was added to each sample. The samples were

boiled for 10 min and centrifuged at 8200*g* for 3 min. The supernatant was loaded onto 4-12% SDS-polyacrylamide gels and subjected to electrophoresis.

In-Gel Pepsin Digestion and MS Analysis of Overexpressed NAT1 in HeLa Cells after Treatment with 4-NO-BP. The 3FLAG-NAT1 bands were cut from the gels and sliced into pieces. Gel pieces were washed with ddH_2O (10 mL) for 60 min. Water was removed and the gel pieces were destained with 5000 μL of 40 mM NH_4HCO_3/50% CH_3CN at 37 ºC for 30 min; the destaining was repeated twice. Gel pieces were dried with a vacuum centrifuge. The dry gel pieces were rehydrated with 800 μL of freshly prepared pepsin solution (50 μg/mL in H_2O, pH 1.3). After incubation overnight at 37 ºC, the pepsin solution was collected. Formic acid (5% v/v) in CH_3CN:H_2O (50% v/v) (500 μL) was added to the gel pieces and the incubation was continued for 30 min; the procedure was carried out three times. All the extracts were combined and dried in a centrivap concentrator. Samples were dissolved in 13 μL of reconstitution solution (CH_3CN:H_2O, 5:95, 0.5% TFA) and desalted with Millipore C18 ZipTips. Peptides were analyzed and sequenced as previously described (*11*).

Results

Inactivation of Recombinant Human NAT1 by Nitrosoarenes. Irreversible inactivation of human NAT1 by 4-NO-BP, 2-NO-F, NO-B, and 2-NO-T resulted in a time-dependent, and concentration dependent loss of the N-acetylation activity of NAT1. The reactions of NAT1 with each of the nitrosoarenes followed pseudo-first-order kinetics (Figure 3) (*24*). The inactivation of NAT1 by either 4-NO-BP or NO-B was a saturable process, with K_I values of 0.67 ± 0.07 μM and 540 ± 151 μM, respectively. However, when NAT1 was treated with either 2-NO-F or 2-NO-T, saturation was not observed within the range of concentrations that were investigated (Figure 3).

The inactivation rate constant (k_{inact}) and dissociation constant (K_I) for inactivation of NAT1 by 4-NO-BP and NO-B were obtained from equation 1, where [I] is the inhibitor concentration, and first order inactivation rate constants (k_{obs}) were obtained from the slopes of the lines in Figure 3. The second-order rate constant (k_{inact}/ K_I) for inactivation of NAT1 by 4-NO-BP was over 2000-fold greater than the corresponding rate constant determined for NO-B (Table 1) (*24*).

The second-order inactivation rate constants (k_2) for inactivation of NAT1 by 2-NO-F and 2-NO-T were obtained by fitting the data to equation 2, in which [I] is the inactivator concentration and n is the order of the reaction with respect to inhibitor (*25*). For both 2-NO-F and 2-NO-T, the n was 1.0 and the k_2 value was 34,500 ± 1020 $M^{-1}s^{-1}$ for 2-NO-F and 23 ± 2.0 $M^{-1}s^{-1}$ for 2-NO-T (Table 1).

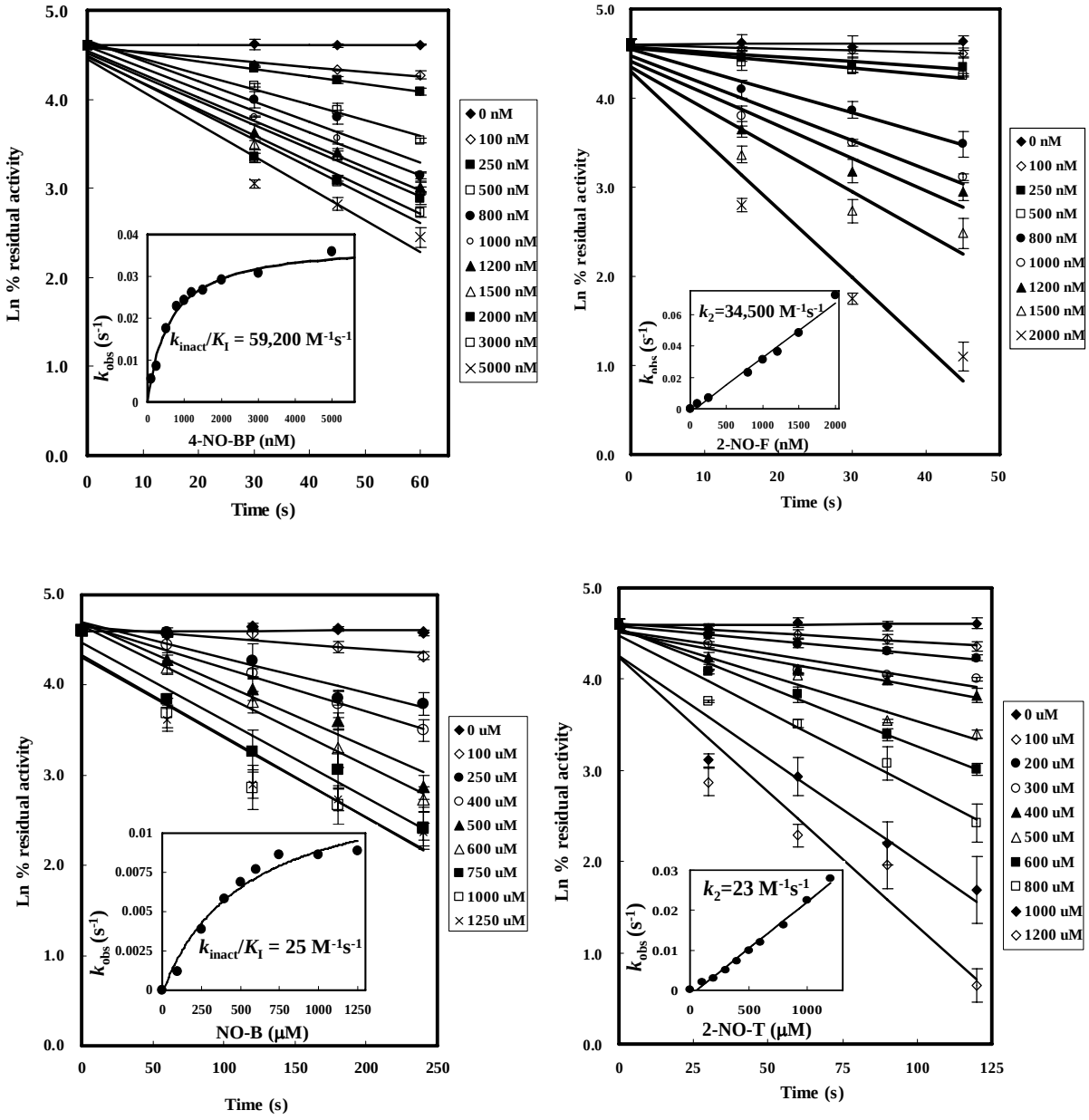

Figure 3. Time- and concentration-dependent inactivation of recombinant human NAT1 by 4-nitrosobiphenyl (4-NO-BP), 2-nitrosofluorene (2-NO-F), nitrosobenzene (NO-B), and 2-nitrosotoluene (2-NO-T). Insets: Plots of k_{obs} values as a function of nitrosoarene concentration. (From reference 24)

Nitrosoarene	K_I (μM)	k_{inact}(s^{-1})	k_{inact}/K_I ($M^{-1}s^{-1}$)	k_2 ($M^{-1}s^{-1}$)
4-NO-BP	0.67 ± 0.07	0.04 ± 0.001	59,200 ± 7,600	
NO-B	540 ± 151	0.01 ± 0.002	25 ± 12	
2-NO-F				34500 ± 1020
2-NO-T				23 ± 2.0

Table 1. Kinetic Parameters for Inactivation of Human NAT1 by Nitrosoarenes. Results are expressed as the means (± SD) of three experiments. See figure 2 for graphical illustrations of the kinetic analyses. (From reference 24)

Therefore, 4-NO-BP and 2-NO-F are potent irreversible inactivators of NAT1, whereas NO-B and 2-NO-T are much weaker inactivators of the enzyme. These results support our hypothesis that for arylamines that are good substrates for human NAT1, the corresponding nitroso derivatives are potent NAT1 inactivators.

$$k_{obs} = k_{inact} / (1 + K_I/[I]) \quad (1)$$

$$\log k_{obs} = \log k_2 + n \log [I] \quad (2)$$

MS Analysis of 2-NO-F-Treated NAT1. To assess the chemical mechanism of inactivation of recombinant NAT1 by 2-NO-F, NAT1 was incubated with 2-NO-F and the adducted protein was analyzed by mass spectrometry. The molecular mass of recombinant NAT1 is 34299.2 Da, which includes four additional amino acids (Gly, Thr, Leu, Glu) at the N-terminus of the recombinant protein. After incubation of NAT1 with 2-NO-F, the ESI-Q-TOF mass spectrum of the adducted protein revealed the probable formation of a (2-fluorenyl)sulfinamide conjugate, as it exhibited a major peak 34494.9 Da, which corresponds to the addition of 195 Da to the native protein (Figure 4) (*24*). MALDI Q-TOF MS analysis of the pepsin digest of 2-NO-F-treated NAT1 revealed one peak, with a monoisotopic mass of 1590.80 Da, that was not present in the pepsin digest of native NAT1 (Figure 5). MALDI Q-TOF MS/MS analysis of the peptide of mass 1590.80 Da revealed the modified (+32 Da) peptide sequence DQVVRRNRGGWCL, which corresponds to Asp57-Leu69 (unmodified theoretical mass 1558.78 Da). The strong b12-H2SO2 ion (1393.72 m/z), the b12 ion (1459.71 m/z), and the b11-NH3 ion (1307.68 m/z) verify that the side chain thiol of Cys68 had been converted to a sulfinic acid (Figure 6). It

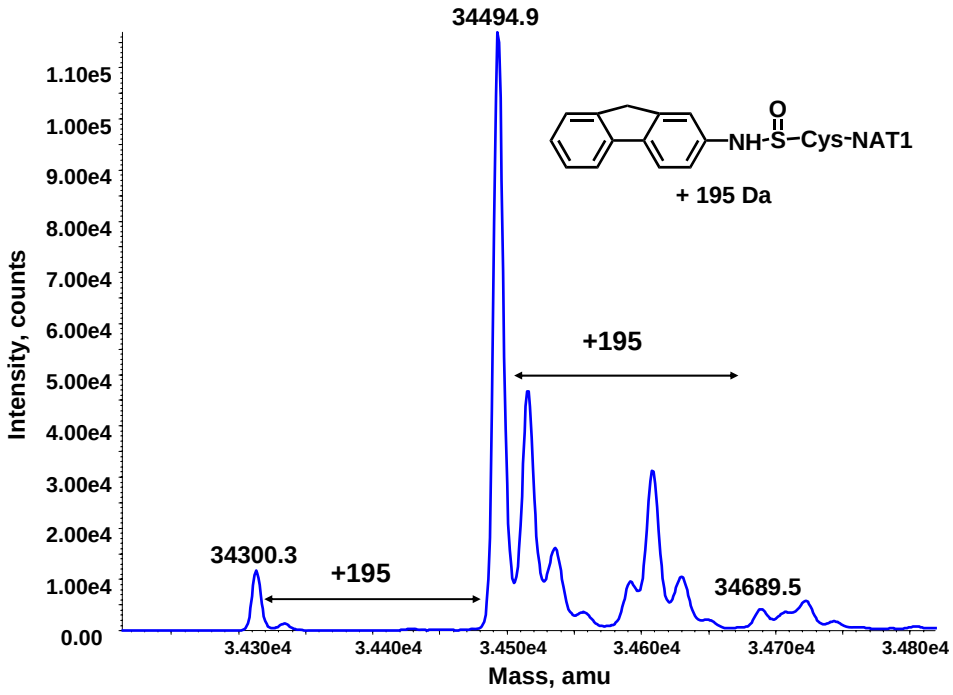

Figure 4. Nano-ESI-Q-TOF mass spectrum of recombinant human NAT1 after incubation with 2-NO-F. The theoretical mass of recombinant NAT1 is 34299.2 Da. (From reference 24)

a.

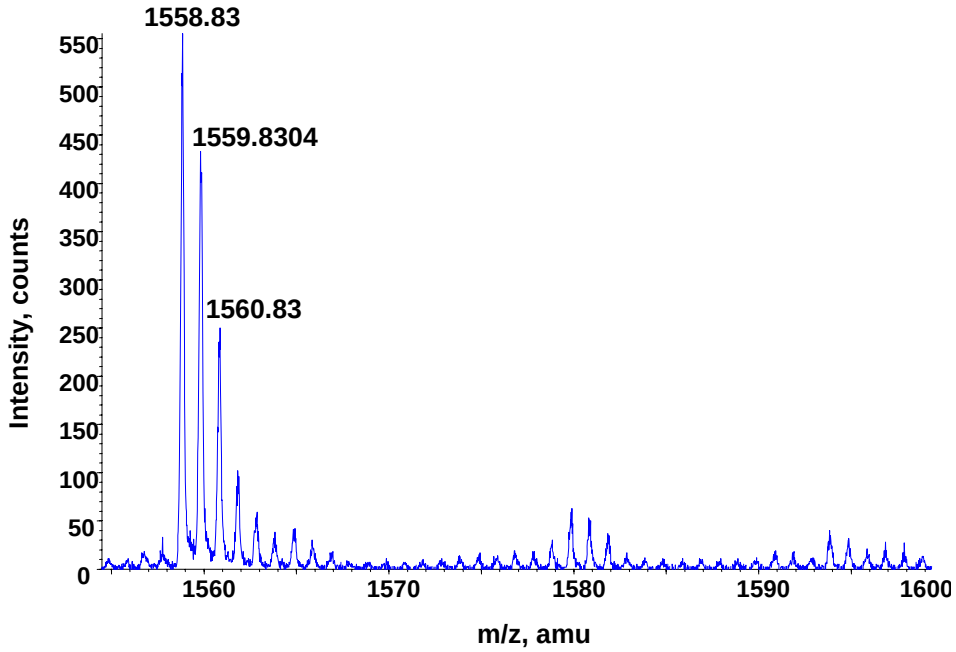

b.

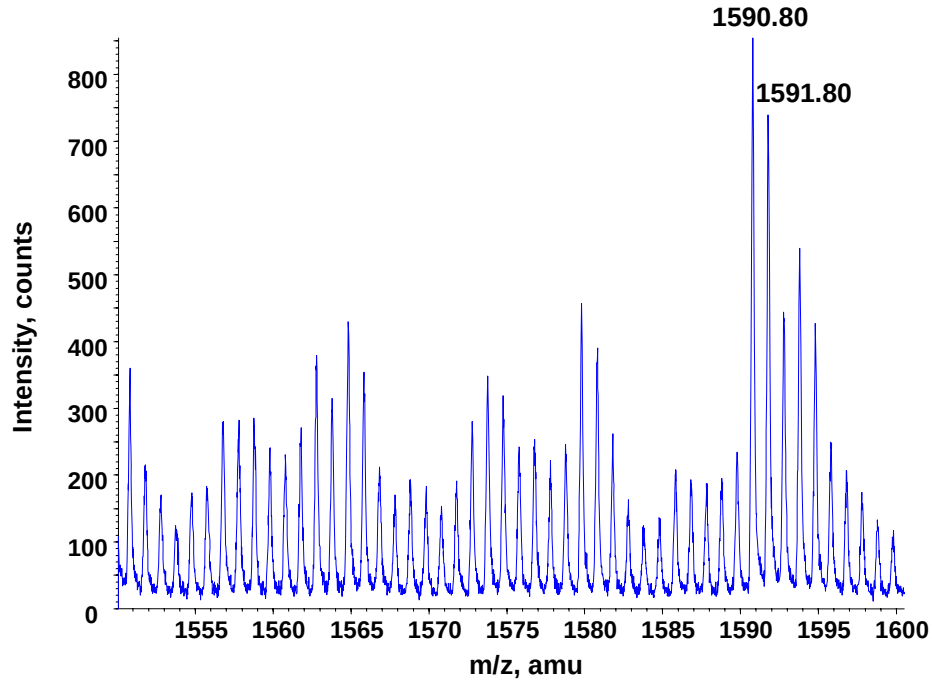

Figure 5. Segments of the MALDI Q-TOF mass spectra of pepsin digests of (a) native recombinant human NAT1; (b) 2-NO-F-inactivated recombinant human NAT1. (From reference 24)

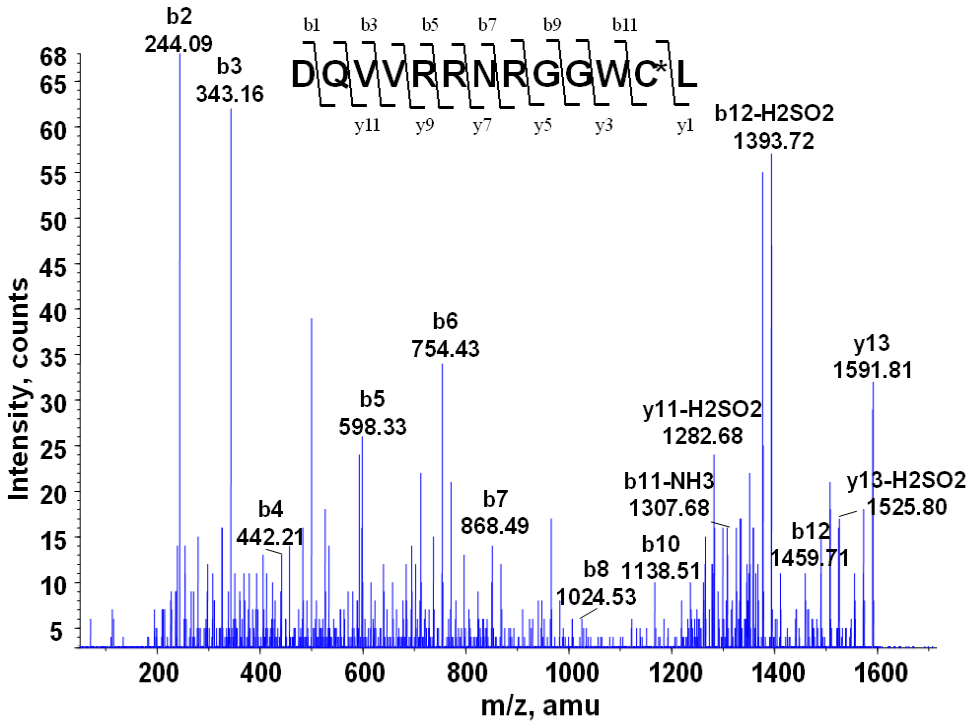

Figure 6. MALDI Q-TOF tandem mass spectrum of the 1590.80 Da peptide obtained by pepsin digestion of 2-NO-F-inactivated recombinant human NAT1. (From reference 24)

has been shown previously that under the acid conditions of pepsin digestion, sulfinamide adducts are hydrolyzed and sulfinic acids are formed (Figure 7) (*10, 11*). These results are consistent with our previous investigations of human NAT1 inactivation by 4-NO-BP and hamster NAT1 inactivation by 2-NO-F, in that Cys68-sulfinamide adducts accounted for the observed losses of NAT activity (*10, 11*).

Effect of AcCoA on the Inhibition of NAT1 by NO-B and 2-NO-T. Incubation of NAT1 (1 μM) with NO-B (250 μM) or 2-NO-T (300 μM) reduced NAT1 activity to 41 (± 3)% and 54 (± 3)% of control activity. Incubation of NAT1 with the endogenous acetyl donor, AcCoA (20 μM), prior to treatment with NO-B or 2-NO-T resulted in recovery of 87 (± 4)% and 96 (± 5)% of control activity. These results suggested that the inactivation of NAT1 by either NO-B or 2-NO-T was due to modification of the active site Cys68 of the enzyme.

Inactivation of NAT1 by 4-NO-BP and 2-NO-F in the Presence of GSH. Because nucleophilic thiols, such as GSH, react readily with nitrosoarenes (*7, 8, 26, 27*), we investigated the ability of physiological concentrations of GSH to protect NAT1 from the effects of 4-NO-BP and 2-NO-F. NAT1 (0.72 μM) was incubated with 4-NO-BP (1 μM and 5 μM) or 2-NO-F (1 μM and 5 μM) in the presence of various concentrations of GSH (0.5 – 5 mM) for either 30 s or 60 s. The results are shown in Figure 8a - 8d.

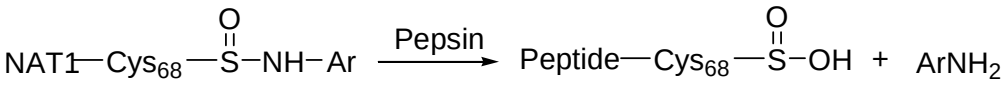

Figure 7. The hydrolysis of sulfinamide to sulfinic acid during the pepsin digestion.

Incubation of NAT1 (0.72 μM) with 4-NO-BP (1 μM) for 30 s caused a 54 (± 3)% loss of NAT1 activity and incubation with 2-NO-F (1 μM) for 30 s caused a 74 (± 3)% reduction in NAT1 activity (Figure 8a). In the presence of 0.5 mM GSH, corresponding to 694-fold excess of GSH over NAT1 and a 500-fold excess over the two nitrosoarenes, 4-NO-BP caused a 37 (± 4)% reduction of NAT1 activity and 2-NO-F caused a 24 (± 1)% reduction of NAT1 activity. In the presence of 1 mM GSH, 4-NO-BP caused 27 (± 6)% and 2-NO-F caused 18 (± 1)% loss of NAT1 activity. In the presence of 5 mM GSH, corresponding to 6944-fold excess of GSH over NAT1 and a 5000-fold excess of GSH over the nitrosoarenes, 4-NO-BP caused 14 (± 2)% and 2-NO-F caused 8 (± 1)% loss of NAT1 activity (Figure 8a).

As shown in figure 8b, incubation of NAT1 with 4-NO-BP (1 μM) for 60 s caused a 71 (± 4)% loss of NAT1 activity and incubation with 2-NO-F (1 μM) for 60 s caused an 89 (± 2)% reduction of NAT1 activity (Figure 8b). In the presence of 0.5 mM GSH, 4-NO-BP caused a 35 (± 4)% reduction of NAT1 activity and 2-NO-F caused a 28 (± 3)% reduction of NAT1 activity. In the presence of 1 mM GSH, 4-NO-BP and 2-NO-F caused 12 (± 6)% and 17 (± 3)% losses of NAT1 activity, respectively. In the presence of 5 mM GSH, both nitrosoarenes caused decreases of about 10% in NAT1 activity.

4-NO-BP (5 μM) and 2-NO-F (5 μM) caused inactivations of 91 (± 2)% and 99 (± 2)%, respectively, during a 30 s incubation with NAT1 (0.72 μM) in the absence of GSH (Figure 8c). In the presence of GSH (0.5 mM), 4-NO-BP caused a 59 (± 3)% reduction in activity and 2-NO-F inhibited NAT1 by 53 (± 1)% in 30

s. 4-NO-BP caused 30 (± 6)% and 12 (± 3)% inactivation in the presence of 1 mM and 5 mM concentrations of GSH, respectively, and the corresponding losses in activity produced by 2-NO-F were 16 (± 9)% and 13 (± 4)%.

As shown in figure 8d, incubation of NAT1 (0.72 μM) with 4-NO-BP (5 μM) for 60 s caused a 97 (± 1)% inactivation and incubation with 2-NO-F (5 μM) for 60 s caused a 99.5 (± 1)% reduction in NAT1 activity. In the presence of 0.5 mM GSH, treatment of NAT1 with 4-NO-BP resulted in a 57 (± 1)% loss of activity and 2-NO-F caused a 60 (± 2)% loss of activity. The incubation with 1 mM GSH decreased the extent of inactivation by 4-NO-BP and 2-NO-F to 26 (± 6)% and 23 (± 7)%, respectively. In the presence of 5 mM GSH, 4-NO-BP and 2-NO-F caused 16 (± 3)% and 21 (± 8)% reductions in NAT1 activity.

Thus, both 4-NO-BP and 2-NO-F react more rapidly with NAT1 than with GSH. These results might indicate that intracellular GSH will not protect endogenous NAT1 from inactivation by either 4-NO-BP or 2-NO-F.

NAT1 in HeLa Cells. Butcher and co-workers have detected NAT1 activity in HeLa cells previously (*28*). To verify the expression of NAT1 protein in HeLa cell cytosol, Western blot analysis was carried out with a NAT1 specific antibody (*16*) (Figure 9). To quantify the constitution of NAT1 in HeLa cell cytosol, densitometric analysis was conducted and a standard curve was made with recombinant NAT1 (Table 2). It was revealed that there was 2.4 (± 0.15) ng of NAT1 protein in 100 μg of cytosolic protein.

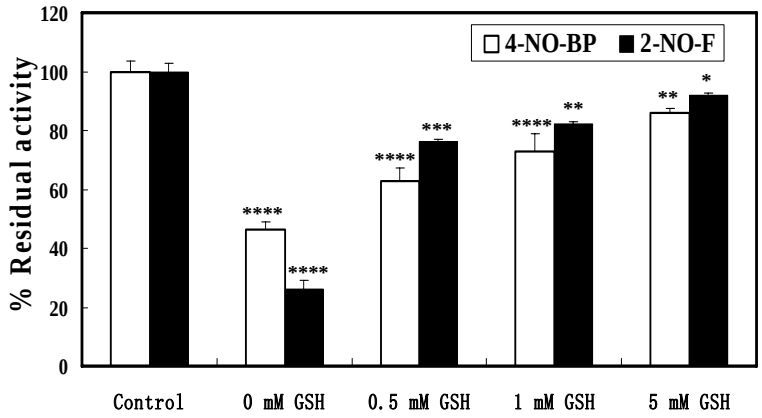

30 s	% Residual Activity	
	4-NO-BP	2-NO-F
Control	100 ± 4	100 ± 3
0 mM GSH	47 ± 3	26 ± 3
0.5 mM GSH	63 ± 4	76 ± 0.5
1 mM GSH	73 ± 6	82 ± 0.7
5 mM GSH	86 ± 2	92 ± 0.6

Figure 8a. Inactivation of NAT1 (0.72 μM) by 4-NO-BP (1 μM) and 2-NO-F (1 μM) in the presence of GSH. The incubation time was 30 s. Each bar represents the mean ± SD of the results of 3 experiments. Asterisks represent significant differences from controls: *$p < 0.05$, **$p < 0.02$, ***$p < 0.01$, and ****$p < 0.001$.

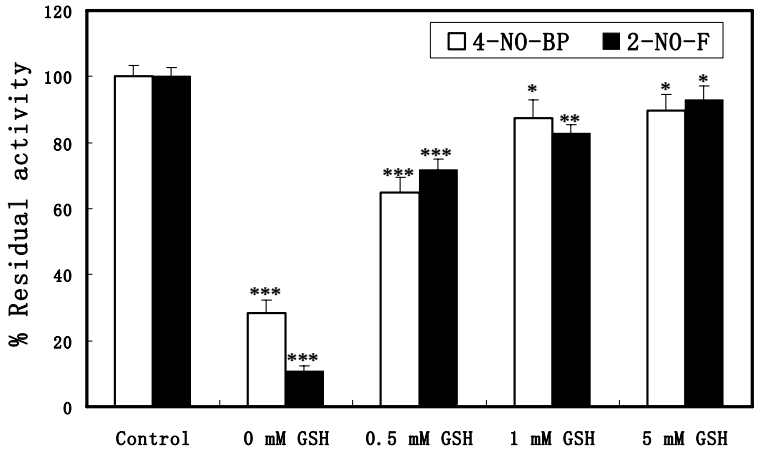

60 s	% Residual Activity	
	4-NO-BP	2-NO-F
Control	100 ± 4	100 ± 3
0 mM GSH	29 ± 4	11 ± 2
0.5 mM GSH	65 ± 4	72 ± 3
1 mM GSH	88 ± 6	83 ± 3
5 mM GSH	90 ± 5	93 ± 4

Figure 8b. Inactivation of NAT1 (0.72 μM) by 4-NO-BP (1 μM) and 2-NO-F (1 μM) in the presence of GSH. The incubation time was 60 s. Each bar represents the mean ± SD of the results of 3 experiments. Asterisks represent significant differences from controls: *$p < 0.05$, **$p < 0.01$, and ***$p < 0.001$.

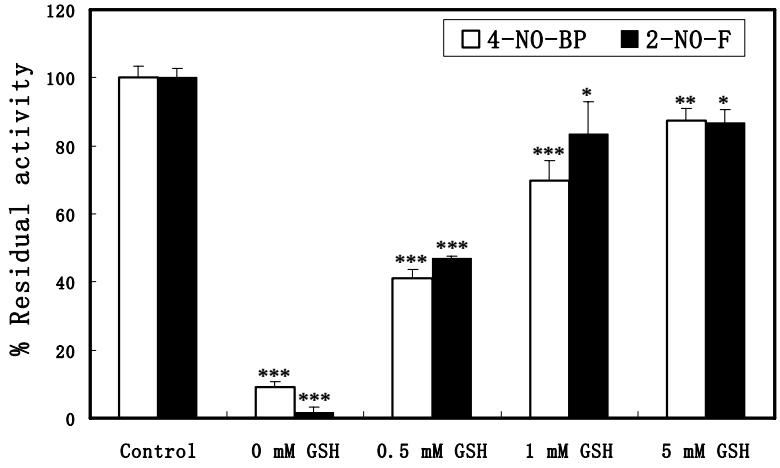

30 s	% Residual Activity	
	4-NO-BP	2-NO-F
Control	100 ± 4	100 ± 3
0 mM GSH	9 ± 2	2 ± 2
0.5 mM GSH	41 ± 3	47 ± 1
1 mM GSH	70 ± 6	84 ± 9
5 mM GSH	88 ± 3	87 ± 4

Figure 8c. Inactivation of NAT1 (0.72 μM) by 4-NO-BP (5 μM) and 2-NO-F (5 μM) in the presence of GSH. The incubation time was 30 s. Each bar represents the mean ± SD of the results of 3 experiments. Asterisks represent significant differences from controls: *$p < 0.05$, **$p < 0.02$, and ***$p < 0.001$.

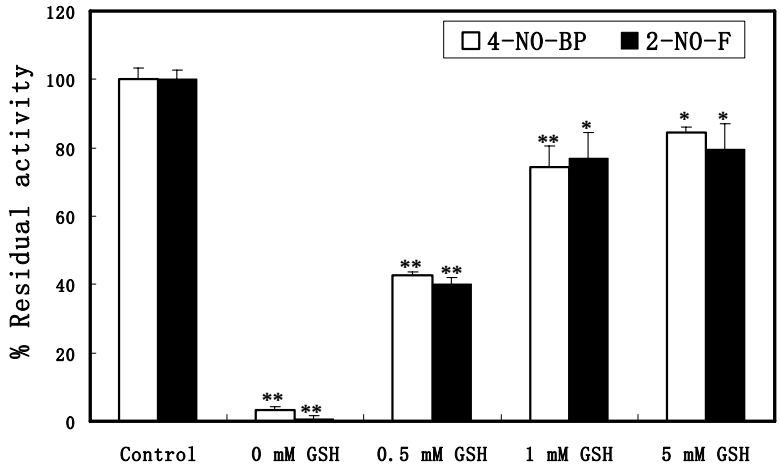

60 s	% Residual Activity	
	4-NO-BP	2-NO-F
Control	100 ± 4	100 ± 3
0 mM GSH	3 ± 1	0.5 ± 1
0.5 mM GSH	43 ± 1	40 ± 2
1 mM GSH	74 ± 6	77 ± 7
5 mM GSH	84 ± 2	80 ± 8

Figure 8d. Inactivation of NAT1 (0.72 μM) by 4-NO-BP (5 μM) and 2-NO-F (5 μM) in the presence of GSH. The incubation time was 60 s. Each bar represents the mean ± SD of the results of 3 experiments. Asterisks represent significant differences from controls: *$p < 0.01$, and **$p < 0.001$.

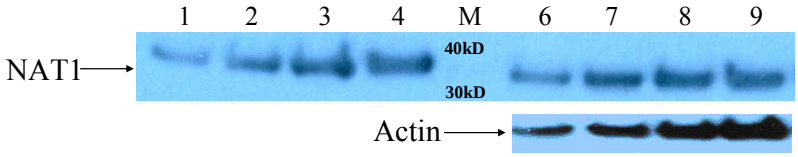

Figure 9. Western blot analysis of recombinant NAT1 and HeLa cell NAT1 with a NAT1-specific antibody. Recombinant NAT1: Lane 1, 0.25 ng; Lane 2, 0.5 ng; Lane 3, 1.0 ng; Lane 4, 1.5 ng. HeLa cell cytosolic protein: Lane 6, 20 μg; Lane 7, 30 μg; Lane 8, 40 μg; Lane 9, 50 μg. The protein was quantified by densitometry. (From reference 24)

Lane		Densitometric Analysis (O. D. x mm)
1	0.25 ng	1.45 e-1
2	0.5 ng	2.8 e-1
3	1.0 ng	5.2 e-1
4	1.5 ng	7.1 e-1
5	Molecular Marker	
6	20 ug HeLa Cytosol	2.5 e-1
7	30 ug HeLa Cytosol	3.7 e-1
8	40 ug HeLa Cytosol	4.9 e-1
9	50 ug HeLa Cytosol	5.5 e-1

Table 2. Densitometric analysis of the Western blot in Figure 7.

Human NAT1 activity in HeLa cell cytosol was measured with AcCoA as the acetyl donor and NAT1 specific substrates, PAS and PABA, as the acetyl acceptors. The specific activity for PAS with cell cytosol was 4.08 ± 0.58 nmol/mg of protein/min and with homogeneous recombinant NAT1 was 337 ± 12 μmol/mg of protein/min. On the basis of the specific activities obtained with PAS, it was concluded that HeLa cell NAT1 concentration is 1.2 ng per 100 μg of protein. When PABA was used as the acetyl acceptor, the specific activity with HeLa cell cytosol was 4.4 ± 0.32 nmol/mg of protein/min and the specific activity with recombinant NAT1 was 237 ± 2.4 μmol/mg of protein/min. By comparison of the specific activities obtained with PABA, HeLa cell cytosol contains 1.8 ng of NAT1 per 100 μg of protein. Thus, on the basis of densitometric analysis and specific activities, NAT1 constitutes approximately 0.002% of HeLa cell cytosol. In a partial purification of NAT2 from human liver, Grant and co-workers have shown that NAT2 also is a low abundance protein and constitutes approximately 0.002% of cytosolic protein (*29*).

NAT1 in MDA-MB-231, MDA-MB-468, and MCF-7 Cells. NAT1 activities have been detected previously in estrogen receptor (ER)-negative MDA-MB-231 breast cancer cells and ER-positive MCF-7 breast cancer cells (*30*). Western blot analysis has been used to verify the expression of NAT1 protein in ER-positive ZR 75-1 breast cancer cells (*30*). In this study, we detected the presence of NAT1 protein in MDA-MB-231, MDA-MB-468, and MCF-7 cells by Western blot analysis (Figure 10). Densitometric analysis revealed the presence of 2.2 ng, 2.1 ng, and 9.6 ± 3.1 ng of NAT1 in 100 μg of MDA-MB-231, MDA-MB-468, and MCF7 cell cytosol, respectively.

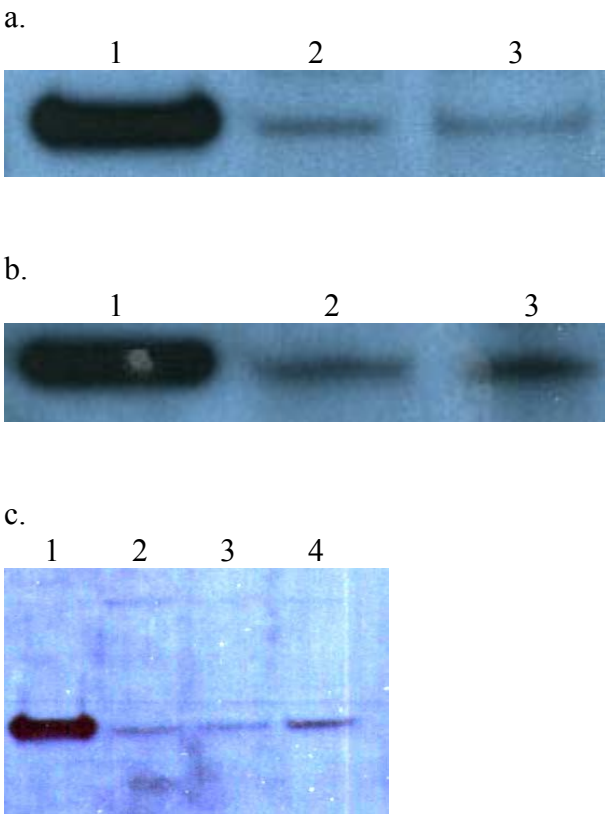

Figure 10. Western blot analysis of recombinant NAT1, MDA-MB-231 cell NAT1, MDA-MB-468 cell NAT1, and MCF-7 cell NAT1 with a NAT1-specific antibody. (a) Recombinant NAT1: Lane 1, 5 ng. MDA-MB-231 cell cytosolic protein: Lane 2, 50 μg; Lane 3, 30 μg. (b) Recombinant NAT1: Lane 1, 5 ng. MDA-MB-468 cell cytosolic protein: Lane 2, 30 μg; Lane 3, 50 μg. (c) Recombinant NAT1: Lane 1, 5 ng. MCF-7 cell cytosolic protein: Lane 2, 8 μg; Lane 3, 15 μg; Lane 4, 25 μg. The protein was quantified by densitometry.

N-acetylation activity in breast cancer cell cytosol was measured by using the NAT1 substrate, PABA, and AcCoA as the acetyl donor. The specific activity in MCF-7 cell cytosol was 11.4 ± 0.3 nmol/mg/min, and in MDA-MB-231 and MDA-MB-468 cell cytosol, it was 4 ± 0.3 nmol/mg/min and 4.2 ± 0.3 nmol/mg/min, respectively. On the basis of the specific activity with homogeneous recombinant NAT1, the NAT1 concentration is 1.8 ng per 100 μg of either MDA-MB-231 or MDA-MB-468 cell cytosol and is 4.8 ng per 100 μg of MCF-7 cell cytosol. Thus, ER-positive MCF-7 breast cancer cell cytosol contains a 3-fold higher concentration of NAT1 than ER-negative breast cancer cell cytosol or HeLa cell cytosol.

Effect of 4-NO-BP, 2-NO-F, NO-B, and 2-NO-T on NAT1, GAPDH, and GR Activities in HeLa Cell Cytosol. HeLa cell cytosol was treated with a range of concentrations of 4-NO-BP, 2-NO-F, NO-B, and 2-NO-T, and the IC_{50} values for inhibition of NAT1, glyceraldehyde 3-phosphate dehydrogenase (GAPDH), and glutathione reductase (GR) were calculated (Table 3) (*24*). For comparison with NAT1, GAPDH and GR were selected because they both contain active site cysteine thiols which react with a variety of electrophiles (*31-33*). GAPDH, which catalyses the conversion of glyceraldehyde-3-phosphate into 1,3-diphosphoglycerate, coupled with the reduction of NAD to NADH, constitutes approximately 1 % of HeLa cell cytosol, which is 500-fold higher than NAT1 (*34*). GR is one of the enzymes of the glutathione redox cycle and plays a key role in maintenance of cellular redox homeostasis (*35, 36*).

	IC_{50} (μM)		
Nitrosoarene	NAT1	GAPDH	GR
4-NO-BP	0.06 ± 0.002	1.0 ± 0.08	0.4 ± 0.03
2-NO-F	0.04 ± 0.003	1.0 ± 0.09	0.8 ± 0.05
NO-B	237 ±10	1105 ± 78	2033 ± 80
2-NO-T	91 ± 16	402 ± 32	1418 ± 103

Table 3. Inhibition of NAT1, GAPDH, and GR in HeLa Cell Cytosol. Results are expressed as the means (± SD) of three experiments. (From reference 24)

The inhibitory effects of nitrosoarenes on NAT1 activity in cell cytosol were consistent with the results obtained with recombinant NAT1. The IC_{50} values for inhibition of cytosolic NAT1 by 4-NO-BP and 2-NO-F were 0.06 μM and 0.04 μM, respectively, and were 1600-5900-fold lower than the IC_{50} values of either NO-B or 2-NO-T. 4-NO-BP and 2-NO-F showed 7-25-fold greater IC_{50} values for the inhibition of cytosolic GAPDH and GR than for the inhibition of NAT1; NO-B and 2-NO-T were much weaker inhibitors of cytosolic GAPDH and GR than either 4-NO-BP or 2-NO-F (Table 3).

Effect of AcCoA on the Inhibition of HeLa Cell Cytosolic NAT1 Activity by Nitrosoarenes. To obtain evidence that inactivation of HeLa cell cytosolic NAT1 by nitrosoarenes was due to interaction of nitrosoarenes with the active sites of the enzyme, AcCoA (400 μM), the endogenous acetyl donor, was added to the cytosols prior to addition of nitrosoarenes. In these experiments, 4-NO-BP (100 nM), 2-NO-F (50 nM), NO-B (500 μM), and 2-NO-T (100 μM) lowered the NAT1 activity by approximately 60% but, in the presence of AcCoA, the enzymes were inactivated to an extent of only 2-10% (Table 4). Protection of the cytosolic NAT1 from inactivation by nitrosoarenes in the presence of AcCoA indicated the interaction of the nitrosoarenes with the active sites of the enzyme.

Comparative Cytotoxicities of 4-NO-BP, 2-NO-F, NO-B, and 2-NO-T. To determine the relative cytotoxicities of the four nitrosoarenes, HeLa cells were seeded into 96 well plates at a density of 6000 cells per well and were treated with various concentrations of 4-NO-BP, 2-NO-F, NO-B, and 2-NO-T. Cell viability was determined by the 96 AQ_{ueous} one Solution Cell Proliferation Assay and LC_{50}

	NAT1 (nmol/mg/min)	% Control Activity
Control	4.3 ± 0.2	100 ± 4
100 nM 4-NO-BP	1.6 ± 0.1	36 ± 3
400 μM AcCoA + 100 nM 4-NO-BP	3.9 ± 0.3	90 ± 8
50 nM 2-NO-F	1.8 ± 0.2	41 ± 5
400 μM AcCoA + 50 nM 2-NO-F	3.9 ± 0.3	90 ± 7
Control	4.1 ± 0.1	100 ± 3
500 μM NO-B	1.6 ± 0.5	39 ± 11
400 μM AcCoA + 500 μM NO-B	3.8 ± 0.3	93 ± 8
100 μM 2-NO-T	1.8 ± 0.3	43 ± 7
400 μM AcCoA + 100 μM 2-NO-T	4.0 ± 0.2	98 ± 5

Table 4. Effect of AcCoA on the Inactivation of NAT1 in HeLa Cell Cytosol by Nitrosoarenes. Results are expressed as the means (± SD) of three experiments.

values were calculated. 4-NO-BP and 2-NO-F, which were potent NAT1 inactivators in vitro and in HeLa cell cytosol (Table 1 and 3), exhibited similar LC_{50} values of 40 ± 3 and 46 ± 3 μM, respectively. NO-B and 2-NO-T, which were weak NAT1 inactivators, showed LC_{50} values of 273 ± 23 and 157 ± 5 μM and were 6-fold and 3.5-fold less toxic than either 4-NO-BP or 2-NO-F.

Effect of Nitrosoarenes on HeLa Intracellular NAT1, GAPDH, and GR Activities. To investigate the inhibitory effects of 4-NO-BP and 2-NO-F on intracellular NAT1 activity, HeLa cells were treated with a range of concentrations of the compounds for various lengths of time. The effects of the compounds on intracellular GAPDH and GR activities were monitored as well (Figures 11-14). Treatment of the cells with 4-NO-BP (2.5 μM) for 1 h depressed NAT1 activity by 39%. 4-NO-BP concentrations of 5 μM, 10 μM, 20μM, and 40 μM reduced NAT1 activity by 42%, 53 %, 60%, and 59%, respectively. GADPH or GR activities were not affected by 2.5 μM, 5 μM, or 10 μM concentrations of 4-NO-BP. The 20 μM and 40 μM concentrations 4-NO-BP caused a statistically significant reduction ($p < 0.05$) of GAPDH or GR activities by approximately 10-20% compared to control values (Figure 11a). Longer incubation (4 h) caused somewhat more inactivation of GAPDH and GR, without much further inactivation of NAT1 (Figure 11b)

To assess the time-dependent effects of 4-NO-BP on HeLa cell NAT1 in more detail, the cells were incubated with a 10 μM concentration of 4-NO-BP (Figure 12a). A 15 min incubation lowered the NAT1 activity by 39%. After 30 min, the decrease in NAT1 activity was 48%. The losses in NAT1 activity at 60

min and 120 min were 58% and 62%, respectively. Approximately 50% of the loss of NAT1 activity, monitored for 2 h, took place within the first 15 min of exposure of the cells to 4-NO-BP, and very little additional loss of activity was observed after 2 h. There was no significant loss of GAPDH or GR activity during the 2 h incubation. Treatment of HeLa cells with a higher concentration of 4-NO-BP (20 μM) did not cause a greater inactivation of NAT1 activity than was caused by the 10 μM concentration (Figure 12b).

Western blot analysis was used to determine whether or not the loss of NAT1 activity observed after incubation of HeLa cells with 4-NO-BP involved a change in NAT1 protein level (Figure 12a). HeLa cell cytosol was prepared at various times during the course of exposure to 4-NO-BP (10 μM) and subjected to Western blot analysis using a NAT1 specific antibody. Although NAT1 activity was significantly ($p < 0.001$) reduced by as early as 15 min after treatment, densitometric analysis showed that there was no significant ($p > 0.05$) loss of NAT1 protein over the 2 h treatment. It has also been shown that N-OH-PABA irreversibly inactivated endogenous NAT1 in peripheral blood mononuclear cells (PBMC) through a time- and concentration-dependent manner, but did not change NAT1 protein content (*37*).

The concentration-dependent effects of 2-NO-F on HeLa cell NAT1, GAPDH, and GR activities are shown in Figures 13a and 13b. One hour-treatment of the cells with 2-NO-F (1 μM) caused a loss of 34% of the NAT1 activity (Figure 13a), whereas NAT1 activity was unaffected by a 1 μM concentration of 4-NO-BP (Figure 11a). Thus, 2-NO-F was a more potent inactivator of HeLa

intracellular NAT1 than 4-NO-BP. Incubation with 2.5 μM to 10 μM concentrations of 2-NO-F caused a 57% to 73% decrease in NAT1 activity. Little additional loss of NAT1 activity was observed when the cells were treated with 20 μM 2-NO-F. GAPDH and GR activities were not affected by 0.5-2.5 μM concentrations of 2-NO-F and were reduced only 13-24% by 5-20 μM of 2-NO-F (Figure 13a). The extent of NAT1 inactivation after 4 h was similar to that after 1 h. Incubation of HeLa cells with 20 μM of 2-NO-F for 4 h caused an approximately 80% decrease in NAT1 activity and 25% decreases in GAPDH and GR activities (Figure 13b).

2-NO-F also caused a time-dependent loss of HeLa cell NAT1 activity. As illustrated in Figure 14, a 10 μM concentration of 2-NO-F caused a 60% loss of NAT1 activity in 15 min. After 30 min, the loss of NAT1 activity increased to 73% and then little additional loss was observed through 120 min. Incubation of the cells with 2-NO-F (10 μM) for 120 min, caused a modest reduction of 20-30% in the activities of GAPDH and GR. Thus, the inactivation of intracellular NAT1 by 2-NO-F is much more rapid and dramatic than the inactivation of either GAPDH or GR.

NO-B and 2-NO-T were also evaluated for their inhibitory effects on HeLa cell NAT1, GAPDH, and GR. Consistent with the results obtained with recombinant NAT1 and cytosolic NAT1, incubation of cells for 6 h with NO-B (250 μM) or for 4 h with 2-NO-T (100 μM) did not lower NAT1, GAPDH, or GR activity (data not shown).

a.

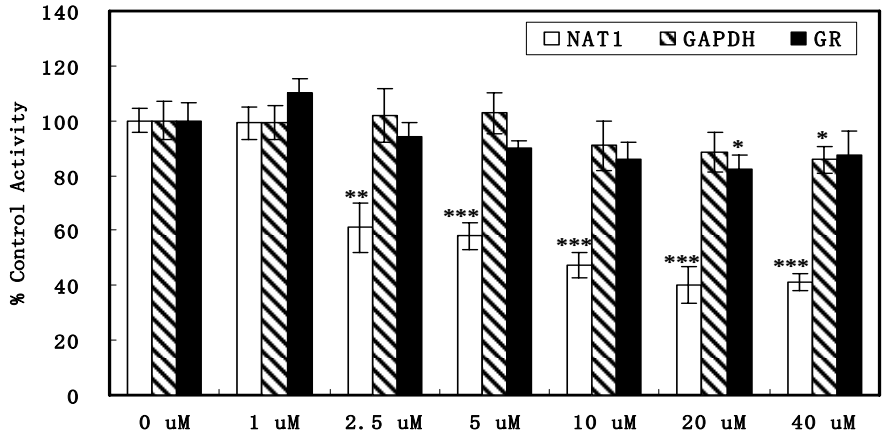

b.

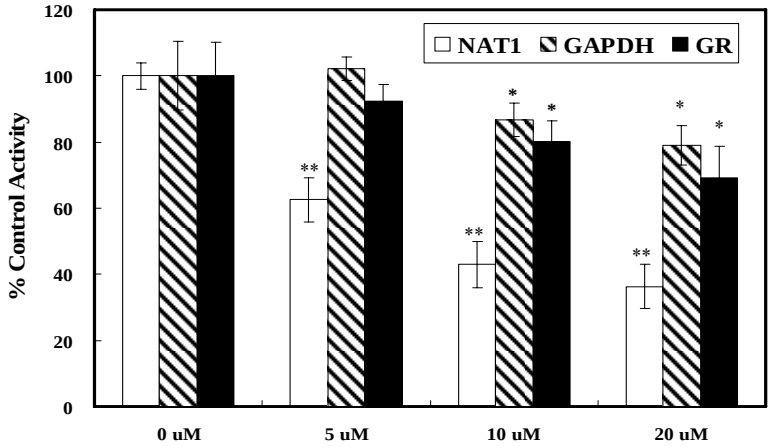

Figure 11. Concentration-dependent inactivation of HeLa cell NAT1, GAPDH, and GR by 4-NO-BP. (a) The incubation time was 1 h. Each bar represents the mean and standard deviation of the results of three experiments. Asterisks represent significant differences from control: *, $p < 0.05$; **, $p < 0.02$; ***, $p < 0.001$. (From reference 24) (b) The incubation time was 4 h. Each bar represents the mean and standard deviation of the results of 3 experiments. Asterisks represent significant difference from control: *, $p < 0.05$; **, $p < 0.001$.

a.

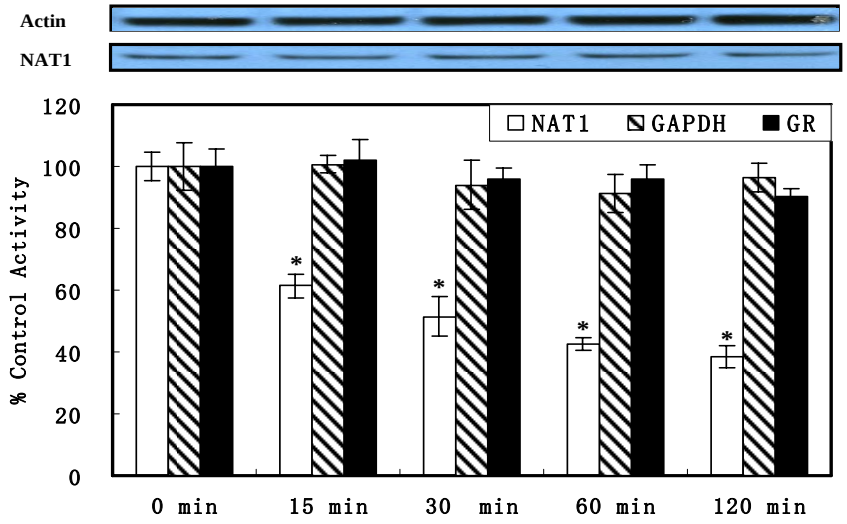

b.

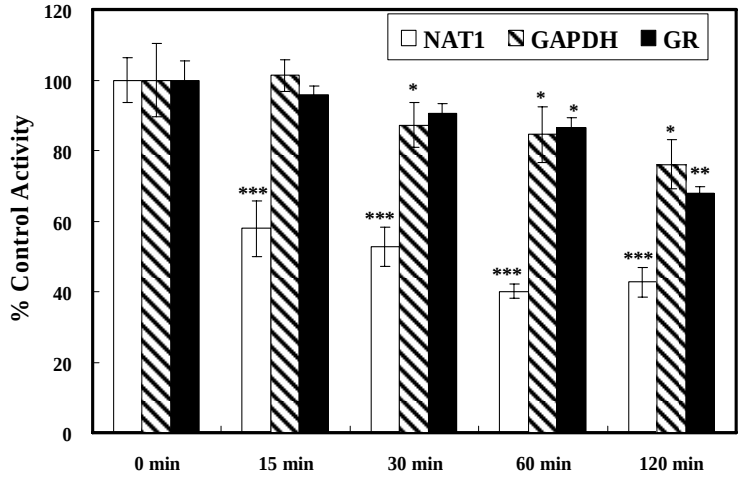

Figure 12. Time-dependent inactivation of HeLa cell NAT1, GAPDH, and GR by 4-NO-BP. (a) The concentration of 4-NO-BP was 10 μM. Upper panels: Western blot analysis of actin and NAT1 in 20 μg of cytosolic protein from HeLa cells that had been treated with 4-NO-BP for various periods of time. Protein was quantified by densitometry. Graph: Each bar represents the mean and standard deviation of the results of 3 experiments. Asterisks represent significant difference from control (0 min): *, $p < 0.001$. (From reference 24) (b) The concentration of 4-NO-BP was 20 μM. Each bar represents the mean and standard deviation of the results of 3 experiments. Asterisks represent significant differences from controls (0 min): *, $p < 0.05$; **, $p < 0.01$; ***, $p < 0.001$.

a.

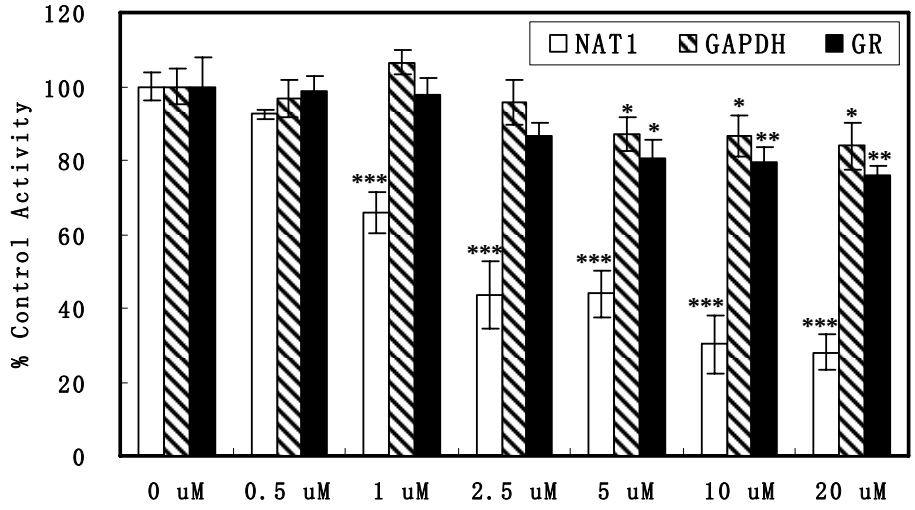

b.

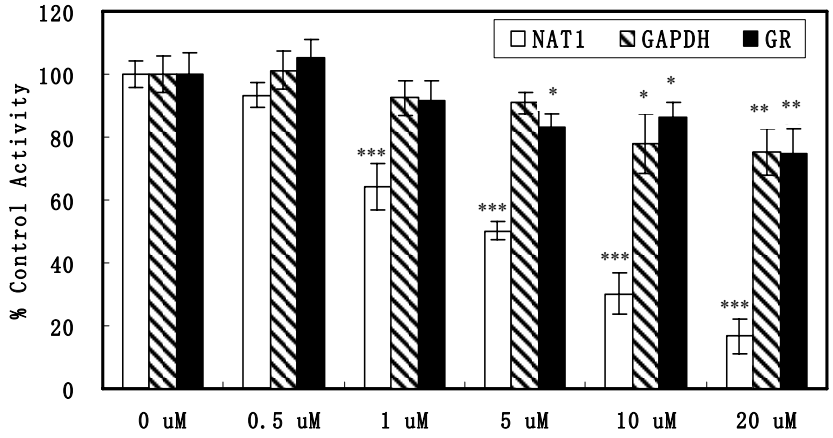

Figure 13. Concentration-dependent inactivation of HeLa cell NAT1, GAPDH, and GR by 2-NO-F. (a) The incubation time was 1 h. Each bar represents the mean and standard deviation of 3 experiments. Asterisks represent significant differences from controls: *, $p < 0.05$; **, $p < 0.01$; ***, $p < 0.001$. (From reference 24) (b) The incubation time was 4 h. Each bar represents the mean and standard deviation of the results of 3 experiments. Asterisks represent significant differences from controls: *, $p < 0.05$; **, $p < 0.01$; ***, $p < 0.001$.

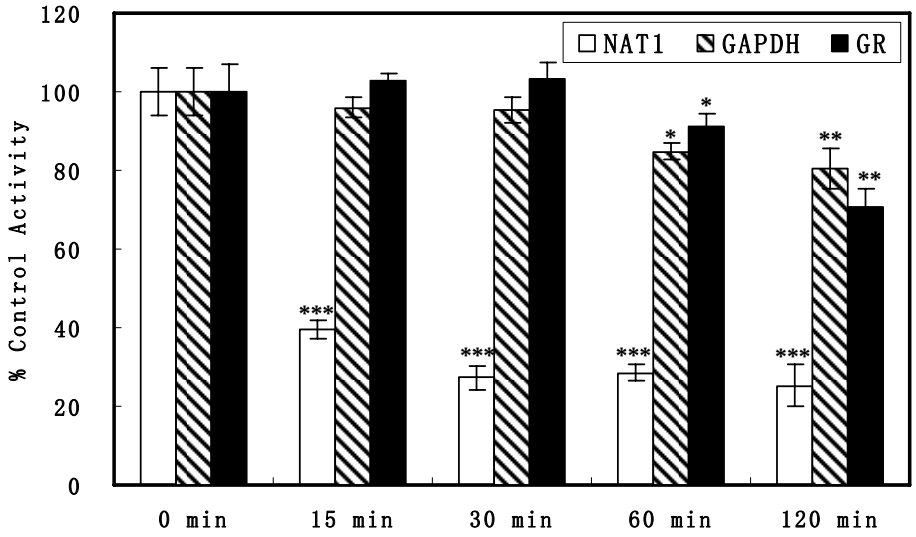

Figure 14. Time-dependent inactivation of HeLa cell NAT1, GAPDH, and GR by 2-NO-F. The concentration of 2-NO-F was 10 μM. Each bar represents the mean and standard deviation of the results of 3 experiments. Asterisks represent significant differences from controls (0 min): *, $p < 0.05$; **, $p < 0.01$; ***, $p < 0.001$. (From reference 24)

Effect of N-Acetylcysteine (NAC) on the Inactivation of HeLa Intracellular NAT1 by 4-NO-BP. GSH is a critical cellular reductant and nucleophile that reacts with various nitrosoarenes to form sulfinamides (*7-9, 26, 27, 38*). It was reported that the GSH content of HeLa cells is 20-30 nmol per 10^6 cells (*39, 40*). It was found that treatment of HeLa cells with a concentration of 20 mM NAC for 4 h caused more than a 4-fold increase in the ratio of reduced to oxidized GSH (*22*). HeLa cells were incubated with NAC (20 mM) for 4 h before being incubated with 4-NO-BP (10 μM) for 1 h. 4-NO-BP caused a 63% reduction in NAT1 activity of HeLa cells and caused a 65% decrease in NAT1 activity when the cells had been treated with NAC before treatment of 4-NO-BP (Table 5). Thus, treatment of HeLa cells with NAC had no effect on the ability of 4-NO-BP to inactivate intracellular NAT1.

Proteolysis and MALDI Q-TOF MS/MS Analysis of 4-NO-BP-Treated 3FLAG-NAT1 Expressed in HeLa Cells. To study the mechanism of inactivation of intracellular NAT1 by 4-NO-BP and to accumulate enough protein for mass spectrometric analysis, 3FLAG-NAT1 was expressed in HeLa cells as previously reported (*23*). By comparing the specific activity of NAT1 in lysates from transfected (472 ± 32 nmol/mg of protein/min) and non-transfected HeLa cells (4.4 ± 0.32 nmol/mg of protein/min), we estimated the concentration of NAT1 to be more than 100-fold greater in transfected cells compared to the endogenous NAT1 levels. Incubation of the cells with 4-NO-BP (200 μM) for 3 h caused an 81 ± 6 % decrease in NAT1 activity. The trypan blue assay showed a cell viability of around 80% under the experimental conditions. Immunoprecipitation of 3FLAG-NAT1 with anti-FLAG M-2 affinity gel was

	NAT1 (nmol/mg/min)	% Control Activity
HeLa Cells	4.66 ± 0.11	100
HeLa Cells + NAC	4.54 ± 0.35	97 *
HeLa Cells + 4-NO-BP	1.72 ± 0.25	37 **
HeLa Cells + NAC + 4-NO-BP	1.61 ± 0.23	35 **

Table 5. Effect of 4-NO-BP on NAT1 Activity after Exposure of HeLa Cells to N-Acetyl-L-Cysteine (NAC). Results are presented as the means (± SD) of three experiments. Asterisks represent significant differences from control values: *, $p > 0.05$; **, $p < 0.001$. (From reference 24)

followed by loading the released protein on SDS-PAGE (Figure 15) and in-gel pepsin digestion. The resulting digests were analyzed by MALDI Q-TOF MS. The mass spectrum of peptides obtained from cells that had not been incubated with 4-NO-BP revealed a peak with molecular mass of 1558.79 Da, which corresponds to the sequence DQVVRRNRGGWCL (Asp57-Leu69; unmodified theoretical mass 1558.78 Da) (Figure 16a). After treatment of cells with 4-NO-BP, the corresponding mass spectrum of the digest contained a new peak at 1590.76 Da, corresponding to the modified (+32 Da) Asp57-Leu69 sequences (Figure 16b). MALDI Q-TOF MS/MS of the peptide of mass 1590.76 revealed a intense b12-H_2SO_2 ion (1393.71 m/z) and a b12 ion of 1459.71 (m/z), which verify that the thiol group of the catalytically essential Cys68 had been converted to a sulfinic acid (Figure 17). As illustrated in Figure 7, it has been established previously that, under the acid conditions of pepsin digestion, sulfinamide adducts are hydrolyzed to sulfinic acids (*10, 11*). Thus, the inactivation of intracellular NAT1 by 4-NO-BP involves formation of a sulfinamide adduct with the active site Cys68 (Figure 18).

Effect of 4-NO-BP and 2-NO-F on Cytosolic NAT1 and Intracellular NAT1 Activity in Breast Cancer Cells. The IC_{50} values for inhibition of NAT1 in MDA-MB-231 cell cytosol by 4-NO-BP and 2-NO-F were 0.07 ± 0.006 μM and 0.05 ± 0.003 μM, which were very similar to the values for inhibition of HeLa cytosolic NAT1. Incubation of cytosol with 4-NO-BP (100 nM) caused 66 ± 5% inhibition of NAT1 activity, but only 13 ± 8% inhibition occurred in the presence of AcCoA (400 μM). Thus, inactivation of MDA-MB-231 cell cytosolic NAT1 by 4-NO-BP involves interaction with the active site of NAT1.

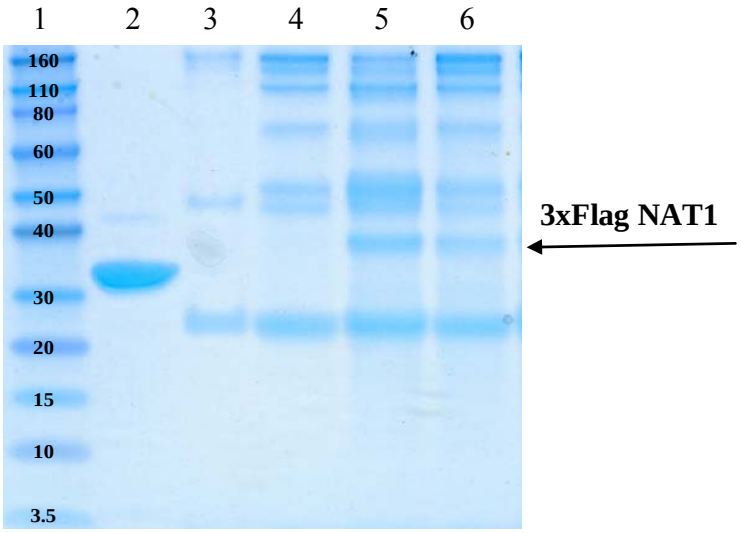

Figure 15. SDS-PAGE for in-gel pepsin digestion and mass spectrometric analysis: lane 1, molecular markers; lane 2, recombinant NAT1; lane 3, ANTI-FLAG M2 Affinity Gel boiled with SDS-PAGE sample buffer; lane 4, immunoprecipitation of control HeLa cell lysate; lane 5, immunoprecipitation of NAT1 transfected HeLa cell lysate; lane 6, immunoprecipitation of 4-NO-BP treated NAT1 transfected HeLa cell lysate.

a.

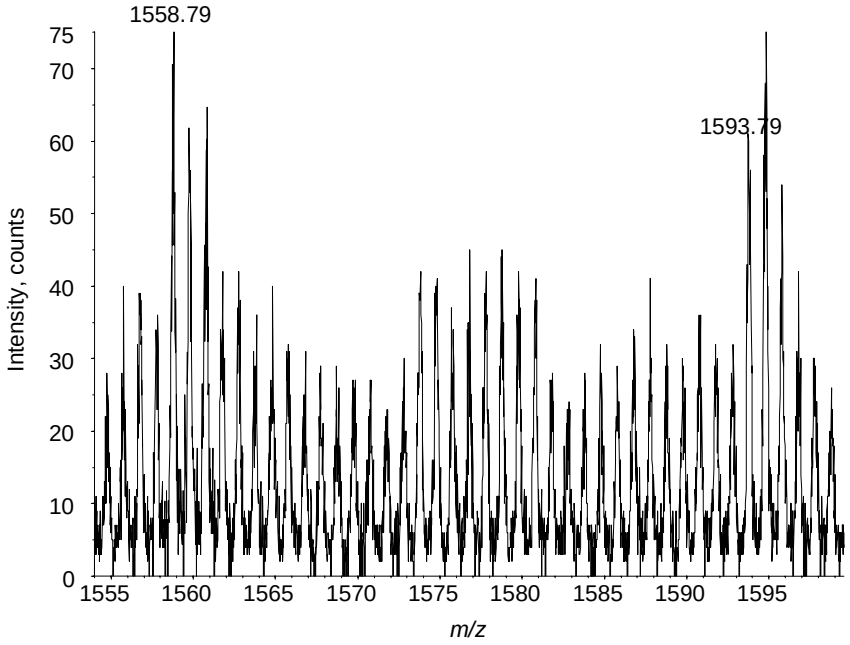

b.

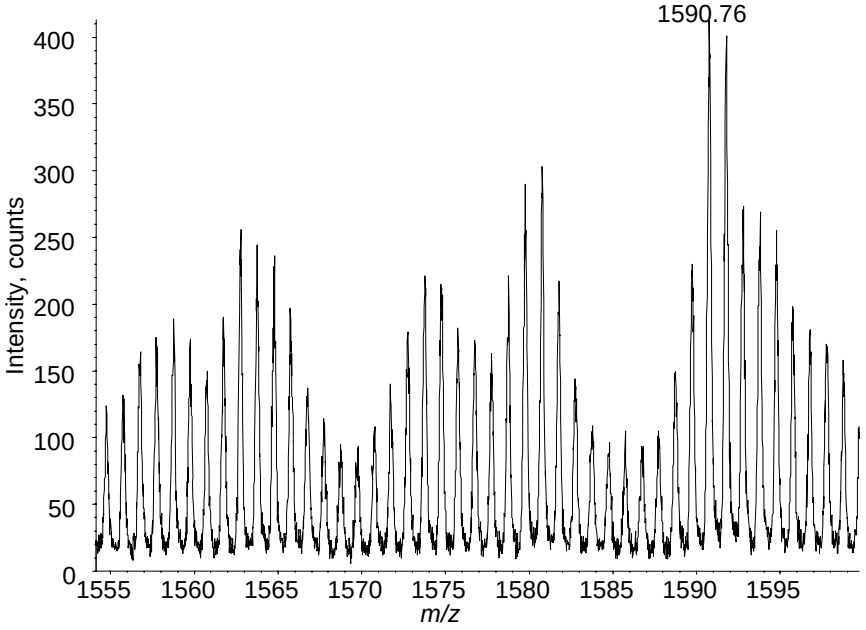

Figure 16. Segments of the MALDI Q-TOF mass spectra of in gel pepsin digests of (a) NAT1 after overexpression in HeLa cells; (b) NAT1 after overexpression in HeLa cells followed by treatment of the cells with 4–NO-BP (200 μM for 3 h). (From reference 24)

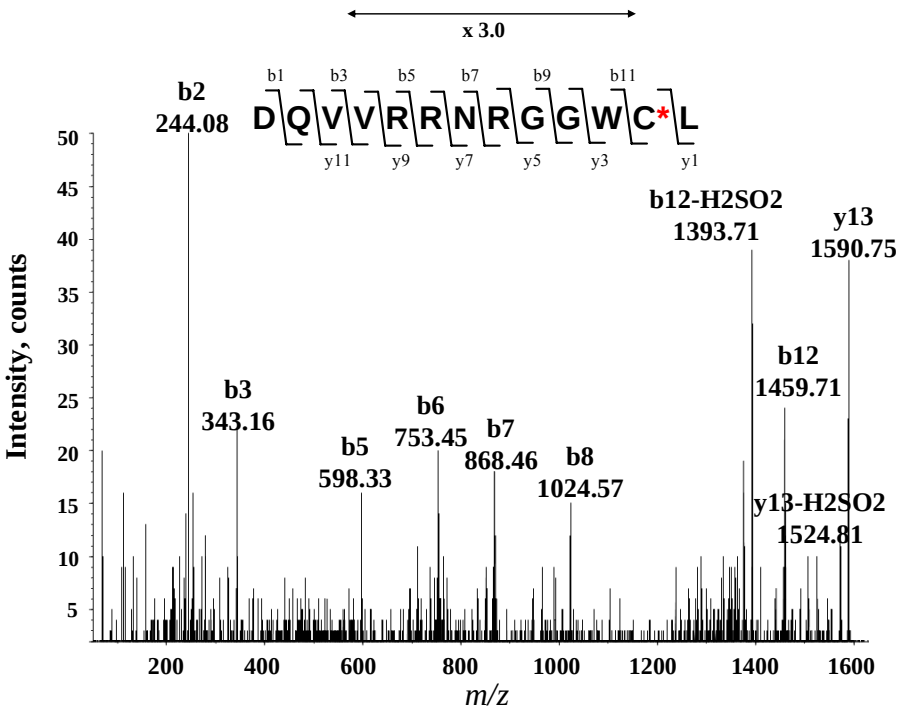

Figure 17. MALDI Q-TOF tandem mass spectrum of the 1590.76 Da peptide obtained by pepsin digestion of NAT1 after overexpression of NAT1 in HeLa cells and treatment of the cells with 4-NO-BP. The asterisk indicates Cys68, which contains a sulfinic acid side chain. (From reference 24)

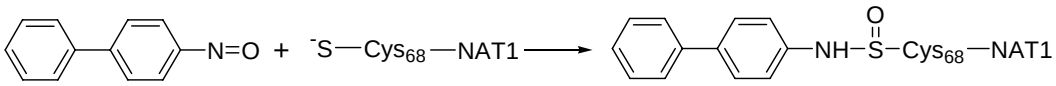

Figure 18. Reaction of a nitrosoarene with the catalytically essential Cys68 of NAT1 to form a sulfinamide. (From reference 24)

Incubation of MDA-MB-231 cells with various concentrations of 4-NO-BP for 4 h caused a concentration dependent inactivation of endogenous NAT1, showing an IC_{50} value of 37 ± 1 μM (Figure 19a). 4-NO-BP also caused the inactivation of intracellular NAT1 in MDA-MB-468 cells, exhibiting an IC_{50} value of 21 ± 1 μM during the 4 h treatment (Figure 19b). Incubation of MCF7 cells with 10 μM of 4-NO-BP for 4 h caused a 74 ± 4 % inhibition of intracellular NAT1 activity. Thus, 4-NO-BP is an effective inactivator of NAT1 in breast cancer cells as well as in HeLa cells.

a.

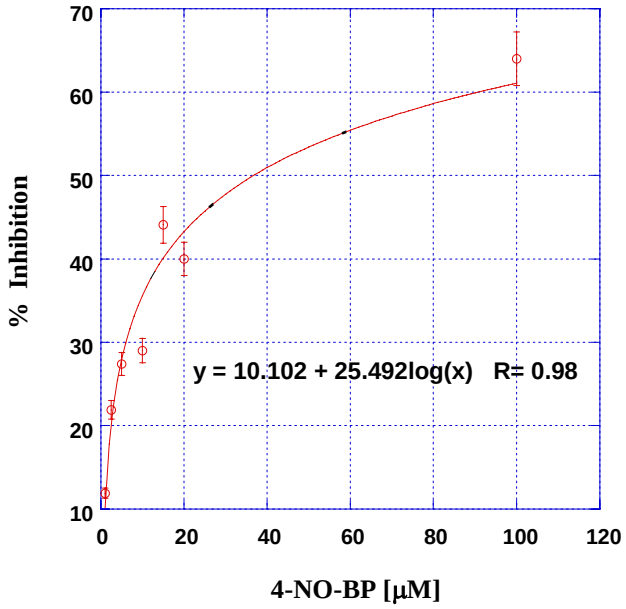

b.

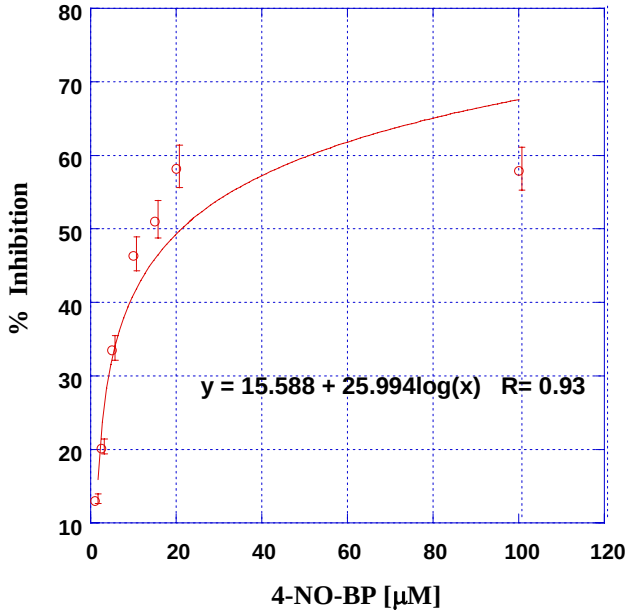

Figure 19. Concentration-dependent inactivation of MDA-MB-231 and MDA-MB-468 cells NAT1. The incubation time was 4 h. (a) MDA-MB-231 cells; (b) MDA-MB-468 cells. The logarithmic curve fit was used to assist in visualization of the trend in the data.

Discussion

The 2007 International NAT Workshop report emphasized that investigation of carcinogenic compounds that may inhibit NAT by directly reacting with the active site of the enzyme is a critical field of eukaryotic NAT functional study (*41*). Previously, our laboratory has shown that N-arylhydroxamic acids, which are metabolites of arylamines, inactivate NATs, in vitro and in vivo (*10, 11, 42-45*). Mass spectrometric analysis revealed that the mechanism of inactivation of NAT by N-arylhydroxamic acids involved an initial NAT-mediated deacetylation to produce N-arylhydroxylamines, which undergo oxidation to the electrophilic nitrosoarenes, which react with the nucleophilic active site Cys68 of the enzyme to form a sulfinamide (*10, 11*). Treatment of hamster NAT1 with 2-NO-F, or exposure of hamster NAT1, hamster NAT2, and human NAT1 to 4-NO-BP resulted in the irreversible inactivation of the enzyme by production of a sulfinamide adduct with the Cys68 thiol group. It is of interest that King and Duffel found that inactivation of rat aryl sulfotransferase IV by N-hydroxyarylamines, such as N-hydroxyaniline and N-hydroxy-2-aminofluorene, was dependent upon oxidation of the hydroxylamines to nitrosoarenes (*46*). Nitrosoarenes, which can be formed from the oxidation of N-hydroxyarylamines, critical intermediates in the bioactivation of many carcinogenic arylamines, arylamides and nitroaromatics, or by the reduction of nitroarenes, are of potential toxicological importance for their ability to inactivate NAT, thereby impairing a crucial detoxification process.

The results of the analysis of inactivation of recombinant human NAT1, HeLa cell cytosolic NAT1, and HeLa intracellular NAT1 by 4-NO-BP, 2-NO-F,

NO-B, and 2-NO-T were consistent with the expectation that nitrosoarene derivatives of primary arylamines that are rapidly N-acetylated by NAT1 should be portent inactivators of the enzyme. The second order rate constants for inactivation of NAT1 by 4-NO-BP and 2-NO-F were 59200 and 34500 $M^{-1}s^{-1}$, respectively, and were 1500-2500-fold greater than the corresponding inactivation rate constants of NO-B and 2-NO-T. 4-NO-BP and 2-NO-F are such potent inactivators of NAT1 that the second order inactivation rate constants are comparable in magnitude to the value 50,000 $M^{-1}s^{-1}$, obtained with peroxynitrite, a highly reactive oxidant (*47*). As a comparison, the rate constants for inactivation of NAT1 by hydrogen peroxide (H_2O_2) and cisplatin, an anticancer agent, are 7 and 12 $M^{-1}s^{-1}$, respectively, which are 2900-8000 fold smaller than those of 4-NO-BP and 2-NO-F (*48, 49*). The effective inactivation of NAT1 by 4-NO-BP and 2-NO-F can be attributed to favorable interaction of the biphenyl and fluorenyl ring systems with hydrophobic residues in the NAT1 binding pocket, and also to the high nucleophility of the active site Cys68 thiol group, which has a pKa of 5.2 and reacts as the unprotonated thiolate in an imidazolium-thiolate ion pair (*50-52*).

Although nitrosoarenes react with GSH, one of the most important cellular thiol-containing molecules, to form sulfinamides, our results showed that 4-NO-BP and 2-NO-F react much more readily with NAT1 than with GSH (*7, 9*). In the presence of 500-fold excess of GSH over both nitrosoarenes and NAT1, 4-NO-BP and 2-NO-F caused substantial losses of NAT1 activity in 60 s. Additionally, a 5000-fold excess of GSH could not provide complete protection of NAT1. Therefore, it was expected that cellular GSH may be insufficient to protect the endogenous NAT1 enzyme from inactivation by 4-NO-BP or 2-NO-F.

Western blot experiments showed that NAT1 was expressed in HeLa cells and in breast cancer cell lines, MDA-MB-231, MDA-MB-468, and MCF-7. Densitometry analysis and specific activity comparisons with purified recombinant NAT1 revealed that NAT1 constituted approximately 0.002% of the cytosolic protein in HeLa, MDA-MB-231, and MDA-MB-468 cells and constituted approximately 0.005-0.01% of cytosolic protein in ER-positive MCF-7 breast cancer cells. It is of interest that several studies have shown that NAT1 genes are significantly overexpressed in ER-positive breast cancers and that expression of NAT1 may be a candidate prognostic marker in ER-positive breast cancer (*30, 53-55*).

The inhibitory effects of 4-NO-BP and 2-NO-F on NAT1 were also observed upon treatment of HeLa cell cytosol and intact HeLa cells with nitrosoarenes. Low concentrations of 4-NO-BP and 2-NO-F caused a dramatic and rapid loss of HeLa cytosolic and intracellular NAT1 activity, whereas NO-B and 2-NO-T were much weaker inhibitors of cytosolic NAT1, showing IC_{50} values of 237 and 91 μM, and were ineffective as inactivators of intracellular NAT1 activity. Treatment of the cells with low concentrations of 4-NO-BP and 2-NO-F or incubation of the cells with 10 μM of the compounds for 15 min caused a pronounced reduction in NAT1 activity, but had no effect on either GAPDH or GR activities. In contrast, cellular oxidants, such as hydrogen peroxide, not only caused reversible inactivation of NAT1 at 200 μM concentration, but also inactivated the proteasome and changed the PI value of cellular GAPDH in human lens epithelial cells (*56, 57*). Thus, in contrast to the effects of less specific

inactivators, NAT1 appears to be a preferred intracellular target of 4-NO-BP and 2-NO-F.

It is of interest that 4-NO-BP and 2-NO-F caused extensive but incomplete inactivation of intracellular NAT1. Approximately 30% of intracellular NAT1 was not susceptible to inactivation by either 4-NO-BP or 2-NO-F. 4-NO-BP (20 μM) and 2-NO-F (10 μM) caused a maximal loss of HeLa NAT1 activity after 1 h treatment. A 40 μM concentration of 4-NO-BP and a 20 μM concentration of 2-NO-F did not lead to significant additional reduction of NAT1 activity in HeLa cells (Figures 11a and 13a). After incubation of HeLa cells with 4-NO-BP or 2-NO-F for 4 h, the maximal reduction of NAT1 activity was approximately 70-80% (Figure 11b and 13b). Treatment of MDA-MB-231 or MDA-MB-468 cells with a 20 μM concentration of 4-NO-BP for 4 h caused approximately 50% inactivation of NAT1 activity and a 100 μM concentration of 4-NO-BP eliminates approximately 60% of the NAT1 activity. These results are consistent with previous reports that 50-100 μM concentrations of N-hydroxy-PABA caused a similar loss of NAT1 activity of approximately 60-80% in PBMC after exposure of 24 h, and 250-500 concentrations of cisplatin reduced NAT1 activity by 60-80% in MDA-MB-231 cells and MCF-7 cells after an exposure of 1 h (*37*, *49*). Because nitrosoarenes and cisplatin inactivate NAT1 through direct reaction with the active site Cys68, which is the "most likely" mechanism of the inactivation by N-hydroxy-PABA as well (*37*), it is possible that the residual NAT1 activity represents a portion of the intracellular NAT1 that is in the acetylated state and cannot react with the inactivators.

Thus, the efficiency of the NAT1-catalyzed acetylation of arylamines can be applied to predict the relative effectiveness of nitrosoarenes as inactivators of NAT1. NAT1 is inactivated by concentrations of 4-NO-BP and 2-NO-F that are not toxic to HeLa cells. Exposure to low concentrations of nitrosoarenes in vivo may lead to a loss of NAT1 activity and damage to the NAT-mediated detoxification process.

References

(1) Kim, D. and Guengerich, F. P. (2005) Cytochrome P450 activation of arylamines and heterocyclic amines. *Annu Rev Pharmacol Toxicol 45*, 27-49.

(2) Hanna, P. E. (1996) Metabolic activation and detoxification of arylamines. *Curr. Med. Chem. 3*, 195-210.

(3) Beije, B. and Moller, L. (1988) 2-Nitrofluorene and related compounds: prevalence and biological effects. *Mutat Res 196*, 177-209.

(4) Zwirner-Baier, I. and Neumann, H. G. (1999) Polycyclic nitroarenes (nitro-PAHs) as biomarkers of exposure to diesel exhaust. *Mutat Res 441*, 135-144.

(5) Boelsterli, U. A., Ho, H. K., Zhou, S. and Leow, K. Y. (2006) Bioactivation and hepatotoxicity of nitroaromatic drugs. *Curr Drug Metab 7*, 715-727.

(6) Neumann, H. G. (2007) Aromatic amines in experimental cancer research: tissue-specific effects, an old problem and new solutions. *Crit Rev Toxicol 37*, 211-236.

(7) Mulder, G. J., Unruh, L. E., Evans, F. E., Ketterer, B. and Kadlubar, F. F. (1982) Formation and identification of glutathione conjugates from 2-nitrosofluorene and N-hydroxy-2-aminofluorene. *Chem Biol Interact 39*, 111-127.

(8) Eyer, P. (1994) Reactions of oxidatively activated arylamines with thiols: reaction mechanisms and biologic implications. An overview. *Environ Health Perspect 102 Suppl 6*, 123-132.

(9) Kazanis, S., and Mc Clelland, R. A. (1992) Electrophilic intermediate in the reaction of glutathione and nitrosoarenes. *J. Am. Chem. Soc. 114*, 3052-3059.

(10) Guo, Z., Wagner, C. R. and Hanna, P. E. (2004) Mass spectrometric investigation of the mechanism of inactivation of hamster arylamine N-acetyltransferase 1 by N-hydroxy-2-acetylaminofluorene. *Chem Res Toxicol 17*, 275-286.

(11) Wang, H., Wagner, C. R. and Hanna, P. E. (2005) Irreversible inactivation of arylamine N-acetyltransferases in the presence of N-hydroxy-4-acetylaminobiphenyl: a comparison of human and hamster enzymes. *Chem Res Toxicol 18*, 183-197.

(12) Liu, L., Von Vett, A., Zhang, N., Walters, K. J., Wagner, C. R. and Hanna, P. E. (2007) Arylamine N-acetyltransferases: characterization of the substrate specificities and molecular interactions of environmental arylamines with human NAT1 and NAT2. *Chem Res Toxicol 20*, 1300-1308.

(13) Wang, H., Vath, G. M., Kawamura, A., Bates, C. A., Sim, E., Hanna, P. E. and Wagner, C. R. (2005) Over-expression, purification, and characterization of recombinant human arylamine N-acetyltransferase 1. *Protein J 24*, 65-77.

(14) Mangold, B. L. and Hanna, P. E. (1982) Arylhydroxamic acid N,O-acyltransferase substrates. Acetyl transfer and electrophile generating activity of N-hydroxy-N-(4-alkyl-, 4-alkenyl-, and 4-cyclohexylphenyl)acetamides. *J Med Chem 25*, 630-638.

(15) Westra, J. G. (1981) A rapid and simple synthesis of reactive metabolites of carcinogenic aromatic amines in high yield. *Carcinogenesis 2*, 355-357.

(16) Stanley, L. A., Coroneos, E., Cuff, R., Hickman, D., Ward, A. and Sim, E. (1996) Immunochemical detection of arylamine N-acetyltransferase in normal and neoplastic bladder. *J Histochem Cytochem 44*, 1059-1067.

(17) Bradford, M. M. (1976) A rapid and sensitive method for the quantitation of microgram quantities of protein utilizing the principle of protein-dye binding. *Anal Biochem 72*, 248-254.

(18) *NIH Guidelines for the Laboratory Use of Chemical Carcinogens* (1981) NIH Publication No. 81-2385, U.S. Government Printing Office, Washington, DC.

(19) Sinclair, J. C., Delgoda, R., Noble. M. E., Jarmin, S., Goh, N. K., and Sim, E. (1998) Purification, characterization, and crystallization of an N-hydroxyarylamine O-acetyltransferase from Salmonella typhimurium. *Protein Expression Purif. 12*, 371-380.

(20) McAlister, L. and Holland, M. J. (1985) Differential expression of the three yeast glyceraldehyde-3-phosphate dehydrogenase genes. *J Biol Chem 260*, 15019-15027.

(21) Cohen, M. B. and Duvel, D. L. (1988) Characterization of the inhibition of glutathione reductase and the recovery of enzyme activity in exponentially growing murine leukemia (L1210) cells treated with 1,3-bis(2-chloroethyl)-1-nitrosourea. *Biochem Pharmacol 37*, 3317-3320.

(22) Goswami, P. C., Sheren, J., Albee, L. D., Parsian, A., Sim, J. E., Ridnour, L. A., Higashikubo, R., Gius, D., Hunt, C. R. and Spitz, D. R. (2000) Cell cycle-coupled variation in topoisomerase IIalpha mRNA is regulated by

the 3'-untranslated region. Possible role of redox-sensitive protein binding in mRNA accumulation. *J Biol Chem 275*, 38384-38392.

(23) Liu, F., Zhang, N., Zhou, X., Hanna, P. E., Wagner, C. R., Koepp, D. M. and Walters, K. J. (2006) Arylamine N-acetyltransferase aggregation and constitutive ubiquitylation. *J Mol Biol 361*, 482-492.

(24) Liu, L., Wagner, C. R. and Hanna, P. E. (2008) Human arylamine N-acetyltransferase 1: in vitro and intracellular inactivation by nitrosoarene metabolites of toxic and carcinogenic arylamines. *Chem Res Toxicol 21*, 2005-2016.

(25) Levy, H. M., Leber, P. D. and Ryan, E. M. (1963) Inactivation of Myosin by 2,4-Dinitrophenol and Protection by Adenosine Triphosphate and Other Phosphate Compounds. *J Biol Chem 238*, 3654-3659.

(26) Eyer, P. (1979) Reactions of nitrosobenzene with reduced glutathione. *Chem Biol Interact 24*, 227-239.

(27) Dolle, B., Topner, W. and Neumann, H. G. (1980) Reaction of arylnitroso compounds with mercaptans. *Xenobiotica 10*, 527-536.

(28) Butcher, N. J., Tetlow, N. L., Cheung, C., Broadhurst, G. M. and Minchin, R. F. (2007) Induction of human arylamine N-acetyltransferase type I by androgens in human prostate cancer cells. *Cancer Res 67*, 85-92.

(29) Grant, D. M., Lottspeich, F. and Meyer, U. A. (1989) Evidence for two closely related isozymes of arylamine N-acetyltransferase in human liver. *FEBS Lett 244*, 203-207.

(30) Wakefield, L., Robinson, J., Long, H., Ibbitt, J. C., Cooke, S., Hurst, H. C. and Sim, E. (2008) Arylamine N-acetyltransferase 1 expression in breast

cancer cell lines: a potential marker in estrogen receptor-positive tumors. *Genes Chromosomes Cancer 47*, 118-126.

(31) Dietze, E. C., Schafer, A., Omichinski, J. G. and Nelson, S. D. (1997) Inactivation of glyceraldehyde-3-phosphate dehydrogenase by a reactive metabolite of acetaminophen and mass spectral characterization of an arylated active site peptide. *Chem Res Toxicol 10*, 1097-1103.

(32) Dennehy, M. K., Richards, K. A., Wernke, G. R., Shyr, Y. and Liebler, D. C. (2006) Cytosolic and nuclear protein targets of thiol-reactive electrophiles. *Chem Res Toxicol 19*, 20-29.

(33) Babson, J. R. and Reed, D. J. (1978) Inactivation of glutathione reductase by 2-chloroethyl nitrosourea-derived isocyanates. *Biochem Biophys Res Commun 83*, 754-762.

(34) Nakano, M., Funayama, S., de Oliveira, M. B., Bruel, S. L. and Gomes, E. M. (1992) D-glyceraldehyde-3-phosphate dehydrogenase from HeLa cells--1. Purification and properties of the enzyme. *Comp Biochem Physiol B 102*, 873-877.

(35) Cotariu, D., Evans, S., Lahat, E., Theitler, J., Bistritzer, T. and Zaidman, J. L. (1992) Inhibition of human red blood cell glutathione reductase by valproic acid. *Biochem Pharmacol 43*, 425-429.

(36) Pai, E. F. and Schulz, G. E. (1983) The catalytic mechanism of glutathione reductase as derived from x-ray diffraction analyses of reaction intermediates. *J Biol Chem 258*, 1752-1757.

(37) Butcher, N. J., Ilett, K. F. and Minchin, R. F. (2000) Inactivation of human arylamine N-acetyltransferase 1 by the hydroxylamine of p-aminobenzoic acid. *Biochem Pharmacol 60*, 1829-1836.

(38) Lotlikar, P. D., Miller, E. C., Miller, J. A. and Margreth, A. (1965) The enzymatic reduction of the N-hydroxy derivatives of 2-acetylaminofluorene and related carcinogens by tissue preparations. *Cancer Res 25*, 1743-1752.

(39) Hao, X. Y., Widersten, M., Ridderstrom, M., Hellman, U. and Mannervik, B. (1994) Co-variation of glutathione transferase expression and cytostatic drug resistance in HeLa cells: establishment of class Mu glutathione transferase M3-3 as the dominating isoenzyme. *Biochem J 297 (Pt 1)*, 59-67.

(40) Lu, S. C., Sun, W. M., Yi, J., Ookhtens, M., Sze, G. and Kaplowitz, N. (1996) Role of two recently cloned rat liver GSH transporters in the ubiquitous transport of GSH in mammalian cells. *J Clin Invest 97*, 1488-1496.

(41) Boukouvala, S., Westwood, I. M., Butcher, N. J. and Fakis, G. (2008) Current trends in N-acetyltransferase research arising from the 2007 International NAT Workshop. *Pharmacogenomics 9*, 765-771.

(42) Hanna, P. E., Banks, R. B. and Marhevka, V. C. (1982) Suicide inactivation of hamster hepatic arylhydroxamic acid N,O-acyltransferase. A selective probe of N-acetyltransferase multiplicity. *Mol Pharmacol 21*, 159-165.

(43) Wick, M. J. and Hanna, P. E. (1990) Bioactivation of N-arylhydroxamic acids by rat hepatic N-acetyltransferase. Detection of multiple enzyme forms by mechanism-based inactivation. *Biochem Pharmacol 39*, 991-1003.

(44) Sticha, K. R., Bergstrom, C. P., Wagner, C. R. and Hanna, P. E. (1998) Characterization of hamster recombinant monomorphic and polymorphic arylamine N-acetyltransferases: bioactivation and mechanism-based inactivation studies with N-hydroxy-2-acetylaminofluorene. *Biochem Pharmacol 56*, 47-59.

(45) Smith, T. J. and Hanna, P. E. (1988) Hepatic N-acetyltransferases: selective inactivation in vivo by a carcinogenic N-arylhydroxamic acid. *Biochem Pharmacol 37*, 427-434.

(46) King, R. S. and Duffel, M. W. (1997) Oxidation-dependent inactivation of aryl sulfotransferase IV by primary N-hydroxy arylamines during in vitro assays. *Carcinogenesis 18*, 843-849.

(47) Dairou, J., Atmane, N., Rodrigues-Lima, F. and Dupret, J. M. (2004) Peroxynitrite irreversibly inactivates the human xenobiotic-metabolizing enzyme arylamine N-acetyltransferase 1 (NAT1) in human breast cancer cells: a cellular and mechanistic study. *J Biol Chem 279*, 7708-7714.

(48) Atmane, N., Dairou, J., Paul, A., Dupret, J. M. and Rodrigues-Lima, F. (2003) Redox regulation of the human xenobiotic metabolizing enzyme arylamine N-acetyltransferase 1 (NAT1). Reversible inactivation by hydrogen peroxide. *J Biol Chem 278*, 35086-35092.

(49) Ragunathan, N., Dairou, J., Pluvinage, B., Martins, M., Petit, E., Janel, N., Dupret, J. M. and Rodrigues-Lima, F. (2008) Identification of the xenobiotic-metabolizing enzyme arylamine N-acetyltransferase 1 as a new target of cisplatin in breast cancer cells: molecular and cellular mechanisms of inhibition. *Mol Pharmacol 73*, 1761-1768.

(50) Zhang, N., Liu, L., Liu, F., Wagner, C. R., Hanna, P. E. and Walters, K. J. (2006) NMR-based model reveals the structural determinants of mammalian arylamine N-acetyltransferase substrate specificity. *J Mol Biol 363*, 188-200.

(51) Wu, H., Dombrovsky, L., Tempel, W., Martin, F., Loppnau, P., Goodfellow, G. H., Grant, D. M. and Plotnikov, A. N. (2007) Structural basis of substrate-binding specificity of human arylamine N-acetyltransferases. *J Biol Chem 282*, 30189-30197.

(52) Wang, H., Vath, G. M., Gleason, K. J., Hanna, P. E. and Wagner, C. R. (2004) Probing the mechanism of hamster arylamine N-acetyltransferase 2 acetylation by active site modification, site-directed mutagenesis, and pre-steady state and steady state kinetic studies. *Biochemistry 43*, 8234-8246.

(53) Richardson, A. L., Wang, Z. C., De Nicolo, A., Lu, X., Brown, M., Miron, A., Liao, X., Iglehart, J. D., Livingston, D. M. and Ganesan, S. (2006) X chromosomal abnormalities in basal-like human breast cancer. *Cancer Cell 9*, 121-132.

(54) Miller, L. D., Smeds, J., George, J., Vega, V. B., Vergara, L., Ploner, A., Pawitan, Y., Hall, P., Klaar, S., Liu, E. T. and Bergh, J. (2005) An expression signature for p53 status in human breast cancer predicts mutation status, transcriptional effects, and patient survival. *Proc Natl Acad Sci U S A 102*, 13550-13555.

(55) Gruvberger, S., Ringner, M., Chen, Y., Panavally, S., Saal, L. H., Borg, A., Ferno, M., Peterson, C. and Meltzer, P. S. (2001) Estrogen receptor status in breast cancer is associated with remarkably distinct gene expression patterns. *Cancer Res 61*, 5979-5984.

(56) Hosler, M. R., Wang-Su, S. T. and Wagner, B. J. (2003) Targeted disruption of specific steps of the ubiquitin-proteasome pathway by oxidation in lens epithelial cells. *Int J Biochem Cell Biol 35*, 685-697.

(57) Paron, I., D'Elia, A., D'Ambrosio, C., Scaloni, A., D'Aurizio, F., Prescott, A., Damante, G. and Tell, G. (2004) A proteomic approach to identify early molecular targets of oxidative stress in human epithelial lens cells. *Biochem J 378*, 929-937.

PART IV: HUMAN ARYLAMINE N-ACETYLTRANSFERASE 2: IN VITRO AND INTRACELLULAR INACTIVATION BY NITROSOARENES

Introduction

Arylamine N-acetyltransferases (NATs) modify drug efficacy/toxicity and cancer risk due to their dual role in detoxification and metabolic activation of arylamine drugs and carcinogens (*1, 2*). Human NAT2 is one of two polymorphic NAT isoforms expressed in human tissues and shares 81% sequence identity with the NAT1 isoform (*3*). NAT1 and NAT2 polymorphisms modify individual cancer risk, drug response and adverse drug reactions (*4-7*). The role of the NAT2 slow acetylator genotype and bladder cancer risk, especially following exposures to aromatic amines, has been subject of numerous studies (*8-12*). It is of interest to characterize the non-genetic factors that may attenuate NAT2 activity and the toxicological implications.

We previously reported that the ability of human NAT1 to N-acetylate an arylamine correlates with the ability of the corresponding nitrosoarene metabolites to inactivate the enzyme. Thus, exposure to low concentrations of 4-nitrosobiphenyl (4-NO-BP) and 2-nitrosofluorene (2-NO-F) (Figure 1) lead to a dramatic loss of NAT1 activity in HeLa cells (*13*). The purpose of this study is to investigate the susceptibility of human NAT2 to inactivation by nitrosoarene metabolites of four environmental arylamines (Figure 1), in vitro and in human cells, and to determine similarities and differences with their inactivation of human NAT1.

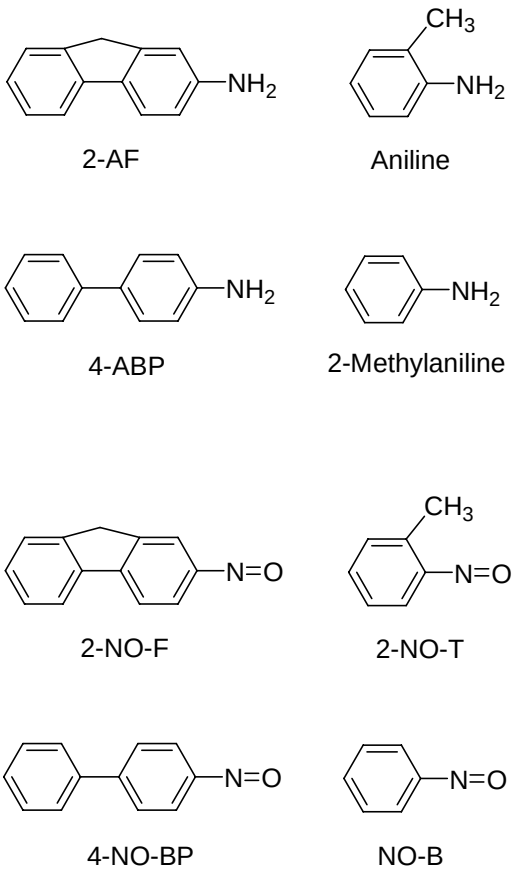

Figure 1. Structures of arylamines and their nitrosoarene metabolites used in this study.

We proposed that, for arylamines which are good substrates for human NAT2, the corresponding nitroso derivatives would be potent NAT2 inactivators. In contrast, the nitrosoarene metabolites of arylamines that are poor substrates for NAT2 are expected to be much less effective inactivators. The k_{cat}/K_m values for N-acetylation of 4-aminobiphenyl (4-ABP) and 2-aminofluorene (2-AF) (Figure 1) by recombinant NAT2 are 527 $s^{-1}mM^{-1}$ and 265 $s^{-1}mM^{-1}$. However, the corresponding rate constants for aniline and 2-methylaniline (o-toluidine) (Figure 1) are 63 $s^{-1}mM^{-1}$ and 15 $s^{-1}mM^{-1}$ (*14*). Thus, 4-NO-BP and 2-NO-F (Figure 1) are proposed to be potent inactivators of NAT2 and nitrosobenzene (NO-B) and 2-nitrosotoluene (2-NO-T) are anticipated to be much weaker inhibitors. The reduction of NAT2 activity by nitrosoarenes might result in elevated sensitivity to environmental arylamines and play a role in arylamine carcinogenesis.

Materials and Methods

Materials were prepared as described in Part III of this thesis.

NAT2 Activity Assay. The assay was performed with PNPA as the acetyl donor and p-anisidine as the acetyl acceptor as described previously (Part I of this thesis).

Time-Dependent Inactivation of NAT2 by Nitrosoarenes at 37 °C. The incubation mixtures contained NAT2 (34.5 μg/mL, 1 μM), 4-NO-BP (0.1-5 μM), 2-NO-F (0.1-2 μM), NO-B (500-4000 μM), or 2-NO-T (100-2000 μM) and potassium phosphate buffer (20 mM, pH 7.4; 1 mM EDTA) in a total volume of 75 μL. The reaction was initiated by addition of nitrosoarenes dissolved in 1.5 μL of DMSO. The final concentration of DMSO was 2%. Aliquots (2 μL) were withdrawn at 15 s (4-NO-BP, 0-45 s), 10 s (2-NO-F, 0-30 s), 30 s (2-NO-T, 0-120 s), or 60 s (NO-B, 0-180 s) intervals and transferred to an assay cuvett. The controls contained DMSO, but not nitrosoarene.

Inactivation of NAT2 by NO-B and 2-NO-T in the Presence of AcCoA. In a total volume of 98 μL, NAT2 (34.5 μg/mL, 1 μM) was incubated with AcCoA (20 μM) for 1 min in potassium phosphate buffer (20 mM, pH 7.4; 1 mM EDTA) at 37 ºC. 2-NO-T or NO-B dissolved in 2 μL of DMSO was added. The final concentration of 2-NO-T was 500 μM and that of NO-B was 800 μM . The incubation was continued for 2 min (2-NO-T) or 3 min (NO-B). Aliquots (2 μL) were withdrawn and assayed for NAT2 transacetylation activity.

Inactivation of NAT2 by 4-NO-BP and 2-NO-F in the Presence of GSH. In a total volume of 147 μL, NAT2 was incubated with GSH for 2 min in potassium phosphate buffer (20 mM, pH 7.4; 1 mM EDTA) at 37 °C. 4-NO-BP or 2-NO-F dissolved in 3 μL of DMSO was added and incubation was continued for 30 or 60 s at 37 °C. The final concentrations were: NAT2, 25 μg/mL (0.73 μM); GSH, 0.5, 1, or 5 mM; 4-NO-BP or 2-NO-F, 1 or 5 μM. Aliquots (2 μL) were withdrawn and assayed for NAT2 activity. Controls contained only potassium phosphate buffer and DMSO. There was no statistically significant difference between control activities determined in the presence and absence of GSH ($p > 0.2$).

Sample Preparation for Nano-ESI-Q-TOF MS of 4-NO-BP-Treated NAT2 and 2-NO-F-Treated NAT2. To NAT2 (84 μg, 40 μM) in potassium phosphate buffer (60 μL, 20 mM, pH 7.4; 1 mM EDTA; 10% glycerol; 0.1 mM DTT) was added 4-NO-BP or 2-NO-F dissolved in 2 μL of DMSO. The final concentration of 4-NO-BP and 2-NO-F were 250 μM and 100 μM, respectively. DMSO only was added to the control incubation mixtures. After a 3 min incubation for 4-NO-BP and a 5 min incubation for 2-NO-F at 37 °C, the residual activity was less than 3% of the control activity. The reaction mixture was loaded onto a Bio Spin 6 Tris Column, which had been equilibrated with the potassium phosphate buffer. After centrifugation at 1000g for 4 min, 8 μL of the solution was used to measure the protein concentration and residual activity. The remaining solution was stored at -80 °C.

Pepsin Digestion of 4-NO-BP, and 2-NO-F-Treated NAT2. The same procedures were carried out to inactivate NAT2 with 4-NO-BP, and 2-NO-F as described above for the sample preparation for Nano-ESI-Q-TOF MS. The solution (50 μL) obtained with the Bio Spin 6 Tris column was concentrated to 30 μL by freeze drying. HCl (2.2 μL, 1 N) was added to adjust the pH to 1.3. Digestion was initiated by addition of pepsin (1 mg/mL in H_2O, pH 1.3). The ratio of pepsin to NAT2 protein was approximately 1:100. After incubation at 37 °C for 3 h, the reaction was terminated by adjusting the pH to 8 with 1 N NaOH (1.7 μL). Acetonitrile (2.1 μL) was added, and the sample was stored at -80 °C. A control digest, to which DMSO only had been added, was obtained by an identical procedure.

Nano-ESI-Q-TOF MS of Unmodified and Modified NAT1 and NAT2. NAT1 and NAT2 samples were desalted with Millipore C4 ZipTips and analyzed by Nano-ESI-Q-TOF MS as previously described (*15*).

MALDI-TOF MS Screening and Sequencing of Peptides. The pepsin digests were desalted with Millipore C18 ZipTips and analyzed by MALDI-TOF MS and sequenced by MALDI-TOF MS/MS as previously described (*15*).

MS Data Analysis. Theoretical masses of proteins, peptides, and fragment ions were generated with Protein Prosepector (http://prospector.ucsf.edu) and with the ABI AS software package.

Cell Culture Conditions. HeLa cells were maintained as monolayers in

DMEM supplemented with 10% fetal bovine serum (FBS) and 1% penicillin-streptomycin-fungizome in a humidified, 5% CO_2 atmosphere at 37 ºC.

NAT2 Activity in HeLa Cell Cytosol. HeLa cell cytosol was prepared as described in Part III of this thesis. Cell cytosol (80 μL) and SMZ, dissolved in 10 μL of assay buffer (20 mM Tris-HCl, 1 mM EDTA, pH 7.5) were incubated at 37 ºC for 5 min. AcCoA dissolved in 10 μL of assay buffer was added. The final concentrations were: SMZ, 200 μM; AcCoA, 800 μM. The incubation was continued at 37 ºC for various lengths of time (30-90 min). Cold trichloroacetic acid (20% w/v) (100 μL) was added, followed by centrifugation for 5 min at 12000g. The supernatant was added to 4-dimethylaminobenzaldehyde (800 μL, 5% w/v in 9:1 acetonitrile/water). The unreacted SMZ was quantitated by measuring the absorbance at 450 nm (ε_{450nm} = 7300 $M^{-1}cm^{-1}$). All assays were performed in triplicate under initial rate conditions. Either AcCoA or SMZ was omitted in control incubations.

NAT1, GAPDH, and GR Activity in HeLa Cell Cytosol. NAT1, GAPDH, and GR activities were measured as reported previously (*16*).

Effect of Nitrosoarenes on Endogenous NAT2, GAPDH, and GR Activities in HeLa Cells. At approximately 90% confluence, cell monolayers were washed twice with PBS. The cells were exposed to 4-NO-BP (5-40 μM), 2-NO-F (2.5-20 μM), NO-B (100-250 μM), or 2-NO-T (100-250 μM) in 10 mL of serum-free DMEM media containing DMSO. The final concentration of DMSO was 0.1%. The incubation was continued at 37 ºC for various periods of time.

Cells were washed with PBS buffer, trypsinized, and harvested. The controls contained DMSO only. Cytosol was prepared as described above, and the NAT2 activity was determined. In the experiments with 4-NO-BP and 2-NO-F, GAPDH and GR activities were also measured. Cell viability was confirmed with the trypan blue assay as described previously (*16*).

Results

Inactivation of Recombinant NAT2 by Nitrosoarenes. Incubation of NAT2 with 4-NO-BP, 2-NO-F, NO-B, and 2-NO-T caused a concentration-dependent and time-dependent loss of NAT2 activity (Figure 2). The reactions of NAT2 with each of the nitrosoarenes followed pseudo-first-order kinetics. Time dependent inactivation of NAT2 by 4-NO-BP and NO-B were saturable processes with K_I values of 0.71 ± 0.09 μM and 2260 ± 760 μM, respectively (Table 1). However, there was a linear relationship between the rates of inactivation of NAT2 and the concentrations of 2-NO-F and 2-NO-T (Figure 2). Saturation was not observed within the range of concentrations that were investigated. The values of the kinetic constants for inactivation of NAT2 by the four nitrosoarenes are listed in Table 1.

The inactivation rate constant (k_{inact}) and dissociation constant (K_I) for inactivation of NAT2 by 4-NO-BP and NO-B were obtained from equation 1 (*17*), and the inactivation rate constants for 2-NO-F and 2-NO-T were obtained by fitting the data to equation 2 (*18*). The second-order rate constant (k_{inact}/ K_I) for 4-NO-BP was 5700-fold greater than that of NO-B. For both 2-NO-F and 2-NO-T, the reaction order (n) was 1.0 and the k_2 value was 50,500 $M^{-1}s^{-1}$ for 2-NO-F and 16 $M^{-1}s^{-1}$ for 2-NO-T (Table 1). Therefore, 4-NO-BP and 2-NO-F are potent irreversible inactivators of NAT2, whereas NO-B and 2-NO-T are much weaker inactivators of NAT2. These results support our hypothesis that the nitrosoarene metabolites of arylamines that are efficiently N-acetylated by NAT2 are potent inactivators of NAT2.

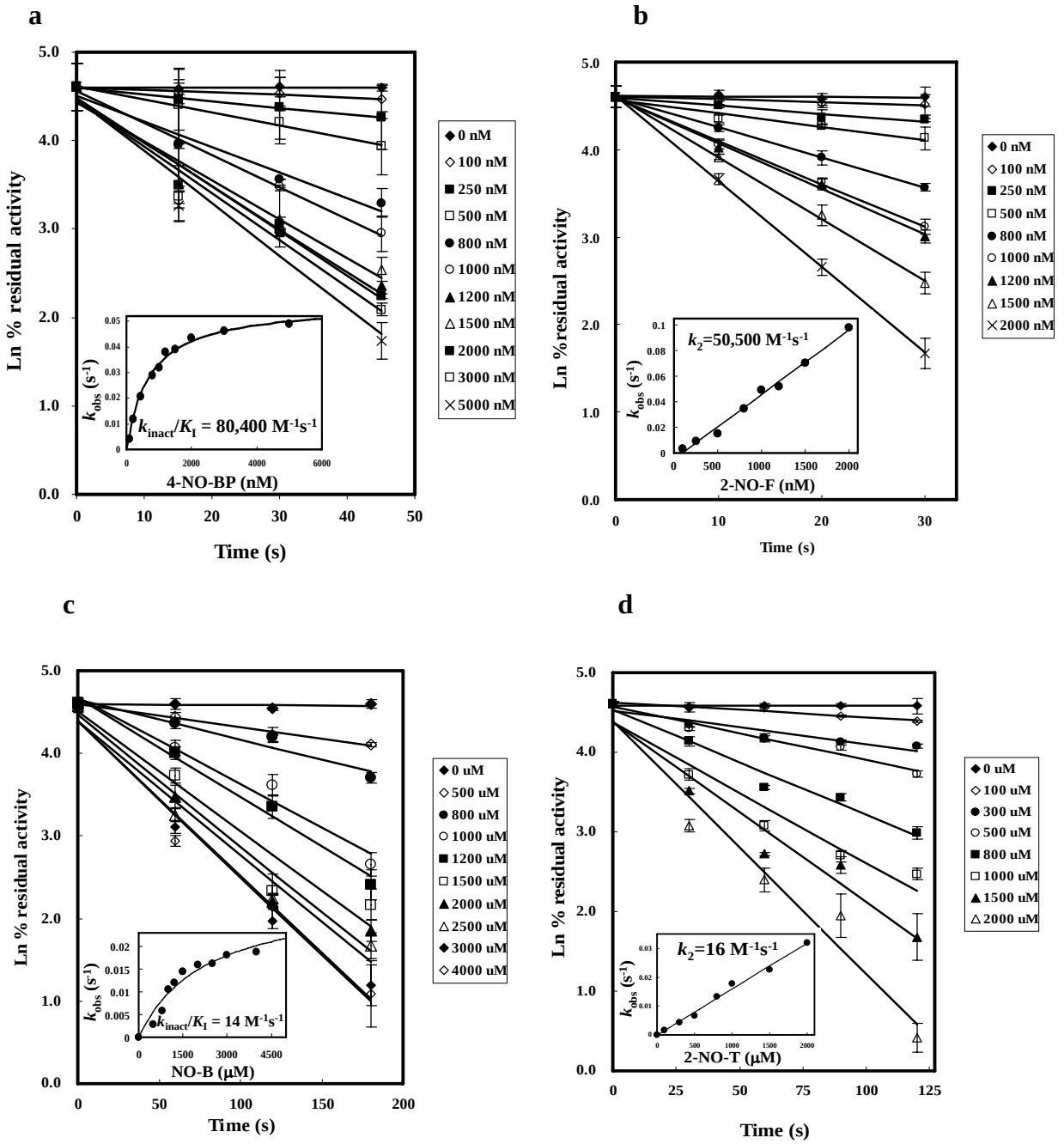

Figure 2. Time- and concentration-dependent inactivation of human NAT2 by (a) 4-NO-BP, (b) 2-NO-F, (c) NO-B, (d) 2-NO-T). Insets: Plots of k_{obs} values as a function of nitrosoarene concentration.

	K_I (μM)	k_{inact} (s^{-1})	k_{inact} / K_I ($M^{-1}s^{-1}$)	k_2 ($M^{-1}s^{-1}$)
4-NO-BP	0.71 ± 0.09	0.06 ± 0.002	80,400 ± 12,800	
NO-B	2260 ± 760	0.03 ± 0.005	14 ± 6	
2-NO-F				50,500 ± 4,300
2-NO-T				16 ±1.4

Table 1. Kinetic Constants for Inactivation of NAT2 by Nitrosoarenes. Results are expressed as the means (± SD) of three experiments.

$$k_{obs} = k_{inact} / (1 + K_I/[I]) \quad (1)$$

$$\log k_{obs} = \log k_2 + n \log [I] \quad (2)$$

MS Analysis of 4-NO-BP-Treated NAT2 and 2-NO-F-Treated NAT2. The ESI Q-TOF mass spectrum of 4-NO-BP-treated NAT2 exhibited a minor peak (33838.1 Da), which corresponded to the native recombinant NAT1 mass of 33841.8 Da, including three additional N-terminal amino acids Gly, Leu, and Glu (*14*). The peak of the greatest intensity (34022.0 Da) showed a mass increase of 184 Da to the native protein, indicating the formation of a (4-biphenyl)sulfinamide adduct. The third peak (34206.3 Da) was a result of mass increase of 368 Da (184 Da + 184 Da), relative to the native recombinant NAT2 (Figure 3a).

MALDI Q-TOF MS analysis of pepsin digested human NAT2 that had been incubated with 4-NO-BP revealed only one new peak with a monoisotopic mass of 1613.80 Da, corresponding to the modified peptide DHIVRRNRGGWCL (Asp57-Leu69; unmodified theoretical mass 1581.82 Da), compared with the pepsin digest of native NAT1 (Figure 4a and 4b). MALDI Q-TOF MS/MS analysis of the peptide of mass 1613.80 Da allowed the assignment of Cys68 as the modified residue, with the b11 ion (1347.73 m/z), b12 ion (1482.68 m/z), and intense b12-H_2SO_2 ion (1416.72 m/z) being diagnostic for the added mass of +32 Da. This result indicates that the thiol of Cys68 had been converted to a sulfinic acid (Figure 5a).

The ESI Q-TOF mass spectrum of 2-NO-F-treated NAT2 exhibited a major peak at 34039.2 Da, corresponding to a 196 Da mass increment relative to

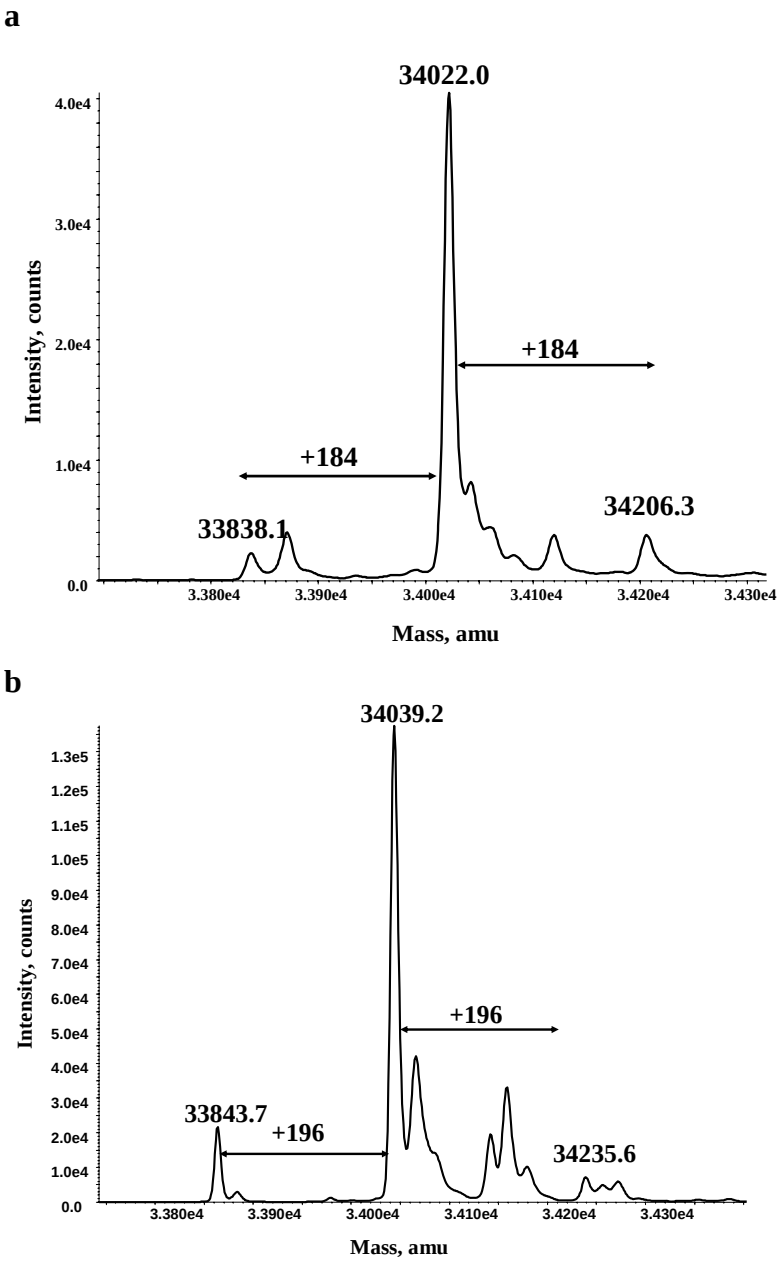

Figure 3. Deconvoluted Nano-ESI Q-TOF mass spectra: (a) 4-NO-BP-inactivated NAT2, (b) 2-NO-F-inactivated NAT2. The theoretical mass of recombinant human NAT2 is 33841.8 Da.

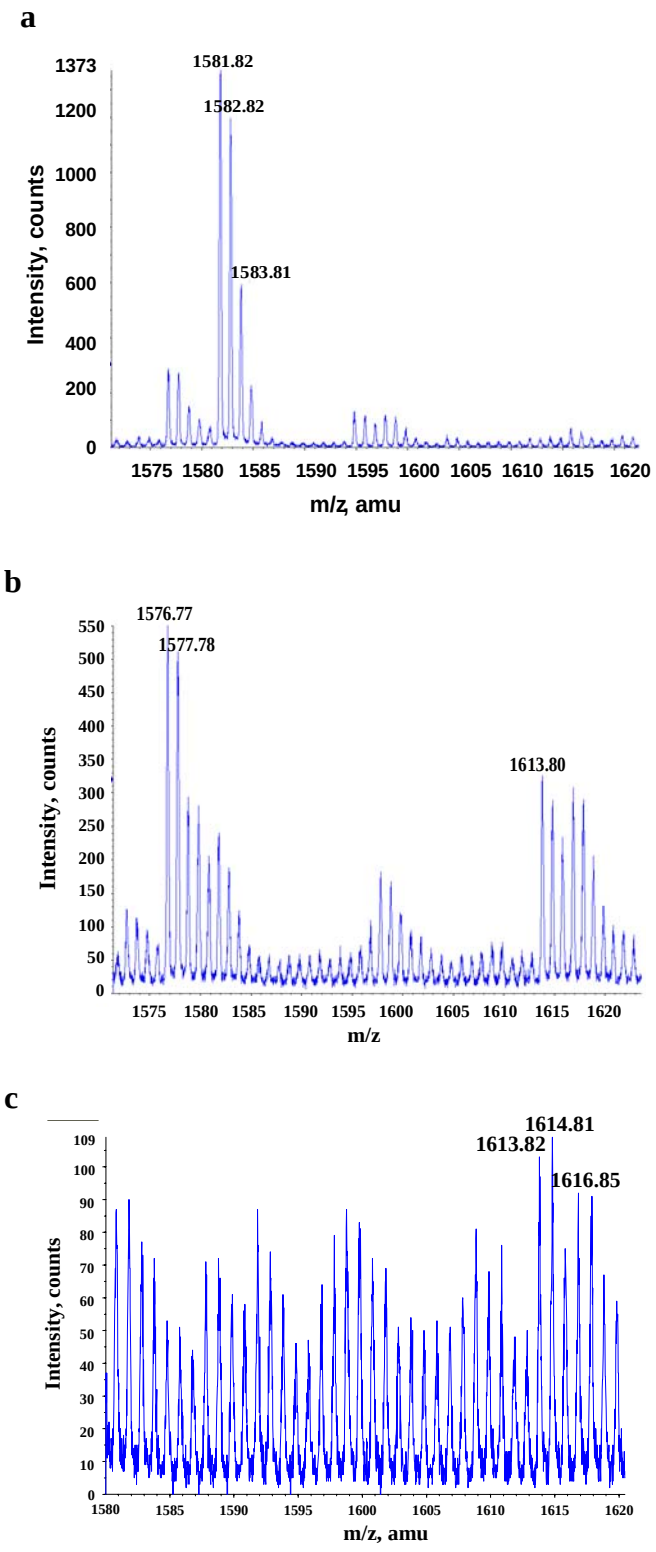

Figure 4. Segments of the MALDI Q-TOF mass spectra of pepsin digests of (a) native human NAT2; (b) 4-NO-BP-inactivated NAT2; (c) 2-NO-F-inactivated NAT2.

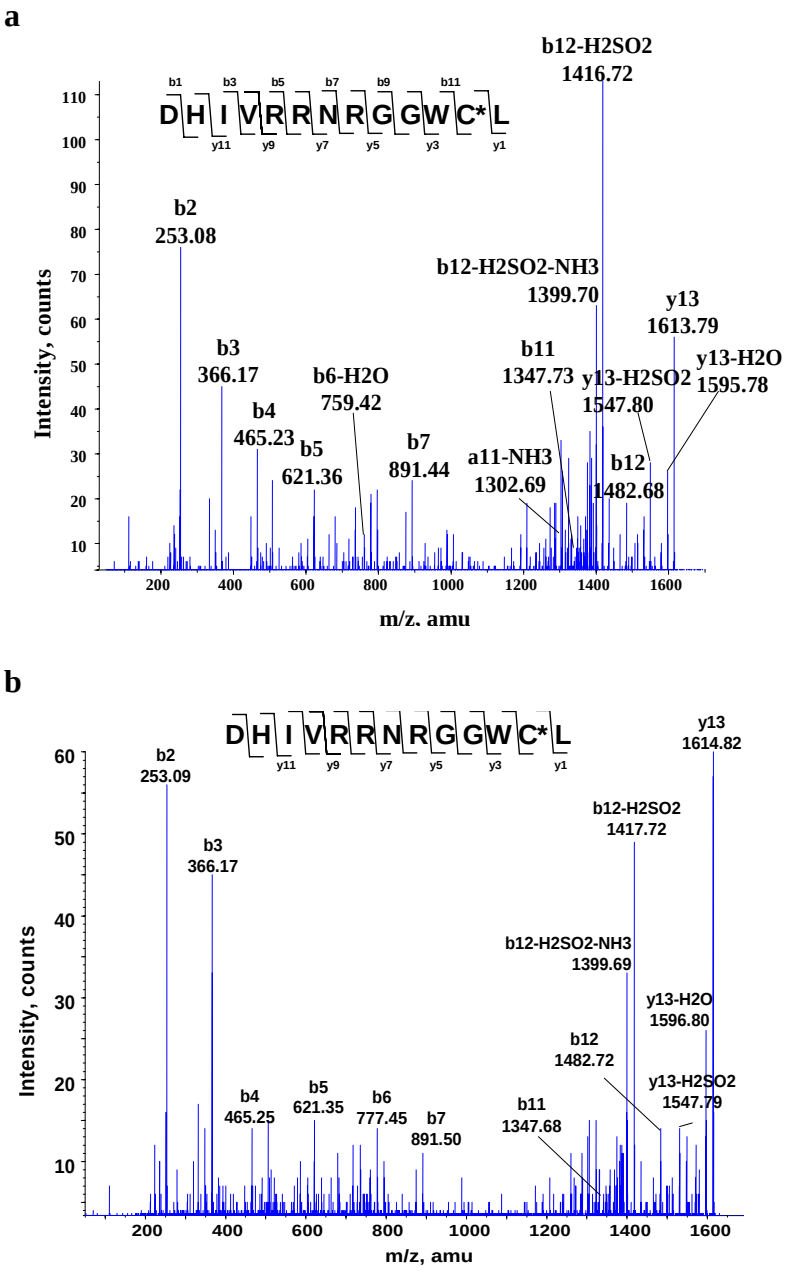

Figure 5. MALDI Q-TOF tandem mass spectra: (a) 1613.80 Da peptide obtained by pepsin digestion of 4-NO-BP-inactivated NAT2, (b) 1613.81 Da peptide obtained by pepsin digestion of 2-NO-F-inactivated NAT2.

the native protein and indicating the probable formation of a (2-fluorenyl)sulfinamide conjugate (Figure 3b). The mass spectrum of 2-NO-F-treated NAT2 also showed a minor peak at 34235.6 Da, corresponding to a 392 Da (196 Da + 196 Da) mass increment relative to the native protein (Figure 3b). MALDI Q-TOF MS of the pepsin digests of 2-NO-F treated (Figure 4c) and untreated NAT2 (Figure 4a) revealed a new peak at 1613.82 Da, corresponding to a 32 Da increment in the peptide DHIVRRNRGGWCL (Asp57-Leu69, unmodified theoretical mass 1581.82 Da). As shown in Figure 5b, tandem MS of the 1613.82 Da peptide revealed the b11 ion (1347.68 m/z), b12 ion (1482.72 m/z), and intense b12-H_2SO_2 ion (1417.72 m/z). This result indicates that the thiol group of Cys68 had been converted to a sulfinic acid.

Effect of AcCOA on the Inactivation of NAT2 by NO-B and 2-NO-T. Incubation of NAT2 (1 μM) with NO-B (800 μM) or 2-NO-T (500 μM) reduced NAT2 activity to 41 ± 5 % and 42 ± 2% of control activity. Incubation of NAT2 with the cofactor, AcCoA (20 μM), prior to treatment with NO-B and 2-NO-T resulted in recovery of 87 ± 6% and 85 ± 6% of control activity. These results suggest that the inactivations of NAT2 by NO-B and 2-NO-T are due to their effects on the active site Cys68 of NAT2.

Inactivation of NAT2 by 4-NO-BP and 2-NO-F in the Presence of GSH. Similar to the results that we observed for human NAT1, we found that 4-NO-BP and 2-NO-F react much more readily with NAT2 than with GSH, the cellular nucelophile that reacts readily with nitrosoarenes to form sulfinamides (*13, 19-22*). NAT2 (0.73 μM) was incubated with 4-NO-BP (1 μM and 5 μM) or 2-

NO-F (1 μM and 5 μM) in the presence of various concentrations of GSH (0.5 – 5 mM) for 30 or 60 s (Figure 6a - 6d).

Incubation of NAT2 (0.73 μM) with 4-NO-BP (5 μM) for 30 s caused a 93 (± 2)% loss of NAT2 activity and incubation with 2-NO-F (5 μM) for 30 s caused a 98 (± 1)% reduction in NAT2 activity (Figure 6a). In the presence of 0.5 mM GSH, corresponding to 685-fold excess of GSH over NAT2 and a 100-fold excess over the two nitrosoarenes, 4-NO-BP caused a 46 (± 4)% reduction of NAT2 activity and 2-NO-F caused a 41 (± 2)% reduction of NAT2 activity. In the presence of 1 mM GSH, 4-NO-BP caused 25 (± 4)% and 2-NO-F caused 27 (± 1)% loss of NAT2 activity. In the presence of 5 mM GSH, corresponding to 6849-fold excess of GSH over NAT2 and a 1000-fold excess of GSH over the nitrosoarenes, 4-NO-BP caused 17 (± 4)% and 2-NO-F caused 19 (± 5)% loss of NAT2 activity (Figure 6a).

As shown in Figure 6b, incubation of NAT2 (0.73 μM) with 4-NO-BP (5 μM) for 60 s caused a 97 (± 1)% inactivation of NAT2 activity and incubation of 2-NO-F (5 μM) for 60 s caused a 99.7 (± 3)% reduction in NAT2 activity. In the presence of 0.5 mM GSH, treatment of NAT2 with 4-NO-BP resulted in a 49 (± 2)% loss of activity and 2-NO-F caused a 62 (± 3)% loss of activity. The incubation with 1 mM GSH decreased the extent of inactivation by 4-NO-BP and 2-NO-F to 29 (± 6)% and 38 (± 3)%, respectively. In the presence of 5 mM GSH, 4-NO-BP and 2-NO-F caused 27 (± 9)% and 27 (± 3)% reductions in NAT2 activity.

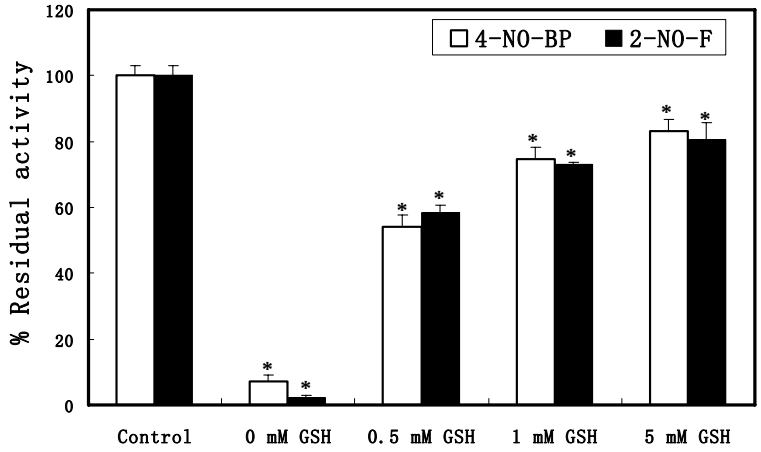

30 s	% Residual Activity	
	4-NO-BP	2-NO-F
Control	100 ± 3	100 ± 3
0 mM GSH	7 ± 2	2 ± 1
0.5 mM GSH	54 ± 4	59 ± 2
1 mM GSH	75 ± 4	73 ± 1
5 mM GSH	83 ± 4	81 ± 5

Figure 6a. Inactivation of NAT2 (0.73 μM) by 4-NO-BP (5 μM) and 2-NO-F (5 μM) in the presence of GSH. The incubation time was 30 s. Each bar represents the mean ± SD of the results of 3 experiments. Asterisks represent significant differences from controls: * $p <$ 0.001.

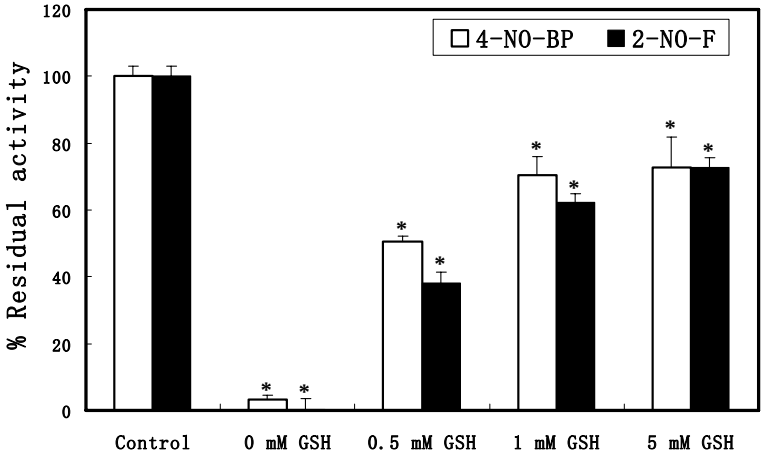

60 s	% Residual Activity	
	4-NO-BP	2-NO-F
Control	100 ± 3	100 ± 3
0 mM GSH	3 ± 1	0.3 ± 3
0.5 mM GSH	51 ± 2	38 ± 3
1 mM GSH	71 ± 6	62 ± 3
5 mM GSH	73 ± 9	73 ± 3

Figure 6b. Inactivation of NAT2 (0.72 μM) by 4-NO-BP (5 μM) and 2-NO-F (5 μM) in the presence of GSH. The incubation time was 60 s. Each bar represents the mean ± SD of the results of 3 experiments. Asterisks represent significant differences from controls: * $p < 0.001$.

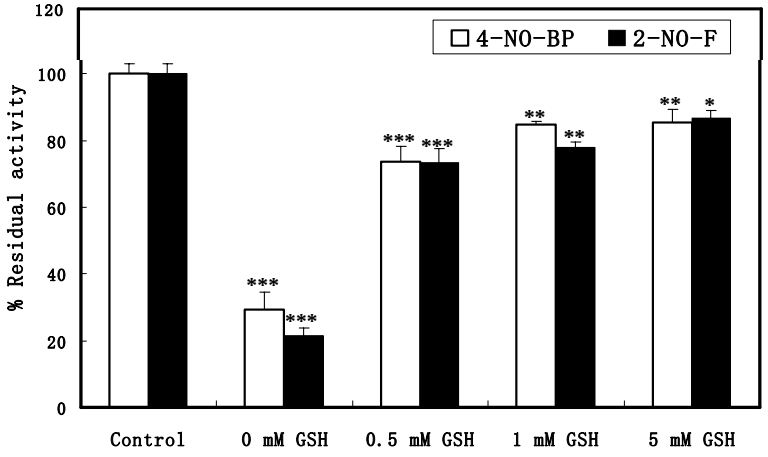

30 s	% Residual Activity	
	4-NO-BP	2-NO-F
Control	100 ± 3	100 ± 3
0 mM GSH	30 ± 5	22 ± 2
0.5 mM GSH	74 ± 4	73± 4
1 mM GSH	85 ± 1	78 ± 2
5 mM GSH	86 ± 4	87 ± 2

Figure 6c. Inactivation of NAT2 (0.73 μM) by 4-NO-BP (1 μM) and 2-NO-F (1 μM) in the presence of GSH. The incubation time was 30 s. Each bar represents the mean ± SD of the results of 3 experiments. Asterisks represent significant differences from controls: *$p < 0.02$, **$p < 0.01$, and ***$p < 0.001$.

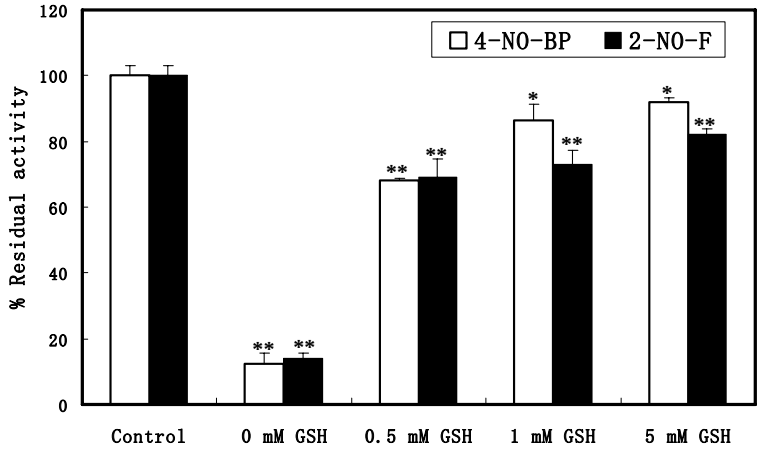

60 s	% Residual Activity	
	4-NO-BP	2-NO-F
Control	100 ± 3	100 ± 3
0 mM GSH	12 ± 3	14 ± 2
0.5 mM GSH	68 ± 1	70 ± 4
1 mM GSH	86 ± 5	73 ± 4
5 mM GSH	92 ± 1	82 ± 2

Figure 6d. Inactivation of NAT2 (0.73 μM) by 4-NO-BP (1 μM) and 2-NO-F (1 μM) in the presence of GSH. The incubation time was 60 s. Each bar represents the mean ± SD of the results of 3 experiments. Asterisks represent significant differences from controls: *$p < 0.05$, and **$p < 0.001$.

4-NO-BP (1 μM) and 2-NO-F (1 μM) caused inactivations of 70 (± 5)% and 78 (± 2)%, respectively, during a 30 s incubation with NAT2 (0.73 μM) in the absence of GSH (Figure 6c). In the presence of GSH (0.5 mM), 4-NO-BP caused a 26 (± 4)% reduction in activity and 2-NO-F inhibited NAT2 by 27 (± 4)% in 30 s. 4-NO-BP caused 15 (± 1)% and 14 (± 4)% inactivation in the presence of 1 mM and 5 mM concentrations of GSH, respectively, and the corresponding losses in activity produced by 2-NO-F were 22 (± 2)% and 13 (± 2)%.

As illustrated in Figure 6d, incubation of NAT2 for 60 s with 4-NO-BP caused an 88 (± 3)% loss of NAT2 activity in the absence of GSH and, in the presence of GSH (0.5 mM), 4-NO-BP caused a 32 (± 1)% reduction in NAT2 activity. Similarly, treatment of NAT2 with 2-NO-F caused an 86 (± 2)% reduction of NAT2 activity and, in the presence of GSH (0.5 mM), a 30 (± 4)% reduction of NAT2 activity was observed. In the presence of 1 mM and 5 mM concentrations of GSH, 4-NO-BP caused 14 (± 5)% and 8 (± 1)% losses in NAT2 activity and 2-NO-F reduced NAT2 activity by 27 (± 4)% and 18 (± 2)%.

Thus, the data in Figures 6a-6d indicate that the cellular nucleophile, GSH, provided only partial protection of human NAT2 from inactivation by 4-NO-BP and 2-NO-F.

NAT2 in HeLa Cells. Human NAT2 activities in HeLa cell cytosol were measured with AcCoA as the acetyl donor and the NAT2 specific substrate, SMZ, as the acetyl acceptor. The specific activity was 0.18 ± 0.02 nmol/mg of protein/min. Control experiments were conducted in the absence of AcCoA.

Without AcCoA present, SMZ was not acetylated in HeLa cytosol. The dependence on AcCoA for N-acetylation of SMZ illustrates the involvement of NAT2 in this assay and the presence of NAT2 in HeLa cytosol. Because of the unavailability of an effective NAT2 antibody (*23*), Western blotting and densitometry analysis, as we conducted for NAT1 (*13*), could not be carried out.

The specific activity for SMZ with recombinant NAT1 is 0.51 ± 0.05 μmol/mg of protein/min and the specific activity for SMZ with recombinant NAT2 is 14.3 ± 0.6 μmol/mg of protein/min. Since NAT1 constitutes 0.002% of HeLa cytosolic protein (*14*), the NAT1 in 1 mg of cytosol will acetylate 0.01 nmol of SMZ per min. Thus, on the basis of the specific activity of SMZ acetylation in HeLa cytosol (0.18 nmol/mg of protein/min), the NAT2 in 1 mg of cytosol is estimated to acetylate 0.17 nmol of SMZ per min. Based on these calculations, it is concluded that NAT2 constitutes 0.0013 ± 0.0002 % of HeLa cytosolic protein. This conclusion is in agreement with the result of a partial purification of NAT2 from human liver, which indicated that NAT2 constitutes approximately 0.002% of cytosolic protein (*24*). Thus, NAT2 is expressed in HeLa cytosol at a level that appears to be very similar to that of NAT1 (Part III of this thesis).

Effect of 4-NO-BP and 2-NO-F on NAT2, GAPDH and GR Activities in HeLa Cells. In our previous study, it was shown that certain nitrosoarenes appear to penetrate HeLa cells readily at low concentrations and effect an inactivation of NAT1 at concentrations that had only modest effects on GAPDH and GR activities (*13*). In this study, the effects of the nitrosoarenes on intracellular NAT2 activity were investigated.

A one hour incubation of HeLa cells with 5 μM and 10 μM concentrations of 4-NO-BP caused 23% and 58% decreases in NAT2 activity, without effect on either GAPDH or GR activities (Figure 7a). The 20 μM and 40 μM concentrations of 4-NO-BP reduced NAT2 activity by 68% and 63%, which are not significantly different ($p > 0.05$) from the effect of 10 μM 4-NO-BP. 4-NO-BP (20 μM and 40 μM) caused 13-20% reduction in the activities of GAPDH and GR.

4-NO-BP (10 μM) caused a 41% reduction in HeLa cell NAT2 activity within 15 min and reduced NAT2 activity by 73% after 2 hours. There were no changes in GR activity and only a minor reduction of 14% in GAPDH activity after the two hour exposure (Figure 7b).

The concentration-dependent inactivations of HeLa NAT2, GAPDH, and GR activities by 2-NO-F are shown in Figure 8a. One hour-treatment of the cells with 2-NO-F (2.5 μM) caused a loss of 22% of the NAT2 activity. Incubation with 5 μM, 10 μM, and 20 μM concentrations of 2-NO-F caused 50%, 65%, and 73% decreases in NAT2 activity, respectively. GAPDH and GR activities were reduced only 10-20% by 20 μM and 40 μM concentrations of 2-NO-F.

As illustrated in Figure 8b, a 10 μM concentration of 2-NO-F caused a 29% loss of NAT2 activity in 15 min. After 2 h, the loss of NAT2 activity

a

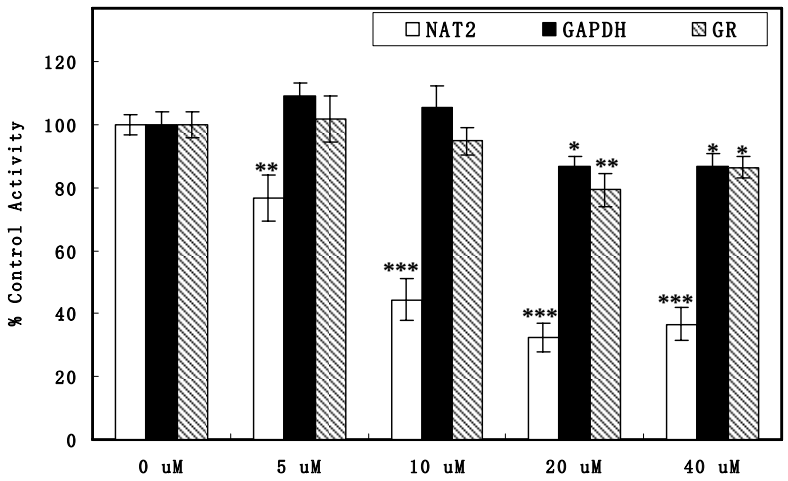

b

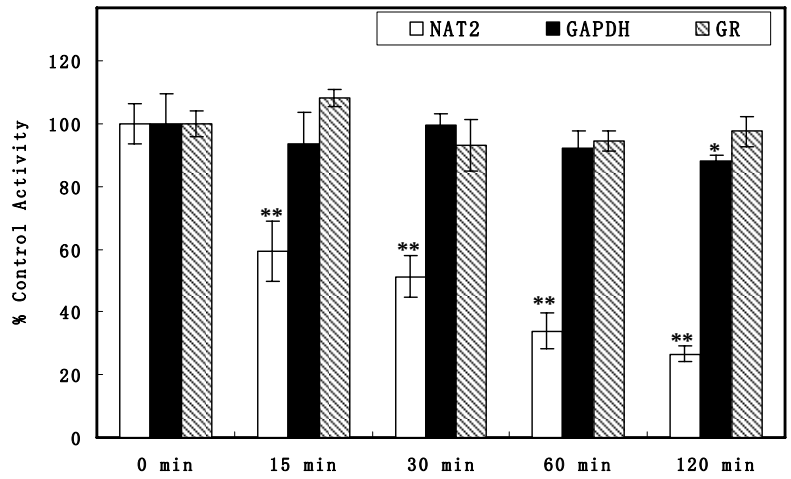

Figure 7. Inactivation of HeLa cell NAT2, GAPDH, and GR by 4-NO-BP. (a) Concentration dependence. The incubation time was 1 h. Each bar represents the mean and standard deviation of the results of three experiments. Asterisks represent significant differences from control: *, $p < 0.05$; **, $p < 0.01$; ***, $p < 0.001$. (b) Time dependence. The concentration of 4-NO-BP was 10 μM. Each bar represents the mean and standard deviation of the results of 3 experiments. Asterisks represent significant differences from control (0 min): *, $p < 0.05$; **, $p < 0.001$.

a

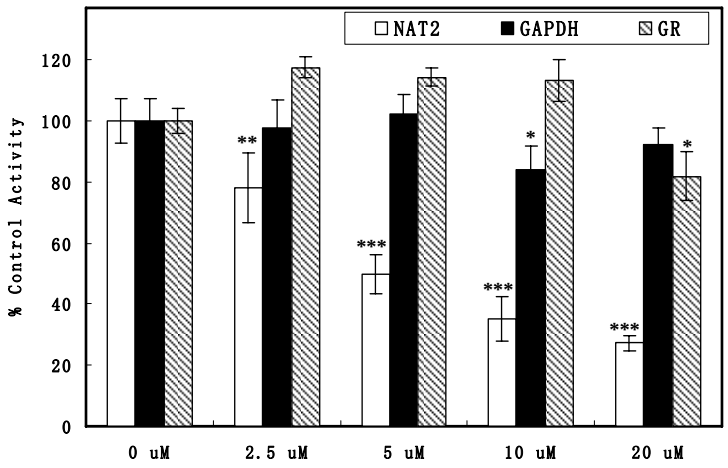

b

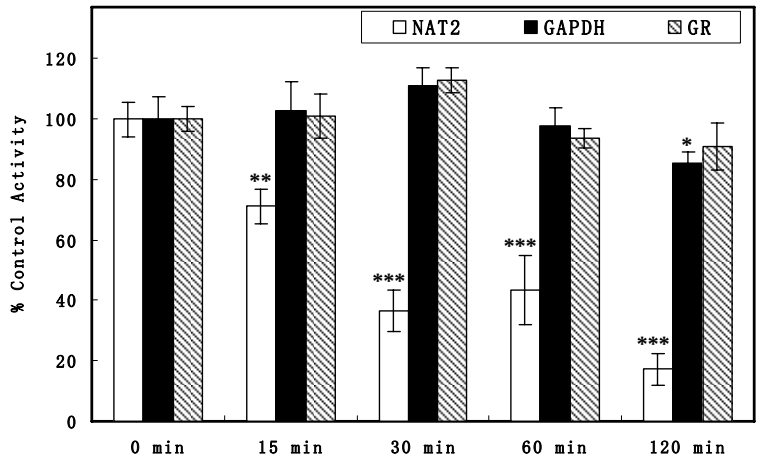

Figure 8. Inactivation of HeLa cell NAT2, GAPDH, and GR by 2-NO-F. (a) Concentration dependence. The incubation time was 1 h. Each bar represents the mean and standard deviation of the results of three experiments. Asterisks represent significant differences from control: *, $p < 0.05$; **, $p < 0.01$; ***, $p < 0.001$. (b) Time dependence. The concentration of 2-NO-F was 10 μM. Each bar represents the mean and standard deviation of the results of 3 experiments. Asterisks represent significant differences from control (0 min): *, $p < 0.05$; **, $p < 0.01$; ***, $p < 0.001$.

increased to 83%. However, there was no decrease in GR activity and only a 14% reduction in GAPDH activity after 2h.

Similar to the results obtained with NAT1, NO-B (250 μM) and 2-NO-T (250 μM) had no significant effect on HeLa intracellular NAT2 activity after six hours of treatment (Table 2).

Thus, 4-NO-BP and 2-NO-F produced a pronounced inhibitory effect on HeLa cell NAT1 and NAT2 activities at concentrations that had only negligible or moderate effects on GAPDH and GR activities. NATs are intracellular targets of nitrosoarene metabolites of 4-ABP and 2-AF.

NO-B (μM)	nmol/mg/min	% Control Activity
0	0.17 ± 0.004	100 ± 2.4
100	0.17 ± 0.008	98.7 ± 4.6
250	0.16 ± 0.012	95.4 ± 7.2
2-NO-T (μM)	nmol/mg/min	% Control Activity
0	0.17 ± 0.017	100 ± 9.8
100	0.16 ± 0.005	96.8 ± 2.8
250	0.17 ± 0.017	104.9 ± 10.5

Table 2. Inactivation of HeLa NAT2 by NO-B and 2-NO-T. The incubation time was 6 h.

Discussion

Recently, non-heritable factors, such as exogenous chemical agents and their metabolic products, which may impair NAT activities, are drawing scientists' attention. Inactivation of endogenous NAT1 through covalent modification of the NAT active site cysteine by several chemical agents, such as N-OH-PABA and cisplatin, has been investigated (*25, 26*).

Similar to our previous results on inactivation of NAT1 by nitrosoarenes, we found that 2-NO-F and 4-NO-BP, the nitroso derivatives of good NAT2 and NAT1 substrates, are potent inhibitors of NAT2. Also, there was little difference in the efficiency of inactivation of the recombinant NATs by 4-NO-BP and 2-NO-F. Incubation of HeLa cells with 4-NO-BP and 2-NO-F caused a time-dependent loss of intracellular NAT1 and NAT2 activities (Figures 7b and 8b; Figures 12a and 14, Part III of this thesis). Treatment of the cells with a 10 μM concentration of 4-NO-BP for 15 min to 2 h produced similar losses of NAT1 and NAT2 activities of approximately 40-70%. There was no significant difference ($p > 0.05$) between the losses of NAT1 and NAT2 activities at any time of measurement.

Treatment of the cells with 10 μM of 2-NO-F for 15 min caused significantly different ($p < 0.001$) decreases in NAT1 and NAT2 activities: 29% reduction in NAT2 activity, but 61% reduction in NAT1 activity. No significantly different ($p > 0.05$) reductions in NAT1 and NAT2 activities was produced by 2-NO-F during incubations longer than 15 min. The decreases in NAT1 and NAT2 activities at 30 min to 2 h were approximately 60-80% (Figure 8b; Figure 14, Part III).

4-NO-BP and 2-NO-F caused a concentration-dependent inactivation of HeLa NAT1 and NAT2 activities (Figures 7a and 8a; Figure 11a and 13a of Part III of this thesis). Incubation of cells with a 5 μM concentration of 4-NO-BP for one hour caused significantly different ($p < 0.05$) reductions of NAT1 and NAT2 activities: 23% loss in NAT2 activity, but 42% loss in NAT1 activity. One hour-incubation of the cells with concentrations greater than 10 μM of 4-NO-BP produced losses of NAT1 and NAT2 activities of approximately 50-70%, and were not significantly different ($p > 0.05$). A 10 μM concentration of 4-NO-BP caused approximately 50% reductions in cellular NAT1 and NAT2 activities and 20 μM and 40 μM concentrations of 4-NO-BP caused approximately 60-70% losses of NAT1 and NAT2 activities.

Incubation of cells with 2-NO-F (2.5 μM) for one hour caused significantly different ($p < 0.01$) effects on NAT1 activity and NAT2 activity: 22% loss in NAT2 activity, but 57% loss in NAT1 activity (Figure 8a; Figure 13a, Part III). No significantly different ($p > 0.05$) reduction in NAT1 and NAT2 activities was produced by concentrations greater than 5 μM 2-NO-F. 2-NO-F (5 μM) caused approximately 50-60% decreases in NAT1 and NAT2 activities and 2-NO-F (10 μM and 20 μM) caused approximately 60-70% losses of NAT1 and NAT2 activities.

Thus, HeLa cell NAT2 is less susceptible to the effects of the lower concentrations of the two nitrosoarenes than is NAT1. NAT1 also is more rapidly inactivated than NAT2 by 2-NO-F. The difference in susceptibility of NATs to

inactivation by nitrosoarenes in HeLa cells might indicate that intracellular NAT2 is somewhat less accessible to nitrosoarenes than NAT1. It is of interest to note that the second order rate constants for inactivation of the recombinant NATs by 2-NO-F and 4-NO-BP were approximately 1.5 and 1.4 fold greater for NAT2 than for NAT1, which is inconsistent with the results obtained for inactivation of the intracellular enzymes (Table 1; Table 1, Part III).

As shown in Figures 7 and 8, approximately 20-30% of intracellular NAT2 was not susceptible to inactivation by 4-NO-BP and 2-NO-F. These results are similar to those observed with NAT1 in that incomplete inactivation was achieved, and the residual NAT2 activity might indicate that a portion of the intracellular NAT2 is in the acetylated form.

The tissue distributions of NATs are potentially important with regard to their relative roles in the local detoxification or bioactivation of xenobiotics. It is well documented that both NAT2 and NAT1 are expressed in hepatic tissue and that NAT1 is distributed throughout the human body (*27, 28*). NAT1 and NAT2 mRNA have been identified in most human tissues (*29, 30*). The levels of NAT2 mRNA in most extrahepatic tissues were found to be no more than 1% of that found in liver (*30*). However, the expression and distribution of NAT2 in extrahepatic tissues is still unclear because of the unavailability of an effective NAT2 specific antibody (*23*). Studies have revealed mouse NAT1 (the mouse counterpart of human NAT2) catalytic activity in all hepatic and extrahepatic tissues examined in NAT2 knockout mice (*31*). NAT1 and NAT2 mRNA levels were found to be similar in mouse liver, gut, pancreas, bladder, and prostate (*31*).

It has been reported that NAT1 activity (PAS as substrate) is 5.9 ± 0.4 nmol/mg of protein/min and NAT2 activity (SMZ as substrate) is 0.8 ± 0.05 nmol/mg of protein/min in human epithelial lens cells; murine NAT1 activity (SMZ as substrate) is 0.9 ± 0.5 nmol/mg of protein/min and NAT2 activity (PAS as substrate) is 5.52 ± 0.31 nmol/mg of protein/min in mouse skeletal muscle (*32, 33*). These results agree with our observations that NAT1 type activity (PAS as substrate) is 4.08 ± 0.58 nmol/mg of protein/min and NAT2 type activity (SMZ as substrate) is 0.18 ± 0.02 nmol/mg of protein/min in HeLa cytosolic protein. By comparison of the specific activities for acetylation of SMZ by recombinant NAT2 and recombinant NAT1 and the NAT1 concentration in HeLa cytosolic protein, we concluded that NAT2 constitutes 0.0013 ± 0.0002% of cytosolic protein. This method of estimation was tested and supported by Western Blot and densitometry data obtained when we calculated the NAT1 concentration in HeLa cytosolic protein (*13*). This result is consistent with a previous report of a partial purification which showed NAT2 constitutes approximately 0.002% of soluble protein in human liver (*24*). The concentrations of NATs in HeLa cytosolic protein are similar to those of two isoforms of glutathione transferases (GSTs), which are members of another family of phase II drug metabolism enzymes: GST M1-1 (0.0053 ± 0.0009%), which is restricted to liver and few other tissues, and GST P1-1 (0.0011 ± 0.0003%), which is the most widely distributed extrahepatic GST isoform (*34-36*).

In this study, we characterized the inactivation of NAT2 by the nitrosoarene metabolites of arylamines. Similar to the results obtained with NAT1 (Part III), we found that, for arylamines that are good substrates for NAT2, the

corresponding nitrosoarenes are potent NAT2 inactivators. Such irreversible decreases in the N-acetylation activities of NAT2 and NAT1 might influence drug-induced toxicities and arylamine carcinogenesis, as has been well documented for genetically determined insufficiencies in NAT activities (*4-6, 8, 37, 38*).

References

(1) Hanna, P. E. (1994) N-acetyltransferases, O-acetyltransferases, and N,O-acetyltransferases: enzymology and bioactivation. *Adv Pharmacol 27*, 401-430.

(2) Hanna, P. E. (1996) Metabolic activation and detoxification of arylamines. *Curr. Med. Chem. 3*, 195-210.

(3) Ohsako, S. and Deguchi, T. (1990) Cloning and expression of cDNAs for polymorphic and monomorphic arylamine N-acetyltransferases from human liver. *J Biol Chem 265*, 4630-4634.

(4) Hein, D. W. (2002) Molecular genetics and function of NAT1 and NAT2: role in aromatic amine metabolism and carcinogenesis. *Mutat Res 506-507*, 65-77.

(5) Walraven, J. M., Zang, Y., Trent, J. O. and Hein, D. W. (2008) Structure/Function evaluations of single nucleotide polymorphisms in human N-acetyltransferase 2. *Curr Drug Metab 9*, 471-486.

(6) Walraven, J. M., Trent, J. O. and Hein, D. W. (2008) Structure-function analyses of single nucleotide polymorphisms in human N-acetyltransferase 1. *Drug Metab Rev 40*, 169-184.

(7) Agundez, J. A. (2008) Polymorphisms of human N-acetyltransferases and cancer risk. *Curr Drug Metab 9*, 520-531.

(8) Hein, D. W. (2006) N-acetyltransferase 2 genetic polymorphism: effects of carcinogen and haplotype on urinary bladder cancer risk. *Oncogene 25*, 1649-1658.

(9) Risch, A., Wallace, D. M., Bathers, S. and Sim, E. (1995) Slow N-acetylation genotype is a susceptibility factor in occupational and smoking related bladder cancer. *Hum Mol Genet 4*, 231-236.

(10) Garcia-Closas, M., Malats, N., Silverman, D., Dosemeci, M., Kogevinas, M., Hein, D. W., Tardon, A., Serra, C., Carrato, A., Garcia-Closas, R., Lloreta, J., Castano-Vinyals, G., Yeager, M., Welch, R., Chanock, S., Chatterjee, N., Wacholder, S., Samanic, C., Tora, M., Fernandez, F., Real, F. X. and Rothman, N. (2005) NAT2 slow acetylation, GSTM1 null genotype, and risk of bladder cancer: results from the Spanish Bladder Cancer Study and meta-analyses. *Lancet 366*, 649-659.

(11) Lubin, J. H., Kogevinas, M., Silverman, D., Malats, N., Garcia-Closas, M., Tardon, A., Hein, D. W., Garcia-Closas, R., Serra, C., Dosemeci, M., Carrato, A. and Rothman, N. (2007) Evidence for an intensity-dependent interaction of NAT2 acetylation genotype and cigarette smoking in the Spanish Bladder Cancer Study. *Int J Epidemiol 36*, 236-241.

(12) Gu, J., Liang, D., Wang, Y., Lu, C. and Wu, X. (2005) Effects of N-acetyl transferase 1 and 2 polymorphisms on bladder cancer risk in Caucasians. *Mutat Res 581*, 97-104.

(13) Liu, L., Wagner, C. R. and Hanna, P. E. (2008) Human arylamine N-acetyltransferase 1: in vitro and intracellular inactivation by nitrosoarene metabolites of toxic and carcinogenic arylamines. *Chem Res Toxicol 21*, 2005-2016.

(14) Liu, L., Von Vett, A., Zhang, N., Walters, K. J., Wagner, C. R. and Hanna, P. E. (2007) Arylamine N-acetyltransferases: characterization of the substrate specificities and molecular interactions of environmental

arylamines with human NAT1 and NAT2. *Chem Res Toxicol 20*, 1300-1308.

(15) Wang, H., Wagner, C. R. and Hanna, P. E. (2005) Irreversible inactivation of arylamine N-acetyltransferases in the presence of N-hydroxy-4-acetylaminobiphenyl: a comparison of human and hamster enzymes. *Chem Res Toxicol 18*, 183-197.

(16) Liu, L., Wagner, C. R., and Hanna, P. E. (2008) Human Arylamine N-Acetyltransferase 1: In Vitro and Intracellular Inactivation by Nitrosoarene Metabolites of Toxic and Carcinogenic Arylamines. *Chem. Res. Toxicol.*

(17) Kitz, R. and Wilson, I. B. (1962) Esters of methanesulfonic acid as irreversible inhibitors of acetylcholinesterase. *J Biol Chem 237*, 3245-3249.

(18) Levy, H. M., Leber, P. D. and Ryan, E. M. (1963) Inactivation of Myosin by 2,4-Dinitrophenol and Protection by Adenosine Triphosphate and Other Phosphate Compounds. *J Biol Chem 238*, 3654-3659.

(19) Mulder, G. J., Unruh, L. E., Evans, F. E., Ketterer, B. and Kadlubar, F. F. (1982) Formation and identification of glutathione conjugates from 2-nitrosofluorene and N-hydroxy-2-aminofluorene. *Chem Biol Interact 39*, 111-127.

(20) Eyer, P. (1994) Reactions of oxidatively activated arylamines with thiols: reaction mechanisms and biologic implications. An overview. *Environ Health Perspect 102 Suppl 6*, 123-132.

(21) Eyer, P. (1979) Reactions of nitrosobenzene with reduced glutathione. *Chem Biol Interact 24*, 227-239.

(22) Dolle, B., Topner, W. and Neumann, H. G. (1980) Reaction of arylnitroso compounds with mercaptans. *Xenobiotica 10*, 527-536.

(23) Stanley, L. A., Coroneos, E., Cuff, R., Hickman, D., Ward, A. and Sim, E. (1996) Immunochemical detection of arylamine N-acetyltransferase in normal and neoplastic bladder. *J Histochem Cytochem 44*, 1059-1067.

(24) Grant, D. M., Lottspeich, F. and Meyer, U. A. (1989) Evidence for two closely related isozymes of arylamine N-acetyltransferase in human liver. *FEBS Lett 244*, 203-207.

(25) Ragunathan, N., Dairou, J., Pluvinage, B., Martins, M., Petit, E., Janel, N., Dupret, J. M. and Rodrigues-Lima, F. (2008) Identification of the xenobiotic-metabolizing enzyme arylamine N-acetyltransferase 1 as a new target of cisplatin in breast cancer cells: molecular and cellular mechanisms of inhibition. *Mol Pharmacol 73*, 1761-1768.

(26) Butcher, N. J., Ilett, K. F. and Minchin, R. F. (2000) Inactivation of human arylamine N-acetyltransferase 1 by the hydroxylamine of p-aminobenzoic acid. *Biochem Pharmacol 60*, 1829-1836.

(27) Upton, A., Johnson, N., Sandy, J. and Sim, E. (2001) Arylamine N-acetyltransferases - of mice, men and microorganisms. *Trends Pharmacol Sci 22*, 140-146.

(28) Minchin, R. F., Hanna, P. E., Dupret, J. M., Wagner, C. R., Rodrigues-Lima, F. and Butcher, N. J. (2007) Arylamine N-acetyltransferase I. *Int J Biochem Cell Biol 39*, 1999-2005.

(29) Husain, A., Zhang, X., Doll, M. A., States, J. C., Barker, D. F. and Hein, D. W. (2007) Functional analysis of the human N-acetyltransferase 1 major promoter: quantitation of tissue expression and identification of critical sequence elements. *Drug Metab Dispos 35*, 1649-1656.

(30) Husain, A., Zhang, X., Doll, M. A., States, J. C., Barker, D. F. and Hein, D. W. (2007) Identification of N-acetyltransferase 2 (NAT2) transcription start sites and quantitation of NAT2-specific mRNA in human tissues. *Drug Metab Dispos 35*, 721-727.

(31) Loehle, J. A., Cornish, V., Wakefield, L., Doll, M. A., Neale, J. R., Zang, Y., Sim, E. and Hein, D. W. (2006) N-acetyltransferase (Nat) 1 and 2 expression in Nat2 knockout mice. *J Pharmacol Exp Ther 319*, 724-728.

(32) Dairou, J., Dupret, J. M. and Rodrigues-Lima, F. (2005) Impairment of the activity of the xenobiotic-metabolizing enzymes arylamine N-acetyltransferases 1 and 2 (NAT1/NAT2) by peroxynitrite in mouse skeletal muscle cells. *FEBS Lett 579*, 4719-4723.

(33) Dairou, J., Malecaze, F., Dupret, J. M. and Rodrigues-Lima, F. (2005) The xenobiotic-metabolizing enzymes arylamine N-acetyltransferases in human lens epithelial cells: inactivation by cellular oxidants and UVB-induced oxidative stress. *Mol Pharmacol 67*, 1299-1306.

(34) Hao, X. Y., Widersten, M., Ridderstrom, M., Hellman, U. and Mannervik, B. (1994) Co-variation of glutathione transferase expression and cytostatic drug resistance in HeLa cells: establishment of class Mu glutathione transferase M3-3 as the dominating isoenzyme. *Biochem J 297 (Pt 1)*, 59-67.

(35) Warholm, M., Guthenberg, C., Mannervik, B., von Bahr, C. and Glaumann, H. (1980) Identification of a new glutathione S-transferase in human liver. *Acta Chem Scand B 34*, 607-621.

(36) Tsuchida, S. and Sato, K. (1992) Glutathione transferases and cancer. *Crit Rev Biochem Mol Biol 27*, 337-384.

(37) Lower, G. M., Jr., Nilsson, T., Nelson, C. E., Wolf, H., Gamsky, T. E. and Bryan, G. T. (1979) N-acetyltransferase phenotype and risk in urinary bladder cancer: approaches in molecular epidemiology. Preliminary results in Sweden and Denmark. *Environ Health Perspect 29*, 71-79.

(38) Hein, D. W. (1988) Acetylator genotype and arylamine-induced carcinogenesis. *Biochim Biophys Acta 948*, 37-66.

PART V: INACTIVATION OF HUMAN ARYLAMINE N-ACETYLTRANSFERASES BY N-ARYLHYDROXAMIC ACIDS

Introduction

In the early 1960s, Cramer et al. reported the N-hydroxylation of the carcinogenic arylamide, 2-acetylaminofluorene (2-AAF), to form N-hydroxy-2-acetylaminofluorene (N-OH-AAF) (Figure 1) in rats, and Miller et al. reported the formation of N-hydroxy-4-acetylaminobiphenyl (N-OH-4-AABP) (Figure 1) from both 4-aminobiphenyl (4-ABP), a widespread environmental carcinogen present in cigarette smoke and cooking oil fumes (*1, 2*), and 4-acetylaminobiphenyl (4-AABP) in rats (*3, 4*). Since those initial reports, N-arylhydroxamic acids have been shown to be in vivo metabolites of a variety of N-arylamines, N-arylamides, and nitroarenes in humans and animals (*5-9*).

Arylamine N-acetyltransferases (NATs) play an important role in the detoxification of arylamines by conversion of arylamines to arylamides, a pathway which competes with the N-hydroxylation of arylamines to form N-arylhydroxylamines, which is a process leading to carcinogenic and toxic metabolites (*10, 11*). Inactivation of intracellular NATs would compromise the critical detoxification pathway of N-acetylation and could result in exacerbation of the untoward effects of arylamines. The toxicological implications of irreversible inactivation of biotransformation enzymes by exogenous agents and their metabolites are of current interest (*12*).

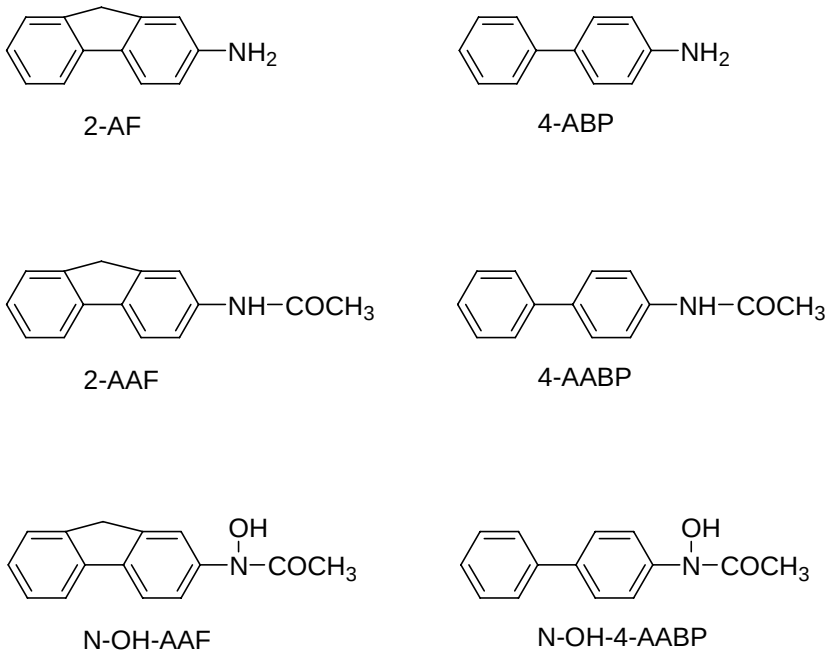

Figure 1. Structures of aryamines, arylamides and N-arylhydroxamic acids.

In 1972, Bartsch et al. reported that administration of N-OH-AAF to rats caused a 20-30% reduction in the acetyltransferase-catalyzed O-acetylation of N-arylhydroxylamines in liver cytosol (*13*). In the 1980s, N-OH-AAF was shown to selectively inactivate hamster NAT1 activity in hamster liver cytosol, and administration of N-OH-AAF to hamsters resulted in loss of hepatic NAT1 activity but had no effect on NAT2 (*14, 15*). N-Arylhydroxamic acids have been shown to inactivate human recombinant NAT1, hamster recombinant NAT1, and hamster recombinant NAT2 (*16, 17*).

It was previously established in our laboratory that inactivation of NATs by N-OH-4-AABP involves an initial NAT-mediated deacetylation to form N-OH-4-aminobiphenyl (Scheme 1, B, Part VI of this thesis), which undergoes oxidation to the electrophilic 4-nitrosobiphenyl (4-NO-BP) (Scheme 1, C, Part VI of this thesis), which reacts with the nucleophilic active site Cys68 to form a sulfinamide (Scheme 1, E, Part VI of this thesis) (*17*). It was proposed that the relative stabilities of the Cys68 thioacetyl esters influence the susceptibilities of NATs to inactivation by N-arylhydroxamic acids. Based on the previous observations with the corresponding hamster NAT homologs, it was proposed that human NAT2 would be more susceptible than human NAT1 to inactivation by N-arylhydroxamic acids such as N-OH-AAF and N-OH-4-AABP, and that the Cys68 thioacetylester of NAT2 would have a shorter half-life than the corresponding thioacetyl ester of NAT1.

Materials and Methods

Materials were prepared as described previously (Part III of this thesis).

NAT1 and NAT2 Activity Assay. The NAT1 and NAT2 activity assay were performed as described previously (Part II of this thesis).

Time-Dependent Inactivation of NAT2 by N-OH-4-AABP and N-OH-AAF at 37 °C. The incubation mixtures contained 24 μg/mL (0.71 μM) of NAT2 and either N-OH-4-AABP (100-1250 μM) or N-OH-AAF (5-150 μM) and tetrasodium pyrophosphate buffer (50 mM, pH 7.0; 0.1 mM DTT; 1% glycerol) in a total volume of 50 μL. The reaction was initiated by the addition of N-OH-4-AABP or N-OH-AAF dissolved in DMSO (2.5 μL). Aliquots (2 μL) were withdrawn at 30 s intervals (0-360 s) in experiments with N-OH-4-AABP or at 45 s intervals (0-270 s) in experiments with N-OH-AAF and were transferred to an assay cuvett. Control incubations contained DMSO but not N-OH-AAF or N-OH-4-AABP.

Time-Dependent Inactivation of NAT1 by N-OH-AAF at 37 °C. The incubation mixtures contained NAT1 (50 μg/mL, 1.46 μM), N-OH-AAF (30-800 μM), and tetrasodium pyrophosphate buffer (50 mM, pH 7.0; 0.1 mM DTT; 1% glycerol) in a total volume of 50 μL. The reaction was initiated by the addition of N-OH-AAF dissolved in DMSO (2.5 μL). Aliquots (2 μL) were withdrawn at 45 s intervals (0-270 s) and transferred to an assay cuvett. NAT1 activity was measured as described previously (*17*). Control incubations contained DMSO but not N-OH-AAF.

Half Life of Acetyl-NAT2 Intermediate. NAT2 (56.5 μg/mL, 1.67 μM) was incubated with PNPA (2 mM) in MOPS buffer (398 μL; 100 mM, pH 7.0; 150 mM NaCl; 0.1 mM DTT) at 37 °C. The reactions were initiated by addition of PNPA dissolved in DMSO (2 μL). The rate of the hydrolysis was determined by monitoring the increase in absorbance at 400 nm due to the formation of *p*-nitrophenol (ε_{400nm} = 9400 M^{-1} cm^{-1}) for 5 min. Control incubations were conducted in the absence of enzyme.

Formation of 2-NO-F and 4-NO-BP during the Incubation of NAT1 or NAT2 with N-OH-AAF or N-OH-4-AABP. In a total volume of 500 μL, NAT1 (4 μM) or NAT2 (4 μM) was incubated with either N-OH-AAF (200 μM) or N-OH-4-AABP (200 μM) in MOPS buffer (100 mM, pH 7.0; 150 mM NaCl; 0.025 mM DTT), which had been extensively degassed under vacuum, at 37 ºC for 30 min. The reactions were initiated by addition of N-OH-AAF or N-OH-4-AABP dissolved in DMSO (4 μL). Formation of 2-NO-F was monitored continuously at A_{380nm} (ε_{380nm} = 19800 M^{-1} cm^{-1}) and formation of 4-NO-BP was monitored at A_{350nm} (ε_{350nm} = 11800 M^{-1} cm^{-1}) for 30 min. Control experiments were conducted in which either enzyme or hydroxamic acid was omitted.

Sample Preparation for Nano-ESI-Q-TOF MS of N-OH-4-AABP-Treated NAT2. To NAT2 (84 μg, 40 μM) in potassium phosphate buffer (60 μL, 20 mM, pH 7.4; 1 mM EDTA; 10% glycerol; 0.1 mM DTT) was added N-OH-4-AABP dissolved in 2 μL of DMSO. The final concentration of N-OH-4-AABP was 500 μM. DMSO only was added to the control incubation mixtures. After a

10 min incubation at 37 °C, the residual activity was less than 3% of the control activity. The reaction mixture was loaded onto a Bio Spin 6 Tris Column, which had been equilibrated with the potassium phosphate buffer. After centrifugation at 1000g for 4 min, 8 μL of the solution was used to measure the protein concentration and residual activity. The remaining solution was stored at -80 °C.

Sample Preparation for Nano-ESI-Q-TOF MS of N-OH-AAF-Treated NAT1 and NAT2. To NAT1 (150 μg, 44 μM) or NAT2 (70 μg, 25 μM) in potassium phosphate buffer (100 μL, 20 mM, pH 7.4; 1 mM EDTA; 10% glycerol; 0.1 mM DTT) was added N-OH-2-AAF dissolved in 2 μL of DMSO. The final concentration of N-OH-2-AAF was 500 μM. DMSO only was added to the control incubation mixtures. The incubation time with NAT1 was 12 min and with NAT2 was 9 min at 37 °C. The residual activity was less than 5% of the control activity. The reaction mixture was loaded onto a Bio Spin 6 Tris Column. After centrifugation, the sample was concentrated to 30 μL by freeze drying.

Pepsin Digestion of N-OH-4-AABP-Treated NAT2 and N-OH-AAF-Treated NAT1 and NAT2. NAT1 or NAT2 was incubated with N-OH-4-AABP or N-OH-AAF as described above for the sample preparation for Nano-ESI-Q-TOF MS. The digestion procedure was the same as described for pepsin digestion of 4-NO-BP-treated NAT2 (Part IV of this thesis).

Nano-ESI-Q-TOF MS of Unmodified and Modified NAT1 and NAT2. NAT1 and NAT2 samples were desalted with Millipore C4 ZipTips and analyzed by Nano-ESI-Q-TOF MS as previously described (*17*).

MALDI-TOF MS Screening and Sequencing of Peptides. The pepsin digests were desalted with Millipore C18 ZipTips and analyzed by MALDI-TOF MS and sequenced by MALDI-TOF MS/MS as previously described (*17*).

NAT1, NAT2, GAPDH, and GR Activity in HeLa Cell Cytosol. NAT1, NAT2, GAPDH, and GR activities were measured as described previously (Part III and IV of this thesis).

Effect of N-OH-AAF and N-OH-4-AABP on NAT1 and NAT2 Activity in HeLa Cell Cytosol. In a total volume of 50 μL, cell cytosol (48 μL) was incubated with either N-OH-AAF (10-500 μM for NAT1, and 2.5-20 μM for NAT2), or N-OH-4-AABP (10-200 μM for NAT1, or 5-50 μM for NAT2) at 37 ºC for 30 min. The reaction was initiated by the addition of the hydroxamic acids dissolved in DMSO (2 μL). PABA and AcCoA, or SMZ and AcCoA dissolved in assay buffer (50 μL) and warmed to 37 ºC for 5 min, were added to the mixtures. The final concentrations were: PABA or SMZ, 200 μM; AcCoA, 400 μM for NAT1 and 800 μM for NAT2. Residual NAT1 or NAT2 activity was measured as described above. The control incubations contained DMSO, but not hydroxamic acids.

Effect of AcCoA on N-OH-AAF and N-OH-4-AABP Inactivation of NAT1 and NAT2 in HeLa Cell Cytosol. To cell cytosol (46 μL) was added AcCoA dissolved in assay buffer (2 μL). The mixture was incubated for 5 min at 37 ºC followed by the addition of either N-OH-AAF or N-OH-4-AABP in DMSO

(2 μL). The final concentrations were: AcCoA, 400 μM for NAT1 and 800 μM for NAT2; N-OH-AAF, 50 μM for NAT1 and 10 μM for NAT2; N-OH-4-AABP, 50 μM for NAT1 and 20 μM for NAT2. After incubation for 30 min at 37 ºC, PABA and AcCoA, or SMZ and AcCoA dissolved in assay buffer (50 μL) were added. The final concentrations were: PABA or SMZ, 200 μM; AcCoA, 400 μM for NAT1 and 800 μM for NAT2. Residual NAT1 and NAT2 activity was measured as described above. For experiments without AcCoA, cell cytosol (46 μL) was incubated with 2 μL of assay buffer for 5 min. Either N-OH-AAF or N-OH-4-AABP (2 μL) were added and incubations were continued for 30 min. PABA and AcCoA, or SMZ and AcCoA dissolved in 50 μL of assay buffer were added and NAT1 or NAT2 activity was measured.

Effect of N-OH-AAF and N-OH-4-AABP on Endogenous NAT1 and NAT2 in HeLa Cells. At approximately 90% confluence, cell monolayers were washed twice with PBS. The cells were exposed to either N-OH-AAF (25-250 μM) or N-OH-4-AABP (25-500 μM) in 10 mL of serum-free DMEM media containing DMSO. The final concentration of DMSO was 0.5%. The incubation was continued at 37 ºC for 2 h and 6 h. Cells were washed with PBS buffer, trypsinized, and harvested. The controls contained DMSO only. Cytosol was prepared as described above, and the NAT1 and NAT2 activities were measured. Cell viability was confirmed with the trypan blue assay as reported previously (*18*).

Results

Inactivation of NAT2 and NAT1 by N-OH-AAF and N-OH-4-AABP. Incubation of human NAT1 and NAT2 with N-OH-AAF caused a time-dependent and concentration-dependent loss of N-acetylation activity. The rates of NAT1 and NAT2 inactivation by N-OH-AAF were dependent on the concentration of N-OH-AAF at lower concentrations, with saturation occurring at approximately 600 μM (NAT1) and 100 μM (NAT2) (Figure 2).

Linear semilog plots of percent remaining N-acetylation activity vs time were obtained with several concentrations of N-OH-AAF, and a first-order inactivation rate constant (k_{obs}) for each concentration was determined from the slopes of the lines (Figure 2). The inactivation rate constant (k_{inact}) and dissociation constant (K_I) were obtained from a non-linear fit of the data according to equation 1 (*19*). The second order rate constant (k_{inact}/ K_I) for inactivation of human NAT2 by N-OH-AAF was 459 ± 80 $M^{-1}s^{-1}$, which was 8-fold greater than that for NAT1. The values of the kinetic constants for inactivation of NAT1 and NAT2 by N-OH-AAF are listed in Table 1. As seen in Figure 2a, there is a delay in loss of NAT1 activity upon incubation with N-OH-AAF, which is similar to that observed for the reaction of NAT1 with N-OH-4-AABP as reported previously (*17*). Little NAT1 activity was lost during the first 45s of incubation with N-OH-AAF (Figure 2a), in contrast to the immediate onset of inactivation observed with NAT2 (Figure 2b).

$$k_{obs} = k_{inact} / (1 + K_I/[I]) \qquad (1)$$

a

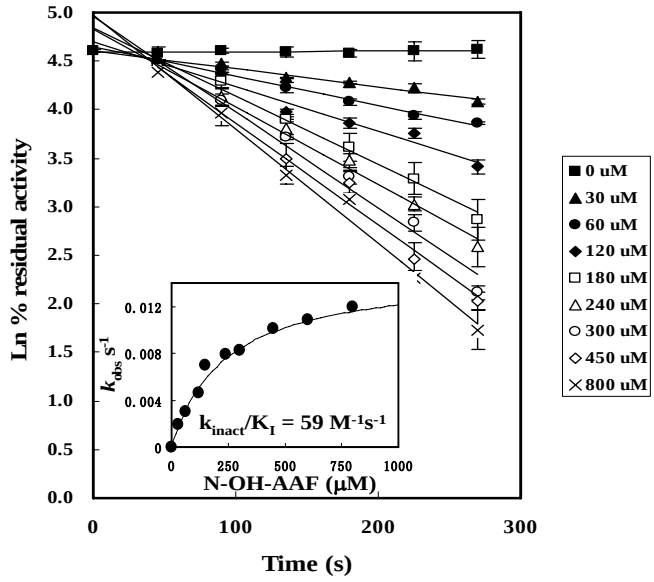

b

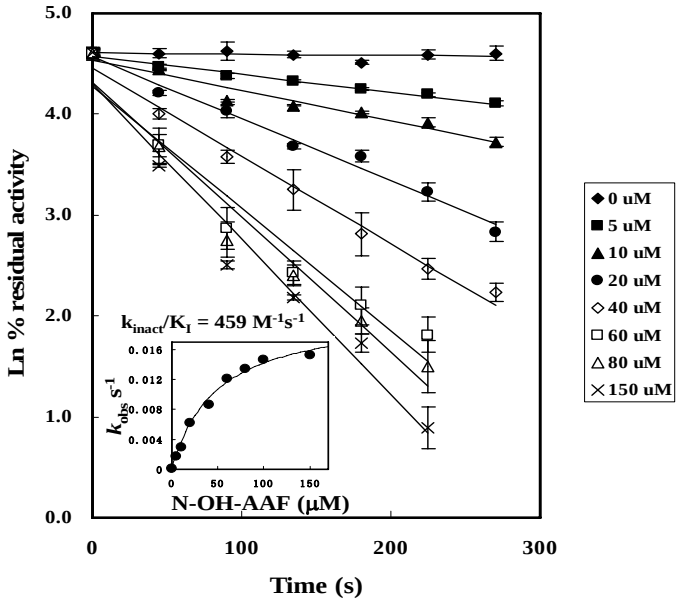

Figure 2. Time- and concentration-dependent inactivation of NATs by N-OH-AAF. (a) human NAT1, (b) human NAT2. The results represent the means ± SD of three experiments. Insets: Plots of k_{obs} values as a function of N-OH-AAF concentration.

Enzyme	N-OH-AAF			N-OH-4-AABP		
	K_I (μM)	k_{inact} (s^{-1})	k_{inact} / K_I ($M^{-1}s^{-1}$)	K_I (μM)	k_{inact} (s^{-1})	k_{inact} / K_I ($M^{-1}s^{-1}$)
NAT1	237 ± 25	0.01 ± 0.001	59 ± 12	1260 [a]	0.01 [a]	7.9 [a]
NAT2	48 ± 6	0.02 ± 0.001	459 ± 80	193 ± 10	0.004 ± 0.001	21 ± 6.3

Table 1. Inactivation of NAT1 and NAT2 by N-OH-AAF and N-OH-4-AABP. Results are expressed as the means (± SD) of three experiments, except the results for inactivation of NAT2 by N-OH-4-AABP, which represent the mean of two experiments.

[a] From reference 17.

In order to verify our proposal that human NAT2 would be more susceptible to inactivation by N-arylhydroxamic acids than NAT1, NAT2 was incubated with another arylhydroxamic acid, N-OH-4-AABP (Figure 3). The k_{inact}/ K_I value for inactivation of NAT2 by N-OH-4-AABP was 21 ± 6.3 $M^{-1}s^{-1}$, which was 2.7-fold greater than the value previously observed for NAT1 (Table 1) (*17*). Furthermore, the inactivation reaction occurred immediately upon incubation of NAT2 with N-OH-4-AABP (Figure 3), in contrast to the 2 min delay in the reaction of NAT1 with N-OH-4-AABP (*17*). Thus, NAT2 was more rapidly inactivated by both N-OH-AAF and N-OH-4-AABP than was NAT1, which is consistent with our hypothesis.

ESI Q-TOF MS Analysis, Proteolysis, and MALDI Q-TOF MS/MS Analysis of N-OH-AAF-Treated Human NAT1 and NAT2. On the basis of the results of our previous investigation of the inactivation of NATs by N-arylhydroxamic acids, it was anticipated that inactivation of human NATs by N-OH-AAF would involve formation of (2-fluorenyl)sulfinamide and 2-AF adducts, corresponding to mass increments of 195 Da and 179 Da, respectively. Human NAT1 that had been treated with N-OH-AAF yielded a mass spectrum that exhibited three principal peaks (Figure 4a). The mass spectrum of the adducted protein exhibited a minor peak (34299.3), which corresponded to the native recombinant NAT1, which has a theoretical mass of 34299.2 Da, including four additional N-terminal amino acids, Gly, Thr, Leu, and Glu (*20*). The peak of the greatest intensity (34495.1 Da) showed a mass increase of 196 Da to the native protein, indicating the formation of a (2-fluorenyl)sulfinamide adduct. The third

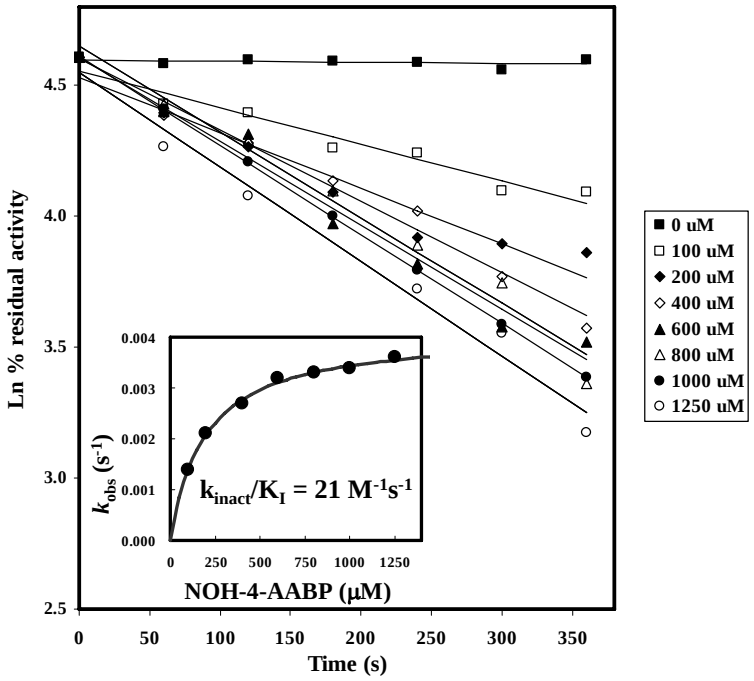

Figure 3. Time- and concentration-dependent inactivation of recombinant human NAT2 by N-hydroxy-4-acetylaminobiphenyl (N-OH-4-AABP). The results represent the mean of two experiments. Insets: Plots of k_{obs} values as a function of N-OH-4-AABP concentration.

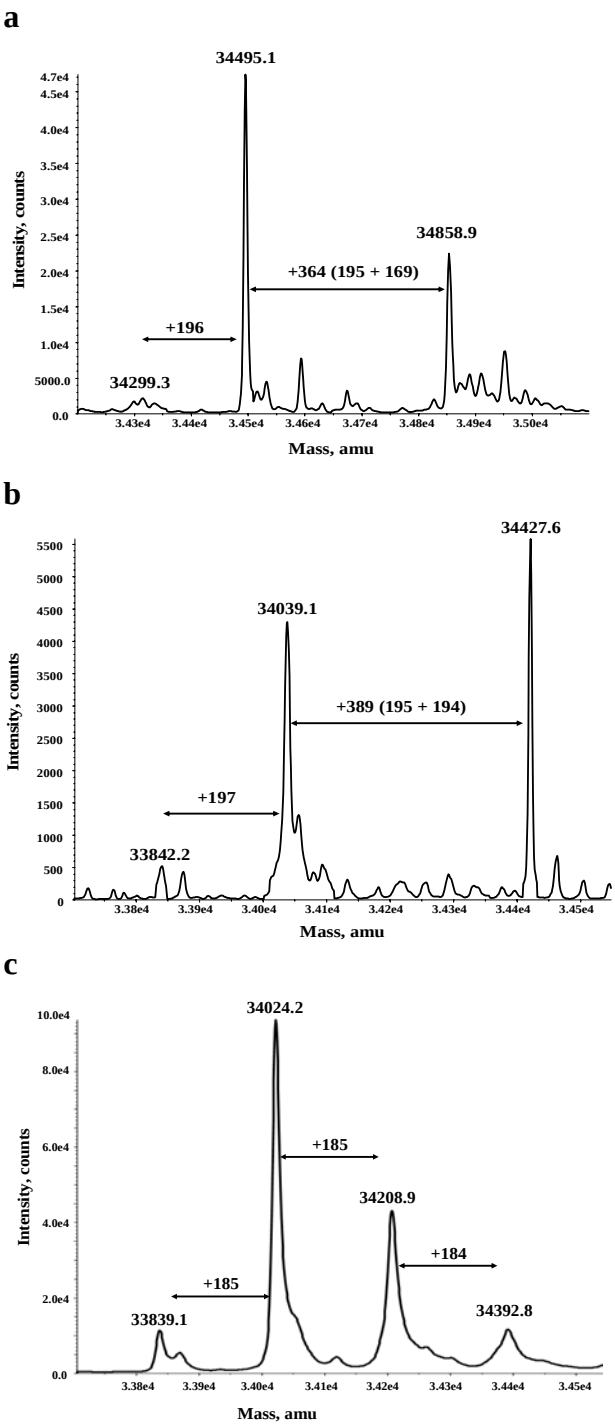

Figure 4. Deconvoluted Nano-ESI Q-TOF mass spectra: (a) N-OH-AAF-inactivated NAT1, (b) N-OH-AAF-inactivated NAT2, (c) N-OH-4-AABP-inactivated NAT2. The theoretical mass of recombinant human NAT1 is 34299.2 Da. The theoretical mass of recombinant human NAT2 is 33841.8 Da.

peak (34858.9 Da) was a result of mass increase of 363.8 Da (169 Da + 195 Da), relative to the 34495.1 Da (Figure 4a).

The N-OH-AAF-treated human NAT1 was hydrolyzed with pepsin and the resulting digest was analyzed by MALDI Q-TOF MS. Two new peaks with monoisotopic masses of 1590.78 Da (+32 Da) and 1727.87 Da (+179 Da) (Figure 5b and5d) were observed, which were not present in the pepsin digest of native NAT1 (Figure 5a and 5c). MALDI Q-TOF MS/MS analysis of the peptide of mass 1590.78 Da revealed the modified (+ 32 Da) sequence DQVVRRNRGGWCL (Asp57-Leu69, unmodified theoretical mass 1558.78 Da). The b11-NH_3 ion (1307.65 *m/z*), the b12 ion (1459.68 *m/z*), and the intense b12-H_2SO_2 ion (1393.71 *m/z*) verify that the thiol group of Cys68 was converted to a sulfinic acid (Figure 6). It was found previously that pepsin digestion of NATs containing a sulfinamide adduct resulted in the formation of a sulfinic acid (-SO_2H), which accounts for a 32 Da increase in the mass of the modified peptide (*16, 17*).

MS/MS analysis of the peptide of mass 1727.87 Da identified the modified (+179 Da) sequence LEDSKYRKIYSF (Leu 181-Phe 192, unmodified theoretical mass 1548.76 Da). The b5-H_2O ion (555.18 *m/z*), b6-H_2O ion (897.38 *m/z*), and the immonium ion (315.14 *m/z*), which is 179 Da greater than the theoretical mass of the tyrosine immonium ion, provide strong evidence that Tyr 186 is covalently bound to 2-aminofluorene (Figure 7). Previous mass spectrometric analyses also showed that treatment of hamster NAT1 with N-OH-

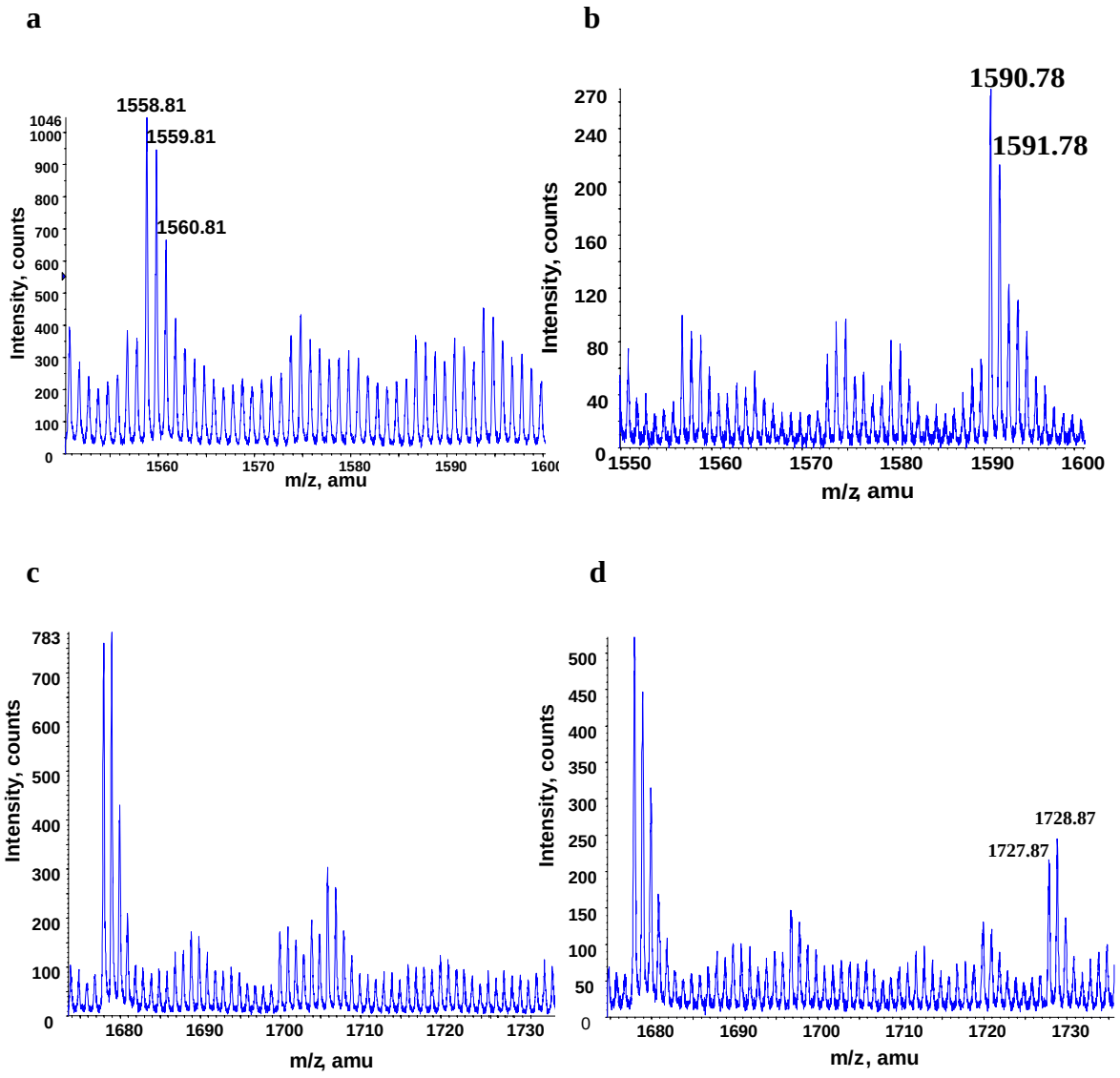

Figure 5. Segments of the MALDI Q-TOF mass spectra of pepsin digests of (a, and c) native human NAT1; (b, and d) N-OH-AAF-inactivated NAT1.

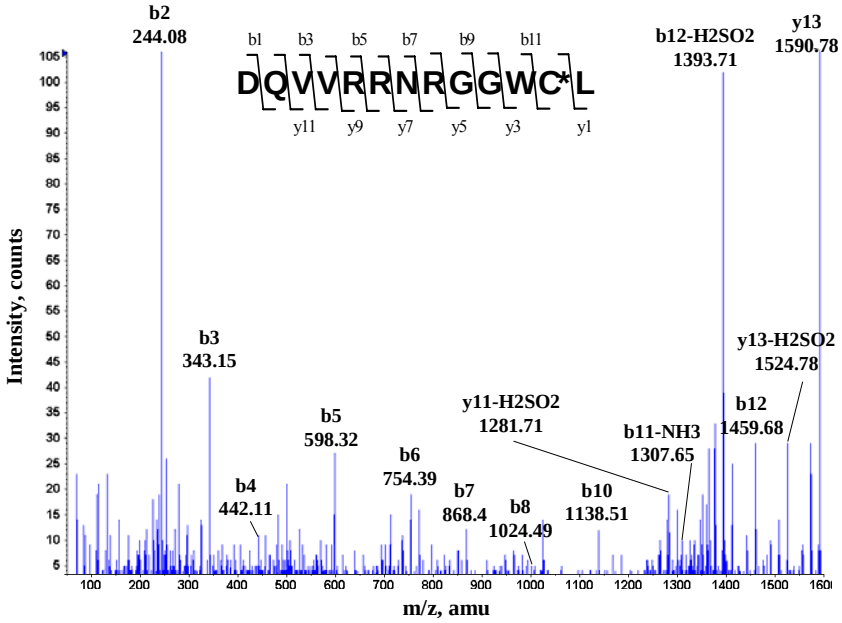

Figure 6. MALDI Q-TOF tandem mass spectra of 1590.78 Da peptide obtained by pepsin digestion of N-OH-AAF-inactivated NAT1.

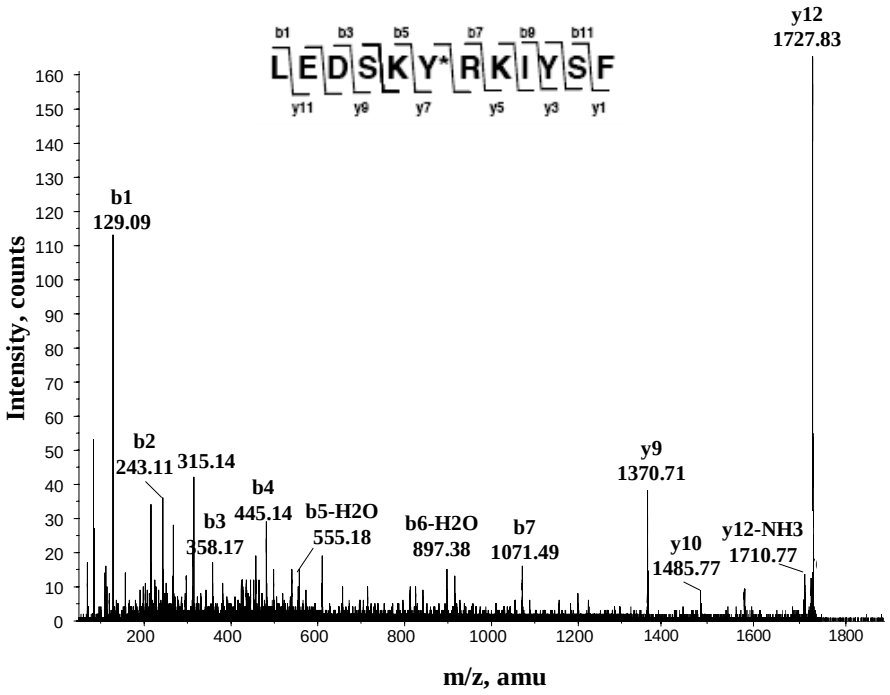

Figure 7. MALDI Q-TOF tandem mass spectra of 1727.87 Da peptide obtained by pepsin digestion of N-OH-AAF-inactivated NAT1.

AAF or human NAT1 with N-OH-4-AABP resulted in minor adducts formed between either 2-AF or 4-ABP and tyrosine residues (*16, 17*).

Human NAT2 that had been treated with N-OH-AAF showed three principal peaks (Figure 4b). The first peak (33842.2 Da) corresponds to native NAT2. The molecular mass of recombinant NAT2 is 33841.8, which includes three additional N-terminal amino acids, Gly, Leu, and Glu (*21*). The second peak (34039.1 Da) corresponds to a mass increase of 197 Da, relative to the 33842.2 Da peak, the native NAT2, indicating a sulfinamide adduct. The most intense peak (34427.6 Da) corresponds to the mass increase of 389 (195 + 194) Da, relative to the 34039.1 Da peak. MALDI Q-TOF MS analysis of pepsin digested human NAT2 that had been incubated with N-OH-AAF revealed only one new peak, a monoisotopic mass of 1613.81 Da (Figure 8b), compared with the pepsin digest of native NAT1 (Figure 8a). MALDI Q-TOF MS/MS analysis of the peptide of mass 1613.81 Da identified the modified (+32 Da) sequence DHIVRRNRGGWCL (Asp57-Leu69, unmodified theoretical mass 1581.82 Da. The b11 ion (1347.62 *m/z*), the b12 ion (1482.66 *m/z*), and the intense b12-H_2SO_2 ion (1416.71 *m/z*) in the MALDI Q-TOF tandem mass spectrum verify that the thiol group of Cys68 had been converted to a sulfinic acid (Figure 9).

ESI Q-TOF MS Analysis, Proteolysis, and MALDI Q-TOF MS/MS Analysis of N-OH-4-AABP-Treated NAT2. Our previous investigation of human NAT1 inactivation by N-OH-4-AABP revealed the formation of a sulfinamide adduct with the active site Cys68 (*17*). The mass spectrum of human NAT2 that had been treated with N-OH-4-AABP contained four peaks, the most

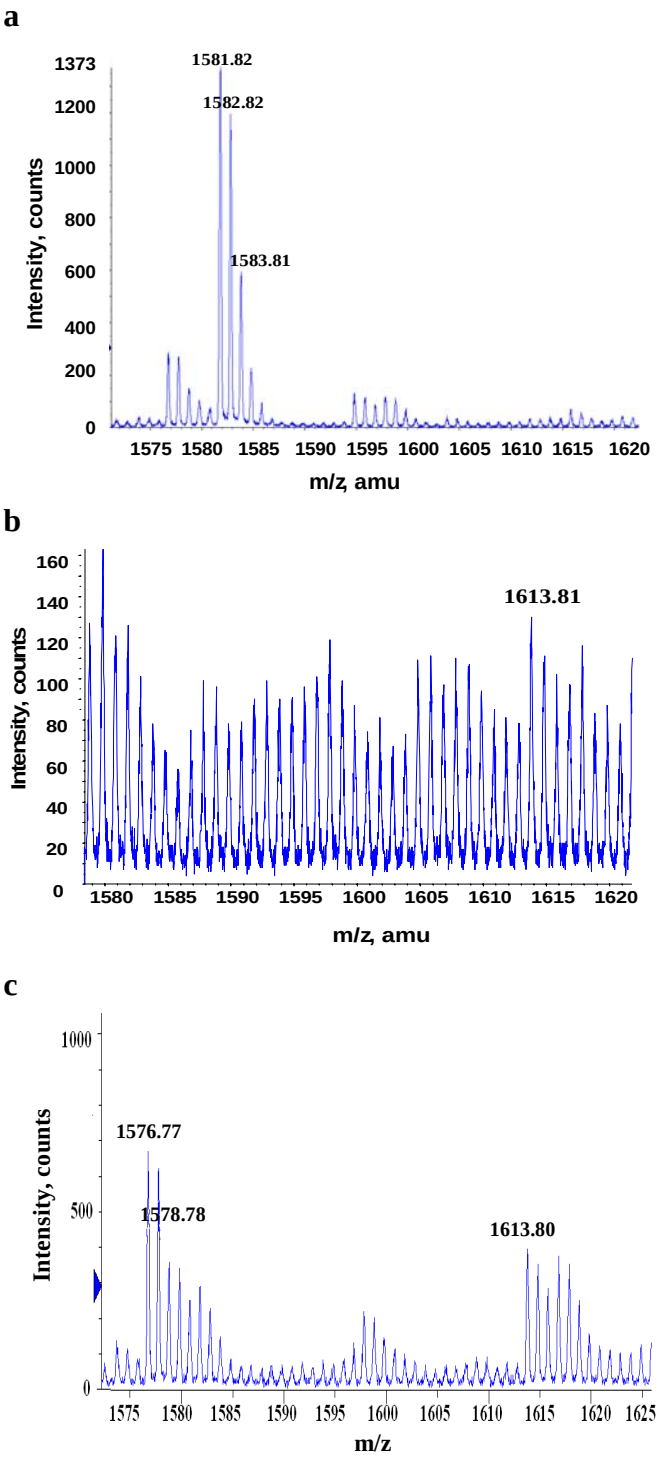

Figure 8. Segments of the MALDI Q-TOF mass spectra of pepsin digests of (a) native human NAT2; (b) N-OH-AAF-inactivated NAT2; (c) N-OH-4-AABP-inactivated NAT2.

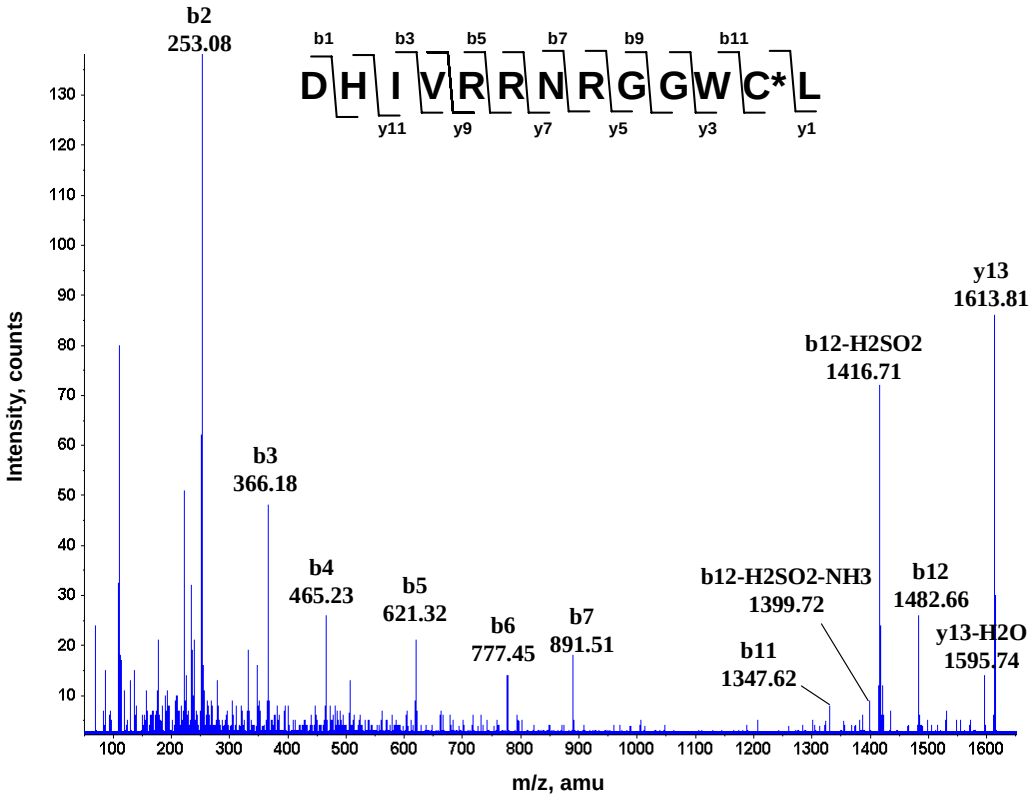

Figure 9. MALDI Q-TOF tandem mass spectra of the 1613.81 Da peptide obtained by pepsin digestion of N-OH-AAF-inactivated NAT2.

intense of which (34024.2 Da) indicates a mass increase of 185 Da relative to the 33839.1 Da peak, which corresponds to unmodified NAT2 (Figure 4c). The third peak in the spectrum (34208.9 Da) represents a mass increase of 185 Da relative to the 34024.2 Da peak. The fourth peak (34392.8 Da) represents a mass increase of 184 Da relative to the mass of 34208.9 Da. The MALDI Q-TOF MS analysis of the pepsin digest of the N-OH-4-AABP modified NAT2 revealed a modified (+32 Da) peptide of mass 1613.80 Da (Figure 8c), which was not present in the digest obtained with NAT2 that had not been treated with N-OH-4-AABP (Figure 8a). MALDI Q-TOF MS/MS of the peptide of mass 1613.80 revealed the modified (+32 Da) sequence DHIVRRNRGGWCL (Asp57-Leu69; unmodified theoretical mass 1581.82 Da). The presence of the b11 ion (1347.71 m/z), the b12 ion (1482.69 m/z) and the strong b12-H2SO2 ion (1416.73 m/z) verified the added mass of 32 Da, and demonstrated that the side chain thiol of Cys68 had been converted to a sulfinic acid (Figure 10).

Hydrolytic Stability of Acetylated NAT2 and Nitrosoarene Formation from N-arylhydroxamic Acids in the Presence of NAT2. After the susceptibilities of NATs to inactivation by N-arylhydroxamic acids were revealed by kinetic analysis and sulfinamide adduct formation was shown to be responsible for N-arylhydroxamic acid-mediated inactivation of NAT2, we tested the proposal that the relative stabilities of the acetyl-enzyme intermediates influence the susceptibilities of NATs to inactivation by N-arylhydroxamic acids. To calculate the half-lives of the acetyl-enzymes ($t_{1/2} = 0.693/k_{H_2O}$), the steady state rate constants, which represent the rate constants for hydrolysis of the acetyl-enzyme (k_{H_2O}) were measured. NAT2 was incubated with the acetyl donor, PNPA, and the

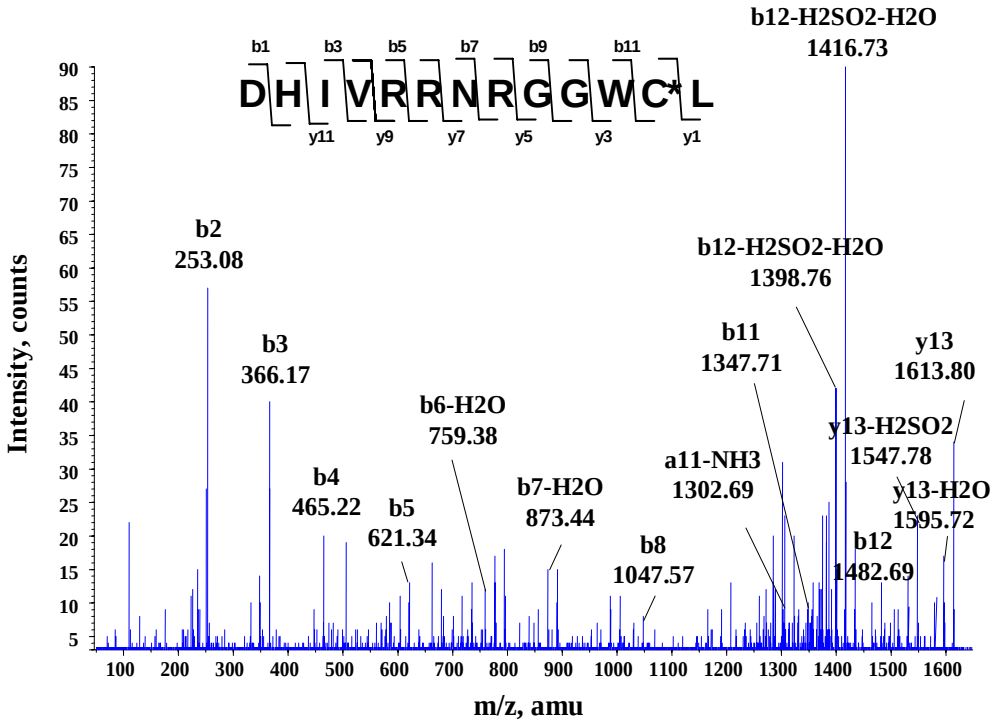

Figure 10. MALDI Q-TOF tandem mass spectra of the 1613.80 Da peptide obtained by pepsin digestion of N-OH-4-AABP-inactivated NAT2.

formation of 4-nitrophenol was monitored at 400 nm. Acetylated NAT2 has a half-life of 7 s at 37 ºC, which is 4.7-fold less than the half life of 33 s determined for acetylated NAT1 (Table 2) (*17*).

The greater stability of the acetyl-NAT1 intermediate and the observable delay in inactivation upon exposure of NAT1 to N-arylhydroxamic acids indicate that greater amounts of nitrosoarenes should accumulate in the incubation mixture during the exposure of NAT1 to N-arylhydroxamic acids than during treatment of NAT2. NAT2 (4 μM) was incubated with either N-OH-4-AABP or N-OH-AAF (200 μM). The generated 4-NO-BP or 2-NO-F was monitored at 350 nm or 380 nm continuously for 30 min. The amount of 2-NO-F that was accumulated with NAT1 was two fold greater than that accumulated with NAT2, and the amount of 4-NO-BP produced by NAT1 was four times greater than the amount produced by NAT2 (Table 2). Therefore, NAT2, which was more efficiently inactivated, and exhibited no delay in the inactivation process after exposure to N-arylhydroxamic acids, generated smaller quantities of the nitroso products, and its acetylated form was less stable than that of NAT1.

Effect of N-OH-AAF and N-OH-4-AABP on NAT1 and NAT2 Activities in HeLa Cell Cytosol. To assess the IC_{50} values for inhibition of cytosolic NAT1 and NAT2 by N-arylhydroxamic acids, HeLa cell cytosol was incubated with a range of concentrations of N-OH-AAF and N-OH-4-AABP. For N-OH-AAF, the IC_{50} values obtained with NAT1 and NAT2 were 27.1 ± 0.19 μM and 9.5 ± 0.6 μM, which were significantly different ($p < 0.001$). For N-OH-4-AABP, the corresponding values were 34 ± 1.3 μM and 19.7 ± 0.57 μM, which

			N-OH-AAF	N-OH-4-AABP
	k_{H2O} (s^{-1})	$t_{1/2}$ (s)	2-NO-F (μM)	4-NO-BP (μM)
NAT1	0.02 ± 0.001 [a]	33 [a]	10 ± 0.9	20 ± 3 [a]
NAT2	0.1 ± 0.002	7 ± 1.4	5 ± 0.7	4 ± 0.9

Table 2. Hydrolysis rate constants (k_{H2O}) and half-Lives ($t_{1/2}$) of acetylated NATs and 2-NO-F and 4-NO-BP formation from N-OH-AAF and N-OH-4-AABP in the presence of NATs**.** [a] Data is from reference 17.

also showed significant difference ($p < 0.001$). Thus, the results obtained with the cytosolic enzymes were consistent with the results obtained with the recombinant NATs and consistent with the expectation that NAT2 would be more susceptible than NAT1 to inactivation by hydroxamic acids.

Evidence that inactivation of NATs in HeLa cell cytosol by N-arylhydroxamic acids involves interaction with the active site was obtained by incubation of the N-arylhydroxamic acids with cell cytosol in the presence of the physiological acetyl donor, AcCoA. Incubation of cell cytosol with a 50 μM concentration of either N-OH-AAF or N-OH-4-AABP caused approximately 60% inhibition of NAT1. Similarly, N-OH-AAF (10 μM) and N-OH-4-AABP (50 μM) caused 60% losses in NAT2 activity. The presence of AcCoA (400 μM) lowered the extent of inhibition of NAT1 to 15-17% and AcCoA (800 μM) lowered the loss of NAT2 activity to 6-10% (Table 3). Thus, inhibition of HeLa cell cytosolic NAT1 and NAT2 by N-OH-AAF and N-OH-4-AABP involves interaction of the N-arylhydroxamic acids with the active sites of enzymes.

Effect of N-OH-AAF and N-OH-4-AABP on NAT1 and NAT2 Activities in HeLa Cells. To assess the effects of N-arylhydroxamic acids on intracellular NAT activities, HeLa cells were incubated with N-OH-AAF (25-250 μM) and N-OH-4-AABP (25-250 μM) for 2 h and 6 h. Cell viability was at least 90% in the 2 h experiments, as determined by trypan blue exclusion. In the 6 h experiments, cell viability was 81-94% in the presence of 25-100 μM concentrations of N-OH-AAF and N-OH-4-AABP; cell viability was 70-75% in the presence of 250 μM concentrations of the hydroxamic acids. A two hour

NAT1	nmol/mg/min	% Control Activity
Control	4.34 ± 0.13	100 ± 3
50 μM N-OH-AAF	1.77 ± 0.28	41 ± 7
AcCoA [b] + 50 μM N-OH-AAF	3.67 ± 0.21	85 ± 5
50 μM N-OH-4-AABP	1.68 ± 0.35	39 ± 8
AcCoA [b] + 50 μM N-OH-4-AABP	3.58 ± 0.70	83 ± 16
NAT2	nmol/mg/min	% Control Activity
Control	0.15 ± 0.006	100 ± 4
10 μM N-OH-AAF	0.05 ± 0.01	38 ± 9
AcCoA [c] + 10 μM N-OH-AAF	0.13 ± 0.02	94 ± 11
20 μM N-OH-4-AABP	0.06 ± 0.02	41 ± 11
AcCoA [c] + 20 μM N-OH-4-AABP	0.13 ± 0.01	90 ± 9

Table 3. Effect of AcCoA on N-OH-AAF and N-OH-4-AABP inactivation of NAT1 and NAT2 in HeLa Cell Cytosol [a].

[a] Results are expressed as the means (± SD) of three experiments.

[b] The AcCoA concentration was 400 μM.

[c] The AcCoA concentration was 800 μM.

incubation of HeLa cells with either N-OH-AAF or N-OH-4-AABP caused no significant change in either intracellular NAT1 or NAT2 activities (Table 4). However, treatment of the cells with either of the compounds for six hours caused a concentration dependent reduction in both NAT1 and NAT2 activities. The inhibition of intracellular GAPDH and GR by the two N-arylhydroxamic acids were also determined (Figure 11).

As shown in Figure 11a, treatment of the cells with 25 μM N-OH-4-AABP for 6 h had no effect on either NAT1 or NAT2 activities. A 50 μM concentration of N-OH-4-AABP had no effect on NAT2 activity, but caused a significant ($p < 0.05$) reduction of 24% in NAT1 activity. Incubation with N-OH-4-AABP (100 μM) for 6 h reduced NAT2 and NAT1 activities by 19 (±7)% and 56 (±1)%, respectively; the reductions in NAT1 and NAT2 activities were significantly ($p < 0.001$) different from each other. N-OH-4-AABP (250 μM) caused similar decreases in NAT1 and NAT2 activities of approximately 50%. N-OH-4-AABP (100 μM and 250 μM) reduced GAPDH and GR activities by approximately 19-24%.

N-OH-AAF was a somewhat more effective inactivator of intracellular NAT1 and NAT2 than N-OH-4-AABP (Figure 11b). Treatment of HeLa cells with 50 μM N-OH-AAF for 6 hours caused significantly ($p < 0.001$) different reductions in NAT2 and NAT1 activities of 11 (±4)% and 33 (±1)%, respectively. N-OH-AAF (100 μM and 250 μM) decreased NAT1 and NAT2 activities by approximately 50%. A six hour-incubation of the cells with N-OH-AAF (100 μM and 250 μM) caused an 11-16% decrease in GAPDH activity and a 28% decrease

in GR activity (Figure 11b). Thus, approximately 10-fold greater concentrations and much longer incubation times were required for N-OH-4-AABP or N-OH-AAF to produce effects on intracellular NATs than were required for either 4-NO-BP or 2-NO-F (Part III and Part IV of this thesis).

	NAT1		NAT2	
	nmol/mg/min	% Control Activity	nmol/mg/min	% Control Activity
N-OH-AAF (μM)				
0	4.22 ± 0.20	100 ± 5	0.14 ± 0.01	100 ± 10
25	4.23 ± 0.12	101 ± 3	0.14 ± 0.02	96 ± 15
50	4.36 ± 0.25	104 ± 6	0.13 ± 0.01	91 ± 6
100	4.04 ± 0.38	96 ± 9	0.15 ± 0.01	102 ± 10
250	4.47 ± 0.21	106 ± 5	0.15 ± 0.003	103 ± 2
N-OH-4-AABP (μM)				
0	4.41 ± 0.13	100 ± 3	0.19 ± 0.02	100 ± 9
25	4.06 ± 0.09	92 ± 2	0.20 ± 0.01	106 ± 4
50	4.23 ± 0.07	96 ± 2	0.19 ± 0.01	98 ± 7
100	4.33 ± 0.09	98 ± 2	0.18 ± 0.01	95 ± 7
250	4.47 ± 0.28	102 ± 6	0.18 ± 0.01	95 ± 5
500	4.15 ± 0.31	94 ± 7	0.19 ± 0.01	100 ± 4

Table 4. Effect of N-OH-AAF and N-OH-4-AABP on endogenous NAT1 and NAT2 activities in HeLa cells. Results are expressed as the means (± SD) of three experiments. The incubation time was 2 hours.

a.

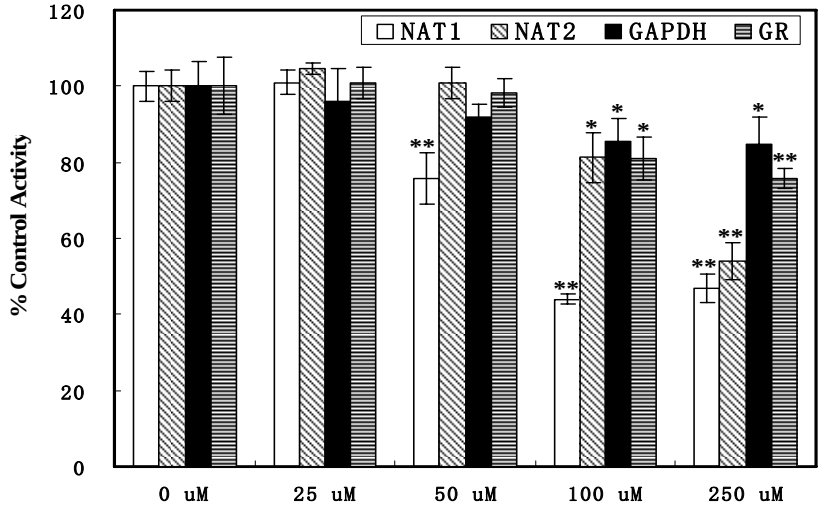

b.

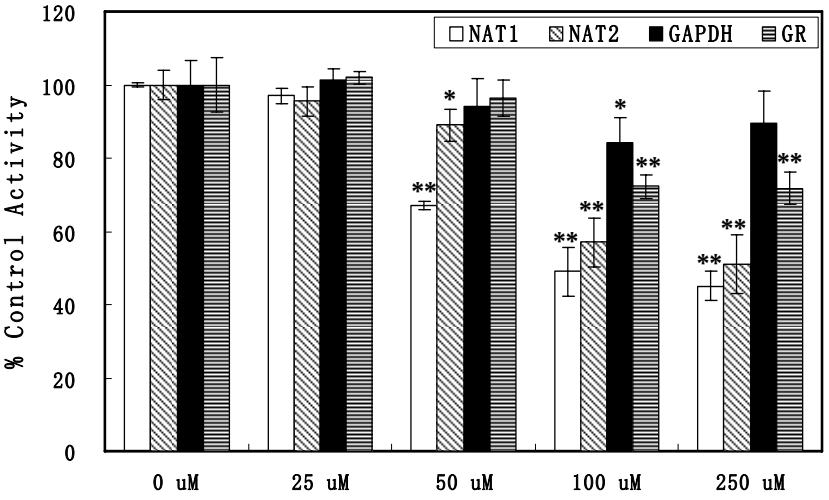

Figure 11. Inactivation of HeLa cell NAT1, NAT2, GAPDH, and GR by N-OH-4-AABP and N-OH-AAF. The incubation time was 6 h. (a) N-OH-4-AABP. Each bar represents the mean and standard deviation of the results of three experiments. Asterisks represent significant differences from control: *, $p < 0.01$; **, $p < 0.001$. (b) N-OH-AAF. Each bar represents the mean and standard deviation of the results of three experiments. Asterisks represent significant differences from control: *, $p < 0.05$; **, $p < 0.001$.

Discussion

N-Arylhydroxamic acids, which are in vivo metabolites of arylamines and arylamides in humans and animals (*3-7*), have been shown to inactivate hamster arylamine N-acetyltransferases (NATs), in vitro and in vivo, and human recombinant NAT1 in vitro (*15-17*). In this study, we explored the inactivation of human NATs by N-arylhydroxamic acids, N-OH-AAF and N-OH-4-AABP, in vitro and in human cells.

As shown in Scheme 1, part VI of this thesis, the mechanism of inactivation of NATs by N-arylhydroxamic acids in vitro involves an initial NAT-mediated deacetylation of the hydroxamic acid, producing an arylhydroxlamine (Scheme 1, B, part VI of this thesis), which after oxidative conversion to a nitrosoarene reacts with the catalytic nucleophile, Cys68, of NAT to form a covalent sulfinamide adduct (Scheme 1, C, E, part VI of this thesis) (*16, 17*). Based on previous observations from reactions of N-OH-4-AABP with hamster NAT1, hamster NAT2, and human NAT1, it was expected that human NAT2 would be more readily inactivated by N-arylhydroxamic acids than human NAT1 because hamster NAT1, the homolog of human NAT2, is more rapidly inactivated by N-OH-4-AABP than hamster NAT2. It was proposed that the relative stabilities of the acetyl-enzyme intermediates formed in the initial step of the inactivation process (Scheme 1, B, part VI of this thesis) influence the susceptibilities of NATs to inactivation by N-arylhydroxamic acids and that the human NAT2 Cys68 thioacetyl ester would be more rapidly hydrolyzed (Scheme 1, D, part VI of this thesis) than that of NAT1 (*17*).

The kinetic analysis revealed that the second order rate constants (k_{inact}/K_I) for inactivation of NAT2 by N-OH-AAF and N-OH-4-AABP were 8-fold greater and 3-fold greater, respectively, for NAT2 than for NAT1 (Table 1). NAT2 forms a less stable acetyl-enzyme intermediate than NAT1, with the acetylated form of NAT2 having a five-fold shorter hydrolysis half-life, which results in greater availability of the Cys68 thiol of NAT2 for reaction with a nitrosoarene, a faster rate of inactivation of NAT2, and larger quantities of nitrosoarene formed in incubations of NAT1 with N-arylhydroxamic acids (Table 2). The inhibitory effects of N-OH-AAF and N-OH-4-AABP on NAT1 and NAT2 activities in HeLa cell cytosol were consistent with the results obtained with the recombinant NATs, as the IC_{50} values for inhibition of NAT2 by N-OH-AAF and N-OH-4-AABP were 2 to 3 times smaller than the IC_{50} for inhibition of NAT1.

Nitrosoarenes, generated from arylhydroxylamines, are expected to be the reactive species that inactivate HeLa intracellular NATs upon exposure to hydroxamic acids. Therefore, the relative susceptibility of HeLa intracellular NAT1 and NAT2 to inactivation after treatment of the cells with N-arylhydroxamic acids might be expected to be consistent with the relative susceptibility of HeLa NATs to inactivation upon direct treatment of the cells with nitrosoarenes. A six-hour treatment of HeLa cells with N-OH-4-AABP (50 μM and 100 μM) and with N-OH-AAF (50 μM) caused significantly greater inhibitory effects on intracellular NAT1 than on NAT2. The k_{inact}/K_I values for inactivation of recombinant NAT1 by N-OH-AAF and N-OH-4-AABP, however, were 8-fold lower and 3-fold lower, respectively, than for NAT2 (Table 1), and the IC_{50} values for inactivation of HeLa cytosolic NATs by the hydroxamic acids

were 2 to 3-fold greater for NAT1 than for NAT2. Thus, HeLa intracellular NATs showed a different relative susceptibility to N-arylhydroxamic acids than either the recombinant NATs or the NATs in HeLa cell cytosol. We have shown previously that HeLa cell NAT1 is more susceptible to the effects of the lower concentrations of 2-NO-F and 4-NO-BP than is NAT2 (Part III and IV of this thesis). Therefore, HeLa cell NATs showed an identical relative susceptibility to inactivation by N-arylhydroxamic acids and by nitrosoarenes.

To produce an inhibitory effect on the intracellular NAT1 and NAT2 activities, it was necessary to treat HeLa cells with relatively higher concentrations of N-arylhydroxamic acids and for longer incubation times, compared to the corresponding nitrosoarenes. One reason for the lower potency of the hydroxamic acids may be that the acetohydroxamic acid group is slightly acidic and more polar than the nitroso group and markedly decreases lipid solubility and cell penetration. The calculated partition coefficients (LogP) for N-OH-AAF and N-OH-4-AABP are reported to be 2.60-2.80 and 2.61-2.92, whereas the calculated LogP values for 2-NO-F and 4-NO-BP are 3.96 and 3.50-4.14 (*22*). Another factor may be that esterase-catalyzed hydrolysis of the hydroxamic acids, followed by the generation of nitrosoarenes from the arylhydroxylamines may be the primary intracellular pathway for production of nitrosoarenes from arylhydroxamic acids. It was found that treatment of hamsters with an esterase inhibitor, bis(*p*-nitrophenyl)phosphate (BNPP), prior to the administration of N-OH-AAF prevented NAT inactivation in vivo (*15*). Thus, the esterase-catalyzed deacetylation of the hydroxamic acids appeared to be essential to produce sufficient quantities of the arylhydroxylamines to cause inhibitory effects in vivo

(Scheme 1, F and C, part VI of this thesis), and NAT-catalyzed deacetylation of hydroxamic acids (Scheme 1, B, part VI of this thesis) may not be important for arylhydroxylamine formation within cells.

We have shown previously that 4-NO-BP and 2-NO-F react more readily with NATs than with GSH, a ubiquitous cellular reductant and nucleophile, (Part III and Part IV of this thesis). Similarly, it had been shown that GSH provided little protection of hamster recombinant NAT1 from inactivation by N-OH-AAF (*16*). These results indicate that intracellular GSH would not be a significant factor in preventing the inactivation of cellular NATs by N-arylhydroxamic acids.

Research on the bioactivation of N-arylhydroxamic acids by NATs has also focused on the NAT-catalyzed formation of N-acetoxyarylamines, which undergo heterolytic cleavage of the N-O bond to produce arylnitrenium ions, which are believed to be the ultimate electrophilic reactants responsible for DNA adduct formation (*23-25*) (equation 2). It is not known whether N-acetoxyarylamines play an important role in formation of protein adducts, but our results do not support their involvement in the inactivation of NATs. Additional studies will be required to elucidate the pathway of inactivation of HeLa NATs by N-arylhydroxamic acids. Experiments should be conducted to determine which enzymes play key roles in hydrolyzing the compounds and what molecular species accumulate in the cells.

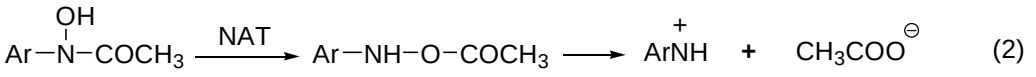

(2)

References

(1) Chiang, T. A., Pei-Fen, W., Ying, L. S., Wang, L. F. and Ko, Y. C. (1999) Mutagenicity and aromatic amine content of fumes from heated cooking oils produced in Taiwan. *Food Chem Toxicol 37*, 125-134.

(2) Stabbert, R., Schafer, K. H., Biefel, C. and Rustemeier, K. (2003) Analysis of aromatic amines in cigarette smoke. *Rapid Commun Mass Spectrom 17*, 2125-2132.

(3) Cramer, J. W., Miller, J. A. and Miller, E. C. (1960) N-Hydroxylation: A new metabolic reaction observed in the rat with the carcinogen 2-acetylaminofluorene. *J Biol Chem 235*, 885-888.

(4) Miller, J. A., Wyatt, C. S., Miller, E. C., and Hartmann, H. A. (1961) The N-hydroxylation of 4-acetylaminobiphenyl by the rat and dog and the strong carcinogenicity of N-hydroxy-4-acetylaminobiphenyl in the rat. *Cancer Res. 21*, 1465-1473.

(5) Enomoto, M., Lotlikhar, P., Miller, J. A., and Miller, E. C. (1962) Urinary metabolites of 2-acetylaminofluorene and related compounds in the rhesus monkey. *Cancer Res. 22*, 1336-1342.

(6) Weisburger, J. H., Grantham, P. H., Vanhorn, E., Steigbigel, N. H., Rall, D. P. and Weisburger, E. K. (1964) Activation And Detoxification Of N-2-Fluorenylacetamide In Man. *Cancer Res 24*, 475-479.

(7) Veronese, M. E., McLean, S., D'Souza, C. A. and Davies, N. W. (1985) Formation of reactive metabolites of phenacetin in humans and rats. *Xenobiotica 15*, 929-940.

(8) Moller, L., Rafter, J. and Gustafsson, J. A. (1987) Metabolism of the carcinogenic air pollutant 2-nitrofluorene in the rat. *Carcinogenesis 8*, 637-645.

(9) Weisburger, J. H. and Weisburger, E. K. (1973) Biochemical formation and pharmacological, toxicological, and pathological properties of hydroxylamines and hydroxamic acids. *Pharmacol Rev 25*, 1-66.

(10) Hanna, P. E. (1996) Metabolic activation and detoxification of arylamines. *Curr. Med. Chem. 3*, 195-210.

(11) Kim, D. and Guengerich, F. P. (2005) Cytochrome P450 activation of arylamines and heterocyclic amines. *Annu Rev Pharmacol Toxicol 45*, 27-49.

(12) Hollenberg, P. F., Kent, U. M. and Bumpus, N. N. (2008) Mechanism-based inactivation of human cytochromes p450s: experimental characterization, reactive intermediates, and clinical implications. *Chem Res Toxicol 21*, 189-205.

(13) Bartsch, H., Dworkin, M., Miller, J. A. and Miller, E. C. (1972) Electrophilic N-acetoxyaminoarenes derived from carcinogenic N-hydroxy-N-acetylaminoarenes by enzymatic deacetylation and transacetylation in liver. *Biochim Biophys Acta 286*, 272-298.

(14) Hanna, P. E., Banks, R. B., and Marhevka, V. C. (1982) Suicide inactivation of hamster hepatic arylhydroxamic acid N,O-acyltransferase. A selective probe of N-acetyltransferase multiplicity. *Mol. Pharmacol. 21*, 159-165.

(15) Smith, T. J. and Hanna, P. E. (1988) Hepatic N-acetyltransferases: selective inactivation in vivo by a carcinogenic N-arylhydroxamic acid. *Biochem Pharmacol 37*, 427-434.

(16) Guo, Z., Wagner, C. R. and Hanna, P. E. (2004) Mass spectrometric investigation of the mechanism of inactivation of hamster arylamine N-acetyltransferase 1 by N-hydroxy-2-acetylaminofluorene. *Chem Res Toxicol 17*, 275-286.

(17) Wang, H., Wagner, C. R. and Hanna, P. E. (2005) Irreversible inactivation of arylamine N-acetyltransferases in the presence of N-hydroxy-4-acetylaminobiphenyl: a comparison of human and hamster enzymes. *Chem Res Toxicol 18*, 183-197.

(18) Liu, L., Wagner, C. R., and Hanna, P. E. (2008) Human Arylamine N-Acetyltransferase 1: In Vitro and Intracellular Inactivation by Nitrosoarene Metabolites of Toxic and Carcinogenic Arylamines. *Chem. Res. Toxicol.*

(19) Kitz, R. and Wilson, I. B. (1962) Esters of methanesulfonic acid as irreversible inhibitors of acetylcholinesterase. *J Biol Chem 237*, 3245-3249.

(20) Wang, H., Vath, G. M., Kawamura, A., Bates, C. A., Sim, E., Hanna, P. E. and Wagner, C. R. (2005) Over-expression, purification, and characterization of recombinant human arylamine N-acetyltransferase 1. *Protein J 24*, 65-77.

(21) Liu, L., Von Vett, A., Zhang, N., Walters, K. J., Wagner, C. R. and Hanna, P. E. (2007) Arylamine N-acetyltransferases: characterization of the substrate specificities and molecular interactions of environmental arylamines with human NAT1 and NAT2. *Chem Res Toxicol 20*, 1300-1308.

(22) http://www.chemspider.com.

(23) Hanna, P. E. (1994) N-acetyltransferases, O-acetyltransferases, and N,O-acetyltransferases: enzymology and bioactivation. *Adv Pharmacol 27*, 401-430.

(24) Novak, M. and Rajagopal, S. (2002) Correlations of nitrenium ion selectivities with quantitative mutagenicity and carcinogenicity of the corresponding amines. *Chem Res Toxicol 15*, 1495-1503.

(25) Kennedy, S. A., Novak, M., Kolb, B.A. (1997) Reactions of ester derivatives of carcinogenic N-(4-biphenyl)hydroxylamine and the corresponding hydroxamic acid with purine nucleosides. *J. Am. Chem. Soc. 119*, 7654-7664.

PART VI: OVERVIEW OF NAT INACTIVATION BY NITROSOARENES AND N-ARYLHYDROXAMIC ACIDS

In this thesis, we explored the inactivation of human arylamine N-acetyltransferase 1 (NAT1) and arylamine N-acetyltransferase 2 (NAT2) by two types of reactive arylamine metabolites, nitrosoarenes and N-arylhydroxamic acids, in vitro and in human cells. The inactivation of human NATs will impair the NAT catalyzed N-acetylation of arylamines to arylamides (Scheme 1), which is a key detoxification pathway, and may result in an increase in the CYP catalyzed oxidation of arylamines to N-arylhydroxylamines (Scheme 1), which is the primary step for toxification of these xenobiotics. Inactivation of NATs should also influence their role in the O-acetylation of N-arylhydroxylamines, which is a bioactivation process.

Nitrosoarenes can be formed from the oxidation of arylamines and N-arylhydroxylamines in vivo (Scheme 1). The electrophilicity of nitrosoarenes allow them to react readily with the highly nucleophilic active site Cys68 thiol group of NATs to form sulfinamides (Scheme 1, E). It was found that the nitroso derivatives of arylamines that are good substrates for human NATs are potent NAT inactivators in vitro and that human NATs appear to be preferred intracellular targets of 4-NO-BP and 2-NO-F. Additionally, it was observed that HeLa intracellular NAT2 is less susceptible to the effects of lower concentrations of the two nitrosoarenes than is NAT1.

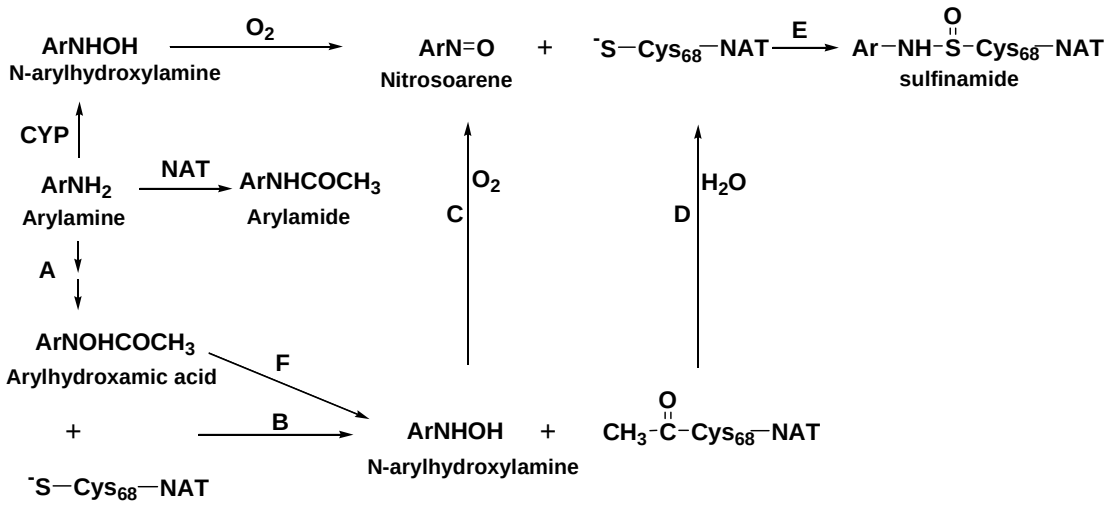

Scheme 1. Pathways for detoxification and/or conversion of arylamines to reactive metabolites that are capable of inactivating NATs.

CYP = cytochrome P450; NAT = arylamine N-acetyltransferase; A = CYP and NAT; B = NAT; C = nonenzymatic oxidation; D = nonenzymztic hydrolysis; E = nonenzymatic sulfinamide formation; F = esterases.

N-Arylhydroxamic acids can be formed from arylamines in vivo (Scheme 1, A) (*1*). The inactivation of recombinant NATs by N-arylacetohydroxamic acids starts with NAT-mediated deacetylation to produce N-arylhydroxylamines and acetylated-NAT intermediates (Scheme 1, B). The subsequently generated nitrosoarenes (Scheme 1, C) react with the active site cysteine to form sulfinamide adducts (Scheme 1, E). It was found that the hydrolysis rates of the acetyl-enzyme intermediates (Scheme 1, D) influence the susceptibilities of recombinant NATs to inactivation by N-arylhydroxamic acids. The stability of the acetyl thioester is inversely related to the rate of inactivation. The inactivation of NATs by N-arylhydroxamic acids in vivo appears to involve an essential esterase-catalyzed deacetylation of the hydroxamic acids to generate N-arylhydroxlamines (Scheme 1, F) (*2*), followed by the formation of nitrosoarenes (Scheme 1, C), which react with the intracellular NATs. The complete details of the intracellular inactivation of NAT1 and NAT2 by N-arylhydroxamic acids in HeLa cells are not known, but the relative susceptibilities of HeLa NAT1 and NAT2 to inactivation by nitrosoarenes and hydroxamic acids are identical, although they differ from the relative susceptibilities to inactivation by the compounds in vitro.

References

(1) Miller, J. A., Wyatt, C. S., Miller, E. C., and Hartmann, H. A. (1961) The N-hydroxylation of 4-acetylaminobiphenyl by the rat and dog and the strong carcinogenicity of N-hydroxy-4-acetylaminobiphenyl in the rat. *Cancer Res. 21*, 1465-1473.

(2) Smith, T. J. and Hanna, P. E. (1988) Hepatic N-acetyltransferases: selective inactivation in vivo by a carcinogenic N-arylhydroxamic acid. *Biochem Pharmacol 37*, 427-434.

BIBLIOGRAPHY

Introduction

(1) Hanna, P. E. (1996) Metabolic activation and detoxification of arylamines. *Curr. Med. Chem. 3*, 195-210.

(2) Kim, D. and Guengerich, F. P. (2005) Cytochrome P450 activation of arylamines and heterocyclic amines. *Annu Rev Pharmacol Toxicol 45*, 27-49.

(3) Hein, D. W. (2002) Molecular genetics and function of NAT1 and NAT2: role in aromatic amine metabolism and carcinogenesis. *Mutat Res 506-507*, 65-77.

(4) Rodrigues-Lima, F., Dairou, J. and Dupret, J. M. (2008) Effect of environmental substances on the activity of arylamine N-acetyltransferases. *Curr Drug Metab 9*, 505-509.

(5) Parkes, H. G., Evans, A. E. J. (1984) Epidemiology of aromatic amine cancers. In: Searle C. E. (ed) Chemical carcinogens, vol 1, American Chemical Society, Washington DC, pp 277-301.

(6) Gan, J., Skipper, P. L., Gago-Dominguez, M., Arakawa, K., Ross, R. K., Yu, M. C. and Tannenbaum, S. R. (2004) Alkylaniline-hemoglobin adducts and risk of non-smoking-related bladder cancer. *J Natl Cancer Inst 96*, 1425-1431.

(7) Gorlewska-Roberts, K., Green, B., Fares, M., Ambrosone, C. B. and Kadlubar, F. F. (2002) Carcinogen-DNA adducts in human breast epithelial cells. *Environ Mol Mutagen 39*, 184-192.

(8) Gago-Dominguez, M., Bell, D. A., Watson, M. A., Yuan, J. M., Castelao, J. E., Hein, D. W., Chan, K. K., Coetzee, G. A., Ross, R. K. and Yu, M. C. (2003) Permanent hair dyes and bladder cancer: risk modification by cytochrome P4501A2 and N-acetyltransferases 1 and 2. *Carcinogenesis 24*, 483-489.

(9) Hazardous substances databand (HSDB) (2008) http:// toxnet.nlm.nih.gov.

(10) Yu, M. C., Skipper, P. L., Tannenbaum, S. R., Chan, K. K. and Ross, R. K. (2002) Arylamine exposures and bladder cancer risk. *Mutat Res 506-507*, 21-28.

(11) Turesky, R. J., Freeman, J. P., Holland, R. D., Nestorick, D. M., Miller, D. W., Ratnasinghe, D. L. and Kadlubar, F. F. (2003) Identification of aminobiphenyl derivatives in commercial hair dyes. *Chem Res Toxicol 16*, 1162-1173.

(12) Gaber, K., Harreus, U. A., Matthias, C., Kleinsasser, N. H. and Richter, E. (2007) Hemoglobin adducts of the human bladder carcinogen o-toluidine after treatment with the local anesthetic prilocaine. *Toxicology 229*, 157-164.

(13) Felton, J. S., Knize, M. G., Roper, M., Fultz, E., Shen, N. H. and Turteltaub, K. W. (1992) Chemical analysis, prevention, and low-level dosimetry of heterocyclic amines from cooked food. *Cancer Res 52*, 2103s-2107s.

(14) http://cancer.org.

(15) Jiang, X., Yuan, J. M., Skipper, P. L., Tannenbaum, S. R. and Yu, M. C. (2007) Environmental tobacco smoke and bladder cancer risk in never smokers of Los Angeles County. *Cancer Res 67*, 7540-7545.

(16) Vineis, P. and Pirastu, R. (1997) Aromatic amines and cancer. *Cancer Causes Control 8*, 346-355.

(17) Talaska, G. (2003) Aromatic amines and human urinary bladder cancer: exposure sources and epidemiology. *J Environ Sci Health C Environ Carcinog Ecotoxicol Rev 21*, 29-43.

(18) Messner, C. and Murkovic, M. (2004) Evaluation of a new model system for studying the formation of heterocyclic amines. *J Chromatogr B Analyt Technol Biomed Life Sci 802*, 19-26.

(19) Skipper, P. L., Trudel, L. J., Kensler, T. W., Groopman, J. D., Egner, P. A., Liberman, R. G., Wogan, G. N. and Tannenbaum, S. R. (2006) DNA adduct formation by 2,6-dimethyl-, 3,5-dimethyl-, and 3-ethylaniline in vivo in mice. *Chem Res Toxicol 19*, 1086-1090.
(20) Hanna, P. E. (1994) N-acetyltransferases, O-acetyltransferases, and N,O-acetyltransferases: enzymology and bioactivation. *Adv Pharmacol 27*, 401-430.
(21) Cramer, J. W., Miller, J. A. and Miller, E. C. (1960) N-Hydroxylation: A new metabolic reaction observed in the rat with the carcinogen 2-acetylaminofluorene. *J Biol Chem 235*, 885-888.
(22) Miller, J. A., Wyatt, C. S., Miller, E. C., and Hartmann, H. A. (1961) The N-hydroxylation of 4-acetylaminobiphenyl by the rat and dog and the strong carcinogenicity of N-hydroxy-4-acetylaminobiphenyl in the rat. *Cancer Res. 21*, 1465-1473.
(23) Beland, F. A., and Kadlubar, F. F. (1990) Metabolic activation and DNA adducts of aromatic amines and nitroaromatic hydrocarbons. *Handbook Exp. Pharmacol 94/I*, 267-325.
(24) Murata, M., Tamura, A., Tada, M. and Kawanishi, S. (2001) Mechanism of oxidative DNA damage induced by carcinogenic 4-aminobiphenyl. *Free Radic Biol Med 30*, 765-773.
(25) Zwirner-Baier, I. and Neumann, H. G. (1999) Polycyclic nitroarenes (nitro-PAHs) as biomarkers of exposure to diesel exhaust. *Mutat Res 441*, 135-144.
(26) Boelsterli, U. A., Ho, H. K., Zhou, S. and Leow, K. Y. (2006) Bioactivation and hepatotoxicity of nitroaromatic drugs. *Curr Drug Metab 7*, 715-727.
(27) Kazanis, S., and Mc Clelland, R. A. (1992) Electrophilic intermediate in the reaction of glutathione and nitrosoarenes. *J. Am. Chem. Soc. 114*, 3052-3059.
(28) Wang, H., Wagner, C. R. and Hanna, P. E. (2005) Irreversible inactivation of arylamine N-acetyltransferases in the presence of N-hydroxy-4-acetylaminobiphenyl: a comparison of human and hamster enzymes. *Chem Res Toxicol 18*, 183-197.
(29) Eyer, P. (1994) Reactions of oxidatively activated arylamines with thiols: reaction mechanisms and biologic implications. An overview. *Environ Health Perspect 102 Suppl 6*, 123-132.
(30) Miller, E. C., Miller, J. A. and Enomoto, M. (1964) The Comparative Carcinogenicities Of 2-Acetylaminofluorene And Its N-Hydroxy Metabolite In Mice, Hamsters, And Guinea Pigs. *Cancer Res 24*, 2018-2031.
(31) Banks, R. B. and Hanna, P. E. (1979) Arylhydroxamic acid N,O-acyltransferase. Apparent suicide inactivation by carcinogenic N-arylhydroxamic acids. *Biochem Biophys Res Commun 91*, 1423-1429.
(32) Guo, Z., Wagner, C. R. and Hanna, P. E. (2004) Mass spectrometric investigation of the mechanism of inactivation of hamster arylamine N-acetyltransferase 1 by N-hydroxy-2-acetylaminofluorene. *Chem Res Toxicol 17*, 275-286.
(33) Humphreys, W. G., Kadlubar, F. F. and Guengerich, F. P. (1992) Mechanism of C8 alkylation of guanine residues by activated arylamines: evidence for initial adduct formation at the N7 position. *Proc Natl Acad Sci U S A 89*, 8278-8282.
(34) Heflich, R. H. and Neft, R. E. (1994) Genetic toxicity of 2-acetylaminofluorene, 2-aminofluorene and some of their metabolites and model metabolites. *Mutat Res 318*, 73-114.

(35) Kennedy, S. A., Novak, M., Kolb, B.A. (1997) Reactions of ester derivatives of carcinogenic N-(4-biphenyl)hydroxylamine and the corresponding hydroxamic acid with purine nucleosides. *J. Am. Chem. Soc. 119*, 7654-7664.
(36) Ricicki, E. M., Luo, W., Fan, W., Zhao, L. P., Zarbl, H. and Vouros, P. (2006) Quantification of N-(deoxyguanosin-8-yl)-4-aminobiphenyl adducts in human lymphoblastoid TK6 cells dosed with N-hydroxy-4-acetylaminobiphenyl and their relationship to mutation, toxicity, and gene expression profiling. *Anal Chem 78*, 6422-6432.
(37) Agundez, J. A. (2008) N-acetyltransferases: lessons learned from eighty years of research. *Curr Drug Metab 9*, 463-464.
(38) Josephy, P. D., and Mannervik, B. (2006) *Molecular Toxicology 2nd edition*, pp 426-447, Oxford University Press, New York.
(39) Grant, D. M., Blum, M., Beer, M. and Meyer, U. A. (1991) Monomorphic and polymorphic human arylamine N-acetyltransferases: a comparison of liver isozymes and expressed products of two cloned genes. *Mol Pharmacol 39*, 184-191.
(40) Minchin, R. F. (1995) Acetylation of p-aminobenzoylglutamate, a folic acid catabolite, by recombinant human arylamine N-acetyltransferase and U937 cells. *Biochem J 307 (Pt 1)*, 1-3.
(41) Kawamura, A., Graham, J., Mushtaq, A., Tsiftsoglou, S. A., Vath, G. M., Hanna, P. E., Wagner, C. R. and Sim, E. (2005) Eukaryotic arylamine N-acetyltransferase. Investigation of substrate specificity by high-throughput screening. *Biochem Pharmacol 69*, 347-359.
(42) Hein, D. W., Doll, M. A., Rustan, T. D., Gray, K., Feng, Y., Ferguson, R. J. and Grant, D. M. (1993) Metabolic activation and deactivation of arylamine carcinogens by recombinant human NAT1 and polymorphic NAT2 acetyltransferases. *Carcinogenesis 14*, 1633-1638.
(43) Sticha, K. R., Sieg, C. A., Bergstrom, C. P., Hanna, P. E. and Wagner, C. R. (1997) Overexpression and large-scale purification of recombinant hamster polymorphic arylamine N-acetyltransferase as a dihydrofolate reductase fusion protein. *Protein Expr Purif 10*, 141-153.
(44) Sticha, K. R., Bergstrom, C. P., Wagner, C. R. and Hanna, P. E. (1998) Characterization of hamster recombinant monomorphic and polymorphic arylamine N-acetyltransferases: bioactivation and mechanism-based inactivation studies with N-hydroxy-2-acetylaminofluorene. *Biochem Pharmacol 56*, 47-59.
(45) Wang, H., Vath, G. M., Kawamura, A., Bates, C. A., Sim, E., Hanna, P. E. and Wagner, C. R. (2005) Over-expression, purification, and characterization of recombinant human arylamine N-acetyltransferase 1. *Protein J 24*, 65-77.
(46) Sinclair, J. C., Sandy, J., Delgoda, R., Sim, E. and Noble, M. E. (2000) Structure of arylamine N-acetyltransferase reveals a catalytic triad. *Nat Struct Biol 7*, 560-564.
(47) Holton, S. J., Dairou, J., Sandy, J., Rodrigues-Lima, F., Dupret, J. M., Noble, M. E. and Sim, E. (2005) Structure of Mesorhizobium loti arylamine N-acetyltransferase 1. *Acta Crystallogr Sect F Struct Biol Cryst Commun 61*, 14-16.
(48) Wu, H., Dombrovsky, L., Tempel, W., Martin, F., Loppnau, P., Goodfellow, G. H., Grant, D. M. and Plotnikov, A. N. (2007) Structural basis of substrate-binding specificity of human arylamine N-acetyltransferases. *J Biol Chem 282*, 30189-30197.

(49) Zhang, N., Liu, L., Liu, F., Wagner, C. R., Hanna, P. E. and Walters, K. J. (2006) NMR-based model reveals the structural determinants of mammalian arylamine N-acetyltransferase substrate specificity. *J Mol Biol 363*, 188-200.
(50) Rodrigues-Lima, F., Dairou, J., Diaz, C. L., Rubio, M. C., Sim, E., Spaink, H. P. and Dupret, J. M. (2006) Cloning, functional expression and characterization of Mesorhizobium loti arylamine N-acetyltransferases: rhizobial symbiosis supplies leguminous plants with the xenobiotic N-acetylation pathway. *Mol Microbiol 60*, 505-512.
(51) Sandy, J., Mushtaq, A., Holton, S. J., Schartau, P., Noble, M. E. and Sim, E. (2005) Investigation of the catalytic triad of arylamine N-acetyltransferases: essential residues required for acetyl transfer to arylamines. *Biochem J 390*, 115-123.
(52) Andres, H. H., Kolb, H. J., Schreiber, R. J. and Weiss, L. (1983) Characterization of the active site, substrate specificity and kinetic properties of acetyl-CoA:arylamine N-acetyltransferase from pigeon liver. *Biochim Biophys Acta 746*, 193-201.
(53) Westwood, I. M. and Sim, E. (2007) Kinetic characterisation of arylamine N-acetyltransferase from Pseudomonas aeruginosa. *BMC Biochem 8*, 3.
(54) Wang, H., Vath, G. M., Gleason, K. J., Hanna, P. E. and Wagner, C. R. (2004) Probing the mechanism of hamster arylamine N-acetyltransferase 2 acetylation by active site modification, site-directed mutagenesis, and pre-steady state and steady state kinetic studies. *Biochemistry 43*, 8234-8246.
(55) Wang, H., Liu, L., Hanna, P. E. and Wagner, C. R. (2005) Catalytic mechanism of hamster arylamine N-acetyltransferase 2. *Biochemistry 44*, 11295-11306.
(56) Storer, A. C. and Menard, R. (1994) Catalytic mechanism in papain family of cysteine peptidases. *Methods Enzymol 244*, 486-500.
(57) Hickman, D., Risch, A., Buckle, V., Spurr, N. K., Jeremiah, S. J., McCarthy, A. and Sim, E. (1994) Chromosomal localization of human genes for arylamine N-acetyltransferase. *Biochem J 297 (Pt 3)*, 441-445.
(58) Butcher, N. J., Tiang, J. and Minchin, R. F. (2008) Regulation of arylamine N-acetyltransferases. *Curr Drug Metab 9*, 498-504.
(59) Husain, A., Zhang, X., Doll, M. A., States, J. C., Barker, D. F. and Hein, D. W. (2007) Functional analysis of the human N-acetyltransferase 1 major promoter: quantitation of tissue expression and identification of critical sequence elements. *Drug Metab Dispos 35*, 1649-1656.
(60) Husain, A., Zhang, X., Doll, M. A., States, J. C., Barker, D. F. and Hein, D. W. (2007) Identification of N-acetyltransferase 2 (NAT2) transcription start sites and quantitation of NAT2-specific mRNA in human tissues. *Drug Metab Dispos 35*, 721-727.
(61) Upton, A., Johnson, N., Sandy, J. and Sim, E. (2001) Arylamine N-acetyltransferases - of mice, men and microorganisms. *Trends Pharmacol Sci 22*, 140-146.
(62) Minchin, R. F., Hanna, P. E., Dupret, J. M., Wagner, C. R., Rodrigues-Lima, F. and Butcher, N. J. (2007) Arylamine N-acetyltransferase I. *Int J Biochem Cell Biol 39*, 1999-2005.
(63) Wakefield, L., Robinson, J., Long, H., Ibbitt, J. C., Cooke, S., Hurst, H. C. and Sim, E. (2008) Arylamine N-acetyltransferase 1 expression in breast cancer cell lines: a potential marker in estrogen receptor-positive tumors. *Genes Chromosomes Cancer 47*, 118-126.

(64) Hein, D. W. (1988) Acetylator genotype and arylamine-induced carcinogenesis. *Biochim Biophys Acta 948*, 37-66.
(65) Lower, G. M., Jr., Nilsson, T., Nelson, C. E., Wolf, H., Gamsky, T. E. and Bryan, G. T. (1979) N-acetyltransferase phenotype and risk in urinary bladder cancer: approaches in molecular epidemiology. Preliminary results in Sweden and Denmark. *Environ Health Perspect 29*, 71-79.
(66) Morton, L. M., Bernstein, L., Wang, S. S., Hein, D. W., Rothman, N., Colt, J. S., Davis, S., Cerhan, J. R., Severson, R. K., Welch, R., Hartge, P. and Zahm, S. H. (2007) Hair dye use, genetic variation in N-acetyltransferase 1 (NAT1) and 2 (NAT2), and risk of non-Hodgkin lymphoma. *Carcinogenesis 28*, 1759-1764.
(67) Ambrosone, C. B., Kropp, S., Yang, J., Yao, S., Shields, P. G. and Chang-Claude, J. (2008) Cigarette smoking, N-acetyltransferase 2 genotypes, and breast cancer risk: pooled analysis and meta-analysis. *Cancer Epidemiol Biomarkers Prev 17*, 15-26.
(68) Sanderson, S., Salanti, G. and Higgins, J. (2007) Joint effects of the N-acetyltransferase 1 and 2 (NAT1 and NAT2) genes and smoking on bladder carcinogenesis: a literature-based systematic HuGE review and evidence synthesis. *Am J Epidemiol 166*, 741-751.
(69) Li, D., Jiao, L., Li, Y., Doll, M. A., Hein, D. W., Bondy, M. L., Evans, D. B., Wolff, R. A., Lenzi, R., Pisters, P. W., Abbruzzese, J. L. and Hassan, M. M. (2006) Polymorphisms of cytochrome P4501A2 and N-acetyltransferase genes, smoking, and risk of pancreatic cancer. *Carcinogenesis 27*, 103-111.
(70) Zienolddiny, S., Campa, D., Lind, H., Ryberg, D., Skaug, V., Stangeland, L. B., Canzian, F. and Haugen, A. (2008) A comprehensive analysis of phase I and phase II metabolism gene polymorphisms and risk of non-small cell lung cancer in smokers. *Carcinogenesis 29*, 1164-1169.
(71) Butcher, N. J., Arulpragasam, A. and Minchin, R. F. (2004) Proteasomal degradation of N-acetyltransferase 1 is prevented by acetylation of the active site cysteine: a mechanism for the slow acetylator phenotype and substrate-dependent down-regulation. *J Biol Chem 279*, 22131-22137.
(72) Liu, F., Zhang, N., Zhou, X., Hanna, P. E., Wagner, C. R., Koepp, D. M. and Walters, K. J. (2006) Arylamine N-acetyltransferase aggregation and constitutive ubiquitylation. *J Mol Biol 361*, 482-492.
(73) Walraven, J. M., Trent, J. O. and Hein, D. W. (2008) Structure-function analyses of single nucleotide polymorphisms in human N-acetyltransferase 1. *Drug Metab Rev 40*, 169-184.
(74) Walraven, J. M., Zang, Y., Trent, J. O. and Hein, D. W. (2008) Structure/Function evaluations of single nucleotide polymorphisms in human N-acetyltransferase 2. *Curr Drug Metab 9*, 471-486.
(75) Butcher, N. J., Ilett, K. F. and Minchin, R. F. (2000) Substrate-dependent regulation of human arylamine N-acetyltransferase-1 in cultured cells. *Mol Pharmacol 57*, 468-473.
(76) Butcher, N. J., Ilett, K. F. and Minchin, R. F. (2000) Inactivation of human arylamine N-acetyltransferase 1 by the hydroxylamine of p-aminobenzoic acid. *Biochem Pharmacol 60*, 1829-1836.
(77) Dairou, J., Atmane, N., Rodrigues-Lima, F. and Dupret, J. M. (2004) Peroxynitrite irreversibly inactivates the human xenobiotic-metabolizing enzyme arylamine N-acetyltransferase 1 (NAT1) in human breast cancer cells: a cellular and mechanistic study. *J Biol Chem 279*, 7708-7714.

(78) Dairou, J., Malecaze, F., Dupret, J. M. and Rodrigues-Lima, F. (2005) The xenobiotic-metabolizing enzymes arylamine N-acetyltransferases in human lens epithelial cells: inactivation by cellular oxidants and UVB-induced oxidative stress. *Mol Pharmacol 67*, 1299-1306.
(79) Ragunathan, N., Dairou, J., Pluvinage, B., Martins, M., Petit, E., Janel, N., Dupret, J. M. and Rodrigues-Lima, F. (2008) Identification of the xenobiotic-metabolizing enzyme arylamine N-acetyltransferase 1 as a new target of cisplatin in breast cancer cells: molecular and cellular mechanisms of inhibition. *Mol Pharmacol 73*, 1761-1768.
(80) Butcher, N. J., Tetlow, N. L., Cheung, C., Broadhurst, G. M. and Minchin, R. F. (2007) Induction of human arylamine N-acetyltransferase type I by androgens in human prostate cancer cells. *Cancer Res 67*, 85-92.
(81) Atmane, N., Dairou, J., Paul, A., Dupret, J. M. and Rodrigues-Lima, F. (2003) Redox regulation of the human xenobiotic metabolizing enzyme arylamine N-acetyltransferase 1 (NAT1). Reversible inactivation by hydrogen peroxide. *J Biol Chem 278*, 35086-35092.
(82) Lee, J. H., Chung, J. G., Lai, J. M., Levy, G. N. and Weber, W. W. (1997) Kinetics of arylamine N-acetyltransferase in tissues from human breast cancer. *Cancer Lett 111*, 39-50.
(83) Kawamura, A., Westwood, I., Wakefield, L., Long, H., Zhang, N., Walters, K., Redfield, C. and Sim, E. (2008) Mouse N-acetyltransferase type 2, the homologue of human N-acetyltransferase type 1. *Biochem Pharmacol 75*, 1550-1560.
(84) Smith, T. J. and Hanna, P. E. (1988) Hepatic N-acetyltransferases: selective inactivation in vivo by a carcinogenic N-arylhydroxamic acid. *Biochem Pharmacol 37*, 427-434.
(85) Wick, M. J. and Hanna, P. E. (1990) Bioactivation of N-arylhydroxamic acids by rat hepatic N-acetyltransferase. Detection of multiple enzyme forms by mechanism-based inactivation. *Biochem Pharmacol 39*, 991-1003.

Part I

(1) Josephy, P. D., and Mannervik, B. (2006) *Molecular Toxicology 2nd edition*, pp 426-447, Oxford University Press, New York.
(2) Grant, D. M., Blum, M., Beer, M. and Meyer, U. A. (1991) Monomorphic and polymorphic human arylamine N-acetyltransferases: a comparison of liver isozymes and expressed products of two cloned genes. *Mol Pharmacol 39*, 184-191.
(3) Glatt, H. and Meinl, W. (2004) Use of genetically manipulated Salmonella typhimurium strains to evaluate the role of sulfotransferases and acetyltransferases in nitrofen mutagenicity. *Carcinogenesis 25*, 779-786.
(4) Andres, H. H., Kolb, H. J., Schreiber, R. J. and Weiss, L. (1983) Characterization of the active site, substrate specificity and kinetic properties of acetyl-CoA:arylamine N-acetyltransferase from pigeon liver. *Biochim Biophys Acta 746*, 193-201.
(5) Andres, H. H., Vogel, R. S., Tarr, G. E., Johnson, L. and Weber, W. W. (1987) Purification, physicochemical, and kinetic properties of liver acetyl-CoA:arylamine N-acetyltransferase from rapid acetylator rabbits. *Mol Pharmacol 31*, 446-456.
(6) Ozawa, S., Abu-Zeid, M., Kawakubo, Y., Toyama, S., Yamazoe, Y. and Kato, R. (1990) Monomorphic and polymorphic isozymes of arylamine N-

acetyltransferases in hamster liver: purification of the isozymes and genetic basis of N-acetylation polymorphism. *Carcinogenesis 11*, 2137-2144.

(7) Cheon, H. G., Boteju, L. W. and Hanna, P. E. (1992) Affinity alkylation of hamster hepatic arylamine N-acetyltransferases: isolation of a modified cysteine residue. *Mol Pharmacol 42*, 82-93.

(8) Doll, M. A. and Hein, D. W. (1995) Cloning, sequencing and expression of NAT1 and NAT2 encoding genes from rapid and slow acetylator inbred rats. *Pharmacogenetics 5*, 247-251.

(9) Dupret, J. M. and Grant, D. M. (1992) Site-directed mutagenesis of recombinant human arylamine N-acetyltransferase expressed in Escherichia coli. Evidence for direct involvement of Cys68 in the catalytic mechanism of polymorphic human NAT2. *J Biol Chem 267*, 7381-7385.

(10) Minchin, R. F., Reeves, P. T., Teitel, C. H., McManus, M. E., Mojarrabi, B., Ilett, K. F. and Kadlubar, F. F. (1992) N-and O-acetylation of aromatic and heterocyclic amine carcinogens by human monomorphic and polymorphic acetyltransferases expressed in COS-1 cells. *Biochem Biophys Res Commun 185*, 839-844.

(11) Bergstrom, C. P., Wagner, C. R., Ann, D. K. and Hanna, P. E. (1995) Hamster monomorphic arylamine N-acetyltransferase: expression in Escherichia coli and purification. *Protein Expr Purif 6*, 45-55.

(12) Wagner, C. R., Bergstrom, C. P., Koning, K. R. and Hanna, P. E. (1996) Arylamine N-acetyltransferases. Expression in Escherichia coli, purification, and substrate specificities of recombinant hamster monomorphic and polymorphic isozymes. *Drug Metab Dispos 24*, 245-253.

(13) Sticha, K. R., Sieg, C. A., Bergstrom, C. P., Hanna, P. E. and Wagner, C. R. (1997) Overexpression and large-scale purification of recombinant hamster polymorphic arylamine N-acetyltransferase as a dihydrofolate reductase fusion protein. *Protein Expr Purif 10*, 141-153.

(14) Chou, T. F., Bieganowski, P., Shilinski, K., Cheng, J., Brenner, C. and Wagner, C. R. (2005) 31P NMR and genetic analysis establish hinT as the only Escherchia coli purine nucleoside phosphoramidase and as essential for growth under high salt conditions. *J Biol Chem 280*, 15356-15361.

(15) Ghosh, P., Cheng, J., Chou, T. F., Jia, Y., Avdulov, S., Bitterman, P. B., Polunovsky, V. A. and Wagner, C. R. (2008) Expression, purification and characterization of recombinant mouse translation initiation factor eIF4E as a dihydrofolate reductase (DHFR) fusion protein. *Protein Expr Purif 60*, 132-139.

(16) Wang, H., Vath, G. M., Kawamura, A., Bates, C. A., Sim, E., Hanna, P. E. and Wagner, C. R. (2005) Over-expression, purification, and characterization of recombinant human arylamine N-acetyltransferase 1. *Protein J 24*, 65-77.

(17) Bradford, M. M. (1976) A rapid and sensitive method for the quantitation of microgram quantities of protein utilizing the principle of protein-dye binding. *Anal Biochem 72*, 248-254.

(18) Ghosh, S. and Lowenstein, J. M. (1996) A multifunctional vector system for heterologous expression of proteins in Escherichia coli. Expression of native and hexahistidyl fusion proteins, rapid purification of the fusion proteins, and removal of fusion peptide by Kex2 protease. *Gene 176*, 249-255.

(19) de Boer, H. A., Comstock, L. J. and Vasser, M. (1983) The tac promoter: a functional hybrid derived from the trp and lac promoters. *Proc Natl Acad Sci U S A 80*, 21-25.

(20) Sticha, K. R., Bergstrom, C. P., Wagner, C. R. and Hanna, P. E. (1998) Characterization of hamster recombinant monomorphic and polymorphic arylamine N-acetyltransferases: bioactivation and mechanism-based inactivation studies with N-hydroxy-2-acetylaminofluorene. *Biochem Pharmacol 56*, 47-59.
(21) Wang, H., Wagner, C. R. and Hanna, P. E. (2005) Irreversible inactivation of arylamine N-acetyltransferases in the presence of N-hydroxy-4-acetylaminobiphenyl: a comparison of human and hamster enzymes. *Chem Res Toxicol 18*, 183-197.
(22) Takasuga, A., Banba, K., Yoshino, K., Izutsu, H., Iwakura, M. and Ohashi, S. (1992) Efficient production of a small peptide by expression as a multimeric form fused with the dihydrofolate reductase affinity handle. *J Biochem 112*, 652-657.
(23) Blakley, R. L. Dihydrofolate reductase, in: R.L. Blakley, S.J. Benkovic (Eds.), Folates and Pterins, Wiley, New York, 1984, pp. 191-253.
(24) Liu, L., Von Vett, A., Zhang, N., Walters, K. J., Wagner, C. R. and Hanna, P. E. (2007) Arylamine N-acetyltransferases: characterization of the substrate specificities and molecular interactions of environmental arylamines with human NAT1 and NAT2. *Chem Res Toxicol 20*, 1300-1308.

Part II

(1) Vineis, P. and Pirastu, R. (1997) Aromatic amines and cancer. *Cancer Causes Control 8*, 346-355.
(2) Talaska, G. (2003) Aromatic amines and human urinary bladder cancer: exposure sources and epidemiology. *J Environ Sci Health C Environ Carcinog Ecotoxicol Rev 21*, 29-43.
(3) Turesky, R. J., Freeman, J. P., Holland, R. D., Nestorick, D. M., Miller, D. W., Ratnasinghe, D. L. and Kadlubar, F. F. (2003) Identification of aminobiphenyl derivatives in commercial hair dyes. *Chem Res Toxicol 16*, 1162-1173.
(4) Gan, J., Skipper, P. L., Gago-Dominguez, M., Arakawa, K., Ross, R. K., Yu, M. C. and Tannenbaum, S. R. (2004) Alkylaniline-hemoglobin adducts and risk of non-smoking-related bladder cancer. *J Natl Cancer Inst 96*, 1425-1431.
(5) Yu, M. C., Skipper, P. L., Tannenbaum, S. R., Chan, K. K. and Ross, R. K. (2002) Arylamine exposures and bladder cancer risk. *Mutat Res 506-507*, 21-28.
(6) Gaber, K., Harreus, U. A., Matthias, C., Kleinsasser, N. H. and Richter, E. (2007) Hemoglobin adducts of the human bladder carcinogen o-toluidine after treatment with the local anesthetic prilocaine. *Toxicology 229*, 157-164.
(7) Gorlewska-Roberts, K., Green, B., Fares, M., Ambrosone, C. B. and Kadlubar, F. F. (2002) Carcinogen-DNA adducts in human breast epithelial cells. *Environ Mol Mutagen 39*, 184-192.
(8) Gago-Dominguez, M., Bell, D. A., Watson, M. A., Yuan, J. M., Castelao, J. E., Hein, D. W., Chan, K. K., Coetzee, G. A., Ross, R. K. and Yu, M. C. (2003) Permanent hair dyes and bladder cancer: risk modification by cytochrome P4501A2 and N-acetyltransferases 1 and 2. *Carcinogenesis 24*, 483-489.
(9) Skipper, P. L., Trudel, L. J., Kensler, T. W., Groopman, J. D., Egner, P. A., Liberman, R. G., Wogan, G. N. and Tannenbaum, S. R. (2006) DNA adduct formation by 2,6-dimethyl-, 3,5-dimethyl-, and 3-ethylaniline in vivo in mice. *Chem Res Toxicol 19*, 1086-1090.

(10) Hanna, P. E. (1996) Metabolic activation and detoxification of arylamines. *Curr. Med. Chem. 3*, 195-210.
(11) Hanna, P. E. (1994) N-acetyltransferases, O-acetyltransferases, and N,O-acetyltransferases: enzymology and bioactivation. *Adv Pharmacol 27*, 401-430.
(12) Grant, D. M., Blum, M., Beer, M. and Meyer, U. A. (1991) Monomorphic and polymorphic human arylamine N-acetyltransferases: a comparison of liver isozymes and expressed products of two cloned genes. *Mol Pharmacol 39*, 184-191.
(13) Hickman, D., Palamanda, J. R., Unadkat, J. D. and Sim, E. (1995) Enzyme kinetic properties of human recombinant arylamine N-acetyltransferase 2 allotypic variants expressed in Escherichia coli. *Biochem Pharmacol 50*, 697-703.
(14) Kawamura, A., Graham, J., Mushtaq, A., Tsiftsoglou, S. A., Vath, G. M., Hanna, P. E., Wagner, C. R. and Sim, E. (2005) Eukaryotic arylamine N-acetyltransferase. Investigation of substrate specificity by high-throughput screening. *Biochem Pharmacol 69*, 347-359.
(15) Wang, H., Vath, G. M., Kawamura, A., Bates, C. A., Sim, E., Hanna, P. E. and Wagner, C. R. (2005) Over-expression, purification, and characterization of recombinant human arylamine N-acetyltransferase 1. *Protein J 24*, 65-77.
(16) Bradford, M. M. (1976) A rapid and sensitive method for the quantitation of microgram quantities of protein utilizing the principle of protein-dye binding. *Anal Biochem 72*, 248-254.
(17) *NIH Guidelines for the Laboratory Use of Chemical Carcinogens* (1981) NIH Publication No. 81-2385, U.S. Government Printing Office, Washington, DC.
(18) Zhang, N., Liu, L., Liu, F., Wagner, C. R., Hanna, P. E. and Walters, K. J. (2006) NMR-based model reveals the structural determinants of mammalian arylamine N-acetyltransferase substrate specificity. *J Mol Biol 363*, 188-200.
(19) Wallace, A. C., Laskowski, R. A. and Thornton, J. M. (1995) LIGPLOT: a program to generate schematic diagrams of protein-ligand interactions. *Protein Eng 8*, 127-134.
(20) Segel, I. H. (1975) Enzyme kinetics: behavior and analysis of rapid equilibrium and steady-state enzyme systems. *pp. 606-612*.
(21) Hein, D. W., Doll, M. A., Rustan, T. D., Gray, K., Feng, Y., Ferguson, R. J. and Grant, D. M. (1993) Metabolic activation and deactivation of arylamine carcinogens by recombinant human NAT1 and polymorphic NAT2 acetyltransferases. *Carcinogenesis 14*, 1633-1638.
(22) Liu, L., Von Vett, A., Zhang, N., Walters, K. J., Wagner, C. R. and Hanna, P. E. (2007) Arylamine N-acetyltransferases: characterization of the substrate specificities and molecular interactions of environmental arylamines with human NAT1 and NAT2. *Chem Res Toxicol 20*, 1300-1308.
(23) Wu, H., Dombrovsky, L., Tempel, W., Martin, F., Loppnau, P., Goodfellow, G. H., Grant, D. M. and Plotnikov, A. N. (2007) Structural basis of substrate-binding specificity of human arylamine N-acetyltransferases. *J Biol Chem 282*, 30189-30197.
(24) U. S. National Toxicology Program (1990) *Toxicology and Carcinogenesis Studies of 2,6-Xylidine (2,6-Dimethylaniline) (CAS No. 87-62-7) in Charles River CD Rats (Feed Studies).* Technical Report Series No. 278, NTP, Research Triangle Park, NC.

(25) Muenzen, J. B., Cerecedo, L. R., and Sherwin, C. P. (1926) Comparative Metabolism of Certain Aromatic Acids. VIII Acetylation of Amino Compounds. *Journal of Biological Chemistry 67*, 469-476.
(26) Jennne, J. W. (1965) Partial purification and properties of the isoniazid transacetylase in human liver. Its relationship to the acetylation of p-aminosalicylic acid. *J Clin Invest 44*, 1992-2002.
(27) Goodfellow, G. H., Dupret, J. M. and Grant, D. M. (2000) Identification of amino acids imparting acceptor substrate selectivity to human arylamine acetyltransferases NAT1 and NAT2. *Biochem J 348 Pt 1*, 159-166.
(28) Sugamori, K. S., Brenneman, D. and Grant, D. M. (2006) In vivo and in vitro metabolism of arylamine procarcinogens in acetyltransferase-deficient mice. *Drug Metab Dispos 34*, 1697-1702.

Part III

(1) Kim, D. and Guengerich, F. P. (2005) Cytochrome P450 activation of arylamines and heterocyclic amines. *Annu Rev Pharmacol Toxicol 45*, 27-49.
(2) Hanna, P. E. (1996) Metabolic activation and detoxification of arylamines. *Curr. Med. Chem. 3*, 195-210.
(3) Beije, B. and Moller, L. (1988) 2-Nitrofluorene and related compounds: prevalence and biological effects. *Mutat Res 196*, 177-209.
(4) Zwirner-Baier, I. and Neumann, H. G. (1999) Polycyclic nitroarenes (nitro-PAHs) as biomarkers of exposure to diesel exhaust. *Mutat Res 441*, 135-144.
(5) Boelsterli, U. A., Ho, H. K., Zhou, S. and Leow, K. Y. (2006) Bioactivation and hepatotoxicity of nitroaromatic drugs. *Curr Drug Metab 7*, 715-727.
(6) Neumann, H. G. (2007) Aromatic amines in experimental cancer research: tissue-specific effects, an old problem and new solutions. *Crit Rev Toxicol 37*, 211-236.
(7) Mulder, G. J., Unruh, L. E., Evans, F. E., Ketterer, B. and Kadlubar, F. F. (1982) Formation and identification of glutathione conjugates from 2-nitrosofluorene and N-hydroxy-2-aminofluorene. *Chem Biol Interact 39*, 111-127.
(8) Eyer, P. (1994) Reactions of oxidatively activated arylamines with thiols: reaction mechanisms and biologic implications. An overview. *Environ Health Perspect 102 Suppl 6*, 123-132.
(9) Kazanis, S., and Mc Clelland, R. A. (1992) Electrophilic intermediate in the reaction of glutathione and nitrosoarenes. *J. Am. Chem. Soc. 114*, 3052-3059.
(10) Guo, Z., Wagner, C. R. and Hanna, P. E. (2004) Mass spectrometric investigation of the mechanism of inactivation of hamster arylamine N-acetyltransferase 1 by N-hydroxy-2-acetylaminofluorene. *Chem Res Toxicol 17*, 275-286.
(11) Wang, H., Wagner, C. R. and Hanna, P. E. (2005) Irreversible inactivation of arylamine N-acetyltransferases in the presence of N-hydroxy-4-acetylaminobiphenyl: a comparison of human and hamster enzymes. *Chem Res Toxicol 18*, 183-197.
(12) Liu, L., Von Vett, A., Zhang, N., Walters, K. J., Wagner, C. R. and Hanna, P. E. (2007) Arylamine N-acetyltransferases: characterization of the substrate specificities and molecular interactions of environmental arylamines with human NAT1 and NAT2. *Chem Res Toxicol 20*, 1300-1308.

(13) Wang, H., Vath, G. M., Kawamura, A., Bates, C. A., Sim, E., Hanna, P. E. and Wagner, C. R. (2005) Over-expression, purification, and characterization of recombinant human arylamine N-acetyltransferase 1. *Protein J 24*, 65-77.
(14) Mangold, B. L. and Hanna, P. E. (1982) Arylhydroxamic acid N,O-acyltransferase substrates. Acetyl transfer and electrophile generating activity of N-hydroxy-N-(4-alkyl-, 4-alkenyl-, and 4-cyclohexylphenyl)acetamides. *J Med Chem 25*, 630-638.
(15) Westra, J. G. (1981) A rapid and simple synthesis of reactive metabolites of carcinogenic aromatic amines in high yield. *Carcinogenesis 2*, 355-357.
(16) Stanley, L. A., Coroneos, E., Cuff, R., Hickman, D., Ward, A. and Sim, E. (1996) Immunochemical detection of arylamine N-acetyltransferase in normal and neoplastic bladder. *J Histochem Cytochem 44*, 1059-1067.
(17) Bradford, M. M. (1976) A rapid and sensitive method for the quantitation of microgram quantities of protein utilizing the principle of protein-dye binding. *Anal Biochem 72*, 248-254.
(18) *NIH Guidelines for the Laboratory Use of Chemical Carcinogens* (1981) NIH Publication No. 81-2385, U.S. Government Printing Office, Washington, DC.
(19) Sinclair, J. C., Delgoda, R., Noble. M. E., Jarmin, S., Goh, N. K., and Sim, E. (1998) Purification, characterization, and crystallization of an N-hydroxyarylamine O-acetyltransferase from Salmonella typhimurium. *Protein Expression Purif. 12*, 371-380.
(20) McAlister, L. and Holland, M. J. (1985) Differential expression of the three yeast glyceraldehyde-3-phosphate dehydrogenase genes. *J Biol Chem 260*, 15019-15027.
(21) Cohen, M. B. and Duvel, D. L. (1988) Characterization of the inhibition of glutathione reductase and the recovery of enzyme activity in exponentially growing murine leukemia (L1210) cells treated with 1,3-bis(2-chloroethyl)-1-nitrosourea. *Biochem Pharmacol 37*, 3317-3320.
(22) Goswami, P. C., Sheren, J., Albee, L. D., Parsian, A., Sim, J. E., Ridnour, L. A., Higashikubo, R., Gius, D., Hunt, C. R. and Spitz, D. R. (2000) Cell cycle-coupled variation in topoisomerase IIalpha mRNA is regulated by the 3'-untranslated region. Possible role of redox-sensitive protein binding in mRNA accumulation. *J Biol Chem 275*, 38384-38392.
(23) Liu, F., Zhang, N., Zhou, X., Hanna, P. E., Wagner, C. R., Koepp, D. M. and Walters, K. J. (2006) Arylamine N-acetyltransferase aggregation and constitutive ubiquitylation. *J Mol Biol 361*, 482-492.
(24) Liu, L., Wagner, C. R. and Hanna, P. E. (2008) Human arylamine N-acetyltransferase 1: in vitro and intracellular inactivation by nitrosoarene metabolites of toxic and carcinogenic arylamines. *Chem Res Toxicol 21*, 2005-2016.
(25) Levy, H. M., Leber, P. D. and Ryan, E. M. (1963) Inactivation of Myosin by 2,4-Dinitrophenol and Protection by Adenosine Triphosphate and Other Phosphate Compounds. *J Biol Chem 238*, 3654-3659.
(26) Eyer, P. (1979) Reactions of nitrosobenzene with reduced glutathione. *Chem Biol Interact 24*, 227-239.
(27) Dolle, B., Topner, W. and Neumann, H. G. (1980) Reaction of arylnitroso compounds with mercaptans. *Xenobiotica 10*, 527-536.
(28) Butcher, N. J., Tetlow, N. L., Cheung, C., Broadhurst, G. M. and Minchin, R. F. (2007) Induction of human arylamine N-acetyltransferase type I by androgens in human prostate cancer cells. *Cancer Res 67*, 85-92.

(29) Grant, D. M., Lottspeich, F. and Meyer, U. A. (1989) Evidence for two closely related isozymes of arylamine N-acetyltransferase in human liver. *FEBS Lett 244*, 203-207.
(30) Wakefield, L., Robinson, J., Long, H., Ibbitt, J. C., Cooke, S., Hurst, H. C. and Sim, E. (2008) Arylamine N-acetyltransferase 1 expression in breast cancer cell lines: a potential marker in estrogen receptor-positive tumors. *Genes Chromosomes Cancer 47*, 118-126.
(31) Dietze, E. C., Schafer, A., Omichinski, J. G. and Nelson, S. D. (1997) Inactivation of glyceraldehyde-3-phosphate dehydrogenase by a reactive metabolite of acetaminophen and mass spectral characterization of an arylated active site peptide. *Chem Res Toxicol 10*, 1097-1103.
(32) Dennehy, M. K., Richards, K. A., Wernke, G. R., Shyr, Y. and Liebler, D. C. (2006) Cytosolic and nuclear protein targets of thiol-reactive electrophiles. *Chem Res Toxicol 19*, 20-29.
(33) Babson, J. R. and Reed, D. J. (1978) Inactivation of glutathione reductase by 2-chloroethyl nitrosourea-derived isocyanates. *Biochem Biophys Res Commun 83*, 754-762.
(34) Nakano, M., Funayama, S., de Oliveira, M. B., Bruel, S. L. and Gomes, E. M. (1992) D-glyceraldehyde-3-phosphate dehydrogenase from HeLa cells--1. Purification and properties of the enzyme. *Comp Biochem Physiol B 102*, 873-877.
(35) Cotariu, D., Evans, S., Lahat, E., Theitler, J., Bistritzer, T. and Zaidman, J. L. (1992) Inhibition of human red blood cell glutathione reductase by valproic acid. *Biochem Pharmacol 43*, 425-429.
(36) Pai, E. F. and Schulz, G. E. (1983) The catalytic mechanism of glutathione reductase as derived from x-ray diffraction analyses of reaction intermediates. *J Biol Chem 258*, 1752-1757.
(37) Butcher, N. J., Ilett, K. F. and Minchin, R. F. (2000) Inactivation of human arylamine N-acetyltransferase 1 by the hydroxylamine of p-aminobenzoic acid. *Biochem Pharmacol 60*, 1829-1836.
(38) Lotlikar, P. D., Miller, E. C., Miller, J. A. and Margreth, A. (1965) The enzymatic reduction of the N-hydroxy derivatives of 2-acetylaminofluorene and related carcinogens by tissue preparations. *Cancer Res 25*, 1743-1752.
(39) Hao, X. Y., Widersten, M., Ridderstrom, M., Hellman, U. and Mannervik, B. (1994) Co-variation of glutathione transferase expression and cytostatic drug resistance in HeLa cells: establishment of class Mu glutathione transferase M3-3 as the dominating isoenzyme. *Biochem J 297 (Pt 1)*, 59-67.
(40) Lu, S. C., Sun, W. M., Yi, J., Ookhtens, M., Sze, G. and Kaplowitz, N. (1996) Role of two recently cloned rat liver GSH transporters in the ubiquitous transport of GSH in mammalian cells. *J Clin Invest 97*, 1488-1496.
(41) Boukouvala, S., Westwood, I. M., Butcher, N. J. and Fakis, G. (2008) Current trends in N-acetyltransferase research arising from the 2007 International NAT Workshop. *Pharmacogenomics 9*, 765-771.
(42) Hanna, P. E., Banks, R. B. and Marhevka, V. C. (1982) Suicide inactivation of hamster hepatic arylhydroxamic acid N,O-acyltransferase. A selective probe of N-acetyltransferase multiplicity. *Mol Pharmacol 21*, 159-165.
(43) Wick, M. J. and Hanna, P. E. (1990) Bioactivation of N-arylhydroxamic acids by rat hepatic N-acetyltransferase. Detection of multiple enzyme forms by mechanism-based inactivation. *Biochem Pharmacol 39*, 991-1003.

(44) Sticha, K. R., Bergstrom, C. P., Wagner, C. R. and Hanna, P. E. (1998) Characterization of hamster recombinant monomorphic and polymorphic arylamine N-acetyltransferases: bioactivation and mechanism-based inactivation studies with N-hydroxy-2-acetylaminofluorene. *Biochem Pharmacol 56*, 47-59.
(45) Smith, T. J. and Hanna, P. E. (1988) Hepatic N-acetyltransferases: selective inactivation in vivo by a carcinogenic N-arylhydroxamic acid. *Biochem Pharmacol 37*, 427-434.
(46) King, R. S. and Duffel, M. W. (1997) Oxidation-dependent inactivation of aryl sulfotransferase IV by primary N-hydroxy arylamines during in vitro assays. *Carcinogenesis 18*, 843-849.
(47) Dairou, J., Atmane, N., Rodrigues-Lima, F. and Dupret, J. M. (2004) Peroxynitrite irreversibly inactivates the human xenobiotic-metabolizing enzyme arylamine N-acetyltransferase 1 (NAT1) in human breast cancer cells: a cellular and mechanistic study. *J Biol Chem 279*, 7708-7714.
(48) Atmane, N., Dairou, J., Paul, A., Dupret, J. M. and Rodrigues-Lima, F. (2003) Redox regulation of the human xenobiotic metabolizing enzyme arylamine N-acetyltransferase 1 (NAT1). Reversible inactivation by hydrogen peroxide. *J Biol Chem 278*, 35086-35092.
(49) Ragunathan, N., Dairou, J., Pluvinage, B., Martins, M., Petit, E., Janel, N., Dupret, J. M. and Rodrigues-Lima, F. (2008) Identification of the xenobiotic-metabolizing enzyme arylamine N-acetyltransferase 1 as a new target of cisplatin in breast cancer cells: molecular and cellular mechanisms of inhibition. *Mol Pharmacol 73*, 1761-1768.
(50) Zhang, N., Liu, L., Liu, F., Wagner, C. R., Hanna, P. E. and Walters, K. J. (2006) NMR-based model reveals the structural determinants of mammalian arylamine N-acetyltransferase substrate specificity. *J Mol Biol 363*, 188-200.
(51) Wu, H., Dombrovsky, L., Tempel, W., Martin, F., Loppnau, P., Goodfellow, G. H., Grant, D. M. and Plotnikov, A. N. (2007) Structural basis of substrate-binding specificity of human arylamine N-acetyltransferases. *J Biol Chem 282*, 30189-30197.
(52) Wang, H., Vath, G. M., Gleason, K. J., Hanna, P. E. and Wagner, C. R. (2004) Probing the mechanism of hamster arylamine N-acetyltransferase 2 acetylation by active site modification, site-directed mutagenesis, and pre-steady state and steady state kinetic studies. *Biochemistry 43*, 8234-8246.
(53) Richardson, A. L., Wang, Z. C., De Nicolo, A., Lu, X., Brown, M., Miron, A., Liao, X., Iglehart, J. D., Livingston, D. M. and Ganesan, S. (2006) X chromosomal abnormalities in basal-like human breast cancer. *Cancer Cell 9*, 121-132.
(54) Miller, L. D., Smeds, J., George, J., Vega, V. B., Vergara, L., Ploner, A., Pawitan, Y., Hall, P., Klaar, S., Liu, E. T. and Bergh, J. (2005) An expression signature for p53 status in human breast cancer predicts mutation status, transcriptional effects, and patient survival. *Proc Natl Acad Sci U S A 102*, 13550-13555.
(55) Gruvberger, S., Ringner, M., Chen, Y., Panavally, S., Saal, L. H., Borg, A., Ferno, M., Peterson, C. and Meltzer, P. S. (2001) Estrogen receptor status in breast cancer is associated with remarkably distinct gene expression patterns. *Cancer Res 61*, 5979-5984.

(56) Hosler, M. R., Wang-Su, S. T. and Wagner, B. J. (2003) Targeted disruption of specific steps of the ubiquitin-proteasome pathway by oxidation in lens epithelial cells. *Int J Biochem Cell Biol 35*, 685-697.
(57) Paron, I., D'Elia, A., D'Ambrosio, C., Scaloni, A., D'Aurizio, F., Prescott, A., Damante, G. and Tell, G. (2004) A proteomic approach to identify early molecular targets of oxidative stress in human epithelial lens cells. *Biochem J 378*, 929-937.

Part IV

(1) Hanna, P. E. (1994) N-acetyltransferases, O-acetyltransferases, and N,O-acetyltransferases: enzymology and bioactivation. *Adv Pharmacol 27*, 401-430.
(2) Hanna, P. E. (1996) Metabolic activation and detoxification of arylamines. *Curr. Med. Chem. 3*, 195-210.
(3) Ohsako, S. and Deguchi, T. (1990) Cloning and expression of cDNAs for polymorphic and monomorphic arylamine N-acetyltransferases from human liver. *J Biol Chem 265*, 4630-4634.
(4) Hein, D. W. (2002) Molecular genetics and function of NAT1 and NAT2: role in aromatic amine metabolism and carcinogenesis. *Mutat Res 506-507*, 65-77.
(5) Walraven, J. M., Zang, Y., Trent, J. O. and Hein, D. W. (2008) Structure/Function evaluations of single nucleotide polymorphisms in human N-acetyltransferase 2. *Curr Drug Metab 9*, 471-486.
(6) Walraven, J. M., Trent, J. O. and Hein, D. W. (2008) Structure-function analyses of single nucleotide polymorphisms in human N-acetyltransferase 1. *Drug Metab Rev 40*, 169-184.
(7) Agundez, J. A. (2008) Polymorphisms of human N-acetyltransferases and cancer risk. *Curr Drug Metab 9*, 520-531.
(8) Hein, D. W. (2006) N-acetyltransferase 2 genetic polymorphism: effects of carcinogen and haplotype on urinary bladder cancer risk. *Oncogene 25*, 1649-1658.
(9) Risch, A., Wallace, D. M., Bathers, S. and Sim, E. (1995) Slow N-acetylation genotype is a susceptibility factor in occupational and smoking related bladder cancer. *Hum Mol Genet 4*, 231-236.
(10) Garcia-Closas, M., Malats, N., Silverman, D., Dosemeci, M., Kogevinas, M., Hein, D. W., Tardon, A., Serra, C., Carrato, A., Garcia-Closas, R., Lloreta, J., Castano-Vinyals, G., Yeager, M., Welch, R., Chanock, S., Chatterjee, N., Wacholder, S., Samanic, C., Tora, M., Fernandez, F., Real, F. X. and Rothman, N. (2005) NAT2 slow acetylation, GSTM1 null genotype, and risk of bladder cancer: results from the Spanish Bladder Cancer Study and meta-analyses. *Lancet 366*, 649-659.
(11) Lubin, J. H., Kogevinas, M., Silverman, D., Malats, N., Garcia-Closas, M., Tardon, A., Hein, D. W., Garcia-Closas, R., Serra, C., Dosemeci, M., Carrato, A. and Rothman, N. (2007) Evidence for an intensity-dependent interaction of NAT2 acetylation genotype and cigarette smoking in the Spanish Bladder Cancer Study. *Int J Epidemiol 36*, 236-241.
(12) Gu, J., Liang, D., Wang, Y., Lu, C. and Wu, X. (2005) Effects of N-acetyl transferase 1 and 2 polymorphisms on bladder cancer risk in Caucasians. *Mutat Res 581*, 97-104.
(13) Liu, L., Wagner, C. R. and Hanna, P. E. (2008) Human arylamine N-acetyltransferase 1: in vitro and intracellular inactivation by nitrosoarene

metabolites of toxic and carcinogenic arylamines. *Chem Res Toxicol 21*, 2005-2016.
(14) Liu, L., Von Vett, A., Zhang, N., Walters, K. J., Wagner, C. R. and Hanna, P. E. (2007) Arylamine N-acetyltransferases: characterization of the substrate specificities and molecular interactions of environmental arylamines with human NAT1 and NAT2. *Chem Res Toxicol 20*, 1300-1308.
(15) Wang, H., Wagner, C. R. and Hanna, P. E. (2005) Irreversible inactivation of arylamine N-acetyltransferases in the presence of N-hydroxy-4-acetylaminobiphenyl: a comparison of human and hamster enzymes. *Chem Res Toxicol 18*, 183-197.
(16) Liu, L., Wagner, C. R., and Hanna, P. E. (2008) Human Arylamine N-Acetyltransferase 1: In Vitro and Intracellular Inactivation by Nitrosoarene Metabolites of Toxic and Carcinogenic Arylamines. *Chem. Res. Toxicol.*
(17) Kitz, R. and Wilson, I. B. (1962) Esters of methanesulfonic acid as irreversible inhibitors of acetylcholinesterase. *J Biol Chem 237*, 3245-3249.
(18) Levy, H. M., Leber, P. D. and Ryan, E. M. (1963) Inactivation of Myosin by 2,4-Dinitrophenol and Protection by Adenosine Triphosphate and Other Phosphate Compounds. *J Biol Chem 238*, 3654-3659.
(19) Mulder, G. J., Unruh, L. E., Evans, F. E., Ketterer, B. and Kadlubar, F. F. (1982) Formation and identification of glutathione conjugates from 2-nitrosofluorene and N-hydroxy-2-aminofluorene. *Chem Biol Interact 39*, 111-127.
(20) Eyer, P. (1994) Reactions of oxidatively activated arylamines with thiols: reaction mechanisms and biologic implications. An overview. *Environ Health Perspect 102 Suppl 6*, 123-132.
(21) Eyer, P. (1979) Reactions of nitrosobenzene with reduced glutathione. *Chem Biol Interact 24*, 227-239.
(22) Dolle, B., Topner, W. and Neumann, H. G. (1980) Reaction of arylnitroso compounds with mercaptans. *Xenobiotica 10*, 527-536.
(23) Stanley, L. A., Coroneos, E., Cuff, R., Hickman, D., Ward, A. and Sim, E. (1996) Immunochemical detection of arylamine N-acetyltransferase in normal and neoplastic bladder. *J Histochem Cytochem 44*, 1059-1067.
(24) Grant, D. M., Lottspeich, F. and Meyer, U. A. (1989) Evidence for two closely related isozymes of arylamine N-acetyltransferase in human liver. *FEBS Lett 244*, 203-207.
(25) Ragunathan, N., Dairou, J., Pluvinage, B., Martins, M., Petit, E., Janel, N., Dupret, J. M. and Rodrigues-Lima, F. (2008) Identification of the xenobiotic-metabolizing enzyme arylamine N-acetyltransferase 1 as a new target of cisplatin in breast cancer cells: molecular and cellular mechanisms of inhibition. *Mol Pharmacol 73*, 1761-1768.
(26) Butcher, N. J., Ilett, K. F. and Minchin, R. F. (2000) Inactivation of human arylamine N-acetyltransferase 1 by the hydroxylamine of p-aminobenzoic acid. *Biochem Pharmacol 60*, 1829-1836.
(27) Upton, A., Johnson, N., Sandy, J. and Sim, E. (2001) Arylamine N-acetyltransferases - of mice, men and microorganisms. *Trends Pharmacol Sci 22*, 140-146.
(28) Minchin, R. F., Hanna, P. E., Dupret, J. M., Wagner, C. R., Rodrigues-Lima, F. and Butcher, N. J. (2007) Arylamine N-acetyltransferase I. *Int J Biochem Cell Biol 39*, 1999-2005.

(29) Husain, A., Zhang, X., Doll, M. A., States, J. C., Barker, D. F. and Hein, D. W. (2007) Functional analysis of the human N-acetyltransferase 1 major promoter: quantitation of tissue expression and identification of critical sequence elements. *Drug Metab Dispos 35*, 1649-1656.
(30) Husain, A., Zhang, X., Doll, M. A., States, J. C., Barker, D. F. and Hein, D. W. (2007) Identification of N-acetyltransferase 2 (NAT2) transcription start sites and quantitation of NAT2-specific mRNA in human tissues. *Drug Metab Dispos 35*, 721-727.
(31) Loehle, J. A., Cornish, V., Wakefield, L., Doll, M. A., Neale, J. R., Zang, Y., Sim, E. and Hein, D. W. (2006) N-acetyltransferase (Nat) 1 and 2 expression in Nat2 knockout mice. *J Pharmacol Exp Ther 319*, 724-728.
(32) Dairou, J., Dupret, J. M. and Rodrigues-Lima, F. (2005) Impairment of the activity of the xenobiotic-metabolizing enzymes arylamine N-acetyltransferases 1 and 2 (NAT1/NAT2) by peroxynitrite in mouse skeletal muscle cells. *FEBS Lett 579*, 4719-4723.
(33) Dairou, J., Malecaze, F., Dupret, J. M. and Rodrigues-Lima, F. (2005) The xenobiotic-metabolizing enzymes arylamine N-acetyltransferases in human lens epithelial cells: inactivation by cellular oxidants and UVB-induced oxidative stress. *Mol Pharmacol 67*, 1299-1306.
(34) Hao, X. Y., Widersten, M., Ridderstrom, M., Hellman, U. and Mannervik, B. (1994) Co-variation of glutathione transferase expression and cytostatic drug resistance in HeLa cells: establishment of class Mu glutathione transferase M3-3 as the dominating isoenzyme. *Biochem J 297 (Pt 1)*, 59-67.
(35) Warholm, M., Guthenberg, C., Mannervik, B., von Bahr, C. and Glaumann, H. (1980) Identification of a new glutathione S-transferase in human liver. *Acta Chem Scand B 34*, 607-621.
(36) Tsuchida, S. and Sato, K. (1992) Glutathione transferases and cancer. *Crit Rev Biochem Mol Biol 27*, 337-384.
(37) Lower, G. M., Jr., Nilsson, T., Nelson, C. E., Wolf, H., Gamsky, T. E. and Bryan, G. T. (1979) N-acetyltransferase phenotype and risk in urinary bladder cancer: approaches in molecular epidemiology. Preliminary results in Sweden and Denmark. *Environ Health Perspect 29*, 71-79.
(38) Hein, D. W. (1988) Acetylator genotype and arylamine-induced carcinogenesis. *Biochim Biophys Acta 948*, 37-66.

Part V

(1) Chiang, T. A., Pei-Fen, W., Ying, L. S., Wang, L. F. and Ko, Y. C. (1999) Mutagenicity and aromatic amine content of fumes from heated cooking oils produced in Taiwan. *Food Chem Toxicol 37*, 125-134.
(2) Stabbert, R., Schafer, K. H., Biefel, C. and Rustemeier, K. (2003) Analysis of aromatic amines in cigarette smoke. *Rapid Commun Mass Spectrom 17*, 2125-2132.
(3) Cramer, J. W., Miller, J. A. and Miller, E. C. (1960) N-Hydroxylation: A new metabolic reaction observed in the rat with the carcinogen 2-acetylaminofluorene. *J Biol Chem 235*, 885-888.
(4) Miller, J. A., Wyatt, C. S., Miller, E. C., and Hartmann, H. A. (1961) The N-hydroxylation of 4-acetylaminobiphenyl by the rat and dog and the strong carcinogenicity of N-hydroxy-4-acetylaminobiphenyl in the rat. *Cancer Res. 21*, 1465-1473.

(5) Enomoto, M., Lotlikhar, P., Miller, J. A., and Miller, E. C. (1962) Urinary metabolites of 2-acetylaminofluorene and related compounds in the rhesus monkey. *Cancer Res. 22*, 1336-1342.
(6) Weisburger, J. H., Grantham, P. H., Vanhorn, E., Steigbigel, N. H., Rall, D. P. and Weisburger, E. K. (1964) Activation And Detoxification Of N-2-Fluorenylacetamide In Man. *Cancer Res 24*, 475-479.
(7) Veronese, M. E., McLean, S., D'Souza, C. A. and Davies, N. W. (1985) Formation of reactive metabolites of phenacetin in humans and rats. *Xenobiotica 15*, 929-940.
(8) Moller, L., Rafter, J. and Gustafsson, J. A. (1987) Metabolism of the carcinogenic air pollutant 2-nitrofluorene in the rat. *Carcinogenesis 8*, 637-645.
(9) Weisburger, J. H. and Weisburger, E. K. (1973) Biochemical formation and pharmacological, toxicological, and pathological properties of hydroxylamines and hydroxamic acids. *Pharmacol Rev 25*, 1-66.
(10) Hanna, P. E. (1996) Metabolic activation and detoxification of arylamines. *Curr. Med. Chem. 3*, 195-210.
(11) Kim, D. and Guengerich, F. P. (2005) Cytochrome P450 activation of arylamines and heterocyclic amines. *Annu Rev Pharmacol Toxicol 45*, 27-49.
(12) Hollenberg, P. F., Kent, U. M. and Bumpus, N. N. (2008) Mechanism-based inactivation of human cytochromes p450s: experimental characterization, reactive intermediates, and clinical implications. *Chem Res Toxicol 21*, 189-205.
(13) Bartsch, H., Dworkin, M., Miller, J. A. and Miller, E. C. (1972) Electrophilic N-acetoxyaminoarenes derived from carcinogenic N-hydroxy-N-acetylaminoarenes by enzymatic deacetylation and transacetylation in liver. *Biochim Biophys Acta 286*, 272-298.
(14) Hanna, P. E., Banks, R. B., and Marhevka, V. C. (1982) Suicide inactivation of hamster hepatic arylhydroxamic acid N,O-acyltransferase. A selective probe of N-acetyltransferase multiplicity. *Mol. Pharmacol. 21*, 159-165.
(15) Smith, T. J. and Hanna, P. E. (1988) Hepatic N-acetyltransferases: selective inactivation in vivo by a carcinogenic N-arylhydroxamic acid. *Biochem Pharmacol 37*, 427-434.
(16) Guo, Z., Wagner, C. R. and Hanna, P. E. (2004) Mass spectrometric investigation of the mechanism of inactivation of hamster arylamine N-acetyltransferase 1 by N-hydroxy-2-acetylaminofluorene. *Chem Res Toxicol 17*, 275-286.
(17) Wang, H., Wagner, C. R. and Hanna, P. E. (2005) Irreversible inactivation of arylamine N-acetyltransferases in the presence of N-hydroxy-4-acetylaminobiphenyl: a comparison of human and hamster enzymes. *Chem Res Toxicol 18*, 183-197.
(18) Liu, L., Wagner, C. R., and Hanna, P. E. (2008) Human Arylamine N-Acetyltransferase 1: In Vitro and Intracellular Inactivation by Nitrosoarene Metabolites of Toxic and Carcinogenic Arylamines. *Chem. Res. Toxicol.*
(19) Kitz, R. and Wilson, I. B. (1962) Esters of methanesulfonic acid as irreversible inhibitors of acetylcholinesterase. *J Biol Chem 237*, 3245-3249.
(20) Wang, H., Vath, G. M., Kawamura, A., Bates, C. A., Sim, E., Hanna, P. E. and Wagner, C. R. (2005) Over-expression, purification, and characterization of recombinant human arylamine N-acetyltransferase 1. *Protein J 24*, 65-77.

(21) Liu, L., Von Vett, A., Zhang, N., Walters, K. J., Wagner, C. R. and Hanna, P. E. (2007) Arylamine N-acetyltransferases: characterization of the substrate specificities and molecular interactions of environmental arylamines with human NAT1 and NAT2. *Chem Res Toxicol 20,* 1300-1308.
(22) http://www.chemspider.com.
(23) Hanna, P. E. (1994) N-acetyltransferases, O-acetyltransferases, and N,O-acetyltransferases: enzymology and bioactivation. *Adv Pharmacol 27,* 401-430.
(24) Novak, M. and Rajagopal, S. (2002) Correlations of nitrenium ion selectivities with quantitative mutagenicity and carcinogenicity of the corresponding amines. *Chem Res Toxicol 15,* 1495-1503.
(25) Kennedy, S. A., Novak, M., Kolb, B.A. (1997) Reactions of ester derivatives of carcinogenic N-(4-biphenyl)hydroxylamine and the corresponding hydroxamic acid with purine nucleosides. *J. Am. Chem. Soc. 119,* 7654-7664.

Part VI

(1) Miller, J. A., Wyatt, C. S., Miller, E. C., and Hartmann, H. A. (1961) The N-hydroxylation of 4-acetylaminobiphenyl by the rat and dog and the strong carcinogenicity of N-hydroxy-4-acetylaminobiphenyl in the rat. *Cancer Res. 21,* 1465-1473.
(2) Smith, T. J. and Hanna, P. E. (1988) Hepatic N-acetyltransferases: selective inactivation in vivo by a carcinogenic N-arylhydroxamic acid. *Biochem Pharmacol 37,* 427-434.

APPENDIX: INACTIVATION OF INTRACELLULAR NAT BY LOW CONCENTRATIONS OF NITROSOARENES

Introduction

In the previous studies (Parts III and IV of this thesis), we characterized the inactivation of NAT1 and NAT2 by nitrosoarene metabolites of arylamines. It was shown that NAT1 and NAT2 are intracellular targets of 4-NO-BP and 2-NO-F, and that HeLa cell NAT2 is less susceptible to the effects of the lower concentrations of the two nitrosoarenes than is NAT1. However, the NAT1 and NAT2 inactivation experiments were conducted with different preparations of HeLa cells. The objective of this study is to verify the previous results by determining the susceptibilities of the NAT isozymes to nitrosoarenes in the same preparation of HeLa cells.

Methods

At approximately 90% confluence, cell monolayers were washed twice with PBS. The cells were exposed to either 4-NO-BP (2.5 μM and 5 μM) or 2-NO-F (1 μM and 2.5 μM) in 10 mL of serum-free DMEM media containing DMSO. The final concentration of DMSO was 0.1%. The incubation was continued at 37 ºC for 1 h. Cells were washed with PBS buffer, trypsinized, and harvested. The controls contained DMSO only. Cytosol was prepared as described above, and the NAT1 and NAT2 activities were measured.

Results and Discussion

Incubation of cells with 4-NO-BP (2.5 μM) for one hour caused significantly different ($p < 0.001$) effects on NAT1 activity and NAT2 activity: 36 (±6)% loss in NAT1 activity, but no loss in NAT2 activity (Figure 1a). Treatment of the cells with 5 μM of 4-NO-BP for one hour also caused significantly different ($p < 0.02$) decreases in NAT1 and NAT2 activities: 50 (±8)% reduction in NAT1 activity, but only 26 (±9)% reduction in NAT2 activity (Figure 1a). Similarly, incubation of cells with 2-NO-F (1 μM and 2.5 μM) for one hour caused significantly greater inhibitory effects on intracellular NAT1 than on NAT2 (Figure 1b). 2-NO-F (1 μM) had no effect on NAT2 activity, but caused a significant ($p < 0.05$) reduction of 30 (±4)% in NAT1 activity. 2-NO-F (2.5 μM) reduced NAT1 and NAT2 activities by 53 (±5)% and 25 (±7)%, respectively, which were significantly ($p < 0.01$) different from each other. Thus, HeLa cell NAT2 is less susceptible to the effects of the lower concentrations of the two nitrosoarenes than is NAT1, which might indicate that intracellular NAT2 is less accessible to nitrosoarenes than NAT1.

a b

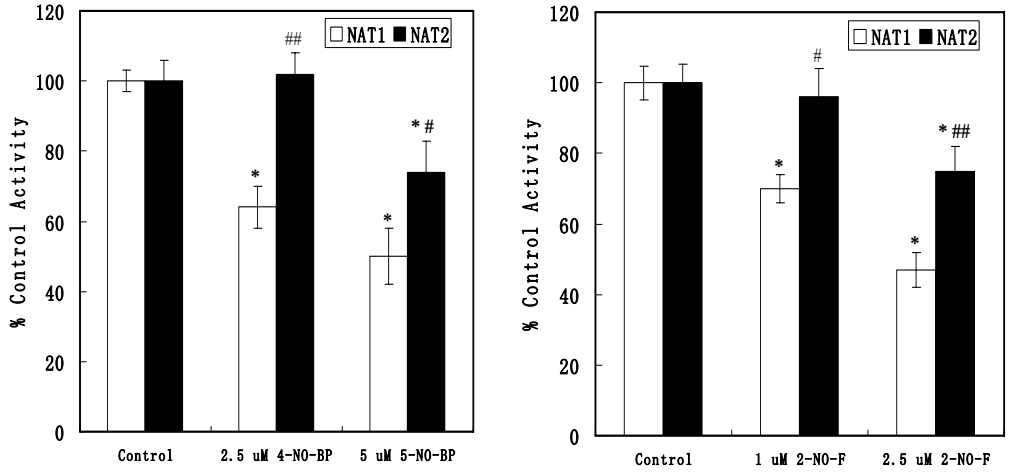

Figure 1. Inactivation of HeLa cell NAT1 and NAT2 by low concentrations of 4-NO-BP and 2-NO-F. The incubation time was 1 h. (a) 4-NO-BP. Each bar represents the mean and standard deviation of the results of three experiments. Asterisks represent significant differences from controls: *, $p < 0.001$. Pound symbols represent significant differences from percentage of NAT1 activity in the same inactivation experiments: #, $p < 0.02$; ##, $p < 0.001$. (b) 2-NO-F. Each bar represents the mean and standard deviation of the results of three experiments. Asterisks represent significant differences from controls: *, $p < 0.001$. Pound symbols represent significant differences from percentage of NAT1 activity in the same inactivation experiments: #, $p < 0.05$; ##, $p < 0.01$.